THE ROLE OF SNARE PROTEINS IN CD4$^+$ T-HELPER CELL SUBSETS

A thesis submitted for the degree of Ph.D.

By

Joseph deCourcey B.Sc

July 2013

Based on research carried out at:
School of Biotechnology,
Dublin City University,
Dublin 9,
Ireland.

Under the supervision of Dr. Christine Loscher

DECLARATION

I hereby certify that this material, which I now submit for assessment on the programme of study leading to the award of Doctor of Philosophy is entirely my own work, and that I have exercised reasonable care to ensure that the work is original, and does not to the best of my knowledge breach any law of copyright, and has not been taken from the work of others save and to the extent that such work has been cited and acknowledged within the text of my work..

Signed: _____ (Candidate) ID No.: _____ Date: _____

ACKNOWLEDGEMENTS

PUBLICATIONS

Rahman A*, DeCourcey J*, Ben Larbi N, Loughran ST, Wall D, Loscher CE† (2013)
"Syntaxin-4 is critical in IgE secretion from plasma cells"
Accepted to Biochemistry and Biophysics Research Communications

Korzeniowska B, Woolley R, Wencel D, DeCourcey J, Loscher CE, McDonagh C* (2013)
"Intracellular pH-sensing using core/shell silica nanoparticles."
Accepted to the Journal of Biomedical Nanotechnology

Kristek M, Collins L, DeCourcey J, McEvoy F, Loscher CE* (2013)
"Soluble factors from colonic epithelial cells contribute to gut homeostasis by modulating macrophage phenotype"
Submitted to Immunology

Draper E, DeCourcey J, Higgins SC, Canavan M, Ryan A, Keogh B, Reynolds C, Roche HM, Mills KH, Loscher CE* (2013)
"A fat to dampen the flames: conjugated linoleic acid suppresses dendritic cell activation and subsequent Th17 responses"
Submitted to PLOS one

.

ABBREVIATIONS

BMDC	Bone marrow-derived dendritic cell
BCA	Bicinchoninic Acid
BSA	Bovine Serum Albumin
CD	Cluster of Differentiation
CFSE	Carboxyfluorescein succinimidyl ester
CTL	Cytotoxic T-lymphocyte
DC	Dendritic cell
DEPC	Diethylpyrocarbonate
DNA	Deoxyribonucleic Acid
DSS	Dextran sodium sulfate
DTT	Dithiotreitol
EDTA	Ethylenediaminetetraacetic acid
ELISA	Enzyme Linked Immuno-Sorbent Assay
FACS	Fluorescence Activated Cells Sorting
FBS	Fetal Bovine Serum
HRP	Horse Radish Peroxidase
IBD	Inflammatory bowel disease
IFN	Interferon
MHC	Major histocompatability complex
MLN	Mesenteric Lymph Nodes
NK	Natural killer
NSF	N-ethylmaleimide sensitive factor
PAF	Para-formaldehyde
PAMP	pathogen associated molecular pattern
PCR	Polymerase Chain Reaction
PI	Propidum Iodide
qRT-PCR	quantitative Real Time-Polymerase Chain Reaction
RNA	Ribonucleic Acid
RORγt	Retinoid orphan receptor γ
SDS	Sodium Dodecyl Sulfide
SNAP	Soluble NSF attachment protein
SNARE	Soluble-N-ethylamide Receptor
SPF	Specific Pathogen Free
STAT	Signal transducer and activator of transcription
STX	Syntaxin
TCR	T-cell receptor complex
TGF	Transforming growth factor
Th	T-helper
TLR	Toll like receptor
TMB	Tetramethylbenzidine
TNF	Tumour necrosis factor
UC	Ulcerative colitis

TABLE OF CONTENTS

TITLE i

DECLARATION ii

ACKNOWLEDGEMENTS iii

PUBLICATIONS iiiv

ABBREVIATIONS v

TABLE OF CONTENTS vi

ABSTRACT xi

CHAPTER 1 – GENERAL INTRODUCTION 1

1.1 INTRODUCTION 2
1.1.1 ADAPTIVE IMMUNITY 2
1.1.2 MAJOR HISTOCOMPATIBILITY COMPLEX 4
1.1.2 $CD4^+$ T-CELL ACTIVATION 5
1.1.3 $CD4^+$ T-CELL SUBSETS 6
1.1.3.1 THE Th1/Th2 PARADIGM 6
1.1.3.2 T-HELPER 2 CELLS 8
1.1.3.2 T-HELPER 1 CELLS 10
1.1.3.2 T-REGULATORY CELLS 13
1.1.3.2 T-HELPER 17 15
1.1.3.2 Th17/Treg AXIS 18
1.1.3.4 Th17 RESPONSES IN INFLAMMATION AND DISEASE 20
1.1.3.4 OTHER EMERGING T-HELPER SUBSETS 24
1.1.4 PROTEIN TRAFFICKING 25
1.1.5 SNARE PROTEINS 27
1.1.5.1 SNARE STRUCTURE 28
1.1.5.2 SNARE FUNCTION 30
1.1.6 SNARE PROTEINS IN IMMUNE CELLS 32
1.1.6.1 NEUTROPHILS 32
1.1.6.2 MAST CELLS 33
1.1.6.2 NATURAL KILLER CELLS 35
1.1.6 SNARE PROTEINS IN TNF-α TRAFFICKING FROM MACROPHAGES 36
1.1.6 SNARE PROTEINS IN T-CELLS 37
1.1.7 PROJECT RATIONALE AND HYPOTHESIS 41
1.1.8 PROJECT AIMS 43

CHAPTER 2 – MATERIALS AND METHODS 44

2.1 – MATERIALS 45
2.2 – ISOLATION AND CULTURE OF $CD4^+$ T-CELLS 49
2.2.1 – CELL ENUMERATION AND VIABILITY ASSESSMENT 49
2.2.2 – ISOLATION OF $CD4^+$ T-CELLS 50
2.2.2.1 – SPLEENOCYTE ISOLATION 50
2.2.2.2 – $CD4^+$ T-CELL MAGNETIC PARTICLE ISOLATION 50
2.2.2.3 – $CD4^+$ T-CELL COLUMN ISOLATION 51
2.2.3 – POLARISATION OF $CD4^+$ T-CELLS 52
2.3 – FLOW CYTOMETRY 53
2.3.1 – BASIC PRINCIPLES OF FLOW CYTOMETRY 53
2.3.2 – FLUORESCENCE ACTIVATED CELLS SORTING (FACS) 53
2.3.3 – CELL SURFACE MARKER STAINING 54
2.3.4 – STAINING ANTIBODY TITRATION 55
2.3.5 – INTRACELLULAR PROTEIN STAINING 55
2.3.5.1 – INTRACELLULAR TRANSCRIPTION FACTOR STAINING 55
2.3.5.2 – INTRACELLULAR CYTOKINE STAINING 56
2.3.6 – PROLIFERATION ANALYSIS USING CFSE DYE 57
2.3.7 – CELL VIABILITY AND DEAD CELL EXCLUSION USING PROPIDIUM IODIDE STAINING 57
2.4 – CYTOKINE ELISA 58
2.4.1 – BASIC PRINCIPLES OF ELISA 58
2.4.2 – TNF-α, IL-4, IL-10 and IL-17 CYTOKINE ELISA 59
2.4.3 – IL-2 AND IFN-γ CYTOKINE ELISA 59
2.4.4 – IL-21 CYTOKINE ELISA 59
2.5 – RNA ANALYSIS 60
2.5.1 – BASIC PRINCIPLES OF REAL-TIME qPCR 60
2.5.2 – RNA EXTRACTION 61
2.5.3 – DNA PRODUCT ANALYSIS BY GEL ELECTROPHORESIS 61
2.5.4 – cDNA SYNTHESIS 62
2.5.5 – qPCR ASSAY OPTIMISATION 63
2.5.6 – RELATIVE QUANTITATION USING qPCR 64
2.6 – *IN VIVO* WORK AND MOUSE MODELS OF DISEASE 65
2.6.1 – DSS MODEL OF COLITIS 65
2.6.2 – ISOLATION OF LAMINA PROPRIA 67
2.6.3 – TISSUE SECTIONING AND IMMUNOHISTOCHEMISTRY 68
2.6.4 – CITROBACTER RODENTIUM INFECTION MODEL 68
2.6.5 – MICE USED FOR $Stx11^{-/-}$ IN VITRO STUDY 69
2.6.6 – MICE USED FOR IN VITRO STUDIES 69
2.7 – STATISTICAL ANALYSIS 65

CHAPTER 3 – ISOLATION AND POLARISATION OF CD4+T- CELLS *IN VITRO* 70
3.1– INTRODUCTION 71

3.2– RESULTS 74
3.2.1 – ISOLATION, ACTIVATION AND CONFIRMATION OF $CD4^+$ T-HELPER CELL POPULATION FROM BALB/C MICE. 74
3.2.2 – ANTIBODIES DIRECTED TO CD3 AND CD28 PROVIDE SIGNALS FOR IN VITRO ACTIVATION OF CD4+ CELLS. 75
3.2.3 – A COMPARISON OF MAGENTIC AND COLUMN PURIFICATION METHODS FOR $CD4^+$ T-CELL ISOLATION. 77
3.2.4 - MAGNETIC ISOLATION OF $CD4^+$ LYMPHOCYTES RESULTS IN ENHANCED CYTOKINE PRODUCTION FOLLOWING STIMULATION. 79
3.2.5 – VARIATIONS IN FETAL BOVINE SERUM (FBS) BATCHES EFFECTS CYTOKINE PRODUCTION IN $CD4^+$ LYMPHOCYTES 80
3.2.6 - ADDITION OF IL-2 INCREASES THE PROLIFERATION OF $CD4^+$ LYMPHOCYTES IN VITRO. 81
3.2.7 – MEDIA SUPPLEMENTED WITH BME IMPROVES THE VIABILITY OF $CD4^+$ T-CELLS IN VITRO. 82
3.2.8 – OPTIMISATION OF Th17 $CD4^+$ T-CELL POLARISATION IN VITRO. 83
3.2.9 – T-CELLS CULTURED IN Th17 POLARISING CONDITIONS EXPRESS THE TRANSCRIPTION FACTOR RORγt 85
3.2.10 – INVESTIGATION OF DIFFERENT Th17 CELL SUBSETS GENERATED IN THE ABSENCE/PRESENCE OF TGF-β. 86
3.2.11 – OPTIMISATION OF Th1 $CD4^+$ T-CELL POLARISATION IN VITRO. 89
3.2.12 – T-CELLS CULTURED IN Th1 POLARISING CONDITIONS EXPRESS THE T-BOX TRANSCRIPTION FACTOR T-BET. 90
3.2.13 – T-CELLS CULTURED IN Th1 POLARISING CONDITIONS EXPRESS THE SURFACE PROTEIN CCR5. 91
3.2.14 – OPTIMISATION OF Th2 $CD4^+$ T-CELL POLARISATION IN VITRO. 91
3.2.15 – T-CELLS CULTURED IN Th2 POLARISING CONDITIONS EXPRESS THE TRANSCRIPTION FACTOR GATA-3. 92

3.3– DISCUSSION 112

CHAPTER 4 – SNARE EXPRESSION IN $CD4^+$ T-CELLS 125

4.1– INTRODUCTION 126

4.2– RESULTS 128
4.2.1 – ANALYSIS OF IFN-γ AND IL-17 CYTOKINE LEVELS FROM POLARISED $CD4^+$ T-HELPER CELLS OVER A 72hr TIME COURSE. 128
4.2.2 – IFN-γ AND IL-17 mRNA EXPRESSION IN Th1 AND Th17 POLARISED $CD4^+$ T-CELLS AT 48hrs 129

4.2.4 – DIFFERENCES IN R-SNARE EXPRESSION IN Th17 CELLS COMPARED TO Th1 CELLS USING qPCR ANALYSIS OF SAMPLES AT 48hrs. 131
4.2.5 – DIFFERENCES IN Qa-SNARE EXPRESSION IN Th17 CELLS COMPARED TO Th1 CELLS USING qPCR ANALYSIS OF SAMPLES AT 48hrs. 132
4.2.6 – DIFFERENCES IN Qb AND Qbc-SNARE EXPRESSION IN Th17 CELLS COMPARED TO Th1 CELLS USING qPCR ANALYSIS OF SAMPLES AT 48hrs. 133
4.2.7 – CYTOKINE mRNA EXPRESSION LEVELS IN NAÏVE, Th1 AND Th17 CELLS AT 48hrs. 134
4.2.8 – SNARE mRNA EXPRESSION LEVELS IN NAÏVE, Th1 AND Th17 CELLS AT 48hrs. 135
4.2.9 – STX11 mRNA EXPRESSION IN MOUSE MODELS OF COLITIS. 137

4.3 – DISCUSSION 158

CHAPTER 5 – THE ROLE OF STX11 IN Th17 CELLS 167

5.1 – INTRODUCTION 168

5.2 – RESULTS 170
5.2.1 – CYTOKINE SECRETION FROM $CD4^+$ T-HELPER CELLS ISOLATED FROM WILD TYPE AND $Stx11^{-/-}$ MICE AND CULTURED IN Th17 POLARISING CONDITIONS IN VITRO. 170
5.2.2 – CYTOKINE SECRETION FROM $CD4^+$ T-HELPER CELLS ISOLATED FROM WILD TYPE AND $Stx11^{-/-}$ MICE AND CULTURED IN Th1 POLARISING CONDITIONS IN VITRO. 172
5.2.3 – INTRA-CELLULAR CYTOKINE STAINING OF $CD4^+$ T-HELPER CELLS ISOLATED FROM WILD TYPE AND $Stx11^{-/-}$ MICE AND CULTURED IN Th17 POLARISING CONDITIONS IN VITRO. 173
5.2.4 – INTRA-CELLULAR CYTOKINE STAINING OF $CD4^+$ T-HELPER CELLS ISOLATED FROM WILD TYPE AND $Stx11^{-/-}$ MICE AND CULTURED IN Th1 POLARISING CONDITIONS IN VITRO. 174
5.2.5 – RORγt STAINING OF $CD4^+$ T-HELPER CELLS ISOLATED FROM WILD TYPE AND $Stx11^{-/-}$ MICE AND CULTURED IN Th17 AND Th1 POLARISING CONDITIONS IN VITRO. 175
5.2.6 – PROLIFERATION OF Th17 POLARISED CELLS ISOLATED FROM WILD TYPE AND $Stx11^{-/-}$ MICE. 176
5.2.7 – PROLIFERATION OF Th1 POLARISED CELLS ISOLATED FROM WILD TYPE AND $Stx11^{-/-}$ MICE. 178
5.2.8 – CELL COUNTS AND VIABILITY OF Th1 And Th17 POLARISED CELLS ISOLATED FROM WILD TYPE AND $Stx11^{-/-}$ MICE. 178
5.2.9 – mRNA EXPRESSION OF SIGNATURE Th17 GENES AND CONFIRMATION OF Th17 POLARISATION IN NAÏVE CELLS FROM WT MICE. 180
5.2.10 – mRNA EXPRESSION OF TRANSCRIPTION FACTOR GENES IN POLARISED NAÏVE CELLS FROM WT AND $Stx11^{-/-}$ MICE. 182

5.2.11 – mRNA EXPRESSION OF CYTOKINE GENES IN POLARISED NAÏVE CELLS FROM WT AND Stx11$^{-/-}$ MICE. 182
5.2.12 – mRNA EXPRESSION OF CYTOKINE RECEPTOR GENES IN POLARISED NAÏVE CELLS FROM WT AND Stx11$^{-/-}$ MICE. 184

5.3– DISCUSSION 212

CHAPTER 6 – GENERAL DISCUSSION 224

CHAPTER 7 – BIBLIOGRAPHY 236

APPENDICES 261
APPENDIX A – MEDIA AND BUFFERS 262
APPENDIX B – PRIMER EFFICIENCY CURVES 264
APPENDIX C – PRIMER SEQUENCES 272

ABSTRACT

It is well established that $CD4^+$ T-helper cells are vital in the adaptive immune response and mediate the clearance of persistent pathogens. Specific T-helper cell phenotypes that secrete distinct profiles of cytokines are generated in response to infection. These cytokines orchestrate homeostasis and pathogen clearance through autocrine and endocrine signalling. Dysregulation of this process can lead to inflammation and autoimmune disease. Secretion of cytokines is facilitated by highly regulated SNARE proteins. SNAREs have been shown to form specific partnerships and facilitate membrane-membrane fusion required for the exocytosis of cytokines and other proteins from immune cells. Using an optimised *in vitro* model, isolated $CD4^+$ T-cells were polarised into T-helper cell subsets in order to profile SNARE expression and regulation. Syntaxin-11 (STX11) was identified as a candidate regulatory SNARE in Th1 and Th17 cells. Further investigation *in vivo* using two mouse models of inflammation suggested that STX11 was regulated in Th17/Th1 mediated disease. Finally, we examined Th1 and Th17 responses in STX11 deficient mice and demonstrated that in the absence of STX11, T helper cell secreted increased levels of IFN-γ and were unable to differentiate into a Th17 subset. The elucidation of SNARE trafficking pathways in $CD4^+$ T-helper cells may represent potential therapeutic targets for blocking cytokine secretion from targeted cells and control inflammation. It may also lead to a better understanding of SNARE deficient immune disorders such as familial haemophagocytic lymphohistocytosis - 4 (FHL-4), characterised by over production of cytokines and high number of activated lymphocytes due to STX11 deficiency.

CHAPTER 1

GENERAL INTRODUCTION

1.1 INTRODUCTION

The immune system has evolved to compose two arms of defence; the innate and adaptive immune system, which together can co-ordinate a response to invading pathogens and parasites. The first line of defence in infection is the innate immune system which is made up of physical barriers, phagocytic cells, granule releasing killer cells and importantly, antigen presenting cells (APCs) (Janeway & Medzhitov 2002). Dendtiric cells (DCs) in particular are highly specialised APCs that form part of an intricate link between the innate and adaptive immune response (Banchereau & Steinman 1998). Many pathogens can overcome the innate system and switch on the adaptive immune system to mount a second specialised response to invaders (Janeway & Medzhitov 2002).

1.1.1 ADAPTIVE IMMUNITY

The adaptive immune system is capable of mounting a targeted specific type of immune response necessary to clear a multitude of different infections. It is a tightly regulated and controlled response that is often self limiting and therefore dysregulation can be the cause of auto immunity or inflammatory disease. The adaptive immune system can mount two main types of response to infection; the first is a humoral response orchestrated by B-cells. B-cells, named for their origin in the bone marrow, present antibodies on their cell surface capable of binding a host of chemical structures (Hardy & Hayakawa 2001). They attempt to target antigens on invading pathogen or infected cells. Successful antibody responses convert B-cells into antibody secreting plasma cells producing large amounts of specific antibody targeting an invading pathogen and neutralising it or tagging it for killing by the innate responder cells (Mauri 2010). Following completion of this task, the response is

suppressed, however some B-cells that recognise specific antigen persist and are converted to memory B-cells which become inert and migrate around the body ready to respond quickly to a repeat infection (Mauri 2010).

The second response is the cellular T-cell mediated response. T-cells develop in the thymus where a number of processes take place before deriving T-cells into one of two specific lineages identified by their cell surface receptor expression; $CD8^+$ cytotoxic lymphocytes (CTLs) and $CD4^+$ T-helper cells (Fink 2013). In the thymus early T-cell progenenitors lack expression of CD4 or CD8 and undergo four cell surface marker stages (CD44 and CD25 derived) of development before a final stage of expressing CD4 ,CD8 and a formed T-cell receptor (TCR) essential for activation and peptide recognition (Germain 2002). The cells are then exposed to self antigens associated with the multiple histocompatability complex (MHC) that present antigen in a complex form on the surface of cells. The MHC are subdivided into two main classes involved in antigen processing and presentation; MHC I and MHC II, which are associated with CD8 and CD4 respectively. If the cells become activated following engagement of MHC they are deleted; this is termed negative selection. If the cells are not engaged they are deleted (Fink 2013). However, an intermediate interaction with self peptide results in the positive selection of the T-cell. Interaction with MHC I peptide self antigen complex leads to $CD8^+$ CTL cells, and interaction with MHC II-self antigen complex leads to the positive selection of $CD4^+$ T-helper cells (Germain 2002).

1.1.2 MAJOR HISTOCOMPATIBILITY COMPLEX

MHC I is expressed by all nucleated cells and its function is to present peptides from within the cell which form part of normal protein production mechanisms, CTLs recognise these as self peptides following the positive selection process, and do not engage with the cell. However, if the cell is cancerous or infected by a virus, it can present antigens on its surface in the MHC I complex which are not usually present and activates naïve CTLs. These CTLs become activated effector cells and respond to target antigen undergoing rapid expansion proliferating up to as many as 15 generations of cells within 7 days to produce an armoury of targeting killer cells (Bevan 2004). CTLs act as directed killers of tumour and pathogen infected cells using two main methods; cell-cell contact and cell targeted secretion of granules containing factors that include perforin and granzymes. Perforin and Granzyme form a complex that allows the granzyme to enter the cell where it induces apoptosis via caspase cleavage and activation. Cell-cell contact cell death is mediated trough the Fas/Fas ligand pathways that also induce cell death via cleavage and activation of caspases in the cell (Russell 2002). Some of these CTLs recognizing specific antigens will become $CD8^+$ memory cells and facilitate a rapid killing response when the antigen is encountered again (Barber et al. 2003).

MHC II is expressed by DCs following the phagocytosis of invading extracellular pathogens (Banchereau & Steinman 1998). Internalised proteins are degraded by proteases and delivered in an MHC II complex to the cell surface. They present peptides from the invading pathogens to $CD4^+$ T-cells which undergo proliferation and differentiation into distinct T-helper subsets of cells when activated (J. Zhu et al. 2010). Activation of $CD4^+$ T-cells requires a number of signals to initiate this differentiation and prevent an

unnecessary immune response which can lead to inflammatory disease or autoimmunity (Jelley-Gibbs et al. 2000)

1.1.2 $CD4^+$ T-CELL ACTIVATION

Dendritic cells are sentinels that reside in the skin and mucosa awaiting activation upon contact and recognition of pathogen associated molecular patterns (PAMPs) via toll like receptors (TLRs). The activated DCs migrate through the lymphatic system to secondary lymphatic structures, spleen and lymph nodes, were T-cells reside. Three signals from the activated DC are required for the full activation of T cells. The first is MHC II which is up-regulated on activated DCs and engages with T-cells that recognise the antigen through the TCR and CD4 surface molecules (Kenneth Murphy Mark Walport 2008). This signal alone is not sufficient to activate the T-cells. DCs may routinely present MHC II in complex with self antigens on their surface, recognition and activation to self antigen results in autoimmunity. Therefore a second signal is required to ensure specific activation of the $CD4^+$ T-cells. Upon activation DCs up-regulate CD80, a member of the B7 family of receptors on the cell surface. CD80 forms a complex with the CD28 surface receptor that is found on naïve $CD4^+$ T-cells activating a co-stimulatory signalling cascade necessary for activation (Lenschow et al. 1996). This leads to up-regulation of CD86 on the surface of DCs, a second member of the B7 family that engages CD28 on the T-cell providing co-stimulatory signals. Activation in the absence of co-stimulatory signals leads to cell anergy or deletion (Greenwald 2005). A third signal that is crucial for activation, and specifically the differentiation of $CD4^+$ T-helper cells, is cytokine signalling (Yamane & Paul 2012). The cytokine environment in which the cell is activated will influence the type of $CD4^+$ T-cell that is generated. This cytokine milieu is dictated in part by the DC,

depending on the nature of its own activation via the TLRs (Banchereau & Steinman 1998). Specific $CD4^+$ T-cell phenotypes are generated in order to adapt and provide a specific immunological response required to clear infection (Jiang & Dong 2013).

1.1.3 $CD4^+$ T-CELL SUBSETS

CD4 T helper cells have a number of different functions. They assist B-cells in the humoral immune response facilitating antibody secretion and memory formation (Crotty 2011). They also enhance and maintain $CD8^+$ T-cells responses and regulate phagocyte function via secretion of cytokines (Bevan 2004). $CD4^+$ T-helper cells play an essential role in immune regulation and clearance of pathogens. They carry out these specialised functions via polarisation into specific cell phenotypes that are defined by the expression of a unique set of transcription factors and secretion of specific key cytokines. Interaction of $CD4^+$ T-cells with APC leads to TCR mediated stimulation which, along with the cytokine environment secreted by the APCs, dictates the transcriptional activation of naïve T-cells directing them towards a distinct Th phenotype (Yamane & Paul 2013).

1.1.3.1 THE Th1/Th2 PARADIGM

The first identification of different T-helper subsets of cells was the classification of Th1 and Th2 cells by Mossmann and Coffman (1986). They distinguished differences in clones in the $CD4^+$ T-cell population; they differentiated the clones by the specific cytokine profiles they secreted and also their differences in cell surface marker expression. Th1 cells were classified by their production of IFN-γ, IL-2 and GM-CSF. Th2 cells on the other hand produced IL-4, IL-5 and IL-13.

Two independent labs demonstrated the generation of IL-4 producing T-cells following activation in the presence of IL-4 (Le Gros 1990; Swain et al. 1990). In the year following these studies, work published by Hsieh *et al* (1993) showed that IL-12, in the absence of IL-4, led to Th1 polarisation *in vitro*. This study highlighted the fact that IL-4, the cytokine that drives Th2/IL-4 producing cells to secrete large amounts of IL-4, inhibited the generation of Th1 cells. Th1 would later be shown to inhibit Th2 cells via IFN-γ mediated inhibition of IL-4 production (Gajewski & Fitch 1988). IFN-γ production also stabilised differentiation of Th1 cells in an autocrine fashion and induce phagocytes to produce IL-12 (Yoshida et al. 1994). Therefore, in response to APC stimulation, Th1 or Th2 cells were polarised via cytokine signals secreted by the APC. This T-cell subset would then produce cytokines to establish extrinsic feedback loops and stabilise differentiation while simultaneously inhibiting the other subset. This provided an explanation for the stable Th1 or Th2 responses observed in patients in response to different chronic infections (Romagnani 1994). Th1 cells were later shown to be involved in delayed type hypersensitivity in which the immune response is cell mediated over a number of days. They promoted intracellular killing of pathogens in macrophages via IFN-γ secretion and promoted IgG production from B-cells. Given that opsonising IgG antibodies tag pathogens for destruction via macrophage phagocytosis or cell-mediated cytotoxicity by $CD8^+$ CTLs (Basu et al. 2013), Th1 cells were identified as the helper cells involved in mobilising the immune system to clear intracellular pathogens.

Th2 cells induced production of IgE and IgG1 antibodies. These antibodies promote mast cell and basopil degranulation, enhance mucus production and promote the development of eosinophils and aid in immune responses to parasitic helminths (Basu et al. 2013). This

hypothesis was shown nicely in a study identifying that human $CD4^+$ T-cell clones specific for *M. tuberculosis* were IFN-γ producing Th1 cells and $CD4^+$ T-cell clones specific for the helminth *Toxocara canis* were mainly IL-4 producing Th2 cells (Delprete et al. 1991).

Cytokine signalling is essential in deciding gene transcription programmes in T-cells via Type I/II cytokine receptor family. Type I/II receptors signal through the Janus kinase-signal transducer and activator of transcription (STAT) signalling pathway in order to initiate signalling pathways differentiating cell populations (Yamane & Paul 2012). The current system of defining T helper subsets attributes specific STAT pathways, activated by cytokine signalling, to the transcription and expression of a "master regulator" gene. Each cell lineage has been attributed to the expression of a master regulator and is in most cases responsible for the transcription of its key cytokine (Vahedi et al. 2013). Following the establishment of Th1 and Th2 $CD4^+$ T-cell clones, subsequent studies led to the identification of the transcriptional pathways that drive the commitment of these cells into a specific lineage (Zheng & Flavell 1997; Szabo et al. 2000)

1.1.3.2 T-HELPER 2 CELLS

Th2 cells have been generated *in vitro* via stimulation of the TCR and the addition of IL-4. IL-4 was shown to drive Th2 polarisation via the activation of STAT6 and STAT6 knockouts fail to induce Th2 polarisation upon stimulation with IL-4 or IL-13 (Shimoda et al. 1996; Takeda et al. 1996; Kaplan et al. 1996). Following this discovery, STAT6 was later revealed to be an activator of the transcription factor GATA-3 (Zheng & Flavell 1997). Ectopic expression of GATA-3 in Th1 cells induced IL-4 production and GATA-3 expression (Ouyang et al. 1998). Conditional GATA-3 knockout in cells led to an inability to drive Th2 polarisation and cells became Th1 polarised in the absence of IL-12 and IFN-

γ. This work also demonstrated the inhibitory role of GATA-3 on Th1 polarisation (Zhu et al. 2004). Deletion of GATA-3 in established Th2 cells resulted in the loss of IL-5 and IL-13 production but not IL-4, indicating that GATA-3 expression is required for the initial polarisation of Th2 cells but late IL-4 is regulated independently of GATA-3. Indeed, IL-4 and STAT6 deficient mice are still able to develop Th2 differentiation in response to infection, however GATA-3 is indispensible and GATA-3 deficient mice develop a Th1 mediated IFN-γ response to infection with *Nippostrongylus brasilienis* (Yamane & Paul 2012). IL-2 mediated activation of STAT5 is also a requirement for Th2 development *in vitro* (Cote-Sierra et al. 2004). Originally recognised as a T-cell growth factor, neutralisation of IL-2 in activated naïve $CD4^+$ T-cell cultures inhibited Th2 polarisation in the presence of IL-4. STAT5a deficient T-cells were unable to differentiate into a Th2 subset following activation in the presence of IL-2. This was rescued following ectopic expression of a constitutively active form of STAT5a demonstrating a requirement in early STAT5 activation in Th2 differentiation. Activated STAT5 binds to the IL-4 genetic region and neutralisation of IL-2 leads to a loss in early IL-4 production but does not effect GATA-3 expression. STAT5 is thought to bind and act to maintain the *Il4* locus in an open configuration allowing access for transcription factors involved in Th2 differentiation. So STAT5 is independent of GATA-3 signalling and over-expression of GATA-3 does not rescue the reduction in IL-4 production in the absence of STAT5 signalling (Zhu et al. 2006). STAT5 also maintains commitment in Th2 cells and its own expression in an autocrine manner. STAT5 regulates expression of the IL-4Rα and is also important in maintaining IL-2R (CD25) expression during T-cell activation. IL-2 produced by the activated cells then interacts with CD25 and activates STAT5. GATA-3 can also act to

maintain a positive feedback loop and acts directly on IL-4 production with STAT5, and IL-4 enhances IL-4Rα expression and also activates STAT6 to up-regulate GATA-3 expression (Zhu 2010).

It is clear that both GATA-3 and STAT5 are major elements that act synergisticically in the differentiation of Th2 cells. The differentiation of these cells *in vivo* remains to be elucidated as IL-4 dependant and independent pathways can lead to Th2 differentiation, as demonstrated by the STAT6 and IL-4 knockout experiments (Yamane & Paul 2012). It is possible that basal expression of GATA-3 is enough to drive Th2 cell responses in certain conditions and TCR receptor activation is also revealing mechanisms of Th2 differentiation depending on peptide dose stimulation; with low-dose stimulation of T-cells preferentially leading to Th2 cell responses. What is clear from these findings is that GATA-3 is necessary for Th2 polarisation, but other cytokines and transcription factors are involved in the fine tuning of Th2 cell responses *in vivo* and their mechanisms are under investigation (Zhu et al. 2006). Despite their important role in defence against extracellular pathogens and their regulated interaction with Th1 cells through inhibition and feedback mechanisms in the Th1/Th2 paradigm, Th2 cells will not be part of the focus of this thesis and therefore will not be discussed further.

1.1.3.2 T-HELPER 1 CELLS

Murphy and colleagues demonstrated that IL-12 induced Th1 cell differentiation via STAT4 (Jacobson et al. 1995). This was later shown to be the inducer of the master regulator T-bet, a transcription factor that transactivates IFN-γ production, the key cytokine produced by Th1 cells. In this study Szabo *et al* (2000) showed that T-bet was expressed in Th1, but not Th2 cells. They also showed that T-bet induced IFN-γ production in

retrovirally transduced naïve T-cells and Th2 committed T-cells (Szabo et al. 2000). Furthermore, subsequent studies in T-bet deficient mice showed that these mice were unable to clear infections requiring an IFN-γ driven response and the cells showed defective IFN-γ production when stimulated with IL-12 *in vitro* (Szabo et al. 2002). In line with the findings that Th1 and Th2 cells both inhibit the development of the other, T-bet was shown to directly inhibit GATA-3 and subsequent Th2 differentiation (Hwang et al. 2005). Conversely GATA-3 inhibits Th1 polarisation via repression of STAT4 and IL-12Rβ2, the active receptor for IL-12 signalling (Usui et al. 2003). IL-12 signalling induces IFN-γ production in Th1 cells and is a potent inducer of T-bet. IFN-γ production therefore in turn stabilises T-bet expression in a positive feedback. However, despite the ability of IFN-γ to induce T-bet expression, IFN-γ alone is not sufficient to drive Th1 differentiation (Macatonia et al. 1993; Seder et al. 1993). IFN-γ drives early T-bet expression, however, this expression is repressed and returns after four days despite no change in IFN-γ expression. This indicted that the second peak in T-bet that commits T-cells to the Th1 lineage is IFN-γ independent (Schulz et al. 2009). The IFN-γR is expressed on naïve $CD4^+$ T-cells, but the IL-12Rβ2 necessary for IL-12 signalling and induction of IFN-γ and Th1 differentiation is not expressed on naïve $CD4^+$ T-cells and remains low in the first few days following activation (Afkarian et al. 2002). This was explained in a two-step regulated sequential mechanism for Th1 differentiation of T-cells. The role of early IFN-γ/STAT1 signalling and late IL-12/STAT4 signalling was shown in an elegant study using *Ifngr*$^{-/-}$ mice and anti-IL-12 antibodies (Schulz et al. 2009). TCR engagement induced early T-bet and IFN-γ expression and simultaneously suppressed IL-12-STAT4 activation via down-regulation of the IL-12Rβ. Loss of antigen signalling and increased IFN-γ production

increased the expression of IL-12Rβ and initiated the late induction of T-bet and commitment to Th1 phenotype via IL-12-STAT4 signalling. This offered an explanation for the strong inhibition of Th1 cell differentiation following IL-12 mediated Th1 differentiation in cells from *Ifngr*$^{-/-}$ mice (Macatonia et al. 1993; Seder et al. 1993). This study shows the synergistic requirement for both early IFN-γ signalling via STAT1 and late IL-12 commitment via STAT4 signalling. Upon stimulation, Th1 derived cells also secrete the cytokine IL-2. IL-2 activates STAT5 and regulates binding of T-bet to the promoter region of the gene encoding IFN-γ production (*Ifnγ*). IL-2 activation of the STAT5 pathway is also responsible for the induction of IL-12Rβ2 which leads to up-regulation of the IL-12R and imprinting of Th1 commitment. The necessity of this pathway in the induction of T-bet and Th1 cell lineage commitment is still not confirmed (Yamane & Paul 2012).

Th1 cells secrete IFN-γ in high amounts in response to intracellular pathogens. The secretion of IFN-γ has a wide range of effects on cell populations *in vivo.* As described above, IL-12 secretion by APCs leads to Th1/IFN-γ responses and inflammation. IFN-γ has also been shown to up-regulate the IL-12Rβ on the surface of T-cells leading to an increased response to IL-12 (Schroder et al. 2004). It also has the effect of up-regulating IL-12 secretion in phagocytes thereby further driving and stabilising a Th1 response (Hochrein et al. 2001). Furthermore, IFN-γ is a potent inducer of T-bet expression, and T-bet regulates IFN-γ production in a number of other cells in the innate response (Schroder et al. 2004). IFN-γ can act in co-ordinating a number of responses. It is active in the response to microbial infection through its influence on macrophages inducing the NADPH-dependant phagocyte oxidase pathway and up –regulation of lysosomal enzymes

promoting microbe destruction. In viral infection responses IFN-γ induces antiviral enzymes and increases intracellular killing through activation of phagocytes creating an anti-viral environment (Schroder et al. 2004).

Th1 cells also play a role in inflammatory responses to bacterial and viral infection in the gut. The effects of Th1 cells in intestinal inflammation have been studied in isolation in the adoptive transfer model of colitis. Naïve T-helper cells are transferred to $RAG^{-/-}$ mice that are lacking mature T and B-cell effectors due to a mutation in the recombination activating gene (Mombaerts et al. 1992). Naïve T-cells migrate to the intestines and induce colitis in acceptor mice. This model allows users to study the role of specific subsets of cells and their role in intestinal inflammation (Ostanin et al. 2009). Interestingly, anti-IFN-γ antibody treatment can prevent intestinal inflammation in these mice. Furthermore, transfer of naïve T-cells deficient in T-bet or STAT4, necessary for Th1 differentiation, fail to induce colitis in the adoptive transfer model. Despite this, other studies suggest that T-cell derived IFN-γ is not necessary for disease or that only early IFN-γ is necessary to initiate colitis in transfer mice (Shale et al. 2013). So it would seem that IFN-γ is necessary to induce inflammation in the intestine but the role of Th1 derived IFN-γ requires further investigation.

1.1.3.2 T-REGULATORY CELLS

T-effector cells undergo extensive expansion once activated, and induce their own autocrine feedback loop in the immune response that stabilises the phenotype while simultaneously inhibiting others. However, this response must be limited in some ways as a cascading inflammatory response would lead to auto inflammation or inflammatory disease without sufficient regulation. Sakaguchi *et al* (1985) showed that the deletion of a

specific subset of $CD5^{hi}$ T-cells led to a variety of autoimmune diseases in mice. In the study $CD5^{lo}$ cells were transferred alone into nude mice which developed autoimmune disease, the transfer of these cells along with $CD5^{hi}$ cells prevented disease suggesting a functional suppressing T-cell subset. This subset was later identified as a $CD4^+$ T cell subset (Powrie & Mason 1990), and subsequent studies characterised these cells as $CD4^+$ $CD25^+$ natural Treg cells (Sakaguchi et al. 1995; Takahashi et al. 1998; Thornton & Shevach 1998). These natural Treg cells differ from T-helper effector cells in that they were derived in the thymus and not from $CD4^+$ naïve pre-cursors in the periphery like Th1 and Th2 cells. Natural Treg cells regulate the immune response via migration to the site of infection and suppression of effector cells, particularly $CD4^+$ T-helper cell subsets. This is carried out via the secretion of anti-inflammatory cytokines including IL-10, and cell-cell contact inhibition. Recently Treg cells were shown to also be inducible from naïve $CD4^+$ T-cells via activation in the presence of TGF-β and further expansion by IL-2 (Curotto de Lafaille & Lafaille 2009). Natural Tregs (nTregs) and inducible Tregs (iTreg) are thought to co-operate in suppressing the immune response and the presence of iTregs greatly expands the antigenic diversity of the nTreg reponse and aids nTregs in immune regulation (Haribhai et al. 2011). The transcription factor FoxP3 has been identified as the master regulating gene in Treg cells (Fontenot et al. 2003). Fontenot *et al* (2003) demonstrated that mice with mutations in Foxp3 showed impaired development or dysregulated function of Treg cells resulting in severe autoimmune disease, inflammatory bowel syndrome and allergy. Furthermore, ectopic expression of Foxp3 conferred a Treg like suppressive phenotype in $CD4^+$ T-helper effector cells (Fontenot et al. 2003).

1.1.3.2 T-HELPER 17

The Th1/Th2 paradigm was studied in detail for over 10 years before a more complicated picture of $CD4^+$ T-cell phenotypes emerged. In the early 2000's, groups working on $CD4^+$ T-cells studied the effects of blocking IFN-γ and IL-12 function in mouse models of autoimmune disease such as experimental autoimmune encephalitis (EAE) and collagen induced arthritis in order to study the suggested role of Th1 cells linked with these disease models. Wild type and *Ifng* knockout mice developed autoimmune disease and demonstrated that the presence of IFN-γ was not crucial for development of EAE (Ferber et al. 1996). The blockade of IL-12 was investigated in detail by Becher *et al* (2002) as previous work involving anti-IL-12 antibodies had shown a crucial role for IL-12 and Th1 cells in EAE, but had targeted the IL-12p40 subunit of IL-12. IL-12 is a heterodimeric cytokine made up of IL-12p35 and a common IL-12p40 subunit that is shared with other cytokines. Interestingly *IL-12p40*$^{-/-}$ mice did not develop EAE, while in contrast *IL-12p35*$^{-/-}$ mice were highly susceptible to EAE. Neither the *p40*$^{-/-}$ or *p35*$^{-/-}$ mice were able to generate an IL-12p70 active heterodimer, therefore a cytokine other than IL-12 that used the IL-12p40 subunit was responsible for the induction of EAE. The authors suggested that the heterodimer IL-23, made up of IL-12p40 and IL-12p19 may be key (Becher et al. 2002). This was confirmed in a later study showing that mice lacking the IL-12p19 subunit were resistant to EAE. The same group went on to demonstrate that the mice lacking IL-23 were resistant to collagen induced arthritis in mice and notably, that there was a correlation with a drop in IL-17 producing $CD4^+$ T-cells suggesting a role for IL-23 in the generation of IL-17 producing $CD4^+$ T-cells and subsequent disease in this model (Murphy et al. 2003). In 2005 two independent groups then identified IL-17 producing $CD4^+$ T-helper

cells as a separate cell lineage from Th1 and Th2 cells (Harrington et al. 2005; H. Park et al. 2005). IL-23 was believed to be responsible for the generation of Th17 cells but was later shown to have no effect on naïve $CD4^+$ T-cells and thought to play a role in their maintenance (Aggarwal et al. 2003). Naïve $CD4^+$ T-cells were soon discovered to differentiate into Th17 cells when activated in the presence of IL-6 and TGF- β (Bettelli et al. 2006; Mangan et al. 2006; Veldhoen et al. 2006). The transcription factor RORγt was identified as the master regulator involved in the differentiation of Th17 cells from naïve $CD4^+$ T-helper cells (Ivanov et al. 2006). In this study, Litmans group demonstrated that IL-17 producing T-cells in the intestinal lamina propria were absent in RORγt deficient mice. Furthermore, they were unable to differentiate naïve RORγt deficient T-cells into Th17 cells upon activation in TGF-β and IL-6 *in vitro* (Ivanov et al. 2006). The same group later showed that IL-6 induced the Th17 differentiation pathway via its essential requirement for STAT3 activation. Furthermore, STAT3 led to the up-regulation of the IL-23R and IL-23 was later confirmed to be an essential signal required in Th17 cell lineage commitment and expansion (McGeachy et al. 2009). STAT3 activation also up-regulated the cytokine IL-21. IL-21 is a member of the IL-2 family of cytokines and although it is produced by Th1 and Th2 cells, it is predominantly produced by Th17 cells (Korn et al. 2009). IL-21 works synergistically with TGF-β to regulate IL-17 and the IL-23R via STAT3 initiating a feedback loop for Th17 development (Korn et al. 2007). This is of particular interest as Th1 and Th2 cells secrete IFN-γ and IL-4 respectively, each of which maintains the subset that they are secreted by in an autocrine fashion. IL-17 does not affect Th17 cells and therefore this role seems to be carried out by secretion of IL-21. The loss of IL-21 or its receptor results in a reduced number of Th17 cells *in vivo* and *in vitro* (Yamane

& Paul 2012). Although IL-21 has been shown to drive a Th17 response with TGF-β in the absence of IL-6 (Yang et al. 2008), IL-6 is the dominant inducer of Th17 cells and IL-21 may play a role in maintaining memory Th17 cells *in vivo* rather than being essential for differentiation (Korn et al. 2009). This is supported by the dispensable role that has been shown for IL-21 as mice deficient in IL-21 or the IL-21R are still able to drive a Th17 response *in vivo* (Sonderegger et al. 2008).

IL-1 cytokine signalling has also been identified as playing a crucial role in Th17 development *in vivo*. The IL-1receptor IL-1Rβ is up-regulated on the surface of activated Th17 cells and was dependant on STAT3 and RORγt signalling. Furthermore, *Il1r1*$^{-/-}$ mice failed to induce EAE in mice and disease was associated with a selective defect in Th17 cells (Chung et al. 2009). This study demonstrated the role of IL-1 in the differentiation of Th17 cells; however, IL-1 was shown to only function in the presence of IL-6. IL-6 was previously demonstrated to enhance $CD4^+$ T-cell responses to IL-1 and IL-23 and produce IL-21 (Yang et al. 2007; Zhou et al. 2007). Interestingly, activation in the presence of IL-6, IL-1β and IL-23 was sufficient to differentiate Th17 cells in the absence of exogenous TGF-β. However, TGF-β was not thought to be absent as it is produced by the T-cells and may be present in the serum. This work presented a model where low concentration of TGF-β in the presence of IL-1 and other cytokines could drive a Th17 response (Chung et al. 2009).

This would suggest that a three step model of differentiation of Th17 cells takes place in which TGF-β and IL-6 initiate the differentiation of Th17 cells through repression of Th1 and Th2 cells subsets, initiation of IL-21 production as well as IL-1R and IL-23R expression. Signalling via IL-21 induces a feedback mechanism that stabilises ROR-γt

expression and Th17 cell differentiation. Finally, IL-23 signalling then commits the Th17 cells and expands the cell population.

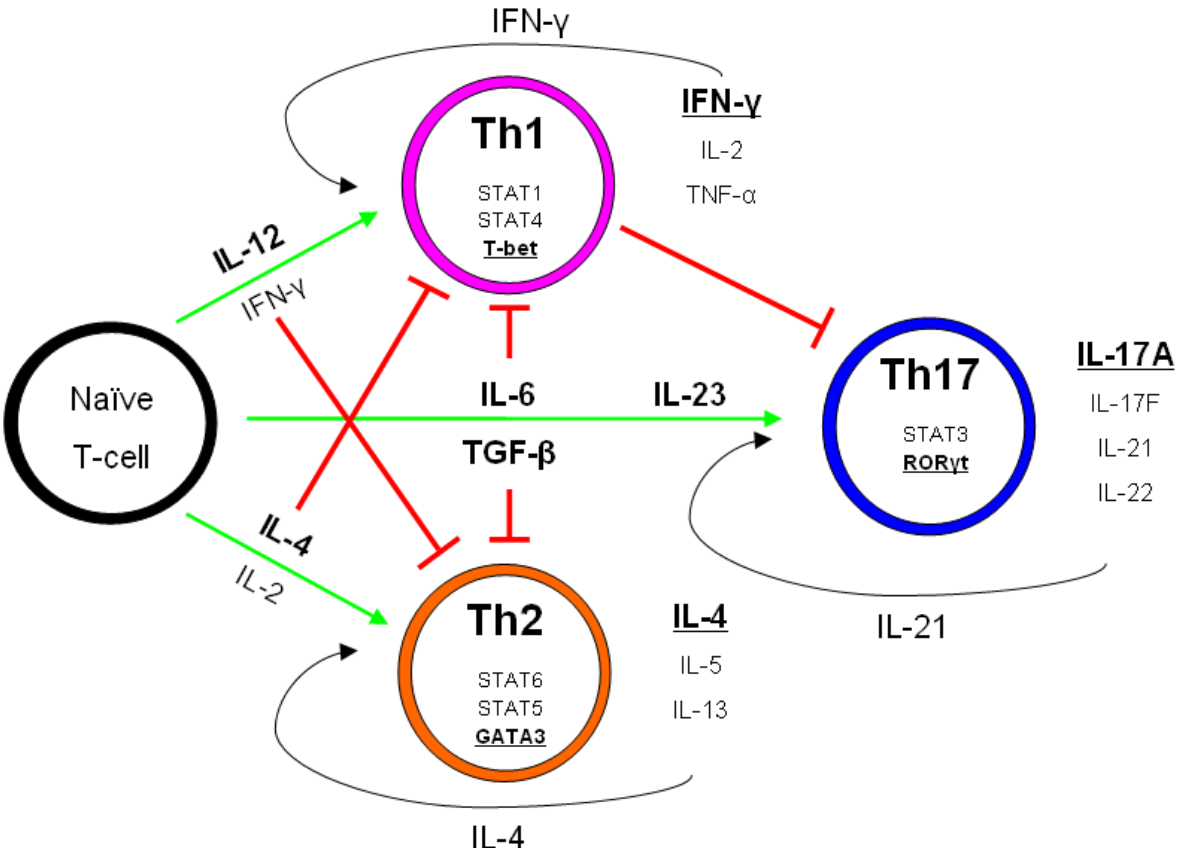

Figure 1.1 - Classical CD4$^+$ T-cell differentiation

1.1.3.2 Th17/Treg AXIS

TGF-β induces the differentiation of Th17 cells by suppressing T-bet and GATA-3 expression in cells allowing for IL-6/STAT3 activation and up-regulation of the master regulator RORγt. The balance of positive feedback loops and suppression of other T-cell effectors therefore is not reserved to the Th1 and Th2 subsets. In fact T-bet has been shown to inhibit RORγt expression and Th17 cell differentiation via runx1 mediated

transactivation (Lazarevic et al. 2011). The shared requirement of TGF-β for Treg and Th17 cells suggests that a balance is maintained between these pathogenic and regulatory subsets and that they share some early transcriptional programming before cell lineage commitment. In fact, recent studies tracing IL-17$^+$ cells in the gut revealed that at some point in their development some of these cells expressed Foxp3. Furthermore, non-Treg cells have been shown to transiently express Foxp3 (Barbi et al. 2013). Naïve CD4$^+$ T-cells stimulated in the presence of TGF-β without IL-6 will up-regulate Foxp3 and repress ROR-γt and IL-23R expression resulting in a Treg cell lineage commitment. However, TGF-β in the presence of IL-6 or IL-21 induces activation of STAT3 and expression of RORγt overcomes Foxp3 repression (Zhou et al. 2008). This leads to up-regulation of IL-23R expression and Th17 cell lineage commitment (Barbi et al. 2013). The balance of Tregs and Th17 cells seems dependant on the presence of IL-6 or other inflammatory cytokines in the presence of TGF-β. This model has been hypothesised to maintain the delicate balance in immune homeostasis and anti-pathogenic clearance of the gut, where the majority of Treg and Th17 cells reside at the mucosal barrier. When maintaining homeostasis, Treg development is favoured and these cells modulate and suppress the immune response. However, when APCs encounter microbial antigens and begin producing pro-inflammatory cytokines such as IL-6, they switch differentiation to favour a Th17 phenotype in order to clear the infection (Maynard et al. 2012)

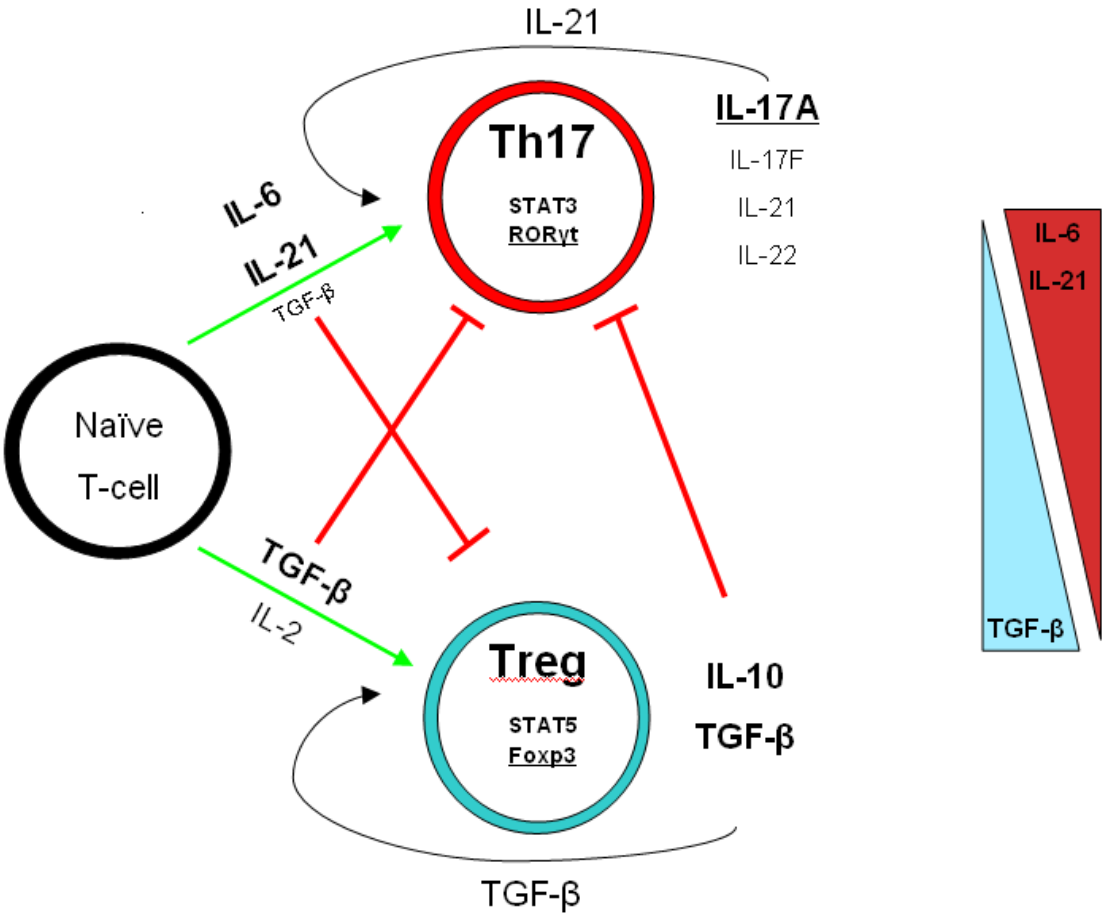

Figure 1.2 - Th17/Treg axis

1.1.3.4 Th17 RESPONSES IN INFLAMMATION AND DISEASE

The Th17 effector response initiates a recruitment and activation of large neutrophil populations. This response is required to clear extracellular pathogens and fungi. A requirement for Th17 cells is demonstrated in patients with Job's syndrome who have a mutation in *Stat3* leading to an inability to mount a Th17 response. Patients are susceptible to infections with *C. albicans* and *S. aureus* in the skin and lungs (Miossec et al. 2009). Prior to the discovery of the Th17 subset of $CD4^+$ T-helper cells, Th1 cells were thought to instigate the progression of autoimmune disease. However studies of mice deficient in

IFN-γ and IL-12 did not confer resistance to autoimmnity, in fact the mice were more susceptible to disease. The finding that the cytokine IL-23 is critical in inflammation and disease led to the discovery of Th17 cells in models of MS (EAE) and collagen induced arthritis clearly identifying crucial roles for Th17 cell in these diseases (H. Park et al. 2005). Th17 effector cells play an important role in immune regulation at mucosal surfaces. They are particularly important in the gut where the majority of Th17 cells develop and is evidenced by high levels of IL-23, IL-1β and IL-6 during gut inflammation (Shale et al. 2013). Furthermore, patients susceptible to inflammatory bowel disease (IBD) show sequence variants in the gene coding for the IL-23R signalling necessary to commit and expand Th17 cell responses (Duerr et al. 2006) The introduction of naïve isolated $CD4^{+}$ RB^{HI} T-cells into *Rag*$^{-/-}$ mice results in the migration of these cells to the gut and symptoms of IBD resulting from a Th17 driven response (Ostanin et al. 2009). The generation of Th17 cells in the gut is of particular importance as noted by the lack of Th17 cells in the intestines of germ-free mice. This is believed to be due to segmented filamentous bacteria (SFB) and their role in early development in Th17 cells. SFB induced DCs to produce IL-6 and IL-23 resulting in the accumulation of Th17 cells in the lamina propria of mice (Ivanov et al. 2009). This finding further supports the role that Th17 cells play in the homeostasis of the gut and balance with commensal bacteria and pathogens.

Indeed, the role of Th17 cells is further complicated by recent work suggesting a degree of plasticity in Th17 cells *in vivo*. The discovery that Th17 cells share a common early transcriptional programme with Tregs led to a study showing that naïve T-cells activated in the absence of TGF-β results in the generation of a pathogenic Th17 cell subset (Ghoreschi et al. 2010). In the case of EAE, an autoimmune mouse model of MS, IL-23 was shown to

be critical in the development of disease suggesting a primary role for Th17 cells. However, T-bet expression usually associated with Th1 cells is also critical in the development of EAE. Indeed, T-bet deficiency confers protection against a number of autoimmune diseases but a lack of IFN-γ infers an increased risk (Lee et al. 2012). This contradictory finding resulted in the authors describing a pathogenic T-cell subset that was generated in the absence of TGF-β and resulted in IFN-γ and IL-17 producing Th17 cells expressing both T-bet and RORγt (Ghoreschi et al. 2010). Therefore the disease is Th17 driven but the cells take on a pathogenic phenotype due to T-bet and IFN-γ expression *in vivo*. Although it is clear that these pathways are inhibitory of each other in development of a cell lineage, Th17 cells are able to undergo some plasticity after late commitment to the Th17 programme. IL-23 has been linked to the expression of T-bet in Th17 cells and T-bet is suggested to increase IL-23R expression in a proposed feed-forward loop (Gocke et al. 2007). These pathogenic IL-17/IFN-γ double producers (DP) are also implicated in colitis and an underlying reliance on the presence of IL-23. Further analysis of this pathogenic subset by the Kuchroo group has resulted in a mechanism of Th17 switching dependant on T-bet expression and increased IL-23 signalling leading to a pathogenic Th17 cell that does not produce IFN-γ (Lee et al. 2012). The pathogenicity of these cells is linked to an increase in IL-23R expression and increased levels of GM-CSF production. GM-CSF as been described as a key cytokine in Th17 mediated disease and GM-CSF deficient mice are protected against EAE (Lee et al. 2012). Furthermore the key cytokine inducing this pathogenic switching of Th17 cells was identified as TGF-β3 which the cells are induced to produce and drives this cell type. Cells induced with TGF-β3 were potent inducers in EAE and the adoptive transfer model of colitis (Lee et al. 2012).

This pathogenic ability of Th17 cells in disease is not only regulated by the Treg cell population but may also be balanced by the discovery of IL-10 secreting Th17 populations activated in the presence of TGF-β and undergoing constant antigenic stimulation. The gene for IL-10 is programmed in the transition to late phase (t=20hrs) in T-cells when stimulated with IL-6 and TGF-β (Yosef et al. 2013). Secretion of IL-10 by Th17 cells may be a mechanism of self inhibition and regulatory control orchestrated by the suppressive effects of IL-10. The suppressive regulatory role played by IL-10 is demonstrated in *Il-10*$^{-/-}$ mice which develop severe colitis (Rennick et al. 1997). A number of studies have now identified IL-17^{+} IL-10^{+} Th17 cells as non-pathogenic Th17 cell and IL-23 would seem to be the driving factor in pathological Th17 cell development by down-regulating IL-10 (McGeachy et al. 2007). It is possible that Th17 cells switch their phenotype in a system that allows the Th17 cells another level of adaptive immunity catering for specific infections, existing within populations of generated Th17 cells. Indeed Th17 cells have been shown to switch their secretion patterns depending on the nature of an infection. Th17 cells generated in mice infected with *Candida albicans* produce IL-17 and IFN-γ as described above. However CD4^{+} Th17 cells from mice infected with *Staphylococcus aureus* are IL-17 and IL-10 producing cells (Shale et al. 2013). It is clear that Th17 cells play a vital role in clearance and homeostasis and also contribute to autoimmune disease due to their inherent plasticity and regulatory role in the gut. Interestingly this switch to a self limiting IL-10 producing subset is not limited to Th17 cells and Th1 cells have also been shown to produce late IL-10 via STAT4 activation and high antigen dose (Saraiva et al. 2009). Clearly these self limiting mechanisms play a crucial role in regulating the pathogenic response of T-helper effector cells. Although the conventional model of T-

helper subset characterisation of STATs and master regulators clearly defines the early transcriptional commitment of these cells to their unique cytokine secretion profiles, more research is required to establish the complex networks involved in T-cell differentiation and plasticity over the lifetime of the subset (Vahedi et al. 2013). Th17 cells in particular seem to display a unique ability to adapt to the cytokine environment and change phenotype necessary to maintain gut homeostasis or clear infection. The balance of this response is clearly critical in the development of inflammatory disease and autoimmunity.

1.1.3.4 OTHER EMERGING T-HELPER SUBSETS

The discovery of Th17 cells lead to two more subsets of $CD4^+$ T-cells being proposed based on their unique cytokine profiles. The Th9 subset of cells is driven from naïve $CD4^+$ cells activated in the presence of TGF-β and IL-4. The identification of the transcription factor PU-1 as the gene necessary for the development of these cells has established them as an independent IL-9 producing subset of T-cells involved in inflammatory responses in the lung (Chang et al. 2010). IL-22 is produced by Th17 cells and has been linked to skin homeostasis and inflammation through its interaction with epithelial cells and keratinocytes. A subset of IL-22 producing Th22 cells were described by three independent labs when activated with IL-6 and TNFα by plasmacytoid DCs (Eyerich et al. 2009; Duhen et al. 2009; Trifari et al. 2009) These cells expressed skin homing receptors and were found in the skin of psoriasis patients indicating a role in skin inflammation (Tian et al. 2013). Although no transcription factor has been identified in the generation of this subset of cells, a genomic transcriptome analysis revealed an up-regulation of Foxo4 and BCN2 in Th22 clones isolated from Th22 patients (Jiang & Dong 2013). Another T-cell subset that is currently seeing a renewed interest is the follicular T-helper subset (Tfh).

These cells are involved in B-cell help and aid antibody production. They are found in the B-cell follicles of secondary lymphoid organs and help B-cells induce germinal centre formation (MacLennan 1994). The recent discovery of the transcription repressor B-cell lymphoma 6 (Bcl-6) as a master regulator following activation of naïve cells in the presence of IL-6 and IL-21 has led to the conclusion that these cells represent an individual T-cell subset. Dysregulated Tfh cell responses lead to autoimmune conditions characterised by production of auto-antigenic antibodies, while deficiencies result in an impaired humoral response to infection (Ma et al. 2012).

1.1.4 PROTEIN TRAFFICKING

Clearly the role of immune mediated cytokine release is essential and tailored to specific infections *in vivo,* creating environments adapted to enhance and regulate clearance. Protein trafficking is particularly important in immune cells that release immune mediators such as cytokines, chemokines and lysosomal enzymes. This trafficking is highly regulated in order to prevent dysregulation, autoimmunity and inflammation and a number of mutations or deficiencies resulting in dysregulated trafficking can have major implications in immune syndromes (Stow et al. 2006).

Depending on the required function of an immune mediator, different pathways exist to transport newly synthesised proteins out of the cell. These pathways are usually shared by a number of factors and their release can be constant (constitutive release) or triggered (regulated release). The pathway through which the mediators are released is dependant on their function and both of these pathways are mediated by vesicular traffic and regulation (Benado et al. 2009).

Proteins produced in the endoplasmic reticulum (ER) can be soluble and contained within vesicles or membrane bound and associated within the plasma membrane of transported vesicles, thus a number of proteins share transport to the plasma membrane to conserve energy (Benado et al. 2009). The release of these proteins can be basal or dependant on their transcription at gene level in response to cellular signalling as discussed in detail above. Proteins are transported from the ER through the cisternae of the golgi and trans-golgi network (TGN) where they may undergo post-translational modifications (Jolly & Sattentau 2007). Finally proteins are sorted and packaged into a vesicle for transport to the cell surface for release via a number of pathways, or incorporated into the plasma membrane of the cell. These pathways are varied and include the use of recycling endosomes that traffic protein to and from the plasma membrane (Murray, Kay, et al. 2005; Hsu & Prekeris 2010).

Regulated release of proteins from cells is inherently conserved in specialised cells such as neurons and secretory cells of the immune system. Immune cells, particularly granulocytes such as mast cells, NK cells, CTLs and endothelial cells are capable of secreting large amounts of cytokine and immune mediators to a specific site on a cell in a rapid response to a specific signal. Proteins can be processed and stored in granules called lysosome-related organelles (LSO) within the cell and held under the control of secretory mechanisms awaiting stimulus coupled rapid release for quick response to injury or indeed cell death signals inducing lytic release from CTL or NK cells (Benado et al. 2009).

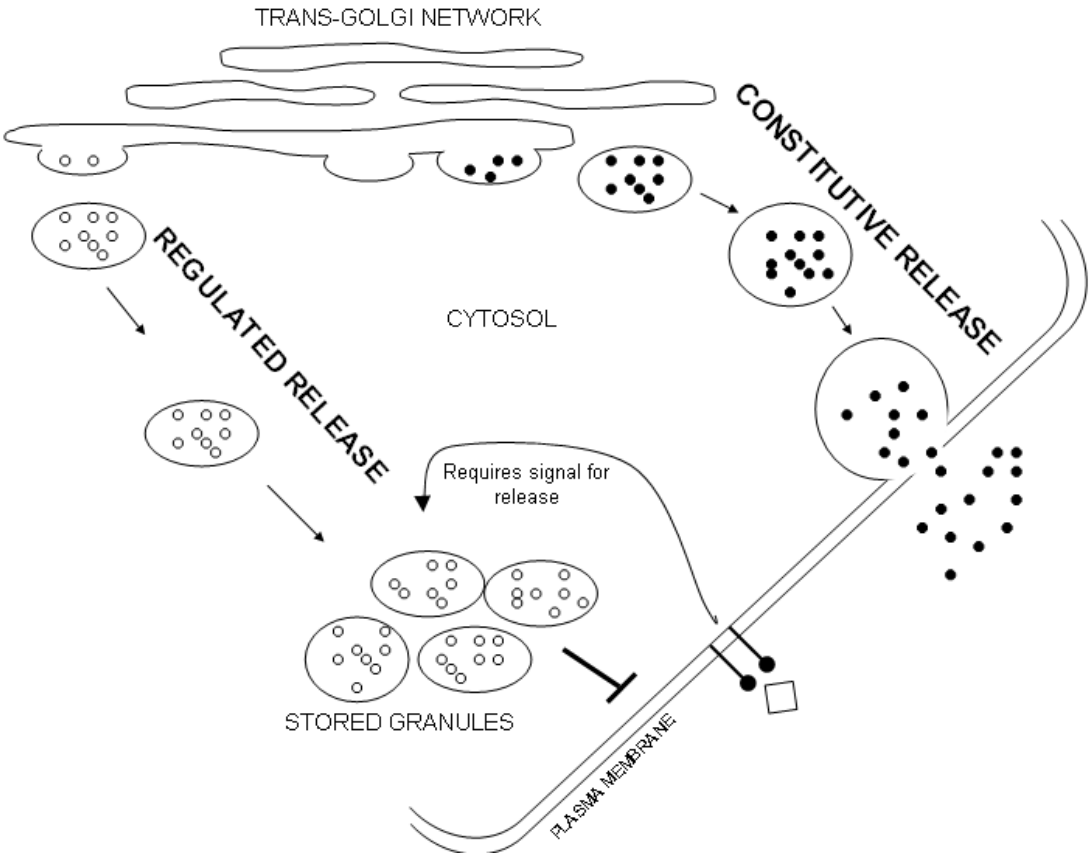

Figure 1.3 - Regulated and constitutive release of cytokines

1.1.5 SNARE PROTEINS

The transport of vesicles between organelles, endosomes and the cell surface plasma membrane is controlled by a complex network of cellular machinery such as membrane associated proteins, lipids and cytoplasmic proteins. The budding and fusion of vesicular carriers is carried out by multi-protein complexes and one family of proteins in particular facilitates the specific fusion of vesicles at target membranes in order to deliver cargo and additional lipids (Malsam et al. 2008). Soluble-N-ethylmaleimide–sensitive factor accessory protein receptor proteins (SNAREs) are a large conserved family identified in the

docking/fusion machinery that allow membranes to overcome opposing forces and fuse docked lipid bilayers (Jahn & Scheller 2006).

1.1.5.1 SNARE STRUCTURE

There are currently 38 known mammalian members of the SNARE family of proteins and they are all identified by a common conserved SNARE motif of 60-70 amino acids arranged in heptad repeats typical for coiled coils (Stow & Murray 2013). Most SNAREs are type II integral membrane proteins that possess a single trans-membrane domain at their carboxy (C-terminal) end that is connected to the SNARE motif by a flexible linker, with the majority of the protein extending into the cytoplasm (Sutton et al. 1998). Some SNAREs lack a trans-membrane domain and attach to membranes by post-translational acyl modifications such as palmitoylation. The SNAP-25 family of SNAREs, including the immune cell enriched variant SNAP-23, express a C-terminal cysteine rich domain ideal for palmitoylation. This process covalently attaches fatty acid groups increasing hydrophobicity and membrane binding potential (Greaves et al. 2010). Similarly, the SNARE STX11 also lacks a transmembrane domain. However, although STX11 also expresses a cysteine rich domain, mutations at this site have shown that it may not be necessary for membrane binding and in fact STX11 may associate with the membrane by binding cognate SNARE complexes (Prekeris et al. 2000)

The conserved coiled-coil SNARE motif is necessary for complex formation and membrane fusion. A SNARE complex crystal structure was solved during the process of exocytosis and revealed the formation of a coiled-coiled four α-helical structure between SNARE proteins on opposing membranes. All four helices arrange themselves so that their C-termini are at the anchor end of the complex leaving the rest of the protein available for

two-helix interactions (Sutton et al. 1998). Vesicle and target membrane contribute helices that are embedded in the lipid bilayer in order to facilitate binding and fusion (Poirier et al. 1998). The complex that is formed is highly thermostable resisting temperatures up to 90^{o}C and resisting the denaturing effects of sodium dodecyl sulphite (SDS). This extremely stable structure indicates that SNARE assembly is associated with a major release of energy (Fasshauer et al. 1998).

When SNARES form in a tight helical bundle they form a conserved structure of an elongated coiled coil of four intertwined α-helices that correspond to the four interacting SNARE motifs occupying specific positions in the complex. There is a highly conserved layer of interacting amino acids in the central hydrophobic core of the helical bundle consisting of three glutamines and one arginine. Each of these contributing motifs contributes an amino acid and their structures are divided into sub-families used to classify the SNARES as R-SNAREs or Q-SNARES.

R-SNARES are usually found on the membrane and have arginine (R) as the central functional residue in the SNARE motif. Q-SNARES are mainly found on the target membrane and are defined by a central glutamine (Q) residue. In order to form a complex and mediate membrane fusion, one R-SNARE and two or three Q-SNARE motifs are required to form a stable RQabc four helical bundle (Bock et al. 2001; Jahn & Scheller 2006).

The N-terminal of SNARE family members is less conserved than the SNARE motif and led to the Q-SNARE family being further divided into three sub-families Qa, Qb and Qc. All the Qa family members but only a portion of Qb and Qc members have an anti-parallel three-helix that varies in length and is connected to the SNARE motif at the N-terminus

and is called the Habc bundle (Jahn & Scheller 2006). The Habc bundle interacts with the C-terminus and forms a closed conformational state in the SNARE preventing complex formation. The role of this change in conformational state is regulatory and may act as a recruitment platform for accessory proteins involved in complex formation (Jahn & Scheller 2006). The R-SNARE family currently consists of seven proteins, all of which are vesicle associated membrane proteins (VAMPs). The N-terminal domains of R-SNARES contain conserved profilin like folds called longin domains (Krzewski et al. 2011).

1.1.5.2 SNARE FUNCTION

The fusion of membranes requires four SNARE motifs with at least one of these present on an opposing membrane. The SNARE proteins interact to form the α-helix bundle that "zippers" together from the N-terminus to the C-terminus forming a trans-SNARE complex (or SNAREpin). SNAREs are thought to act as catalysts in membrane fusion through this complex assembly which exerts mechanical forces on the complex that is then transferred to the membranes. The energy provided by the zippering complex formation pulls the membranes together displacing the water and hydrostatic pressure keeping them apart, thereby facilitating the mixing of hydrophobic lipids (Jahn & Scheller 2006). Once the membranes have fused, the trans-SNARE conformation is converted to a highly stable inert cis-SNARE conformation on the resulting fused membrane. In order to dissociate this stable structure metabolic energy is required and this is provided by two chaperone proteins; N-ethylmaleimide-sensitive factor (NSF) and Soluble NSF attachment protein (SNAP) (Block & Rothman 1992; Clary & Rothman 1992). It was the studies that identified these chaperone proteins as part of a complex necessary for efficient intracellular

transport that lead to the discovery of SNARE proteins. The complex consists of NSF, SNAP and the cis-SNARE conformation resulting in a 20s particle structure (Hohl et al. 1998). NSF provides the energy required for disassembly, it is a member of the AAA+-protein family that have been shown to function in unfolding proteins and aggregates (Jahn & Scheller 2006). NSF is unable to bind without SNAP which binds to the surface of the SNARE proteins, a number of ATP-hydrolysis events then leads to the dissociation of the SNARE complex (Hohl et al. 1998). This dissociation facilitates the recycling of SNARE proteins and prevents accumulation of SNAREs on the membrane. Blocking NSF in cells *in vivo* has been shown to lead to accumulation of SNARES in membranes and cell death (Littleton et al. 2001). The result of this disassembly is energy rich largely unfolded SNAREs that are available for repeated use in subsequent membrane fusion events (Malsam et al. 2008).

The recycling of SNAREs transports them back to a specific location in the cell in which the SNARE operates. They are carried on membranes and returned to their intracellular membrane where they function. Most SNAREs function with specific partners although some SNAREs are more promiscuous and function in a number of complexes, and there is also a level of redundancy in SNARE partnerships with other SNAREs substituting in a less efficient fusion reaction (Hohenstein & Roche 2001). Many SNAREs operate predominantly in a specific subcellular compartment with their partners and some Qa SNAREs such as syntaxin 2 and syntaxin 4 are found on the plasma membrane and involved in fusion of vesicles and secretion of their contents from the cell. Other Qa SNAREs including syntaxin 5 and the R-SNARE VAMP4 are localised in the golgi apparatus (Hong 2005). These SNAREs are therefore found in the membranes of the donor

compartment, acceptor compartment and the intermediate trafficking vesicles (Jahn & Scheller 2006).

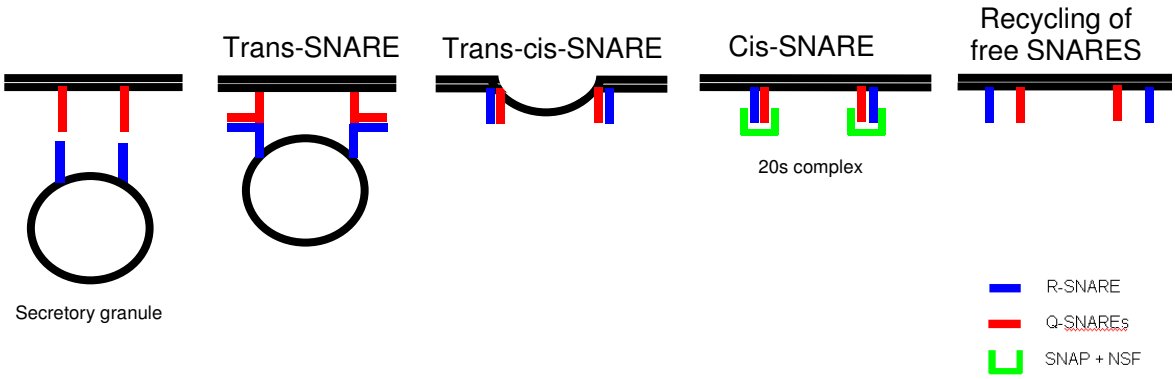

Figure 1.4 – Functional SNARE cycle

1.1.6 SNARE PROTEINS IN IMMUNE CELLS

The specific locations and partnerships in which SNAREs operate means that studies defining the localisation of SNAREs and the proteins that they transport have led to the mapping of intracellular pathways in cells. As previously discussed, some specialised cells of the immune system can store cytokines and immune mediators in pre-formed granules within cells primed for release via specific cell receptor signalling These include cells of the innate immune system; neutrophils, mast cells, eosinophils, NK cells and the $CD8^+$ CTLs of the adaptive immune response (Abraham & St John 2010; Melo et al. 2008; Borregaard et al. 2007; de Saint Basile et al. 2010).

1.1.6.1 NEUTROPHILS

Neutrophils make up the majority of circulating leukocytes and can rapidly enter tissue from the capillaries via the secretion of extravasating factors during inflammation.

Neutrophils secrete four different types of granules and vesicles from the cell containing a large number of cytokines as well as surface receptors and adhesion proteins that promote extravasation. These include primary (azurophilic), secondary (specific), and gelitinase (tertiary) granules and a pool of small secretory vesicles (Häger et al. 2010). SNARE proteins and complexes have been described in the secretion of each of these populations however, specific mechanisms associated with cytokine release have not been reported therefore the data so far is implied but not directly demonstrated (Stanley & Lacy 2010). To date the SNARE complex of VAMP2-SNAP23-STX4 has been implicated in the release of secondary and gelitinase granule contents (Mollinedo et al. 2003; Martín-Martín et al. 2000). Another study indicated that VAMP1, VAMP2, and SNAP23 complexes were involved in the release of specific and gelitinase granules while VAMP1 and VAMP7 are mainly involved in the release of contents from azurophilic granules and most likely partners again with SNAP23 and STX4 at the surface (Mollinedo et al. 2006).

Recently D'Orlando *et al* (2013) showed impaired degranulation from activated neutrophils isolated from STX11 deficient mice, suggesting a critical requirement for STX11 in this process. However the mechanism or binding partners of this regulated release have not been established (D'Orlando et al. 2013).

1.1.6.2 MAST CELLS

Mast cells are tissue resident granulocytes secreting a large amount of cytokines, chemokines and growth factors via large granule and smaller secretory vesicle release that regulate wound healing and innate immunity. The release of secretory granules is triggered by stimulation of mast cells by aggregated IgE through the FcεRI receptor and this has

served as a model for studying granule release from mast cells and mast cell lines (Lorentz et al. 2012).

To date a number of SNAREs have been reported in mast cells including; SNAP23, the Qa SNAREs STX2, 3 and 4, and the VAMP family SNARES 2, 3, 4, 7 and 8 (Lorentz et al. 2012). SNAP23 and STX4 complex formation is again important for fusion at the cell surface. Antibody inhibition of SNAP23 inhibited the release of granules from mast cells while in a separate study, the over expression of SNAP23 enhanced cell excytosis. Both studies show that upon activation, SNAP23 relocated to the cell surface to facilitate degranulation and secretion (Guo et al. 1998; Vaidyanathan et al. 2001). Similarly, siRNA knockdown of STX4 and over expression of STX4 but not STX2 or STX3 led to inhibited degranulation response in mast cells. STX4 was also shown to localise at the membrane with SNAP23 following IgE induced activation of mast cells (Paumet et al. 2000; Woska & Gillespie 2011).

A role for VAMP8 was investigated using cells from VAMP8 deficient mice. This study revealed that the granule mediated release of histamine and β-hexosaminidase was reduced upon stimulation, but release of TNF, CCL2, IL-6 and IL-4 was not affected suggesting that VAMP8 is involved in pre-formed mediator secretion in mast cells. This was further confirmed by the finding that VAMP8 deficient mice had diminished passive systemic anaphylaxis responses *in vivo* (Tiwari et al. 2008)

Although a large arsenal of cytokines are released via degranulation from mast cells, some cytokines are transcribed and secreted via constitutive pathways following activation. TNF has been shown to be up-regulated and expressed 1-2 hrs following degranulation of mast cells, and a study by Tiwari *et al* (2008) suggested that this is trafficked through VAMP3

mediated membrane fusion. Similarly IL-6 is also newly synthesised and is not secreted via degranulation pathways, although the specific trafficking pathway has yet to be elucidated (Kandere-Grzybowska et al. 2003; Stow & Murray 2013). Mast cells have been shown to make use of a secretion mechanism called piecemeal degranulation to constitutively secrete cytokines. In this process small secretory vesicles bud from the larger secretory granules and then transport cytokines to the cell surface for release independently from the granules (Lacy & Stow 2011). Similar to neutrophils, there is little in the literature describing constitutive release mechanisms from mast cells, more work is needed to map the secretory pathways of cytokines and mediators from these cells (Lorentz et al. 2012) .

1.1.6.2 NATURAL KILLER CELLS

Natural killer (NK) cells perform a similar function to $CD8^+$ CTLs and kill virally infected or tumorigenetic target cells through cytotoxic release of lytic granules (Stinchcombe & Griffiths 2007). In a similar fashion to the mast cells, cytokines can be secreted from NK cells via degranulation or alternative vesicle secreting pathways. Lytic granules in NK and CTL cells are targeted to the immunological synapse, the point at which the cell interacts with a target cell. The lytic granules are released in a specific direction at the synapse to isolate effects to the target cell; however cytokine release from NK cells is multidirectional (Reefman et al. 2010) . NK cells secrete TNF and IFN-γ in this manner and are believed to share the pathway of exocytosis as vesicles leaving the golgi have been shown to contain both cytokines (Reefman et al. 2010). Although it is not known if TNF and IFN-γ leave the cell via the same mechanism, there is evidence to suggest that both VAMP7 and STX11

may be involved. However, more research is required to elucidate these pathways and the specific roles of these SNARE proteins (Krzewski et al. 2011; D'Orlando et al. 2013).

1.1.6 SNARE PROTEINS IN TNF-α TRAFFICKING FROM MACROPHAGES

The most understood and studied pathway for constitutive cytokine secretion in immune cells is the exocytosis of TNF from macrophages. Upon activation by invading pathogens via toll like receptors or cytokine stimulation, cells of the immune system upregulate protein trafficking and secrete large amounts of protein under regulated mechanisms. TNF in particular is secreted rapidly upon macrophage activation and can be detected within 10mins post activation (Shurety et al. 2000). TNF is somewhat unique in that it is synthesised as a pre-formed transmembrane cytokine that requires post translational modification via proteolytic cleavage by TNF-α converting enzyme (TACE) thereby releasing TNF outside the cell (Moss et al. 1997). The inhibition of TACE in macrophages has allowed for detailed imaging and tracking experiments on the constitutive release of TNF-α from macrophages and led to detailed mapping of its secretion pathway. Initially the Qa-SNARE syntaxin 4 (STX4), located on the plasma membrane in eukaryotic cells, was shown to increase in expression in response to LPS activation in macrophages, indicating that SNARE expression is regulated in response to increased trafficking in these cells (Pagan et al. 2003). Pagan *et al* (2003) further showed the requirement for STX4 at the cell surface by expressing a mutant form of STX4 in the macrophage cells that blocked delivery of TNF to the cell surface indicating a rate limiting step and requirement for specific SNAREs in exocytosis. In a similar approach, Stow and colleagues showed that a SNARE complex consisting of STX6-STX7-Vti1b (vesicle transport through interaction

with t-SNAREs homologue 1b) was up-regulated and facilitates transport of TNF from the trans-golgi network (TGN) (Murray, Wylie, et al. 2005). VAMP3 was later identified as the required associated R-SNARE in both of these fusion events, and interestingly was localised on the recycling endosomes suggesting a novel two-step pathway for secretion of TNF from the macrophage (Murray, Kay, et al. 2005). TNF is transported from the TGN to recycling endosomes via membrane fusion facilitated by a SNARE complex of STX6-STX7-Vti1b-VAMP3. This recycling endosome then moves to the surface where the VAMP3 on the vesicle interacts with STX4 and SNAP23 at the surface. SNAP23 contributes two SNARE motifs to the complex resulting in a full trans SNARE bundle and membrane fusion (Murray, Kay, et al. 2005; Stow et al. 2006). The relevance of the TNF being secreted through the recycling endosomes was later shown to be related to the contribution of membrane from the recycling endosomes to the plasma membrane to facilitate phagocytosis carried out by the cell. TNF-α secretion is therefore explicitly linked to phagocytosis and VAMP3 was shown to be necessary for efficient phagocytosis (Stow et al. 2006).

1.1.6 SNARE PROTEINS IN T-CELLS

Tools such as TACE inhibitors to block TNF secretion, siRNA inhibition, transfection and triggered granule release mechanisms have all proved to be valuable tools in the elucidation of mechanisms and SNARE complexes playing a role in innate immune cell exocytosis. However, little work is published on T-cells which have proved more difficult to work with, for instance naïve T-cells cannot be transfected effectively *in vitro* by traditional methods without changing their phenotype and function. This has resulted in new methods

of gene inhibition being developed which may lead to more in depth studies on SNARE trafficking in T-cells (Yosef et al. 2013).

T-cell cell lines are limited in their functionality and studies to date have mainly focused on formation and trafficking at the immunological synapse (the point at which the cell interacts with an APC or target cell) using human leukemia Jurkat T-cells (Das et al. 2004). These studies have identified SNAREs and their location within the cells indicating potential roles in secretion. For example, SNAP23 and STX4 have been identified on the surface of Jurkat T-cells clustered at the immunological synapse (Das et al. 2004). These SNAREs have been identified as receptor SNAREs for degranulation and vesicle fusing in neutrophils (Mollinedo et al. 2003; Martín-Martín et al. 2000) and mast cells (Paumet et al. 2000; Woska & Gillespie 2011) and may play a similar role in T-cells.

$CD8^+$ CTL cells are capable of secreting cytokines via regulated lytic granule or constitutive vesicle release in a similar fashion to the innate granulocytes. VAMP8 has been implicated in the secretion of lytic granules at the plasma membrane of CTLs. Cells from VAMP8 deficient mice showed reduced efficiency in the secretion of lytic granules although the contents of the granules were unaffected when compared to the wild type controls (Loo et al. 2009). A similar role for VAMP8 was shown in mast cells (Tiwari et al. 2008). However, degranulation was reduced and not lost in these cells suggesting some redundancy in this pathway.

Similarly, Vti1b has been shown to mediate lytic granule docking and release at the immunological synapse. Vti1b was up-regulated at the transcriptional level in CTLs and lytic granules release was impaired in CTL cells from Vti1b deficient mice (Dressel et al. 2010; Qu et al. 2011).

Another SNARE shown to be crucial for lytic granule release and cytotoxicity in CTLs is STX11. Cells from STX11 deficient mice showed impaired degranulation when compared to cell from wild type mice. Interestingly, constitutive cytokine secretion of TNF and IFN-γ was also affected by the deficiency in STX11 suggesting a possible role for STX11 in lytic granule and constitutive cytokine release pathways (D'Orlando et al. 2013).

Recently a detailed study of SNARE expression and localisation in human CTLs was published by Pattu *et al* (2012). In this study the authors looked at a panel of SNAREs and co localised them with lytic granules in the cell and the immune synapse to try and identify SNAREs involved in exocytosis in these cells. This study showed the co-localisation of STX8 and STX16 with lytic granules at the immunological synapse as well as Vti1b which has been previously described (Pattu et al. 2012).

Interestingly STX11 was localised at the immunological synapse, but despite its crucial role in lytic granule release, it was not co-localised with these structures suggesting an alternative function for STX11 prior to membrane fusion at the cell surface (Pattu et al. 2012).

There is limited research on the expression, regulation and function of SNAREs in $CD4^+$ T-cells. In a study by Huse *et al* (2006), $CD4^+$ Th1 like cells were derived from Th blasts from transgenic mice recognising a peptide of moth cytochrome c amino acids (MCC). Using these cells they identified two distinct directions for cytokine secretion in T-cells; synaptic and multi-directional, each co-localising with different pools of trafficking proteins during exocytosis (Huse et al. 2006). The cytokines IL-2, IL-10 and IFN-γ were all secreted at the immunological synapse and co-localised with Vti1b, Rab3d and Rab19. Rab GTPases are a family of trafficking proteins involved in compartmental identity (Zerial

& McBride 2001). Conversely, TNF, IL-4 and the chemokine MIP-1α was secreted in a multi-directional fashion and co-localised with Vti1b and STX6. Each group of cytokines was also shown to co-localise with each other indicating that they share the secretion pathways. A model of synaptic and multi-directional release allows a further level of control for T-cells to either influence the APC directly to modulate its response, or to secrete cytokines into the environment surrounding the cell and influence the cytokine milieu in response to a pathogen and recruit other cells to the site of inflammation. There is evidence that the secretion of cytokines on these pathways is temporal and may be dependant on the requirements of the cells depending on the need to secrete at the synapse or in a multi-direction (Huse et al. 2006). The steps to commitment and regulation of these pathways are unknown. Furthermore, despite the identification of two differentially regulated pathways for secretion, the specific role of SNARE proteins in these pathways remains to be elucidated (Huse et al. 2008). It is possible that SNAP23 and STX4 play a role in cytokine release from $CD4^+$ T-cells evidenced by their identification on the surface of jurkat T-cells (Das et al. 2004). Evidence from other immune cells suggest that these SNAREs may play a role in vesicle secretion at the immunological synapse, however the lack of SNAP23 in CTLs suggests that there are difference between T-cell phenotypes. VAMP3 was also identified as the cognate R-SNARE on the vesicles at the membrane (Das et al. 2004). A two directional pathway of secretion suggests a viable model for trafficking groups of cytokines through a limited number of potential pathways to save cell energy. However, the temporal nature of the directional secretion, the polarisation of naïve cells into specific phenotypes and the plasticity of committed $CD4^+$ T-cells suggest a more complicated level of regulation involving trafficking proteins and SNAREs.

1.1.7 PROJECT RATIONALE AND HYPOTHESIS

It is well established that $CD4^+$ T-helper cells are vital in the adaptive immune response and clearance of persistent pathogens. Individual subsets are generated in response to signals from APCs that drive highly regulated, targeted T-helper cell subsets. Dysregulation of this process can lead to inflammation and autoimmune disease. Individual T-helper subsets release a distinct profile of cytokines that play role in homeostasis and disease mediated by autocrine and endocrine cytokine signalling (J. Zhu et al. 2010). The profile of cytokines secreted is controlled at the transcriptional level depending on early cytokine signals and cell programming; however there is strong evidence that T-helper cells show considerable plasticity in late stages of differentiation, suggesting a number of complex regulatory pathways are involved (Vahedi et al. 2013; Bluestone et al. 2009)

The release of cytokines from cells is facilitated by highly regulated SNARE proteins. SNAREs have been shown to form specific partnerships and facilitate membrane-membrane fusion required for excytosis of cytokines and other proteins from immune cells (Stow et al. 2006). These specific SNARE partnerships may have a regulatory function in the cell providing another layer of control in the secretion of cytokines which can have such a profound effect on immune responses and inflammatory disease. Therefore defining a role for SNAREs in these T-helper cells may uncover new therapeutic targets in such diseases.

At present we have little understanding about the SNARE proteins that regulate the secretion of cytokines. Defining which SNAREs regulate release of cytokines such as IFNγ and IL-17 may help us better understand these complex trafficking pathways. T-helper

cells are capable of producing a number of cytokines depending on their stimulation and subset differentiation. A number of regulatory steps must therefore control the secretion of one cytokine but not another in a specific subset. Given that T-cells are capable of secreting both IFN-γ and IL-17, we investigated the SNARE expression in early regulatory steps leading to either IFN-γ production, or IL-17 production in Th1 and Th17 cells respectively. Using a combination of recombinant cytokines and neutralising antibodies, it is possible to polarise isolated $CD4^+$ T-cells into T-helper cell subsets *in vitro* in order to study their regulation. Once candidate SNAREs were identified using this model, they were investigated *in vivo* using mouse models of inflammation in order to confirm a regulatory role for SNAREs in T-helper mediated disease.

The identification of trafficking pathways may present potential therapeutic targets for blocking cytokine secretion from targeted cell types and control inflammation. It may also lead to a better understanding of SNARE deficient disorders such as familial haemophagocytic lymphohistocytosis - 4 (FHL-4), characterised by over production of cytokines and high numbers of activated lymphocytes due to STX11 deficiency. To our knowledge there are currently no published data identifying SNARE proteins that play a direct role in the secretion of specific cytokines from $CD4^+$ T-cells.

1.1.8 PROJECT AIMS

- Establish a model of $CD4^+$ T-helper cell isolation and differentiation
- Characterise the T-cell subsets and their cytokine secretion profiles
- Identify SNARE candidates involved in secretion of key cytokines from T-helper subsets
- Investigate candidate SNAREs in *in vivo* models of inflammation
- Elucidate a role for candidate SNAREs in T helper cell cytokine regulation using a specific knockout model deficient in a candidate SNARE

CHAPTER 2

MATERIALS AND METHODS

2.1 – MATERIALS

CELL CULTURE MATERIALS

Material	Source
Fetal Calf Serum	Gibco
Penicillin Streptomycin/Glutamine	Gibco
RPMI-1640	Gibco
DPBS	Gibco
Beta-mercaptoethanol	Sigma-Aldrich
6, 24, 96 well tissue culture plates	Sarstedt
Trypan Blue (0.4% w/v)	Sigma-Aldrich

TABLE 2.1 CELL CULTURE MATERIALS: All tissue culture materials/reagents used and corresponding sources.

T-CELL DIFFERENTIATION REAGENTS

Material	Source
rmIL-1b	R&D systems
rmIL-2	R&D systems
rmIL-4	R&D systems
rmIL-6	R&D systems
rmIL-12	R&D systems
rmIL-23	R&D systems
rmIFN-γ	R&D systems
rhTGF-β	BioLegend
Anti-mouse IL-4 neutralising antibody	R&D systems
Anti-mouse IFN-γ neutralising antibody	R&D systems
Anti-mouse CD3 monoclonal antibody	BD
Anti-mouse CD28 monoclonal antibody	BD

TABLE 2.2 DIFFERENTIATING CYTOKINES AND ANTIBODIES: All differentiating reagents used and corresponding sources.

ELISA REAGENTS

Material	Source
96-well microtitre plate	Nunc
3,3',5,5'-tetramethyl-benzidine (TMB)	R&D systems
Tween 20	Sigma-Aldrich
Bovine serum albumin	Sigma-Aldrich
ELISA DuoSet kits	R&D systems
Sodium azide (NaN_3)	Sigma -Aldrich
Ready Set Go IL-21 ELISA kit	eBiosciences
1X PBS	Gibco
TMB Reagent	eBiosciences

TABLE 2.3 ELISA REAGENTS: All ELISA reagents used and corresponding sources.

FLOW CYTOMETRY AND FACS REAGENTS

Material	Source
FACS Flow	BD
FACSRinse	BD
FACSClean	BD
37% (v/v) paraformaldehyde	Sigma-Aldrich
Fetal bovine serum	Sigma-Aldrich
Sodium azide	Sigma-Aldrich
EDTA	Sigma-Aldrich
Propidium iodide solution	Miltenyi biotech
CFSE	eBiosciences
Tween 20	Sigma-Aldrich
Triton X-100	Sigma-Aldrich
Saponin from quillaja bark	Sigma-Aldrich
Anti-IFN-γ antibody	BD
Anti-IL-17 antibody	BD
Anti-RORγt antibody	eBioscience

Anti-T-bet antibody	BD
Anti-CD3 antibody	BD
Anti-CD4 antibody	BD
Anti-CD44 antibody	BD
Anti-CD62L antibody	BD
Anti-CCL5 antibody	BD
Anti-CD25 antibody	BD

TABLE 2.4 FLOW CYTOMETRY AND FACS REAGENTS: All flow cytometry reagents used and corresponding sources.

RNA ISOLATION AND cDNA SYNTHESIS

Material	Source
Nucleospin RNA II Columns	Fisher Scientific
DEPC treated water	Invitrogen
High Capacity cDNA Reverse Transcription Kit	Applied Biosystems
Molecular grade ethanol (EtOH)	Sigma-Aldrich
Molecular grade isopropanol	Sigma-Aldrich

Table 2.5 RNA ISOLATION REAGENTS: All reagents used in the isolation of mRNA and corresponding sources.

qPCR REAGENTS

Material	Source
TaqMan® Universal Mastermix	Applied Biosystems
MicroAmp® Optical 96-well plate	Applied Biosystems
MicroAmp® Optical Adhesive Film	Applied Biosystems
TaqMan® Gene Expression Assays	Integrated DNA technologies

TABLE 2.6 QUANTATIVE PCR REAGENTS: All qPCR reagents used and corresponding sources.

LAMINA PROPRIA ISOLATION REAGENTS

Material	Source
HBSS (calcium, magnesium free)	Gibco
EDTA	Sigma-Aldrich
Collagenase V	Sigma-Aldrich
Collagenase D	Gibco
Dispase	Roche
DNase	Roche
RPMI	Gibco

TABLE 2.7 LAMINIA PROPRIA ISOLATION REAGENTS: All reagents used and corresponding sources.

IMMUNOHISTOCHEMISTRY REAGENTS

Material	Source
Acetone	Sigma-Aldrich
HCl	Sigma-Aldrich
Sodium bicarbonate	Sigma-Aldrich
EtOH	Sigma-Aldrich
Harris Haematoxylin	Sigma-Aldrich
Eosin	Sigma-Aldrich
Histoclear	National diagnostics
Histobond Microscope slides	RA Lamb
OCT compound	Tissue-Tek

TABLE 2.8 LAMINIA PROPRIA ISOLATION REAGENTS: All reagents used and corresponding sources.

2.2 – ISOLATION AND CULTURE OF $CD4^+$ T-CELLS

All tissue culture was carried out using aseptic technique in a class II laminar airflow unit (Holten 2010- ThermoElectron Corporation, OH, and USA). Cells were maintained in a 37°C incubator with 5% CO_2 and 95% humidified air (Model381- ThermoElectron Corporation, OH, and USA). Cells were grown in complete RPMI-1640 medium (cRPMI) (Krummel et al. 2000). FBS was heated at 57°C for 30 mins and then aliquoted for storage at -20°C. Supplemented medium was stored at 4°C for no longer than three months.

2.2.1 – CELL ENUMERATION AND VIABILITY ASSESSMENT

Cell viability was assessed using the Trypan blue exclusion method. This method is based on the principal that dead or dying cells which do not have an intact cell membrane will allow the trypan blue to enter the cell, staining the cell blue and allowing it to be excluded from the viable cell count. Trypan blue solution (0.4% (v/v)) was mixed in a 1:1 solution with the cell suspension (diluted as necessary) and after ~2 min cells were applied to a brightline haemocytometer (Sigma) and examined under high-power magnification (×40) using an inverted microscope (Olympus CKX31, Olympus Corporation, Tokyo, Japan). Cells inside the 1mm square grid at each corner were counted and averaged [figure 2.1, circled in red]. The number of cells was then calculated using the formula: Cells/ml = N x D (x 10^4). Where N = average number of cells counted in each of the squares and D = the dilution of cells in PBS.

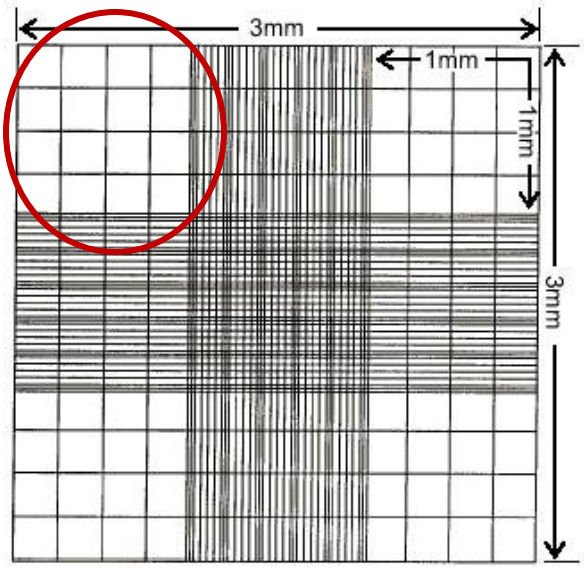

***Figure 2.1**:* Cell enumeration using the haemocytometer

2.2.2 – ISOLATION OF CD4⁺ T-CELLS

Primary T-cells were isolated aseptically from female Balb/c mice aged 6-12 weeks. All mice were sourced from Charles River and housed in a Specific Pathogen Free (SPF) unit.

2.2.2.1 – SPLEENOCYTE ISOLATION

Spleens were removed aseptically and collected in RPMI/10% (v/v) FBS on ice. A single cell suspension was achieved by pushing each spleen through a cell strainer (40µm, BD falcon). Cells were then washed with RPMI/10% (v/v) FBS and counted.

2.2.2.2 – CD4⁺ T-CELL MAGNETIC PARTICLE ISOLATION

(Stemcell technologies- Easysep© Mouse CD4⁺ T-cell isolation kit #19852)

(Stemcell technologies- Easysep© Mouse naïve CD4⁺ T-cell isolation kit #19765)

Cells were prepared in recommended medium at a concentration of $1x10^6$ cells/ml. The cell solution was then placed in a 5ml polystyrene falcon tube (BD Biosciences). The Easysep™ mouse $CD4^+$ T-cell enrichment cocktail was then added at 50µl/ml of cells, mixed well and left at room termperature for 10 minutes. The cocktail contains a selection of antibodies targeting cell surface markers of all cells excluding T-cells. The cocktail for the $CD4^+$ T-cell isolation consisted of antibodies directed against all non-$CD4^+$ cells: CD8, CD11b, CD11c, CD19, CD24, CD45R, CD49b, TCRγ/δ and TER119. The naïve $CD4^+$ T-cell isolation cocktail contained antibodies directed to all non-naïve $CD4^+$ T-cells: CD8, CD11b, CD11c, CD19, CD24, CD25, CD44, CD45R, CD49b, TCRγ/δ. The Easysep™ streptavidin rapidspheres™ were vortexed well, added at 75µl/ml of cells, mixed well and left at room temperature for 2.5 minutes. The suspension was then made up to 2.5mls total volume and mixed gently before placing in the Easysep™ magnet at room temperature for 2.5 minutes. The supernatant that was poured off contained the $CD4^+$ T-cells and naïve $CD4^+$ T-cells. These cells were centrifuged at 300g for 5mins, enumerated and resuspended in cRPMI media.

2.2.2.3 – $CD4^+$ T-CELL COLUMN ISOLATION

(R&D systems – mouse $CD4^+$ T cell subset column kit MCD4C-1000)

$2X10^8$ spleenocytes in 2ml of column wash were mixed with 1 vial of monoclonal antibody cocktail and incubated at room temperature for 15 minutes. During this incubation period the column was washed with 10mls of column buffer. After incubation, cells were washed twice with 10mls of column wash and finally resuspended in 1ml of column wash. The cells were added to the column and any liquid displaced from the column collected in a sterile falcon tube. Once the cells had moved into the

column, the bottom cap was replaced and cells left in the column at room temperature for 10 minutes. This allowed B cells, non-selected T cells and monocytes to bind to the glass beads coated with anti-immunoglobulin via both F(ab) and Fc interations. The column was eluted with 10mls of column buffer. Eluted $CD4^+$ positive T-cells were centrifuged (250g for 5 minutes), resuspended in cRPMI and counted using trypan blue exclusion method. Cells were adjusted to the required concentration with cRPMI.

2.2.3 – POLARISATION OF $CD4^+$ T-CELLS

Cells were stimulated using agonist antibodies directed to CD3 (clone: 145-2C11 BD bioscience) and CD28 (clone: 37.51 BD). Cells were stimulated in the presence of polarising cytokines. The cocktails used to drive specific T-cell subsets and their concentrations are represented in **Table 2.9**.

Phenotype	Cocktail	Concentration	Clone	Source
Naïve	rmIL-2	10ng/ml		R&D
T_H1	rmIL-12	10ng/ml		R&D
	anti-IL-4	10µg/ml		R&D
T_H2	rmIL-2	10ng/ml		R&D
	rmIL-4	10ng/ml		R&D
	anti-IFN-γ	10ug/ml		R&D
T_H17	rmIL-1β	10µg/ml		R&D
	rmIL-6	20ng/ml		R&D
	rmIL-23	10ng/ml		R&D
	rhTGF-β	2ng/ml		R&D
	anti-IFN-γ	10µg/ml		R&D
	anti-IL-4	10µg/ml		R&D

Table 2.9 List of polarising cocktails and concentrations

2.3 – FLOW CYTOMETRY

2.3.1 – BASIC PRINCIPLES OF FLOW CYTOMETRY

Flow cytometry uses the principles of hydrodynamic focussing to present cells for interrogation to a laser light source, one cell at a time. Data is collected for each individual cell, providing information about the size and granularity. Expression of individual protein markers on the surface, or within a cell, can be measured using targeted monoclonal antibodies. These antibodies are conjugated to fluorochromes emitting light at various wavelengths. Following excitation from the flow cytometer LASER light source, scattered light is collected by photomultiplier tubes (PMT) measuring fluorescence intensity and side scatter (SSC), an indication of cell granularity and complexity. The size of the cell is determined from the forward scatter (FSC) detector usually a photodiode. A photodiode (as opposed to a PMT) is used as the detector for the forward scatter owing to the intensity of the light from the LASER source emitted directly at the FSC detector.

Using these parameters individual cells in a complex mixture can be characterised and identified.

2.3.2 – FLUORESCENCE ACTIVATED CELLS SORTING (FACS)

As the flow cytometer measures the characteristic features on each cell, some machines have the capacity to sort cells into individual tubes resulting in pure yields of a single cell type. This is referred to as Fluorescence Activated Cell Sorting (FACS). FACS machines work using charged droplets and an electrostatic deflection system. An oscillation device is used to vibrate the stream and cause it to break into droplets. The

machine is tuned so that each droplet contains a single cell. This droplet has a charge applied to it and it is directed through the electrostatic deflection system into an individual tube. Target tubes for each cell type are assigned when setting the sort parameters. Cells are then sorted to target tubes based on the analysis of each individual cell immediately before breaking into a drop from the stream. In this way individual populations of cells can be obtained from heterogenous mixtures at high speed and with accuracy.

2.3.3 – CELL SURFACE MARKER STAINING

Cells were removed from tissue culture and placed in a 96-well round bottomed plate for staining with each well containing 200,000-400,000 cells. An equal amount of FBS was added to block non-specific binding sites on the cell surface. Cells were then centrifuged at 250g for 5mins. The supernatant was removed and the cells resuspended in FACS buffer [See **Appendix A**]. The plates were centrifuged again and the cell pellet was resuspended in 100µl of antibody or isotype mixture as determined by a titre of each antibody used. The plates were incubated in the dark at 4^{o}C for 30mins. Following incubation cells were washed twice with 200µl FACS buffer, and centrifuged for 5mins at 250g between washes. Cells were analysed immediately. Alternatively cells were fixed using a 4% formaldehyde/PBS solution and stored at 4^{o}C in labelled falcon tubes for analysis at a later time. Data was acquired using a FACS Aria (BD Bioscience). Data was analysed using FlowJo Software (TreeStar).

2.3.4 – STAINING ANTIBODY TITRATION

All antibodies used were titrated to acquire the best possible fluorescent signal using the least amount of antibody possible. This technique leads to more efficient staining and a reduction in steric hindrance where bulky fluorophores such as Phycoerythrin (PE) can block potential binding sites when using multi-colour flow cytometry analysis. This is especially prevalent in intracellular staining. Cells were stained with a serial dilution of antibody. The Mean Fluorescence Intensity (MFI) was measured for each sample and the log MFI was plotted against the concentration of antibody used. This curve shows a point of saturation and a concentration of antibody was selected after this point.

2.3.5 – INTRACELLULAR PROTEIN STAINING

Intracellular protein staining involves permeabilisation of the cell membrane to allow staining antibodies to pass into the cell and bind target epitopes. The method of permeabilisation can greatly affect the cell membrane and the epitopes immediately inside or on the surface of the cell. For this reason, when staining both surface markers and intracellular proteins, the cells are surface stained as described in **2.3.3** before fixing and permeabilising for intracellular staining.

2.3.5.1 – INTRACELLULAR TRANSCRIPTION FACTOR STAINING

Following the surface staining, cells were washed with FACS buffer and resuspended in 1% Triton-X100 detergent in PBS. Triton X-100 is a detergent that partially dissolves the nuclear membrane and is therefore very suitable for nuclear antigen staining. Cells were washed twice in a 0.1% Triton-X100 solution by centrifuging at 300g for 5 mins. The cells were resuspended in a 1% Triton-X100 solution containing the antibodies and

incubated for 30mins at 4°C. Following this cells were washed twice in 0.1% Triton-X100/PBS solution. The cells were then washed twice with FACS buffer and finally resuspended in FACS buffer for analysis.

2.3.5.2 – INTRACELLULAR CYTOKINE STAINING

T-cells were cultured in polarising conditions for 4 days. On the last day monensin was added to the culture and the cells were stimulated with Phorbol 12-Myristate 13-Acetate (PMA) (50ng/ml) and Ionomycin (1µg/ml). These chemicals are useful for quickly inducing and stimulating T-cell populations. PMA stimulates cells through the protein kinase C activation and ionomycin is a calcium ionophore. The monensin halts transport of synthesized proteins from the cell trapping large amounts of cytokine within the cell allowing characterisation of cell cytokine production. The cells were stimulated for 4 hrs with monensin added for the last 2 hrs. The cells were collected by centrifuging at 690g for 5mins. Cell surface epitopes were stained as described in **2.3.3** before $1x10^6$ cells were resuspended in cold 3% para-formaldehyde (PAF) in PBS and incubated for 15mins at room temperature to fix the cells. The cells were then washed twice in cold FACS buffer and resuspended in 1% Saponin in FACS buffer and incubated for 15mins at room temperature. Cells were then centrifuged and resuspended in 50µl of 1% saponin/FACS buffer. An aliquot of 20µl cytokine antibody cocktail was added to each tube and incubated for 30mins at room temperature in the dark. Cells were washed twice with 1% saponin/FACS buffer and resuspended in FACS buffer for analysis.

2.3.6 – PROLIFERATION ANALYSIS USING CFSE DYE

CarboxyFluorescein Sucinimidyl Ester (CFSE) is a fluorescent cell staining dye. This dye is supplied in a non-fluorescent form carboxyfluorescein diacetate succinimidyl ester (CFDA-SE). CFDA-SE contains acetate groups and is highly cell permeable and toxic. When it is added to cells at optimum levels it enters the cytoplasm of the cells where the acetate groups are removed converting the molecule to the fluorescent molecule CFSE which is highly stable within the cell. When the cell undergoes proliferation the dye is halved evenly between daughter cells allowing the tracking of cell proliferation up to 8 generations. Isolated cells were centrifuged at 170g for 5 mins and resuspended in PBS + 5% FBS. The FBS buffers the cells to the toxic effects of CFSE. The CFSE was added at a final concentration of 5μM and the tube was inverted quickly and vortexed to evenly distribute the dye. The cells were incubated for 5 mins and then washed twice with PBS + 5%FBS before re-suspending in RPMI media.

2.3.7 – CELL VIABILITY AND DEAD CELL EXCLUSION USING PROPIDIUM IODIDE STAINING

Propidium Iodide (PI) is a fluorescent intercalating dye that binds DNA. PI is used to distinguish live and dead cells. Cell death leads to a compromised cell membrane. This allows PI to enter the cell and stain DNA. Once PI intercalates with the DNA the fluorescence is enhanced allowing dead cells to be distinguished from live cells. PI is added as the last step before analysis and cannot be used with fixed or permeabilised cells as these cells are killed in the process. Cells were removed from culture and washed with

FACS buffer. PI (Miltenyi Biotech) was added at a working concentration of 1µg/ml and left for 10mins before reading on the FACS Aria.

2.4 – CYTOKINE ELISA

2.4.1 – BASIC PRINCIPLES OF ELISA

Enzyme Linked ImmunoSorbent Assay (ELISA) is an accurate method used for the detection of proteins in cell supernatant. The method of ELISA used in all studies was a sandwich ELISA. In this method a capture antibody specific to the target molecule was diluted in PBS and coated on a 96-well plate. The wells were then washed to remove unbound antibody and blocked using a PBS/BSA solution to block non-specific binding sites. Samples containing an unknown concentration of the target antigen were then added to the wells along with a series of diluted standards of a known concentration of recombinant target protein. The plate was incubated overnight at $4^{o}C$ and then washed to remove unbound antigen and a biotinylated detection antibody specific to the target was added and incubated for 2 hours at RT. This method of using two antibodies to effectively "sandwich" the target molecule results in low, accurate detection levels to the picogram range. The plate was then washed and incubated with a streptavidin-horseradish-peroxidase (HRP) for 20mins. The streptavidin and biotin bind with a high affinity and the amount of HRP is proportional to the amount of target antigen in the sample. Tetramethylbenzidine (TMB) was added to the wells and the HRP enzyme catalyses the oxidation of the TMB substrate transforming it to a blue compound. The intensity of the colour is proportional to the concentration of target antigen present. To prevent further oxidation the reaction was stopped by the addition of sulphuric acid to

each well and the blue turns to a yellow colour. The intensity of this yellow colour was read at 450nm and was then compared to the standards to accurately calculate the concentration of antigen present in the sample.

2.4.2 – TNF-α, IL-4, IL-10 and IL-17 CYTOKINE ELISA

The recommended reagents were used for R&D duo ELISA kits and included: Blocking buffer/reagent diluent 1% (w/v) BSA/PBS and R&D TMB solution. Washing buffer was made up of PBS + 0.05% tTween-20.

2.4.3 – IL-2 AND IFN-γ CYTOKINE ELISA

The method above was followed with two deviations: Blocking buffer used was 1% (w/v) BSA/PBS + 0.05% (w/v) NaN_3 and the reagent diluent was 0.1% (w/v) BSA/TBS + 0.05% (v/v) Tween-20.

2.4.4 – IL-21 CYTOKINE ELISA

The IL-21 ELISA kit was obtained from eBioscience. The protocol was followed according to manufacturer's instructions. All the buffers including the TMB were supplied with this kit.

2.5 – RNA ANALYSIS

2.5.1 – BASIC PRINCIPLES OF REAL-TIME qPCR

Real-time quantitative polymerase chain reaction (qPCR) is a molecular biology method based on the principles of PCR where a region of DNA is amplified using primers to surround a specific targeted portion of DNA and amplify it to orders of magnitude using a heat stable DNA polymerase. In qPCR the amount of DNA amplified is quantified in real time and allows for absolute (total copies) or relative quantification (normalisation to a control gene) of target DNA in a sample.

When qPCR is combined with reverse transcription it allows for the quantification of messenger RNA. A reverse transcription polymerase is used to make complimentary DNA (cDNA) copies of total RNA, including mRNA, isolated from cells of interest. The cDNA is used as the template for qPCR and the amount of mRNA in the sample is quantified. Quantification is accomplished using two methods; the intercalating dye SYBR or primer-probes.

The intercalating dye SYBR green non-specifically binds to double stranded DNA. When SYBR forms a dye complex with DNA products of PCR it is excited by light at 492nm and emits light at 520nm. The non-specific nature of the cyanine dye SYBR green can lead to non-specific double-stranded reaction products resulting in increased background or false positives. The use of probes ensures specificity of the signal and quantification reducing non-specific products. The DNA probe is dual labelled with a reporter dye and a quencher. The assay uses unlabelled primers to amplify the region of

interest and exploits the 5'-3' nuclease activity of DNA polymerase to cleave the probe and release the reporter dye from the quenching protein resulting in a signal. The disadvantage of this method is the time and cost required to design individual probe assays for each gene target and the cost of running the patent protected technique.

2.5.2 – RNA EXTRACTION

T-cells were removed from the 24 well plate and centrifuged at 690g for 10mins to remove media. Cells were then re-suspended in RA1 buffer from the Nucleospin® RNA II (Machery-Nagel, Germany). The RNA extraction was then carried out using the Nucleospin® RNA II kit according to the manufacturer's instructions. The kit works by immediately inactivating RNAses in the lysed cell solution and changing the conditions to allow absorption of the RNA to a silica membrane. Contaminating DNA is then removed using an rDNAse solution, before washing the silica membrane with two buffers (RA2 and RA3) to remove salts, metabolites and macromolecular cellular components. The pure RNA is then eluted from the silica membrane in RNA free H_2O. The concentration of the RNA was then measured using the Nanodrop 1000 spectrophotometer (Thermo-Fisher scientific, USA). The purity of the RNA was determined using the A260nm and A280nm absorption wavelengths. All the RNA used in this study had an A280/260 ratio between 1.8 and 2.1, within the accepted range for RNA purity for use in PCR experiments.

2.5.3 – DNA PRODUCT ANALYSIS BY GEL ELECTROPHORESIS

Gel electrophoresis was used to check DNA products following qPCR. Samples were run on a 2% agarose gel. Gels were prepared by dissolving 2g of agarose (Thermo-Fisher

scientific, USA) in 100mls of TAE buffer and heating to boiling point. After cooling, 10µl of SYBR® safe (10'000X concentration) was added to the gel mix before pouring into a gel mould and setting the well comb. DNA samples were mixed with loading buffer (Fermentas) and loaded straight onto the gel. Gels were run for 1hour in TAE buffer at 100v. Gels were visualised using the G-Box cell imaging system (Syngene, UK)

2.5.4 – cDNA SYNTHESIS

Complimentary DNA (cDNA) is required as a template in two step quantitative PCR. cDNA is generated from RNA in a separate step to the qPCR reaction using reverse transcriptase PCR (RT-PCR). The RT-PCR was carried out using the RNA generated from the samples and the High Capacity cDNA Reverse Transcriptase Kit (Applied Biosystems, USA). The kit contains a master mix of dNTP, random primers and the enzyme reverse transciptase. Reverse transcriptase synthesises single strand cDNA using the RNA strands as template. The cDNA that is produced in this reaction is a more stable and amplified copy of the RNA. This is then used as the template for the subsequent qPCR experiments. This method is used as opposed to one-step qPCR where the RT-PCR and qPCR are carried out sequentially in the one tube in a qPCR method. This method uses more sample and introduces more potential errors in the reaction.

Using quantitative measurements of the RNA, 1µg of RNA was used in each cDNA synthesis reaction. The settings in **[Table 2.10]** were used in the PCR reaction on a PTC-200 MJ research thermocycler.

.

2.5.5 – qPCR ASSAY OPTIMISATION

In order to ensure accuracy and robustness of qPCR gene expression measurements each assay performance had to be evaluated. This was carried out by assessing the PCR efficiency, the linear dynamic range, the limit of detection and the assay precision (Bustin et al. 2009). Primer pairs were purchased from Sigma-Aldrich or IDT [**See Appendix C**].

The Amplification efficiency was determined by carrying out a ten fold dilution of the PCR product and constructing a standard curve of C_T vs log of the dilution of product. Each change in C_T represents a 2-fold change. If the co-efficient of determination was R^2 >0.980, the equation of the line was used to determine the amplification efficiency (E) of the assay using the following formula:

$$\mathbf{E = 10^{\wedge\ (-1/slope)} - 1 \times 100}$$

If the efficiency is 100% (Slope 3.32) then the C_T values will be 3.3 cycles apart. The accepted range for the amplification efficiency of each assay was between 90% and 110% (slope 3.1-3.3).

The linear dynamic range and limit of detection was determined from the efficiency curves generated for each sample, the assay precision was determined by carrying out all assays and technical replicates in triplicate. Non-template controls (NTC) were included in all experiments for assay targets. Samples with an NTC within 5 cycles of the sample Ct value were disregarded and new primers were ordered. Ct values >36 cycles were also disregarded as they are at the limit of detection in this assay and the accuracy is

compromised. The efficiency curve, linear range and limit of detection for each assay used in this study are shown in [**Appendix B].**

2.5.6 – RELATIVE QUANTITATION USING qPCR

This method compares the relative expression of different samples, one of which is a calibrator or control such as untreated tissue. Samples were normalised to a housekeeping gene. The housekeeping gene is an endogenous gene that maintains expression levels despite treatment. In order to identify a suitable housekeeping gene for this experiment, 8 potential common mouse reference genes were investigated. From the endogenous genes examined, the 2 most suitable were selected. It was necessary to have a minimum of 2 housekeeping genes to ensure accuracy in real time assays (Bustin et al. 2009). Samples were normalised to the geometric mean of the two housekeeping genes C_T values. Samples were then compared using the comparative C_T method or ddCt method:

ddCt= dCt sample – dCT reference

Where dCt sample is the normalised Ct value of the treated sample and dCt reference is the normalised Ct value of the control sample.

Quantitative-Real Time PCR (qPCR) was carried out on the ABI Prism 7500 (Applied Biosystems, USA). cDNA was generated as described above and diluted in order to bring the target into the range of detection. PCR reactions were prepared in triplicate for each sample with an appropriate dilution of cDNA. Primers were added for a final concentration of 500mM for each primer. ROX reported dye was used as an internal

reference signal to normalise for non-PCR-related fluorescence occurring from well to well.

Samples were added to a 96-well reaction plate and covered with an adhesive cover (Applied Biosystems, USA). Plates were centrifuged for 2mins at 690g and stored at 4^{o}C until run. Samples were run on the ABI Prism 7500 under the following conditions:

	STEP 1	STEP 2	STEP 3 (a)	STEP 3 (b)
Temperature (^{O}C)	50	95	95	60
Time	2 min	10 min	15 sec*	1 min*
			* Repeat step 3 for 40 cycles	

Table 2.10 – qPCR programme

The results were analysed using the ABI prism sequence detection software (Applied Biosystems, USA) and Excel software (Microsoft, USA).

2.6 – *IN VIVO* WORK AND MOUSE MODELS OF DISEASE

2.6.1 – DSS MODEL OF COLITIS

Dextran sodium sulphate (DSS) model of colitis is one of the most widely used chemically induced models of inflammatory bowel disease. It is directly toxic to the colonic epithelial cells in the basal crypts and induces an acute inflammatory response. When the end point of the model is extended in C57BL/6 mice, it results in a chronic inflammatory response.

DSS mouse work was carried out in collaboration with Silvia Melgar in the Alimentary Pharmabiotic Centre, University College Cork (UCC). 25 C57BL/6 female mice weight

18-20g at arrival were housed in the Biological Services Unit (BSU) at UCC. DSS was administered to the mice in drinking water. A final concentration of 3% DSS was prepared fresh every day in normal tap water and administered *ad libitum*. Mice were split into 4 groups for the study depending on the length of time that mice were left following DSS treatment:

1. **Control**

   No DSS was administered to the control mice.

2. **Early acute**

   Mice were administered DSS for 5 days (Day 0-Day 4) followed by 2 days on water and sacrificed for sample and tissue processing on Day 7

3. **Late acute**

   Mice were administered DSS for 5 days (Day 0-Day 4) followed by 7 days on water and sacrificed for sample and tissue processing on Day 12

4. **Chronic**

   Mice were administered DSS for 5 days (Day 0-Day 4) followed by 21 days on water and sacrificed for sample and tissue processing on day 26

The clinical symptoms recorded in DSS-treated and the control mouse were body weight and fur texture/posture on day 0, and 2 times/week from day 4. These were used to generate a daily disease activity index. At the end point of each group the length & weight of each colon was also measured and used as an indication of colitis in the mouse model. Sections of distal colon were collected for tissue homogenisation and RNA purification.

2.6.2 – ISOLATION OF LAMINA PROPRIA

The large intestines of mice were removed and placed on paper towels soaked in PBS and the fat was removed. The intestines were opened longitudinally, washed in Hank's balanced salt solution (HBSS) 2% FCS, and cut into 0.5cm sections. The tissue was then shaken vigorously in 10ml HBSS 2% FCS, and the supernatant was discarded. To remove the epithelial layer, 10ml fresh CMF (calcium, magnesium free) HBSS containing 2mM EDTA was then added, the tube placed in a shaking water bath for 15mins at 37^{o}C, before being shaken vigorously and the supernatant discarded. 10ml fresh CMF HBSS was then added, the tube shaken again and the supernatant discarded. After a second incubation in 2mM EDTA CMF HBSS, the washes were repeated and the remaining tissue was digested with pre-warmed 1.25mg/ml collagenase D, 0.85mg/ml collagenase V, 1mg dispase, and 30U/ml DNase in complete RPMI medium for 40 minutes in a shaking water bath at 37^{o}C until complete digestion of the tissue. At the start of the incubation, and at 10 mins intervals thereafter, the tube was shaken vigorously and finally the supernatant (containing lamina propria cells) was removed and passed through a 40um filter.

The cells were collected and resuspended in complete RPMI medium. Cells were passed through a 40um filter, counted and kept on ice until use. Approximately 10-15 x10^{6} lamina propria cells are isolated per mouse.

2.6.3 – TISSUE SECTIONING AND IMMUNOHISTOCHEMISTRY

Tissue sections of 0.5cm were removed from washed colons and covered in optimum cutting temperature (OCT) compound in plastic moulds. The sections were then flash frozen by submerging in liquid nitrogen for 20 seconds. The sections were cut in a controlled temperature cryostat at -20^{o}C and mounted onto slides and left overnight at room temperature. Sections were then fixed in acetone/alcohol mix for 5 mins at room temperature and washed in PBS. Slides were then stained in Harris haemotoxylin for 10 minutes and washed again under a running tap for 5 mins. The slides were differentiated in 1% acid/alcohol for 30 secs 3 times and then washed under a tap for 1 min. After washing, slides were placed in 0.1% sodium bicarbonate for 1 min and washed under the tap for 5 mins. The slides were then rinsed in 95% alcohol for 10 dips before counterstaining in Eosin for 1 min by dipping up & down. Finally the slides were dehydrated by dipping in 75% ETOH for 3 mins, 95% ETOH for 3 mins (x2), followed by 100% ETOH for 3 mins and 3 mins in Histoclear. Slides were then mounted with mounting medium and the cover slides pushed down firmly to remove bubbles.

2.6.4 – CITROBACTER RODENTIUM INFECTION MODEL

The *C. rodentium* model of infection is a widely studied mouse model of colitis. *C. rodentium* induces a Th17 response in mice leading to a transient inflammatory state in the colon that is clinically similar to ulcerative colitis. Infection is usually cleared after 21 days.

C. *rodentium* work was carried out in collaboration with Silvia Melgar in the Alimentary Pharmabiotic Centre, University College Cork. C57BL/6 mice were housed in the

Biological Services Unit at UCC. Mice were divided into groups of 6-8 and inoculated orally by a 200µl gavage of approximately $200x10^9$ CFU C. *rodentium*. Mice were sacrificed at day 9, 14, 21 and 28 for tissue processing. The colons were removed and washed and the length and weight of each colon was measured individually as an indication of inflammation of the gut. Sections of distal colon were collected for tissue homogenisation and RNA purification.

2.6.5 – MICE USED FOR Stx11$^{-/-}$ IN VITRO STUDY

Wild type C57BL/6 and *Stx11*$^{-/-}$ mice on a C57BL/6 background were obtained from the Borstel research institute in Hamburg, Germany in collaboration with Silvia Bulfone-Paus and Udo Zur Stadt. Mice were used between 10-12 weeks old and housed in a specific pathogen free unit in the Borstel Research Centre animal facility.

2.6.6 – MICE USED FOR IN VITRO STUDIES

All other mice used in this study were purchased from Charles River and housed in the specific pathogen free biological resources unit in Dublin City University. Mice were kept in controlled conditions and used between 8-14 weeks old.

2.7 – STATISTICAL ANALYSIS

The student T-test was used to determine if differences measured between samples were significantly different from one another. The level of statistical significance was indicated by * ($p<0.05$), ** ($p<0.01$) and *** ($p<0.001$).

CHAPTER 3

ISOLATION AND POLARISATION OF $CD4^+$ T- CELLS *IN VITRO*

3.1– INTRODUCTION

Antigen presenting cells (APCs) phagocytose invading pathogens and present molecules to T-helper cells in the lymph nodes via the MHC molecule activating T-helper cells and the CD3 associated T-cell receptor complex (TCR). CD4 is a marker of mature T helper cells, binds a non-antigen specific region of the MHC and plays an important role in boosting T-cell sensitivity to antigen (Krummel et al. 2000; Bour-Jordan et al. 2011). This activation must be accompanied by two other molecular signals; the co-stimulatory signal and the cytokine milieu. The co-stimulatory signal is necessary to prevent cells from mounting immune responses to "self antigens" (Lenschow et al. 1996). This signal is provided by the B7 family of proteins on APCs and will bind with its natural ligand CD28 on the T-helper cell to provide a co-stimulatory signal to the antigen presented on the APC cells MHC complex. This combined signalling leads to cell activation and cloning. Without this signal the T-cells will not become fully activated by the interaction with the APC and the cell will become anergic (Bour-Jordan et al. 2011). The cell signalling required for T-cell activation can be replicated in *vitro* using anti-CD3 antibody which acts as an agonist by cross-reacting the TCR, and an anti-CD28 antibody which cross reacts with the CD28 molecule providing activation and co-stimulatory signals respectively to the cell. The cytokine milieu can have a number of effects on the fate of the T-cell depending on the cytokines present during activation of the cell. Various cytokines can activate signalling cascades leading to T-cell cloning, cell inactivation, up-regulation of secreted cytokines, and importantly in the case of this work, activation of signal transducers and activators of transcription (STATs) and transcription

factors leading to the commitment of a $CD4^+$ T-helper cells to a specific subtype (Vahedi et al. 2013).

In order to maintain $CD4^+$ T-helper cells *in vitro*, isolation and culture conditions needed to be optimised. $CD4^+$ labelled cells are found in the lymph nodes of mice and humans alike, and are abundant in the spleen. A number of commercial and lab based methods exist for the retrieval of $CD4^+$ cells from a spleenocyte solution. Cells are sensitive to culture conditions and supplementation of media is necessary to keep them viable for the long periods of time necessary to complete studies *in vitro*. The aim of this chapter was to optimise the method to isolate pure, viable $CD4^+$ T-helper cells and identify ideal conditions for culturing them *in vitro*. In order to identify the conditions required for the isolation and activation of $CD4^+$ T-helper cells, surface marker expression and cytokine secretion were measured. Cell viability and proliferation studies were also carried out in various conditions. Following this optimisation, the next step was to further polarise the cells into subsets of T-helper cells.

T-helper cells are capable of polarising into specialised subsets of lymphocytes that deal with the many diverse challenges posed to the immune system from day to day. These subsets secrete defined cytokine profiles which are tailored to induce conditions required for an effective immune response. The Th1 subset of cells primarily deals with invading intracellular pathogens and viral infections. It does this partly though the secretion of large amounts of IFN-γ, the signature cytokine for this cell type (Szabo et al. 2000). Th2 cells direct immune defences against invading parasites and aid the humoral immune response (Mosmann et al. 1986). Th17 cells are a recently described subset that are characterised by their signature cytokine IL-17 and express the transcription factor

RORγt showing a separate lineage commitment to Th1 and Th2 cells. Th17 cells defend against fungal infections and extracellular pathogens. Th17 cells have also been implicated in inflammatory disease (Ivanov et al. 2006).

Using combinations of recombinant cytokines and neutralising antibodies in optimised culture conditions, it was possible to polarise isolated $CD4^+$ T-cells *in vitro* into T-helper cell subsets in order to study them in detail. Given that each cell subset produces a different key signature cytokine in abundance and each cell subset originates from a common source containing identical proteins and pathways, this presents an ideal model to determine the SNARE proteins involved in the secretion of specific cytokines from $CD4^+$ T-helpers cell subsets.

3.2– RESULTS

3.2.1 – ISOLATION, ACTIVATION AND CONFIRMATION OF CD4⁺ T-HELPER CELL POPULATION FROM BALB/C MICE.

$CD4^+$ T-cells develop in the thymus and reside in the spleen and lymph nodes. In order to isolate these cells from BALB/c mice, the spleen was removed from the mouse aseptically and homogenised through a 50μm filter. The spleenocytes were then re-suspended in fully supplemented RPMI and T-helper cells were isolated using the easysep™ mouse $CD4^+$ T-cell isolation kit available from Stemcell Technologies as described in the materials and methods **[Section 2.2.2.2]**. The CD4 antigen is present on mature T-helper cells but is also expressed by some macrophages and dendritic cells; therefore it was important to confirm the purity of the T-helper cell population. CD3 makes up the TCR complex and is a marker of all T-cells including $CD3^+/CD8^+$ cytotoxic T-cells, so double staining for the CD3 antigen population was necessary to confirm the $CD3^+/CD4^+$ T-helper cell population (Krummel et al. 2000)**.** Isolated $CD4^+$ cells were blocked and stained with primary PE conjugated anti-CD4 and primary FITC conjugated anti-CD3 antibodies for 30 mins and washed before analysis on a BD FACS Aria, and data analysed using flowjo software. **Figure 3.1(a)** shows dead cell removal based on FSC and SSC, dead cells and debris have a small FSC and SSC and were gated out from the main population. Plot **[Figure 3.1(b)]** shows cells single stained with the primary PE conjugated anti-CD4 antibody, the dots represent a single cell event and as they shift to the right the intensity of the staining increased (a shift up in the case of a vertical axis). The isolated population was confirmed to be an 89% $CD3^+$ $CD4^+$ T helper cell population

as indicated by a shift to the top right quadrant. Purified cells were stained with directly labelled fluorescent antibodies to the cell antigens and analysed using the BD FACS Aria **[Figure 3.1(c)]**.

The surface marker CD25 (IL-2 receptor) is up-regulated on T-cells upon activation and aids in proliferation of T-helper cells (Smith et al. 1980). It is stained as a marker for activated $CD4^+$ T-cells. In order to demonstrate that the cells isolated were viable and could be activated, cells were treated with anti-CD3 (5µg/ml) and anti-CD28 (2.5µg/ml) antibodies and stained for CD25 using a PE primary conjugated anti-CD25 antibody (BD) (0.5µg/100µl). Cells were cultured and stimulated for 3 days were stained and analysed on the BD FACS Aria. **Figure 3.2** shows an increase in CD25 expression. Median has increased from 2.75 to 20.1 and the mean fluorescence intensity increase from 4.93 to 27.2. These data show an increase in CD25 expression on cells, confirming T-cell activation **[Figure 3.2]**. .

3.2.2 – ANTIBODIES DIRECTED TO CD3 AND CD28 PROVIDE SIGNALS FOR IN VITRO ACTIVATION OF CD4+ CELLS.

Three signals are required for T-cell activation; signalling through the T-cells receptor complex (TCR), activation of the CD28 co-stimulation pathways, and cytokine signalling (Kenneth Murphy Mark Walport 2008). CD3 makes up part of the TCR complex and activation depends on signalling through this pathway. Anti-CD3 antibody (BD Clone:145-2C11) that cross-links CD3 and activates the TCR complex was used to simulate the interaction of MHC complex (found on an antigen presenting cells (APC)) with the TCR (Nobrega et al. 1986; Lu & Durkin 1997). This method was compared to

activation using the anti-CD3 antibody coupled with an anti-CD28 antibody. The anti-CD28 antibody cross-links and activates the CD28 pathway which is required to provide a co-stimulation signal to the T-cell and prevent cell anergy. This signal is usually provided by the CD80-CD86 ligands on APCs during T-cell activation (Lenschow et al. 1996).

There was significant variation in the literature regarding the dose of anti-CD28 used to activate the T-cells. Therefore anti-CD3 alone and in combination with two concentrations of anti-CD28 (2.5µg/ml and 5µg/ml) was assessed on the T-cells. Spleenocytes were isolated from BALB/c mice and were pooled and enriched for $CD4^+$ cells using EasySep Mouse CD4+ T Cell Enrichment Kit (Stemcell technologies). Isolated $CD4^+$ cells were cultured with anti-CD3 alone (5µg/ml) or anti-CD3 with 2 concentrations of anti-CD28 (2.5µg/ml and 5µg/ml). Cells were stimulated for 3 days under these conditions and supernatants were collected for the measurement of IFN-γ, IL-2, IL-4 and IL-17.

Figure3.3 shows that the response of the T-cells to CD3 and CD3/CD28 were similar with significant production of IFN-γ, IL-2, IL-4 and IL-17 by stimulated cells. The two doses of anti-CD28 (2.5µg/ml and 5µg/ml), in combination with anti-CD3, induced a similar profile of cytokine secretion from activated cells, with both inducing secretion of IFN-γ, IL-2, IL-4 and IL-17. The doses of anti-CD28 were also similar to the control of anti-CD3 by itself **[Figure 3.3]**. While anti-CD3 was able to stimulate the cells to secrete cytokines alone, CD3 stimulation alone can lead to cell anergy in T-cells as the co-stimulation signal is not present (Bour-Jordan et al. 2011). Therefore plate bound anti-CD3 and anti-CD28 at a 2.5µg/ml dose was selected as the method of stimulation.

3.2.3 – A COMPARISON OF MAGENTIC AND COLUMN PURIFICATION METHODS FOR CD4⁺ T-CELL ISOLATION.

In order to determine the best method of $CD4^+$ T-cell isolation, two methods of cell isolation were investigated. A number of commercial methods are available for the isolation of specific cells based on antigen markers. Two of the main methods available are column enrichment and magnetic isolation. Both of these methods are negative isolation methods meaning that cells of interest are not bound by antibodies which may interfere with downstream assays.

Spleenocytes isolated from BALB/c mice were enriched for $CD4^+$ cells using EasySep™ Mouse $CD4^+$ T Cell Enrichment Kit (Stemcell technologies) and the Mouse $CD4^+$ T Cell Enrichment Column (R&D systems). In the column kit, spleenocytes were first treated to lyse the erythrocytes from the cell suspension; this was carried out using an ammonium chloride solution. The cell suspension was then mixed with a monoclonal antibody cocktail which binds T-cells and other cells that are not of interest during the 15min incubation. This mixed suspension was then loaded into the enrichment column which contains glass beads coated with Ig and anti-Ig. The mixture flows though the column by gravitational flow and cells tagged with the monoclonal antibody are bound to the column during an additional 15min incubation period. The anti-Ig beads and Ig also bind to B-cells via F(ab)-surface Ig, and monocytes via Fc interactions respectively removing them from the flow-through. The column is then washed and the sample is collected, centrifuged and made up in media before counting the cells.

Stemcells EasySep™ system uses negative selection to enrich the $CD4^+$ population from single cell suspensions of spleenocytes. Unwanted cells are removed by targeting

biotinylated antibody cocktails to non-$CD4^+$ T-cells. Tetrameric antibody complexes recognizing both biotin and dextran-coated magnetic particles then bind to these antibodies. The cell suspension is placed into a magnetic field which holds the labelled cells in place and the desired unlabelled $CD4^+$ T-cells are poured off. No column is involved in the isolation and there is no requirement to lyse erythrocytes before carrying out the isolation.

Following enrichment, cells were stained with anti-CD4 PE conjugated antibody (BD) and analysed using flow cytometry in order to compare the percentage purity of $CD4^+$ cells. Cells were gated on FSC, SSC in order to exclude cell debris **[Figure 3.4(a)]**. Cells were then gated on the PE positive population. This population represents the percentage of $CD4^+$ cells in the sample.

The percentage of $CD4^+$ cells obtained using the EasySep Magnetic enrichment was 94.8% **[Figure 3.4(b)]**. This method consistently yielded purities >90%, in agreement with the suppliers information. The T Cell Enrichment Column yielded lower purity 68.38% **[Figure 3.4(c)]**. Supplier's information indicates a purity of ~85%, however the percentage obtained was consistently ~70% when using this method. It is clear from these data that the magnetic separation method resulted in a higher percentage purity of $CD4^+$ cells. The magnetic cell separation method also required less preparation and less steps involving centrifuging the cells, which resulted in a higher viability in the magnetically separated cells. Viability was calculated using a haemocytometer and trypan blue exclusion **[Table 3.1]**. When cells become apoptotic, their membranes are compromised and allow the flow of material through an otherwise highly regulated membrane. Trypan blue can pass into the cell and stain the DNA in the nucleus a blue

colour. Counting the viable and non-viable blue stained cells using a haemocytometer determines the percentage of viable cells in culture. The magnetically isolated cells had a viability of 76.9%, which was higher than the viability observed for the column separation method of 73.5% **[Table 3.1].** It is possible that this loss of viability when using the column separation method is due to mechanical stress on the cells using the column method as discussed above.

3.2.4 - MAGNETIC ISOLATION OF CD4⁺ LYMPHOCYTES RESULTS IN ENHANCED CYTOKINE PRODUCTION FOLLOWING STIMULATION.

The two methods of $CD4^+$ cell enrichment were next compared by assessing the cytokine production from T-cells after isolation using the column and magnetic separation methods. $CD4^+$ cells were isolated using the magnetic enrichment or column enrichment kit and stimulated with 5µg/ml plate bound anti-CD3 and 2.5µg/ml anti-CD28 agonists. Cells were stimulated for 3 days and supernatants were collected and measured for IFN-γ, IL-4 and IL-17. Activation of T-cells induced significant levels of IFN-γ, IL-4 and IL-17. Magnetically enriched $CD4^+$ cells show an almost 2-fold higher production of all cytokines measured by ELISA **[Figure 3.5]**. This may be in part due to the increased viability observed in the previous comparison of the two methods. This confirmed the magnetic isolation as a more suitable method for enriching $CD4^+$ T-helper cells.

3.2.5 – VARIATIONS IN FETAL BOVINE SERUM (FBS) BATCHES EFFECTS CYTOKINE PRODUCTION IN CD4⁺ LYMPHOCYTES.

During the initial optimisation experiments some variability was observed in the levels of cytokines produced by the cells in independent experiments, therefore the media and culture conditions were examined in order to reduce these variations. The first component of the media examined was the Fetal Bovine Serum (FBS). Earlier experiments used different batches of FBS, furthermore, there was also variation in the method used in lab for heat inactivation of the FBS before use. In order to investigate the variability between batches and the effects of heat inactivation, batches of FBS were obtained from two companies, Gibco and Fisher, summarised in **[Table 3.2]**. Isolated $CD4^+$ cells were cultured in RPMI containing 1% PenStrep and 10% FBS from the various batches. The FBS tested were assigned letters, **A** and **B** are two different batches of the same FBS product sourced from GIBCO (Invitrogen life sciences), **C** is HyClone FetalClone FBS (ThermoFisher) and **D** is HyClone Research Grade (ThermoFisher). The FBS was heat-inactivated according the Gibco protocol for FBS heat-inactivation. Cells were stimulated in naïve conditions for 3 days. Supernatants were collected and assessed for levels of IFN-γ, IL-2, IL-4 and IL-17. There was variation in the levels of cytokine secreted by the cells when different FBS was used. The non-heat-inactivated samples from Gibco (A and B) resulted in low levels of cytokines following stimulation. All non heat-inactivated FBS (A, B, C, D) resulted in low or no secretion of IFN-γ, IL-2, IL-4 and IL-17. Heat-inactivated A and B from Gibco induced significant levels of IFN-γ, IL-2, IL-4 and IL-17. Heat inactivated C and D did not consistently result in high levels of cytokines with no IL-17 or IL-2 for heat-inactivated C **[Figure 3.6]**.

Given that the levels of cytokines were high using heat inactivated GIBCO batches A and B, and the fact that there was consistency between these batches, the Gibco FBS was selected for future use. A single batch of Gibco FBS was ordered in bulk in order to use the same batch in all future experiments. The heat inactivation method was set as a standard protocol and all FBS was heat inactivated on arrival and stored in aliquots at -20^{o}C.

3.2.6 - ADDITION OF IL-2 INCREASES THE PROLIFERATION OF CD4^{+} LYMPHOCYTES IN VITRO.

IL-2 has been identified as a proliferative factor for cloning CD4^{+} T-cells acting in an autocrine fashion (Smith 1988). Upon activation T-cells produce IL-2, however to further optimise the culture conditions the effects of adding additional IL-2 to the media was assessed with regards to proliferation of the cells.

Cells were stained with carboxyfluorescein succinimidyl ester (CFSE) dye before culturing. CFSE is a dye that converts to a fluorescent ester upon removal of acetate groups in the cell cytosol where it remains due to covalent bonds formed with intracellular molecules. As cells divide, so too does the dye and the intensity of the fluorescence is halved. Each peak of halved fluorescence intensity represents a generation of cells and generation numbers can be calculated using software algorithms (Quah et al. 2007). Dead cells were excluded from analysis using propidium iodide dye (PI) which was added 10 minutes before cell analysis. PI can pass through compromised membranes in apoptic/necrotic cells and stains the DNA thereby marking non-viable cells (Nicoletti et al. 1991). Cells were analysed using the BD FACs Aria; cells were gated on the viable population (PI negative cells) and fit using the CFSE proliferation algorithm on

the Flowjo Software (treestar). The software fits a Gaussian curve to each peak and the sum of the curves equals the distribution of the cells measured. This data can give the number of cell generations and the number of cells in each population.

Addition of IL-2 led to an increase in the number of generations of viable $CD4^+$ cells in culture **[Figure 3.7]**. The analysis shows there to be cells in the fifth generation of cells treated with IL-2 compared to only four generation of cells cultured without. This data confirms that IL-2 has a proliferative effect on T-cells in culture and may assist in maintaining T-cells *in vitro*. The next step in optimising the culture conditions was to assess the effects of supplementing the media with beta mercapto-ethanol (BME) in order to improve viability of the cells in culture.

3.2.7 – MEDIA SUPPLEMENTED WITH BME IMPROVES THE VIABILITY OF $CD4^+$ T-CELLS IN VITRO.

Beta mercapto-ethanol (BME) breaks down cystine provided by the FBS allowing T-cells to convert it into the amino acid cysteine which is necessary for cell growth. It is also a reducing agent and has the ability to break down toxic metabolites in the media leading to improved culture conditions (Chang et al. 1982)**.** Therefore, the addition of BME was assessed as to whether it would further improve supplemented media for optimal conditions to culture primary $CD4^+$ cells. Enriched $CD4^+$ cells were cultured for 5 days in media with and without 50μM BME. As previous experiments have shown, the addition of IL-2 increases the proliferation of $CD4^+$ T-cells *in vitro*. Therefore the viability over 5 days was also assessed after the addition of IL-2 alone and IL-2 in combination with BME. Propidium iodide dye (PI) was used to assess cell death. As

previously described above, cells that are apoptotic have a compromised membrane that allows the dye to enter the cell and stain the nucleus.

Samples were taken on day 1, 2, 3 and 5 and cells were gated on live cells as determined by PI staining and analysed on the BD FACs Aria. The percentage of viable cells in each condition over the 5 days is represented in **Figure 3.8.** The control cells and all treatment conditions have the same viability on day one with the combination of BME and IL-2 showing the highest viability. On day 2 there is a further improvement in viability for all groups. By day 3 the control and IL-2 treated cells have a significant decrease in viability, this is not the case for the BME and BME+IL-2 treated cells which show further improvement with a small decrease for all groups on day 5. The common factor in the groups showing an improved viability over 5 days was the addition of BME, IL-2 alone was not sufficient to improve the viability of the cells over the 5 days and BME alone had a similar effect to the addition of BME in combination with IL-2. BME significanlty increased the viability of $CD4^+$ T-cells *in vitro* and was added to the culture media for all cell culture work at a final working concentration of 50μM.

3.2.8 – OPTIMISATION OF Th17 $CD4^+$ T-CELL POLARISATION IN VITRO.

Following the optimisation of the cell isolation, activation and media conditions required for $CD4^+$ T-helper cells, the next step was to optimise the polarisation of $CD4^+$ T-cells into specific cell subsets. The first to be optimised was the Th17 cell subset. IL-17 is the characteristic cytokine secreted from the class of $CD4^+$ T helper cells designated Th17 cells. In order to obtain this subset it is necessary to activate STAT3 and the transcription factor RORγt. This is the master regulator for the IL-17 gene and defines the Th17

subset. IL-6 is also necessary for the activation of STAT3 and RORγt and is required for the Th17 polarisation (Ivanov et al. 2006; Zhou et al. 2007). TGF-β was later recognised as a necessary stimulator of both Th17 cells and Treg cells, however, in the presence of IL-6 it drives cells to a Th17 cell subset. IL-23 is responsible for expanding Th17 cells but is not sufficient on its own to drive naïve cells into Th17 cells (Zhou et al. 2007). IL-1β, one of the last cytokines that has been linked with Th17 cell subsets, has been shown to induce naïve T-cells to produce IL-17 *in vitro* (Chung et al. 2009). Combinations of these cytokines were tested in order to determine the cytokines necessary for generating Th17 cells. A neutralising anti-IFN-γ antibody was also added to block the generation of a Th1 subset which inhibits Th17 cell polarisation**.**

$CD4^+$ enriched T-helper cells were cultured in media supplemented with IL-6 (20ng/ml), IL-23 (20ng/ml), IL-1β (10ng/ml) and neutralising anti-IFN-γ antibody (10μg/ml) with and without the addition of TGF-β (0.2ng/ml). Cells were stimulated with 5μg/ml coated anti-CD3 and 2.5μg/ml anti-CD28 for 3 days. Cells were then transferred to fresh media without recombinant cytokines and further stimulated with 5μg/ml coated anti-CD3 and 2.5μg/ml anti-CD28 for 24 hours before collecting supernatants for ELISA cytokine analysis (R & D duosets). Both cells cultured with and without TGF-β showed a typical Th17 profile with high IL-17 and low IFN-γ and IL-4 [**Figure 3.9]**. While the cells stimulated in the presence of TGF-β resulted in a small increase in IL-17; this data indicates that there is no requirement for TGF-β in the polarisation of Th17 cells *in vitro.*

3.2.9 – T-CELLS CULTURED IN Th17 POLARISING CONDITIONS EXPRESS THE TRANSCRIPTION FACTOR RORγt

In order to confirm the Th17 subset it was necessary to stain for the transcription factor RORγt. RORγt is the master regulator and transcription factor necessary to commit naïve T-cells to a Th17 lineage. It is activated by IL-6 and along with activation of the STAT3 transcription factor, leads to the production of IL-17 in T-cells. $CD4^+$ enriched cells were isolated and stimulated with plate bound anti-CD3 and anti-CD28 in the presence of IL-6, IL-1β, IL-23 and a neutralising anti-IFN-γ antibody. Cells were stimulated over three days, permeablised and stained for intracellular RORγt using a primary conjugated APC labelled anti RORγt antibody (eBioscience) at a number of timepoints (2, 18, 48 and 72hrs). In order to optimise the staining of these cells, the amount of antibody required was also titrated and a time course was carried out. The results show an increase in the expression of RORγt over time in the cells **[Figure 3.10(a)]**. The grey shaded peak is the isotype control staining antibody which is an antibody of the same isotype and conjugated with APC but not targeted to RORγt, it acts as a control for non-specific staining. The biggest increase is detectable at 18hrs with an increase of mean fluorescence intensity (MFI) of 45.9 between the isotype and the sample, although significant RORγt staining is still present at 48 and 72hrs.

At all time points supernatants were collected and measured for levels of IL-17**.** The secretion of IL-17 is evident at 18hrs and increased steadily over the 72hrs **[Figure 3.10(b)]**.

3.2.10 – INVESTIGATION OF DIFFERENT Th17 CELL SUBSETS GENERATED IN THE ABSENCE/PRESENCE OF TGF-β.

Up to this point all experiments were carried out by polarising Th17 cells using IL-6, IL-1β, IL-23 and neutralising IFN-γ antibody in supplemented media. Although the literature suggests a requirement for the presence of TGF-β, a Th17 cell subset was confirmed by ELISA and intracellular transcription factor staining without TGF-β. A paper published by Ghoreschi K *et al* (2010) described a Th17 cells subset generated in the presence of IL-6, IL-1β and IL-23 with no TGF-β. The paper describes the subset used in this study generated without TGF-β and also compares them to the subset generated in the presence of TGF-β.

Ghoreschi *et al* (2010) describe the subset generated in the absence of TGF-β as a more pathogenic Th17 cell. These cells are able to class switch to express T-bet after committing to RORγt transcription factor expression and are capable of simultaneous IFN-γ and IL-17 production in certain conditions. Given the aim of this model was to define the SNARE components involved in IFN-γ and IL-17 production separately in Th1 and Th17 cells, this method of Th17 polarisation was not suitable for the study. It was therefore necessary to reassess the effects of TGF-β and investigate these subsets to ensure that a single IL-17 producing cell subset is obtained.

T-cell isolations to this point have been based on the isolation of $CD4^+$ cells from the spleenocytes of mice. This population contains naïve $CD4^+$ effector cells capable of polarising into specific subsets, but it also contains a population of effector memory cells which have already polarised into a specific cells subtype. Although this population can be effectively polarised into T-helper cell subsets and is suitable for the screening of T-

cell populations for SNARE associated cytokine secretion, in order to specifically investigate the effects of TGF-β on polarisation of naïve $CD4^+$ T-helper cells, T-cells enriched using the easysep™ stemcell $CD4^+$ enrichment kit were further sorted for pure naïve T-cells based on high CD62L ($CD62L^{Hi}$) and low CD44 ($CD44^{Lo}$) surface marker expression. Sorting cells using Fluorescent Activated Cell Sorting (FACS) allows pure naïve T-cells ($CD62L^{Hi}$/ $CD44^{Lo}$) to be separated from effector and central memory T-cells. This will allow the study of TGF-β to be carried out specifically on the naïve polarising cells.

Sorted naïve T-helper cells were stimulated with 5μg/ml plate bound anti-CD3 and 2.5μg/ml anti-CD28 antibody in the presence of neutralising IFN-γ (10μg/ml), IL-1β (10ng/ml), IL-6 (20ng/ml), IL-23 (20ng/ml) and with or without TGF-β (0.2ng/ml) for 3 days. Cells were put in fresh media and re-stimulated for 24 hours. Supernatants were collected and analysed for cytokines**.** Cells cultured with TGF-β have similarly high levels of IL-17 to the cells generated without TGF-β. However, while levels of IL-2 are detected in the Th17 cells generated without TGF-β, IL-2 levels are significantly reduced in the Th17 cells polarised with TGF-β. Levels of IL-10 are significantly reduced in naïve sorted T-helper cell subsets that have been polarised into Th17 cells **[Figure 3.11]**. The two subsets generated show similar results to the cells described in the paper. This was further confirmation of the Th17 cell subsets which correlated with the study by Ghoreschi *et al* (2010).

To confirm the Th17 subsets, and to investigate the culture for IFN-γ/IL-17 double producing cells, the cells were stained for intracellular cytokines to assess the total percentage of IL-17 and IFN-γ producing cells. Cells were cultured for 3 days and re-

stimulated with anti-CD28 and plate bound anti-CD3 antibody for 24 hours. Monensin, a carboxylic ionophore that interrupts intracellular transport leading to an accumulation of cytokine in the Golgi complex, was added for the final 4 hours. This allows cytokines in the cells to be stained using fluorescent antibodies and cytokine production from individual cells to be characterised (Foster et al. 2007).

Cells cultured in Th17 skewing environment show positive staining for intracellular IL-17. Of the cells cultured with TGF-β, more than 10% of these cells were IL-17 producing cells. This is compared to the IL-23 polarised cells of which ~4% are IL-17 producing cells. Cells cultured in both of these conditions have low levels of IFN-γ and IL-4 producing cells **[Figure 3.12]**.

Despite the low levels of IFN-γ or IFN-γ/IL-17 double producers, studies have shown that cells polarised without TGF-β have the ability to class switch to T-bet/RORγt positive, IFN-γ/IL-17 double producing cells in Th1 polarising conditions even after commitment to the Th17 cell subset. Therefore it was necessary to use TGF-β in the conditions for polarising Th17 cells; these conditions also have the added benefit of producing a higher percentage of IL-17 secreting cells *in vitro*. Isolating naïve T-cell populations greatly decreases the number of cells obtained from the spleens of mice. Therefore, the $CD4^+$ enriched T-cells were used to identify initial SNARE candidates as described in the next chapter, and a naïve $CD4^+$ T-cell population will be used in later chapters to study specific SNAREs in detail.

3.2.11 – OPTIMISATION OF Th1 CD4$^+$ T-CELL POLARISATION IN VITRO.

Th1 cells are characterised by production of the hallmark cytokine IFN-γ. In order to identify a Th1 polarised T-cell subset the levels of IFN-γ relative to other T helper cell cytokines produced by the cells are assessed. To drive cells into Th1 subset it is necessary to activate the master regulator T-box transcription factor TBX21 (T-bet). T-bet controls transcription of the Th1 hallmark cytokine IFN-γ. IL-12 has been identified as a signalling cytokine responsible for triggering STAT4 and subsequent T-bet activation leading to an IFN-γ production. IFN-γ, a strong inducer of T-bet, then acts in an autocrine fashion to further drive Th1 polarisation (Schulz et al. 2009; Szabo et al. 2000). T-bet transcription is inhibited by GATA-3 expression as it down-regulates STAT4 expression and independently suppresses IFN-γ expression (Usui et al. 2003; Yagi et al. 2010). GATA-3 is activated through IL-4 signalling, a product of Th2 polarised cells. Therefore, in order to block IL-4 signalling an anti-IL-4 antibody was added with IL-12 to trigger T-bet activation and IFN-γ expression.

In order to establish a method for the generation of a Th1 subset, CD4$^+$ T helper cells were cultured in media supplemented with and without 10ng/ml rmIL-12 and 10μg/ml anti-IL-4 antibody (R & D) and stimulated in fully supplemented RPMI using 5μg/ml plate bound anti-CD3 and 2.5μg/ml anti-CD28 antibody. Supernatants were collected on day 3 and measured for cytokine secretion using ELISA. Cytokine analysis showed that the secretion of IFN-γ from these cells is significantly greater than their secretion of IL-4 and IL-17, which were secreted in very low levels in comparison **[Figure 3.13(a)]**. Next the IFN-γ secretion profile of the Th1 cells was compared to the Th17 cell subsets. As

expected, Th1 cells had a significantly higher level of IFN-γ production when compared to Th17 generated cells **[Figure 3.13(b)].** For further experiments involving the Th1 subset, Th1 polarisation was carried out using 10ng/ml IL-12 and 10μg/ml anti-IL-4 antibody.

3.2.12 – T-CELLS CULTURED IN Th1 POLARISING CONDITIONS EXPRESS THE T-BOX TRANSCRIPTION FACTOR T-BET.

In order to confirm that cells generated in the Th1 conditions used are indeed Th1 cells, it was necessary to stain the cells and confirm the expression of the transcription factor and master regulator T-bet which has been identified as a master regulator of IFN-γ producing Th1 cells (Szabo et al. 2000)**.** To measure expression of T-bet, $CD4^+$ cells were cultured and activated in Th1 and Th17 polarising conditions for 3 days. Cells were permeablised and stained for intracellular transcription factor T-bet using PE conjugated anti T-bet antibody (BD). Given that Th0 stimulated cells secrete an array of cytokines and express high levels of transcription factors from all subsets, T-bet expression of the Th1 cells was compared to a Th17 polarised subset of cells which expresses T-bet at lower levels.

Figure 3.14 demonstrates that the expression of the T-bet transcription factor in Th1 cells is higher than that of Th17 cells with an increase in the MFI from 25.9 to 33.6, and in an increase in the PE Median from 12.0 to 15.8, further confirmation for a polarised Th1 subset *in vitro.*

3.2.13 – T-CELLS CULTURED IN Th1 POLARISING CONDITIONS EXPRESS THE SURFACE PROTEIN CCR5.

To further confirm the Th1 cell subset, cells were stained for the chemokine surface protein receptor CCR5. CCR5 has been shown to be up-regulated on the surface of Th1 cells following activation with 10ng/ml IL-12 (Qin et al. 1998). $CD4^+$ enriched cells were cultured and activated in Th1 polarising conditions for 3 days. The cells were then transferred to fresh media and re-stimulated for a further 24 hours. Cells were blocked and stained for the surface receptor CCR5 using a PE conjugated anti CCR5 antibody (BD). Cells were acquired on the BD FACS Aria and data was analysed using the FlowJo software (treestar). Stimulation of cells in Th1 polarising conditions resulted in an up-regulation of surface chemokine receptor CCR5. PE median intensity increased from 10.4 to 13.8 between the naïve and Th1 cells **[Figure 3.15]**.

3.2.14 – OPTIMISATION OF Th2 $CD4^+$ T-CELL POLARISATION IN VITRO.

Although Th2 cells are not the main focus of this thesis, this subset may be necessary for comparison to Th1 and Th17 subsets in future experiments. Therefore the culture protocol was optimised to generate a Th2 subset. IL-4 is the characteristic cytokine secreted by Th2 cells. In order to polarise naïve T-cells into a Th2 cell subset it is necessary to culture cells in the presence of IL-4 and a neutralising IFN-γ antibody. IFN-γ is responsible for driving a Th1 cell subset, which directly inhibits the generation of Th2 cells (Gajewski & Fitch 1988; Ouyang et al. 1998). IL-4 is a direct inducer of STAT6 which leads to GATA-3 activation and Th2 polarisation (Zheng & Flavell 1997).

As well as being a T-cell growth factor, as shown previously, IL-2 is a strong inducer of STAT5. STAT5, independent of GATA-3, enhances IL-4 production which acts in a autocrine fashion as an inducer of STAT6 and GATA-3 activation and further polarisation of Th2 cells (Cote-Sierra et al. 2004).

Isolated $CD4^+$ enriched T-cells were stimulated in supplemented RPMI in the presence of 10μg/ml neutralising anti-IFN-γ antibody, 10ng/ml IL-4 and 20ng/ml IL-2 for 3 days. Cells were then transferred to fresh medium and re-stimulated with 5μg/ml plate bound anti-CD3 and 2.5μg/ml anti-CD28 and for 24 hours without recombinant cytokines and antibody. This was in order to accurately measure the concentration of IL-4 produced by the cells. These cells were measured for cytokines using ELISA (R&D). The profile of cytokines observed was as expected with high levels of IL-4 and IL-2 and low levels of IL-17 and IFN-γ **[Figure 3.16]**.

3.2.15 – T-CELLS CULTURED IN Th2 POLARISING CONDITIONS EXPRESS THE TRANSCRIPTION FACTOR GATA-3.

In order to confirm the Th2 subset, cells were stained for the Th2 master regulator GATA-3. Th2 cells are polarised from naïve cells after IL-4 signalling and STAT6 activation of the transcription factor GATA-3 (Zheng & Flavell 1997)**.** In order to stain Th2 cells for GATA-3, $CD4^+$ T-cells were stimulated with 5μ/ml plate bound anti-CD3 and 2.5μg/ml anti CD28 antibodies for 3 days in Th2 and Th17 (for comparison) polarising conditions. Cells were then transferred to fresh media containing no recombinant cytokines and re-stimulated with plate bound anti-CD3 and anti CD28 for a further 24 hours. Cells were permeabilised and stained for the intracellular transcription factor GATA-3 using an APC-Cy7 conjugated anti-GATA-3 antibody (BD). Cells were

acquired on the BD FACS Aria and data was analysed using the FlowJo software (treestar). Stimulation of cells in Th2 polarising conditions resulted in an up-regulation of GATA-3 in Th2 polarised cells when compared to Th17 polarised cells with an increase to 14.56 MFI for Th2 cells compared to 8.65 MFI for the Th17 cells **[Figure 3.17]**.

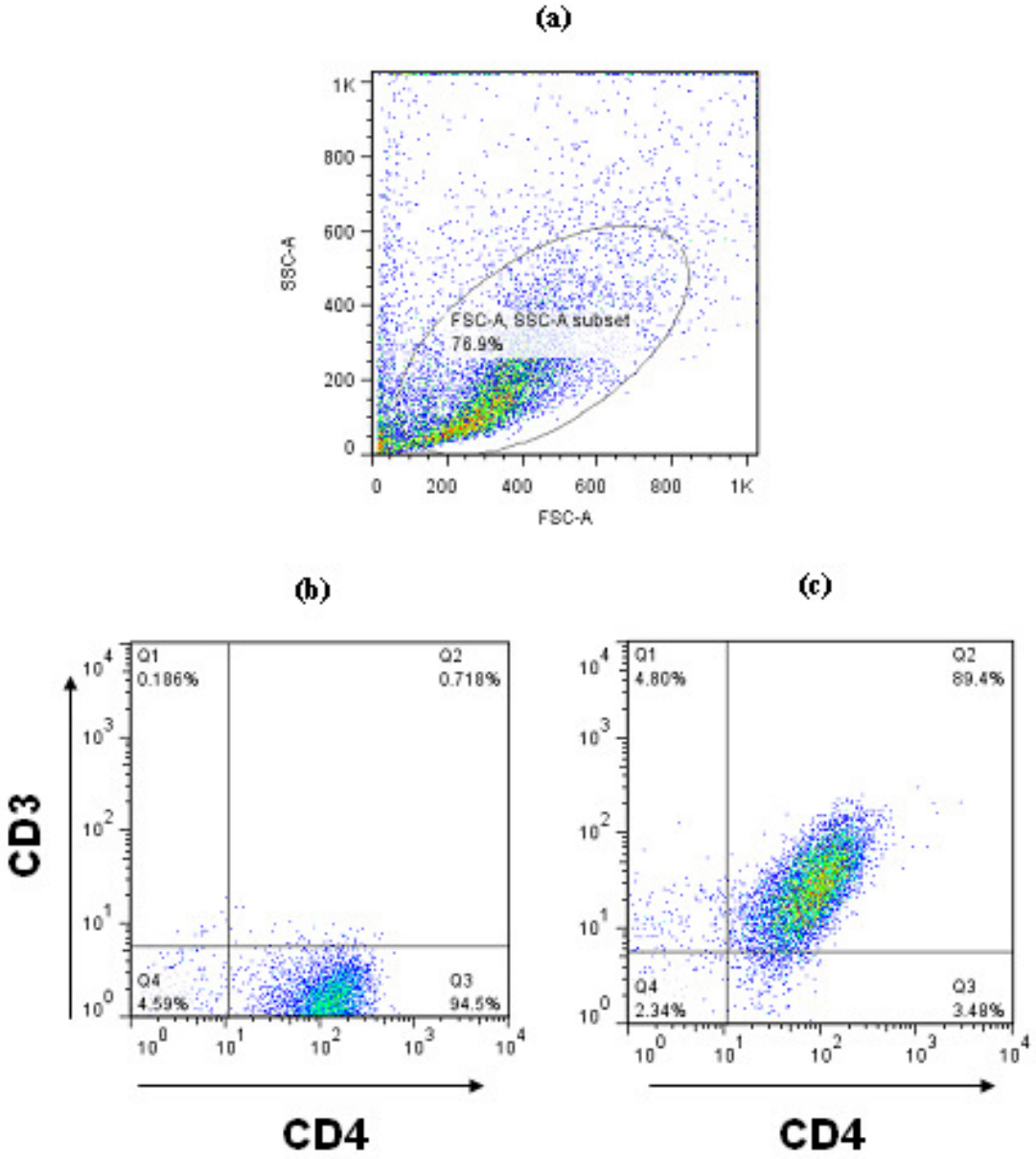

Fig.3.1 – CD3 and CD4 surface staining on CD4$^+$ T-helper subset. Cells were isolated from the spleens of female balb/c mice. Erythrocytes were lysed using an erythrocyte lysing kit (BD). CD4+ T cells were negatively selected using magnetic separation (Stemcell) according to manufacturer's instructions. Cells were stained with anti mouse antibodies from BD. Cells were analysed using the BD FACS Aria flow cytometer. **(a)** FSC and SSC gating to remove dead cells and debris from analysis. **(b)** The dot plot represents magnetically isolated CD4$^+$ cells stained with a primary PE conjugated anti-CD4 antibody. The dot plot indicates that the cells are 94.5% CD4$^+$ cells. **(c)** Cells were stained with primary PE conjugated anti-CD4 antibody and primary FITC conjugated anti-CD3 antibody. The cells were double stained and single stained samples were used to compensate for the fluorescent emission overlap of FITC and PE. The dot plot indicates 89.4% of the cells are positive for both CD3 and CD4 (Q2).

	Spleenocytes (x10^6)	$CD4^+$ T-cells (x10^6)	% Purity	% Viability
Magnet	200	21.32	94.80	76.9
Column	200	13.66	63.63	73.5

Table 3.1 – Comparison of magnetic and column isolation methods

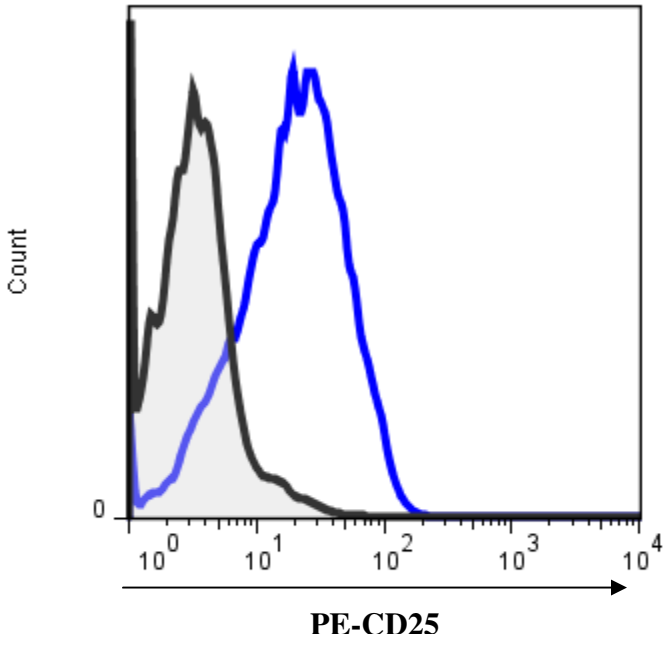

	Sample Name	Mean , PE-A	Median , PE-A
	Specimen_001_Group 5- Unstim.fcs	4.93	2.75
	Specimen_001_Group 5-Stim1.fcs	27.2	20.1

Fig.3.2 – Comparison of CD25 expression on unstimulated and stimulated T-cells. $CD4^+$ T-cells were negatively selected using magnetic isolation (Stemcell) according to manufacturer's instructions. Cells were either stimulated with plate-bound anti-CD3 (5 µg/ml) plus anti-CD28 (2.5 µg/ml) or left in culture unstimulated for three days. Cells were collected and stained for CD25 using PE labelled primary conjugated anti-CD25 antibody (BD). Cells were analysed using a BD FACS Aria and data was analysed using FlowJo Software (treestar). Cells were gated on $CD4^+$ expressing cells and histograms of CD25 expression are overlayed showing an increase in expression of CD25 on stimulated cells.

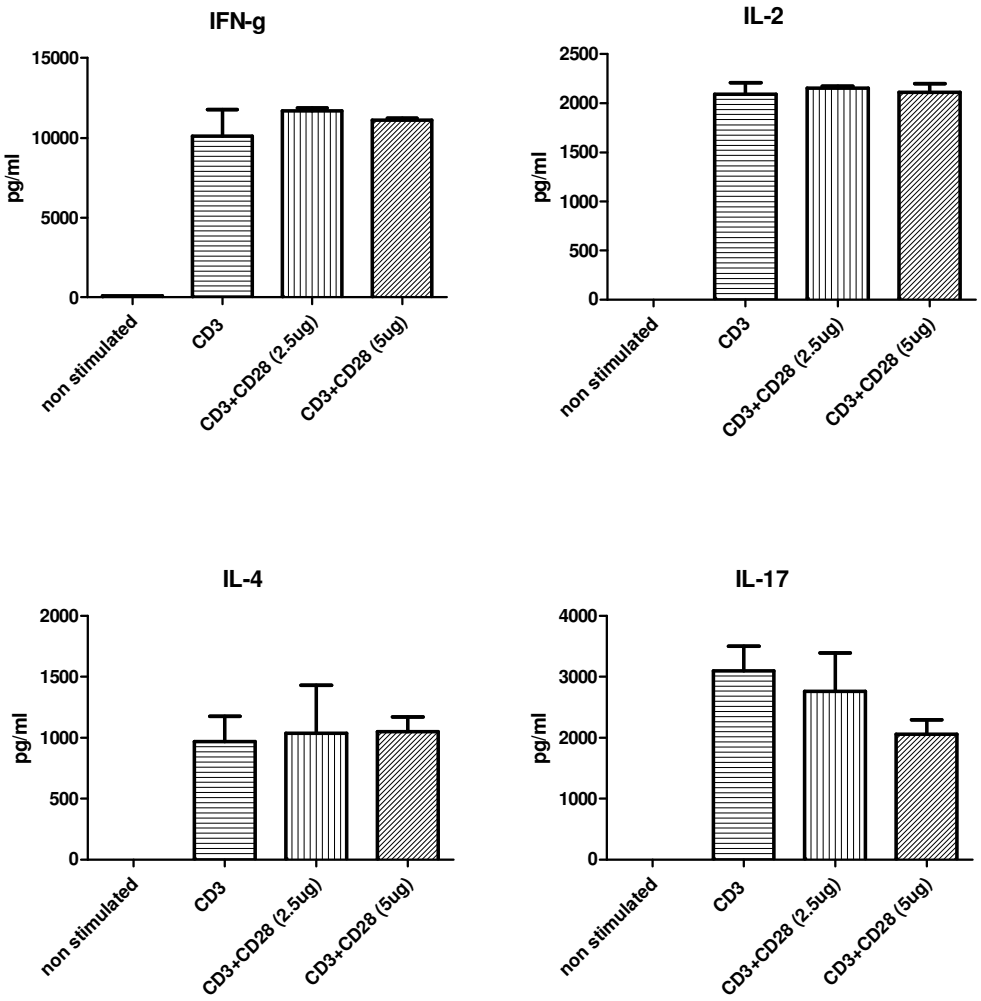

Fig. 3.3 – Comparison of CD3 and different doses of anti CD28 agonist. Cells were isolated from the spleens of female balb/c mice. Erythrocytes were lysed using an erythrocyte lysing kit (BD). $CD4^+$ T cells were negatively selected using magnetic separation (Stemcell) according to manufacturer's instructions. Plates were coated with anti-CD3 antibody (5μg/ml) for two hour at room temperature. Cells were then plates in either uncoated wells, wells with anti-CD3 only or in wells with two different concentrations of anti-CD28 (2.5μg/ml and 5μ/ml). T-cells were left for 3 days in media and supernatants were collected for measurement of cytokines by ELISA.

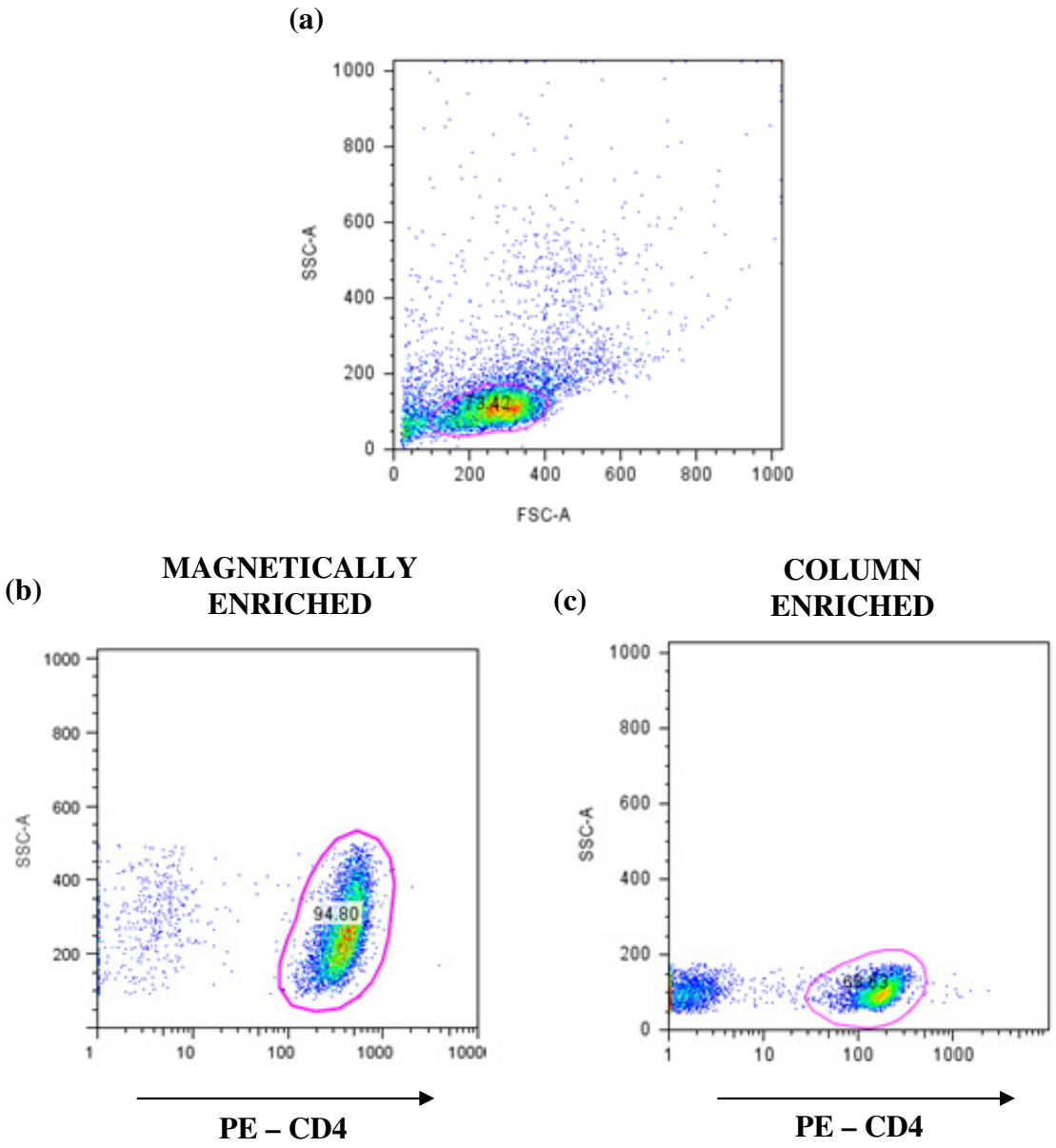

Fig.3.4 - Magnetic isolation of CD4$^+$ cells yields a higher purity when compared to column separation methods. Cells were isolated from the spleens of female balb/c mice. Erythrocytes were lysed using an erythrocyte lysing kit (BD). CD4+ T cells were negatively selected using column (R&D) or magnetic separation (Stemcell) according to manufacturer's instructions. Cells were stained with anti mouse CD4 antibody (BD). Cells were analysed using the BD FACS Aria flow cytometer. **(a)** FSC and SSC plot showing gating of the cells to exclude dead cells and debris. **(b)** Dot plot of magnetically enriched CD4$^+$ cells. Cells are gated on the PE positive population, 94.8% are PE positive cells. **(C)** Dot plot of column separated enriched CD4$^+$ cells. Cells are gated on PE positive population, 68.8% are PE positive. Data was generated using Flowjo software (treestar). Cells were selected after gating out dead cells and debris based on FSC and SSC.

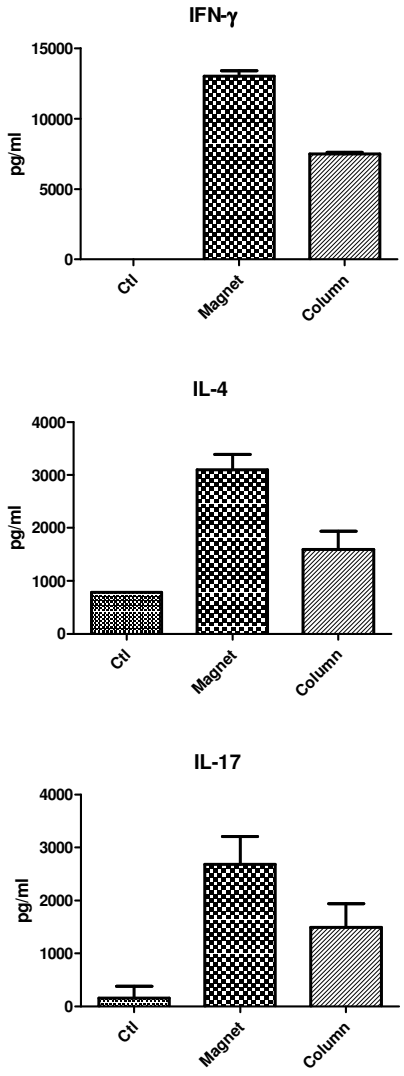

Fig.3.5 – Comparison of magnetic and column purified cells after stimulation. CD4+ T cells were negatively selected using magnetic (Stemcell) or column (R&D) separation according to manufacturer's instructions. Cells were stimulated with plate-bound anti-CD3 (5 μg/ml; 145-2C11) plus anti-CD28 (2.5 μg/ml; 37.51); Cells were stimulated and supernatants were collected after three days and analysed using ELISA duo kits from R&D.

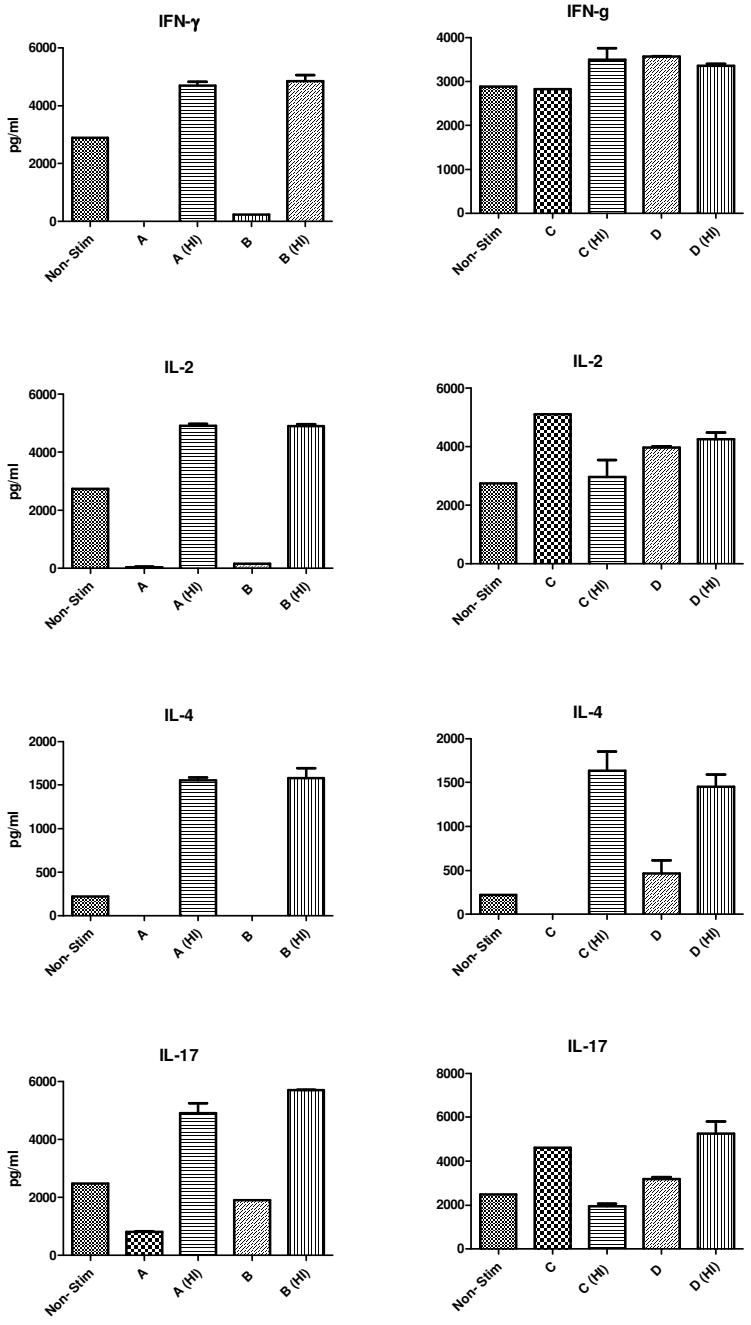

Fig 3.6 - Batch testing of heat inactivated Fetal Bovine Serum. CD4+ T cells were negatively selected using magnetic separation (Stemcell Cat# 19752) according to manufacturer's instructions. Cells were stimulated with plate-bound anti-CD3 (5 ug/ml) plus anti-CD28 (2.5 ug/ml). Media was supplemented with a range of Fetal Bovine Serum batches from Sigma, Gibco and ThermoFisher (10%). Fetal Bovine Serum was heat inactivated for 30mins at 56^{o}C and left to cool at room temperature. Cells were stimulated and supernatants were collected and analysed after three days in culture using ELISA duo kits from R&D.

Designation	Brand Name	Cat Number	Lot Number
A	GIBCO FBS	10270	41G8102K
B	GIBCO FBS	10270	41F8294K
C	HyClone FetalClone	SH30080.02	AVK53532
D	HyClone Research Grade	SV30160.02	RVE38189

Table 1.2 – Description of FBS suppliers and lots analysed and designated labels

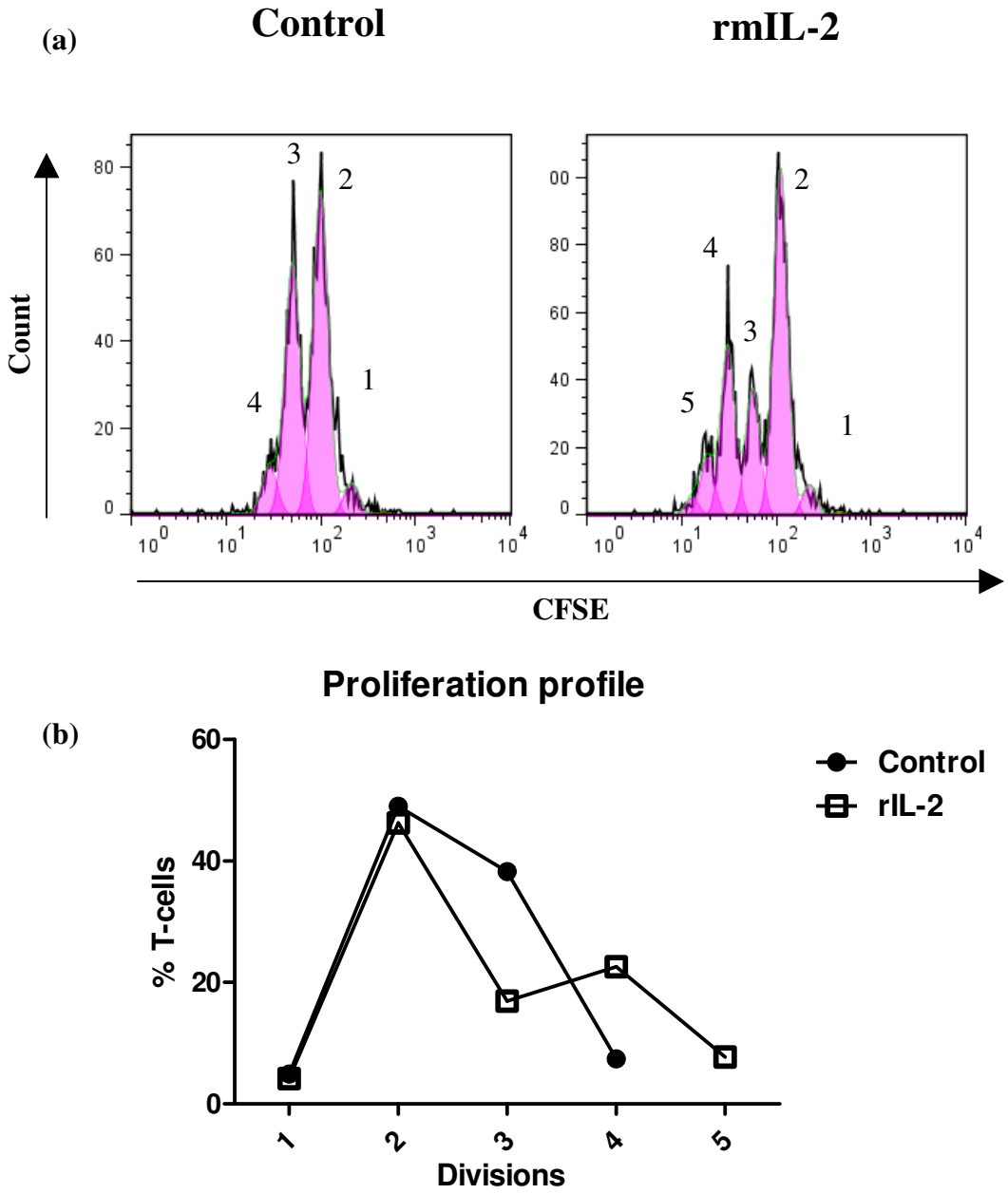

Fig 3.7 – Effects of IL-2 on cell proliferation in supplemented media. Cells were isolated from female balb/c mice using easysep CD4+ Isolation (Stemcell Cat# 19752). Cells were stained with CFSE dye (5µM; eBioscience) for 10 minutes before washing with PBS and fresh medium and plated at 2x106/ml in a 24 well plate. Cells were stimulated with plate-bound anti-CD3 (5 µg/ml) plus anti-CD28 (2.5 µg/ml). Cells were re-stimulated for 3 days and stained with Propidium Iodide (Miltenyi Biotech) for dead cell exclusion and read on a BD FACS Aria. Data was analysed using Flowjo software (Treestar). (a) Proliferation curves generated for each sample using Flowjo software. Each generation of cells is indicated by a number above the peak. (b) Graph of the proliferation profile showing the numbers of cells in each generation calculated using the proliferation algorithm in flowjo analysis software.

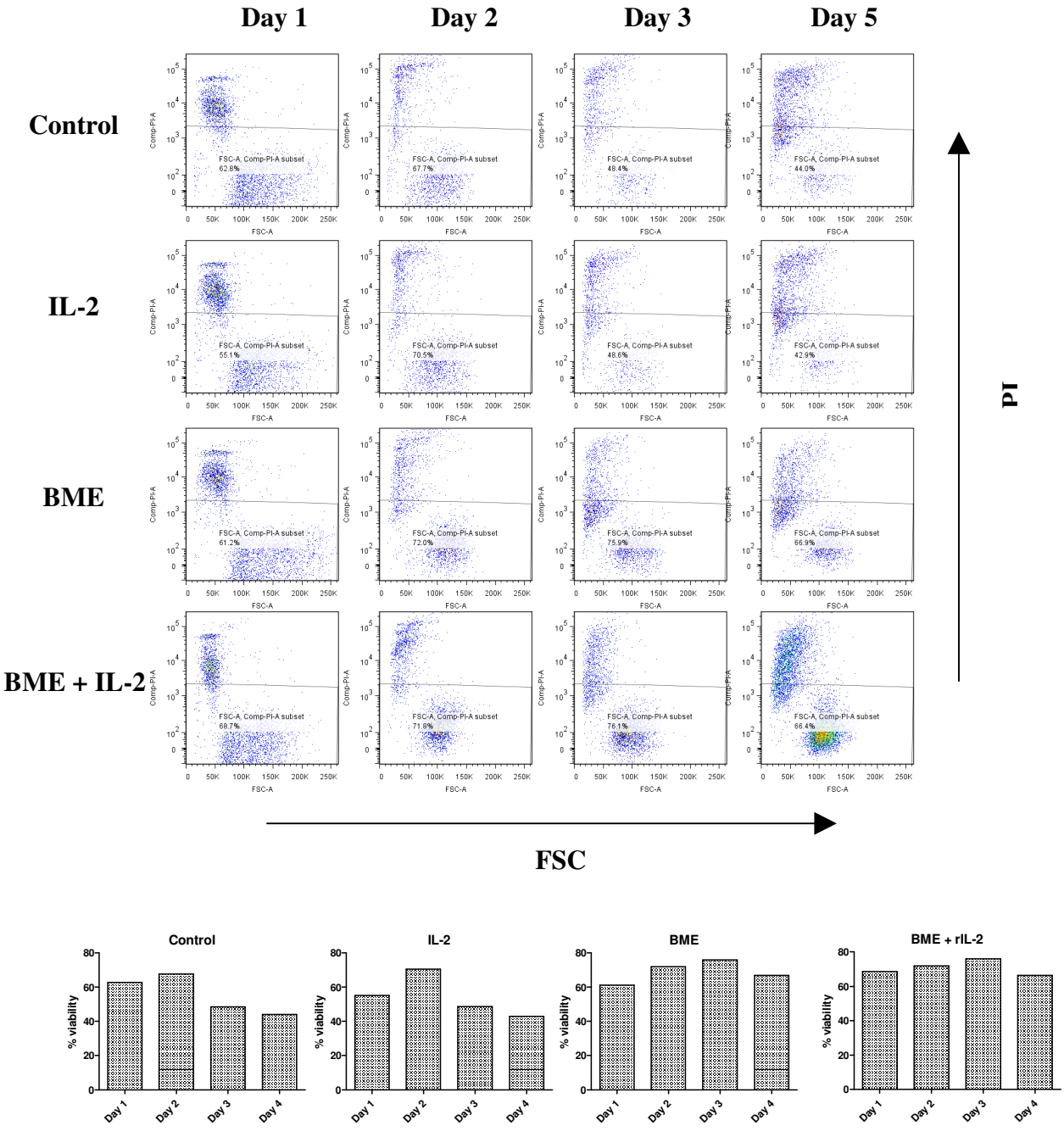

Fig 3.8 – Effects of BME on cell viability. Cells were isolated from female balb/c mice using easysep CD4+ Isolation (Stemcell Cat# 19752). Cells were stained with CFSE dye (5µM; eBioscience) Cells were plated at 2x106/ml in a 24 well plate. Cells were stimulated with plate-bound anti-CD3 (5 ug/ml; 145-2C11) plus anti-CD28 (2.5 ug/ml; 37.51. Cells were re-stimulated in fresh media on day 3. 50µl of cell culture was removed on days 1, 2, 3, 5 and 6 and stained with Propidium Iodide (Miltenyi Biotech) and read on a BD FACS Aria I within 30mins**.**

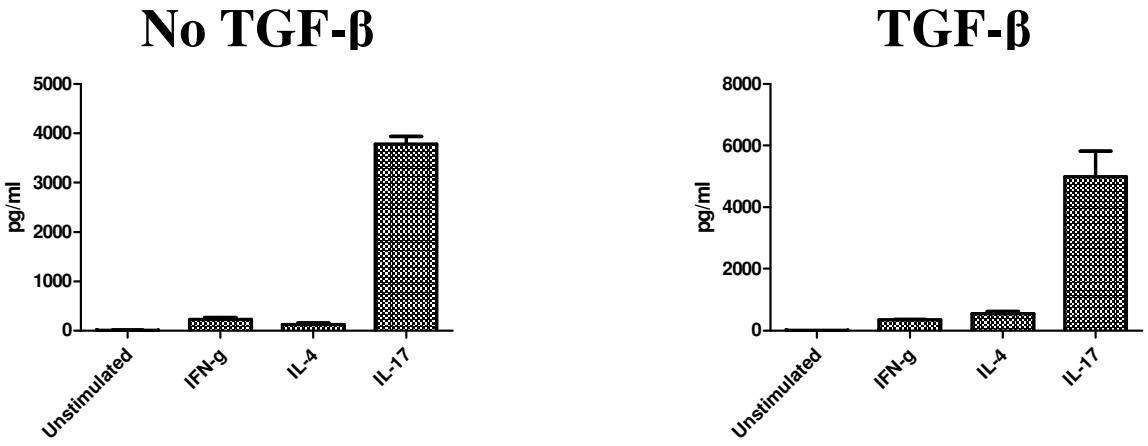

Fig 3.9 – Cytokine profiles for polarised Th17 T-cells with and without TGF-β. Cells were isolated from female balb/c mice using easysep CD4+ Isolation (Stemcell). Cells were plated at $2x10^6$/ml in a 24 well plate. Cells were stimulated with plate-bound anti-CD3 (5 μg/ml) plus anti-CD28 (2.5 μg/ml) in media supplemented with anti-IFN-γ, IL-1β, IL-6 and IL-23 with and without TGF-β. Cells were re-stimulated in fresh media on day 3 with anti-CD28 and anti-CD3 for 24hours. Supernatants were collected and analysed using ELISA according to manufacturer's instructions (R&D duoset). Profile shows an increase in IL-17 relative to IFN-γ and IL-4. The high level of IL-17 in relation to these cytokines is indicative of a Th17 cell subset. TGF-β stimulated cells secrete a higher level of IL-17.

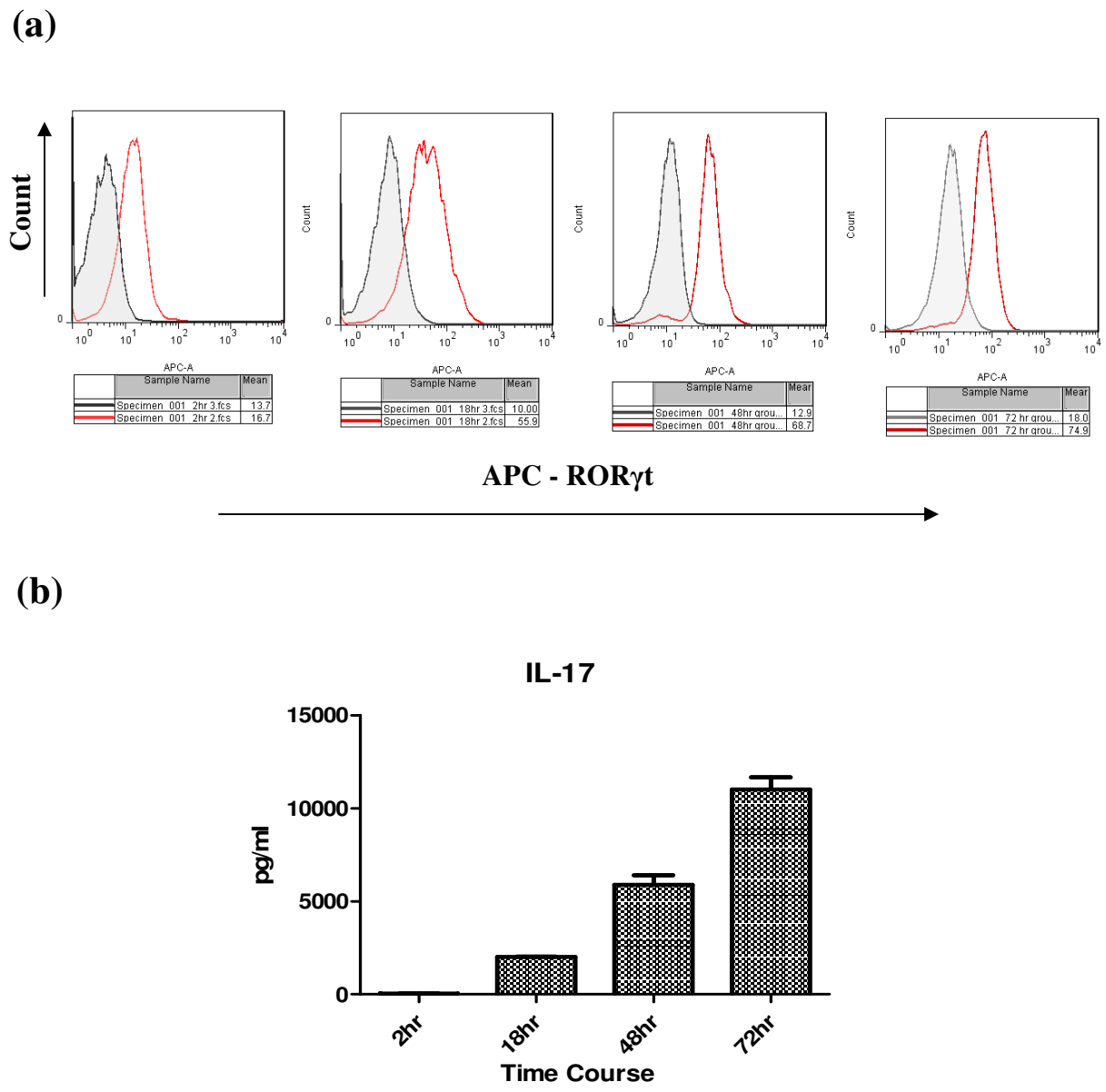

Fig 3.10 – Transcription factor staining for T-helper subsets. Cells were isolated from female balb/c mice using easysep CD4+ Isolation (Stemcell Cat# 19752). Cells were plated at $2x10^6$/ml in a 24 well plate. Cells were stimulated with plate-bound anti-CD3 (5 μg/ml) plus anti-CD28 (2.5 μg/ml) in the media supplemented with neutralising anti-IFN-γ, IL-1β, IL-6 and IL-23 cytokines for 3 days. Samples were taken at 2, 18, 48 and 72hrs. **(a)** Cells were collected at each time point and stained for intracellular IL-17 using APC primary conjugated anti RORγt transcription factor antibody (ebioscience). Cells were analysed on BD FACs Aria I, data was analysed using Flowjo software (treestar). Cells were stained with an APC conjugated isotype (grey) and overlayed with the RORγt staining (red). Cells were gated on $CD4^+$ cells and histograms represent the fluorescence intensity measured for each conjugated antibody relative to protein expression. Flow cytometry show an increase in RORγt staining over time, there is also a slight increase in non specific staining with the isotype at 24 hours. **(b)** Supernatants were collected and analysed by ELISA (R&D) to confirm the production of Il-17 over time at each time point. ELISA results show an increase in IL-17 cytokines over time.

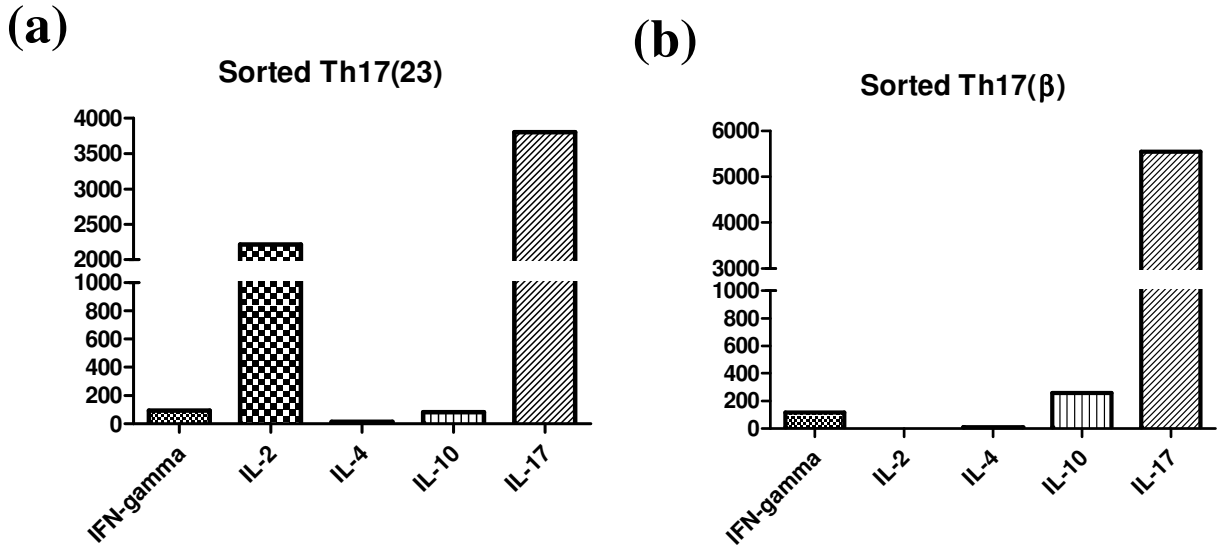

Fig 3.11 - Cytokine profiles for sorted T-helper subsets Th17(23) and Th17(β) . Cells were isolated from female balb/c mice using easysep CD4+ Isolation (Stemcell). Cells were stained with anti-mouse CD4, CD44 and CD62L antibodies (BD) and sorted on a BD FACS Aria I for $CD4^{+}$, $CD62L^{LO}$, $CD44^{+}$ Cells. Cells were plated at $2x10^{6}$/ml in a 96 well plate. Cells were stimulated with plate-bound anti-CD3 (5 μg/ml) plus anti-CD28 (2.5 μg/ml) in media supplemented with anti-IFN-γ, IL-6, IL-1β and either **(a)** IL-23 (Th17(23)) or **(b)** TGF-γ (Th17(β)). Cells were re-stimulated in fresh media on day 4 with anti-CD28 and anti-CD3 for 24hours. Supernatants were collected and analysed using ELISA according to manufacturer's instructions (R&D duoset). Cells show a large amount of IL-17 in both cell stimulations. There is IL-2 present in the Th17(23) population but no Il-2 in the Th17(β) population.

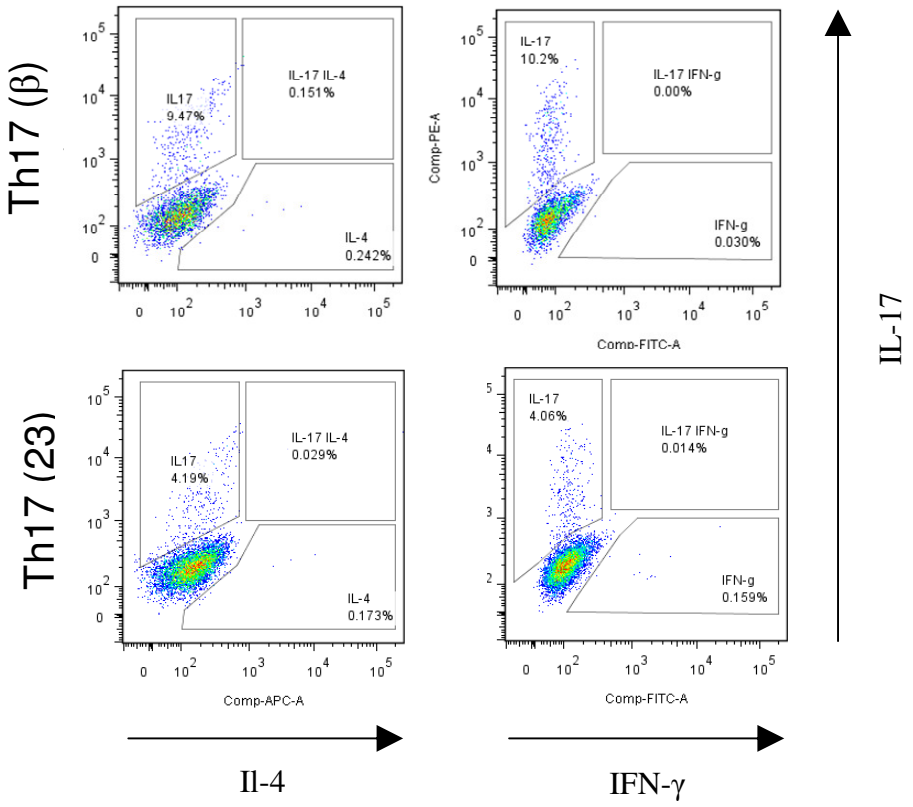

Fig 3.12 - Intracellular cytokine staining profiles for sorted T-helper subsets. Cells were isolated from female balb/c mice using easysep CD4+ Isolation (Stemcell). Cells were stained with anti-mouse CD4, CD44 and CD62L antibodies. Cells were sorted on a BD FACS Aria I for $CD4^+$, $CD62L^{LO}$, $CD44^+$ Cells. Cells were plated at $2x10^6$/ml in a 96 well plate. Cells were stimulated with plate-bound anti-CD3 (5 µg/ml; 145-2C11) plus anti-CD28 (2.5 µg/ml; 37.51) in media supplemented with anti-IFN-γ, IL-6, IL-1β and either IL-23 (Th17(23) or TGF-β Th17(β). Cells were re-stimulated in fresh media on day 4 with anti-CD28 and anti-CD3 for 24hours. Brefeldin A (BD Golgi stop) was added for the last 4 hours. Cells were collected and stained using mouse $CD4^+$ T-cell phenotyping kit (BD) according to manufacturer's instructions. Cells were analysed on BD FACs Aria, data was analysed using Flowjo software (treestar). Both subsets have Th17 producing cells. The Th17(23) has around 4% IL-17 producing cells, Th17(β) cells have a 10% IL-17 producing population.

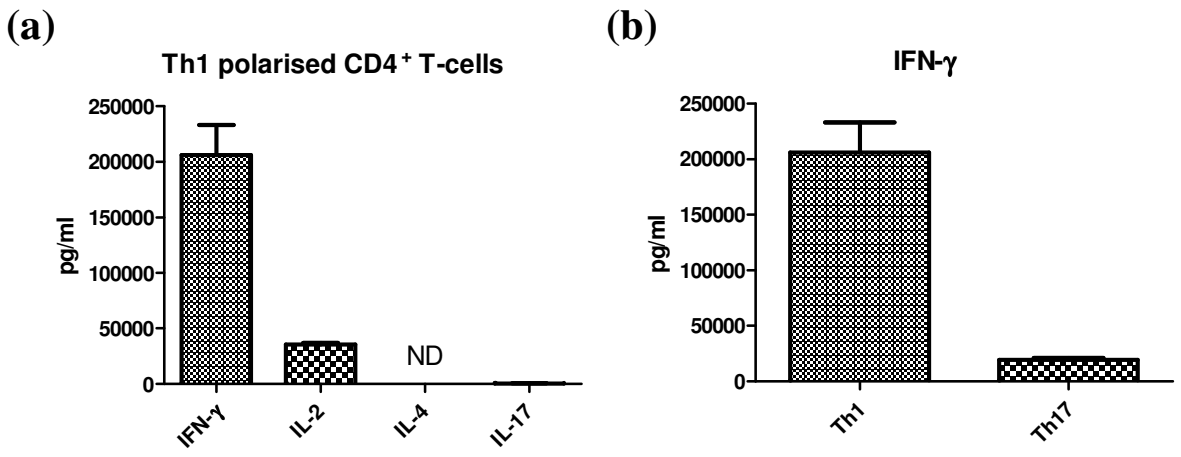

Fig 3.13 – Cytokine profiles for Th1 polarised T-cells stimulated in media supplemented with IL-12 and anti-IL-4 antibody. Cells were isolated using easysep CD4+ magnetic Isolation (Stemcell Cat# 19752). Cells were plated at $2x10^6$/ml in a 24 well plate. $1x10^6$ cells were stimulated with plate-bound anti-CD3 (5 μg/ml) plus anti-CD28 (2.5 μg/ml) with 20ng/ml IL-2, 20ng/ml IL-12 and 10μg/ml anti-IL-4 antibody for 3 days for Th1 polarising conditions. Supernatants were collected and measured for cytokines by ELISA (R&D Duoset). **(a)** Cytokine profile for cells stimulated with IL-12 and anti-IL-4 antibody. Levels of IFN-γ are high relative to IL-4 and IL-17 cytokines. **(b)** Levels of IFN-γ between polarised subsets of cells. Th17 cells were polarised in media supplemented with 10μg/ml anti-IFN-γ antibody, 20ng/ml IL-6, 20ng/ml IL-23 and 10ng/ml IL-1β for 3 days. Th1 subset of cells shows a significant increase in IFN-γ level relative to the Th17 cell subset.

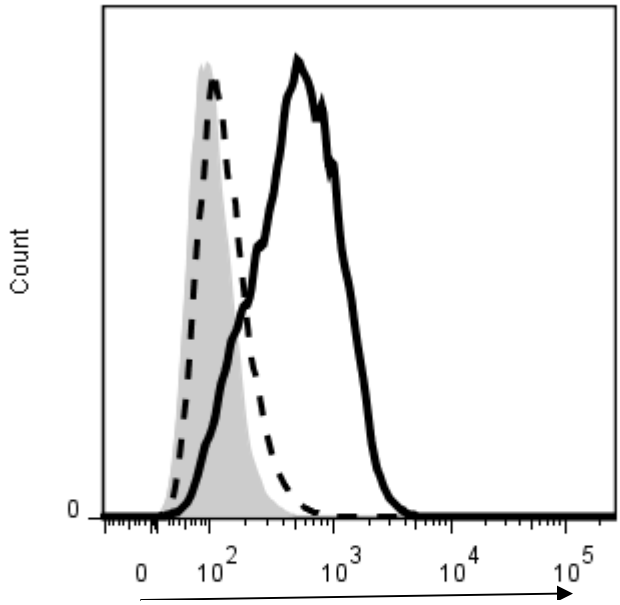

	Sample Name	Median , Comp-PE-
———	Specimen_001_WT T1.fcs	489
– – –	Specimen_001_WT T17.fcs	120
———	Specimen_001_FMO2.fcs	92.9

Fig 3.14 – T-Bet transcription factor. Cells were enriched for $CD4^+$ cells using the $CD4^+$ negative Isolation kit (Stemcell Cat# 19752). Cells were plated at $2x10^6$/ml in a 24 well plate. Cells were stimulated with plate-bound anti-CD3 (5 μg/ml) plus anti-CD28 (2.5 μg/ml) in media supplemented with 10ng/ml IL-12 and 10μg/ml anti-IL-4 anti-body for Th1 cells and 10ng/ml IL-1β, 20ng/ml IL-23, 20ng/ml IL-6, 0.2ng/ml TGF-β, 10μg/ml anti-IL-4 and 10μg/ml anti-IL-6 for Th17 cells. The cells were re-stimulated in fresh media on day 3 with anti-CD28 and anti-CD3 for 24hours. Cells were collected and stained for intracellular T-bet transcription factor using primary PE conjugated anti T-bet antibody (BD). Cells were analysed on BD FACs Aria and data was analysed using Flowjo software (Treestar). Cells were gated on $CD4^+$ expressing cells and histograms represent T-bet expression on Th1 and Th17 cells. The Th1 subset shows an increased expression of intracellular T-bet.

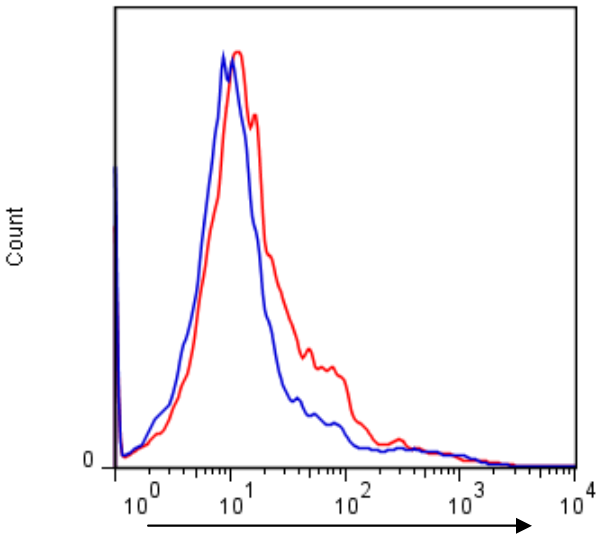

	Sample Name	Mean , PE-A	Median , PE-A
	Specimen_001_Magnet DSorted_PE_001.fcs	49.6	10.4
	Specimen_001_TH1 Magnet DSorted_PE.fcs	53.5	13.8

Fig 3.15 – CCR5 expression in Th1 polarised T-cells. Cells were plated at $2x10^6$/ml in a 24 well plate. Cells were stimulated with plate-bound anti-CD3 (5 µg/ml) plus anti-CD28 (2.5 µg/ml). For Th1 cells media was supplemented with 10ng/ml IL-12 and 10µg/ml anti-IL-4 anti-body. Cells were collected on day 3 and stained using primary conjugated anti-mouse CCR5 antibody (BD). Cells were analysed on BD FACs Aria I, data was analysed using Flowjo software (treestar). Histograms represent the fluorescence intensity of the stained cells relative to CCR5 expression on naïve T-cells (blue) and Th1 polarised T-cells (red). There is an increase in the expression of CCR5 expression on the Th1 polarised cells.

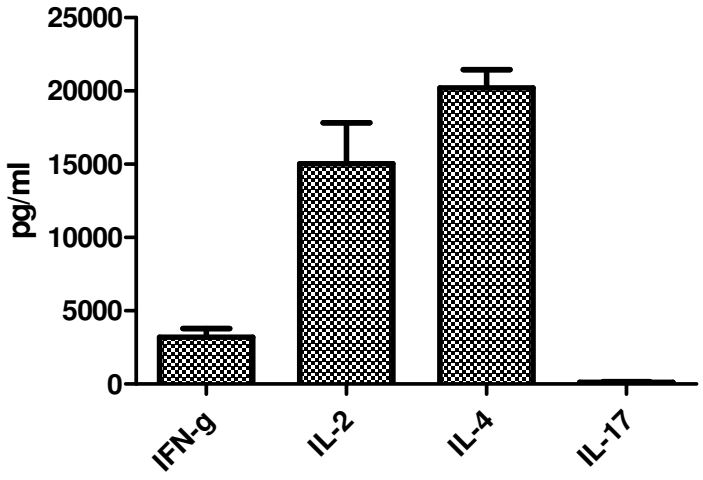

Fig 3.16 – Th2 polarised cells. Cells were isolated using easysep $CD4^+$ negative isolation kit (Stemcell). Cells were plated at $2x10^6$/ml in a 24 well plate. Cells were stimulated with plate-bound anti-CD3 (5 μg/ml) plus anti-CD28 (2.5 μg/ml) in media supplemented with 10μg/ml neutralising anti-IFN-γ antibody and 10ng/ml IL-4. After 3 days in culture, cells were put in fresh media and re-stimulated with (5 μg/ml) plate bound anti-CD3 and (2.5 μg/ml) anti-CD28 for 3 days. On day 6 Supernatants were collected and analysed using ELISA according to manufacturer's instructions (R&D duoset). The analysis shows a large amount of IL-4 and Il-2 relative to the IFN-γ and IL-17 levels, indicative of a Th2 polarised subset.

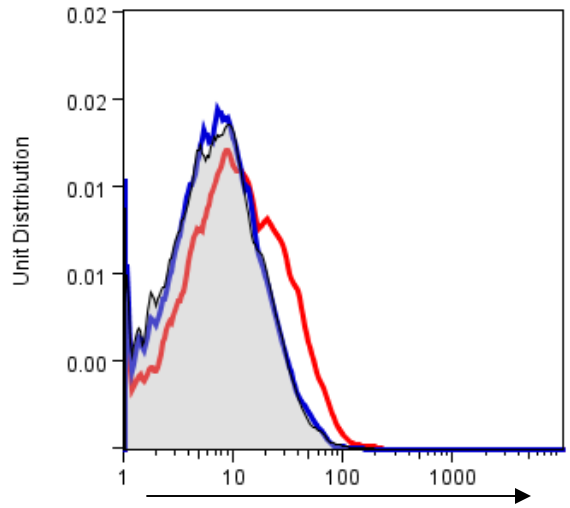

FSC-A, SSC-A subset/SSC-H, SSC-W subset/FSC-H, FSC-W subset

Sample Name	Mean , PE-Cy7-
Specimen_001_FITC 2.fcs	8.26
Specimen_001_Th17 Gata3 2.fcs	8.65
Specimen_001_Th2 Gata3 2.fcs	14.56

Fig 3.17 – CD4$^+$ cells culture in Th2 polarising conditions express the transcription factor GATA-3. Cells were isolated from female balb/c mice using easysep CD4+ Isolation (Stemcell). Cells were plated at 2x10^6/ml in a 24 well plate. Cells were stimulated with plate-bound anti-CD3 (5 µg/ml) plus anti-CD28 (2.5 µg/ml), for Th2 cells supplemented media was further supplemented with 10ng/ml IL-4, 20ng/ml IL-2 and 10µg/ml anti-IFN-γ neutralising anti-body. Th17 cell media was supplemented with 10µg/ml anti-IFN-γ, 20ng/ml IL-6, 10ng/ml IL-1β and 20ng/ml IL-23. Cells were re-stimulated in fresh media on day 3 with anti-CD28 and anti-CD3 for 24hours. Cells were collected and stained using PE-CY7 primary conjugated anti-GATA-3 antibody (BD). Cells were analysed on BD FACs Aria, data was analysed using Flowjo software (treestar). The shaded grey area represents the naive cell population, the blue line represents the expression of GATA-3 in Th17 polarised cells and the red line represents GATA-3 expression in Th2 cells. There is an increase in the expression of GATA-3 in Th2 cells.

3.3– DISCUSSION

In this chapter a pure viable $CD4^+$ T-cell population was isolated. The conditions for culturing and polarising the cells into differentiated T-helper cell subsets were optimised. Column and magnetic based protocols for obtaining $CD4^+$ pure cells from mouse spleenocytes were investigated. The magnetic method of isolation led to a higher purity of cells with better viability and response to stimulation. This technique works using a cocktail of antibodies directed against markers on cells that are not of interest. Magnetic nano-particles are then added and form a nano-particle bound complex the antibodies. Unwanted cells are then removed by placing the cells in a magnetic field which holds the cells bound to a nano-particle in place while the unbound $CD4^+$ cells are poured off and collected. It is important to note that there is no centrifugation or mechanical stress placed on the cells during this purification. The second separation protocol investigated was a column kit that works in a similar fashion using a monoclonal antibody cocktail to bind spleenocyes that are not of interest. The mixed suspension is then loaded into the enrichment column which contains glass beads coated with Ig and anti-Ig. Following an incubation step the mixture flows though the column by gravity and cells that are not of interest are bound to the column enriching the flow through. The column is then washed with buffer to recover the $CD4^+$ cell population. It is possible that the interaction with the column has an affect on cell viability. The washing step may also contribute to the lower purity observed in the column isolated cells. There was a lot more variation in the yields and purity obtained from the column method, which may also be attributed to the column washing and elution steps. Magnetic and column isolated cells were also compared post stimulation, with cells showing higher levels of cytokines secreted from

the magnetically isolated cell population. This is most likely due to the higher purity of $CD4^+$ T-cells obtained and the higher viability of the cells, which would then lead to an improved response following stimulation. Magnetic isolation was selected as it was a faster, more reliable and effective method of isolation resulting in a $CD4^+$ cell population with higher purity, viability and response to activation.

In order to confirm that the isolated cells were indeed $CD4^+$ T-helper cells, the cells were counter-stained for the T-cell surface protein CD3, which is a part of the TCR complex involved in cell antigen recognition (Krummel et al. 2000). Routinely ~90% of the cells isolated were $CD3^+/CD4^+$ T-cells. The remainder is made up of contaminating cells owing to the method of isolation used and a very small population of $CD4^+$ cells that may be present in the spleen that are not bound by the antibody cocktail. Once isolation of $CD4^+$ T-cells was confirmed, the next step was to investigate the effective activation of these cells *in vitro*.

Activation of T-cells requires the stimulation of both the TCR receptor and the CD28 co-stimulatory molecule (J. Zhu et al. 2010). In order to replicate these signals *in vitro,* cells were stimulated with anti-CD3 and anti-CD28 antibodies which cross-react the receptors leading to activation and cytokine secretion. Another method of activation considered was chemical stimulation of the cells using Phorbol 12-myristate 13-acetate (PMA). PMA does not interact with the cascade and activates protein kinase C late in the pathway leading to cell activation and cytokine secretion (Nobrega et al. 1986)**.** Although PMA stimulation *in vitro* leads to cell activation and cytokine secretion, CD3 and CD28 activation represents a more physiological method of stimulation, interacting with surface proteins on the cell and activating corresponding signalling pathways. PMA activation

has also been shown to have an effect on the expression of IL-2R (CD25) and may lead to problems with T-cell proliferation using this model over a longer time period (Chopra et al. 1989). It also leads to over expression of IL-2 via the protein kinase C pathway which may interfere with polarisation of T-cells into a Th17 subset in later experiments (Laurence et al. 2007; P. Zhu et al. 2010). PMA was however used in later experiments to stimulate non-specific cytokine secretion in polarised cells in order to facilitate intracellular staining. Two concentrations of anti-CD28 antibody were investigated in combination with plate bound anti-CD3 activation of the T-cells. Soluble anti-CD3 has been shown to lead to cell anergy and low proliferation *in vitro* and was therefore plate bound at a single concentration for 2hrs prior to activation (Clement et al. 1985). The two concentrations of antit-CD28 investigated appeared to make no difference to the activation of Th0 (non-polarised) cells and the lower dose of anti-CD28 was selected for the activation of the cells. Activation strength can however have an effect on the polarisation of cells, with recent studies showing the effects of varying concentrations of anti-CD28 on the polarisation of Th17 cells in particular (Bouguermouh et al. 2009; Purvis et al. 2010). The method of isolation and dose of antibodies used in this study appear to have been effective in the activation and polarisation of the $CD4^+$ T-cells into Th1, Th2 and Th17 cells subsets.

In initial experiments using these conditions isolated cells did not proliferate well in culture, therefore different components of the media were assessed in order to identify the optimal conditions for culturing $CD4^+$ T-helper cells *in vitro* over a number of days. Fetal bovine serum (FBS) is an undefined media supplement necessary for *in vitro* cell culture. Stocks of FBS are created commercially in large batches and even FBS ordered

from the same company can vary greatly. Batch testing was carried out in order to investigate if different sources and batches could affect the activation and culture of $CD4^+$ T-cells. The results obtained show evidence of variation as there is a difference in cytokine secretion between cells cultured with FBS from different sources. Heat inactivation of FBS is carried out routinely in cell culture labs. It was initially introduced to kill heat labile complement protein, viruses and mycobacteria. A study by Triglia and Linscott (1980) observed that modern FBS contains a negligible amount of complement and any inactivation required is be carried out when the media is heated to 37^{o}C before use. Modern triple filter systems that filter down to 0.1μm in size remove mycobacteria from serum. However, heat activation protocols are still in place in many research labs and heat inactivated serum is available to purchase commercially despite the fact that there is also an inherent possibility of degrading heat sensitive growth factors present in the sera. The results in this chapter show that regardless of these reports of heat inactivation becoming a redundant method, there is a marked increase in cytokine secretion levels following stimulation in media supplemented with heat inactivated sera, this is contrary to findings in other labs (Leshem et al. 1999). No detailed study has been reported on the effects of heat inactivation of FBS in T-cell models and more work is required to understand affects on *in vitro* systems of T-cell activation (Schulz et al. 2009; Szabo et al. 2000). This is made difficult by the undefined nature of FBS. In order to reduce variability between experiments due to FBS, a large stock batch was ordered and a standard heat inactivation protocol was established and used for all experiments.

Once the variability in FBS between experiments was removed, other additions to the media were investigated in order to improve culture conditions for T-cells. β mercapto-

ethanol (BME) has been reported to improve the viability of cells in a number of cell culture systems (Inui et al. 1997). The amino acid cysteine is required for T-cell proliferation but is in short supply in media supplemented with FBS. T-cells are unable to transport its pre-cursor cystine, which is present in the media, to the cytosol. BME reduces cystine to cysteine making it available to T-cells to utilise for cell growth (Chang et al. 1982; Aidoo et al. 1991).

IL-2 is a proliferation factor and stimulation of T-cells leads to up-regulation of the IL-2 receptor CD25. IL-2 has been shown to sustain T-cells and aid in their proliferation as shown here and by others (Smith 1988). The addition of IL-2 leads to an increase in proliferation of unpolarised T-cells in culture and improved cell viability. However, IL-2 has also been show to play an important role in T-helper cell polarisation, particularly in the inhibition of Th17 cell differentiation (Laurence et al. 2007; Cote-Sierra et al. 2004). Therefore IL-2 was selectively added to experiments rather than being included in the cell culture media with BME.

Having optimised the conditions for culturing cells the next aim was to optimise a system to generate differentiated T-helper subsets *in vitro*. This was achieved by stimulating $CD4^+$ T-helper cells in media supplemented with the relevant combination of recombinant cytokines and neutralising antibodies.

Th17 cells are a recently characterised lineage shown to be independent of Th1 and Th2 cells (Harrington et al. 2005; H. Park et al. 2005). Th17 cell produce large amounts of predominantly IL-17A and they have been linked to a number of chronic inflammatory diseases which makes the study of IL-17 secretion pathways of particular interest (Miossec et al. 2009). The signalling that leads to the establishment of Th17 cells is still

under scrutiny with contradicting studies leading to some contention. Part of this is due to a number of factors that were identified as necessary for the commitment of Th17 cells being later identified as dispensable. IL-23 was initially identified as the factor driving cells to produce IL-17 in a number of cells types (McKenzie et al. 2006), at this time it was not known if IL-17 producing T-cells were a distinct cell type from Th1 and Th2 cells. Th17 cells were later established as a distinct $CD4^+$ T-helper cell lineage producing IL-17, IL-21 and IL-22 (H. Park et al. 2005). Initially IL-23 was attributed to the induction of Th17 cells signalling via STAT3, however this was later identified as a growth factor and inducer of committed Th17 cells as the IL-23 receptor (IL-23R) is not expressed on naïve T-cells and is up-regulated on T-cells in an IL-6 dependant manner. IL-6, an activator of the STAT3 pathway and inducer of IL-17 production has been identified as a cytokine required for polarisation of a Th17 cell subtype (Zhou et al. 2007). However, a study by Chen *et al* (2007) has shown that stimulation in the presence of IL-21 and TGF-β is sufficient to induce RORγt and IL-23 receptor expression (Chen et al. 2007). Furthermore, in the presence of IL-6, $CD4^+$ T-cells produce IL-21 which acts through the IL-21 receptor and activates STAT3, committing cells to a Th17 phenotype in an autocrine fashion (Korn et al. 2007). Interestingly, early in this study TGF-β was also shown to be dispensible in the differentiation of Th17 cells. Further investigation confirmed these cells as a Th17 cell subset with up-regulation of RORγt, the transcription factor and master regulator of the Th17 subset (Ivanov et al. 2006), These results were contradictory to published work at the time showing a requirement for TGF-β (Yang et al. 2008; O'Garra et al. 2008). This was later corroborated in a study by Ghoreschi *et al* (2010) confirming the generation of a Th17 subset in the absence of TGF-β (referred to

as Th17(23)). In this study the authors describe these cells to be a pathogenic Th17 cells subset separate from the conventional Th17 T-cells generated *in vivo* in the presence of TGF-β (referred to as Th17(β)) (Ghoreschi et al. 2010). However, Ghoreschi *et al* (2010) and others have shown that Th17 cells generated in the absence of TGF-β (Th17(23)) demonstrate a degree of cell plasticity and are not entirely committed to a Th17 lineage. When Th17 cells were put in media containing IL-23 or IL-12, but no TGF-β they switched to IFN-γ/IL-17 double producing cells. They also expressed T-bet and RORγt simultaneously, each identified as the Th1 and Th17 master regulator transcription factor respectively. These cells have been identified mainly in the gut and have been identified as an overly pathogenic cell subset that is hypothesised to play a role in inflammatory disease (Lee et al. 2009; Lee et al. 2012). Given that the premise for this study was to generate two distinct cell types producing large amounts of the subset signature cytokine but derived from the same progenitor cells, the potential plasticity of the Th17 cells and their ability to produce both IFN-γ and IL-17 could lead to complications when screening potential SNARE candidates. It was therefore necessary to generate both Th17(23) and Th17(β) cells subsets and investigate the cell plasticity in this *in vitro* model.

In order to study these cells in detail, a pure naïve $CD4^+$ T-cell population was isolated from the $CD4^+$ spleenocytes obtained from the spleen. Work to this point was optimised for the cell culture and polarisation of $CD4^+$ enriched T-cells populations from the spleen. This population contains both $CD4^+$ unpolarised naïve T-cells and $CD4^+$ memory T-cells. Memory cells are usually associated with an acute immune challenge where by a portion of T-cells take on a memory phenotype in order to respond quickly to a second challenge of antigen. The balb/c mice used in this study were unchallenged, however it has been

suggested that the memory phenotype present in naïve mice is likely generated to exposure from gut flora and environmental antigens. These cells have the capability of producing cytokines upon re-stimulation with TCR ligands. They are sustained and proliferate in the same conditions as $CD4^+$ naïve helper T-cells (Seddon et al. 2003). Another source of contamination is the presence of $CD4^+$ regulatory cells (Tregs). Tregs are a suppressive T-cell phenotype that is largely studied for its ability to suppress and control immune responses (Littman & Rudensky 2010; Wing & Sakaguchi 2010). In the spleens of mice, 6-10% of $CD4^+$ T-cells are Tregs and these present a potential source of contamination. Although this contamination is present in the $CD4^+$ T-cells isolated and optimised for polarisation into subsets of cells, these cell purities were sufficient for the screening steps that follow in chapter 4. They also allow for a larger cell number to be obtained and the effective use of resources available for the screening stages of the project. However, it was clear that later in the project it would be necessary to study a pure naïve $CD4^+$ population for any SNARE candidates that arise in the screening stages. Cells were sorted using Fluorescent Activated Cell Sorting (FACS), a method that analyses cells for fluorescently labelled antibodies that are targeted to cellular proteins and sorts them into individual populations. The $CD4^+$ cells were stained for the cell surface markers CD44 and CD62L and sorted into CD44 low expressing CD62L high expressing cell population ($CD44^{lo}$, $CD62L^{hi}$), which have been identified as a pure naïve cell phenotype (Seddon et al. 2003). CD62L (also known as L-selectin) is a cell adhesion module that is a marker of naïve effector T-cells. Naïve cells by their nature have not encountered antigen and in order to do that they must enter secondary lymphoid structures, CD62L expression allows cells to enter lymph nodes where it can encounter

antigen. Effector memory T-cells do not express CD62L as they do not reside in the lymph node structures, but circulate in the periphery, cells are therefore sorted for high expression of CD62L (Bradley et al. 1992). Central memory T-cells however also express CD62L as they reside in lymph nodes in order to respond to previously encountered antigens, a second marker is therefore necessary. CD44 is a marker of developed memory T-cells and is involved in cell migration and adhesion (Budd et al. 1987). Hence cells were also sorted for low CD44 expression. The populations obtained were >98% pure and were cultured in polarising conditions for Th17(23) and Th17(β) cell types. The cytokine profiles measured were similar to those measured previously in this study and by Ghoreschi *et al* (2010). No IFN-γ/IL-17 double producing cells were observed in the intracellular cytokine experiments; however there were some differences in the derived subsets. Th17(β) cell polarisation results in a significant increase in the number of IL-17 producing cells, as measured by intracellular cytokine staining. They also show an increase in the amount of IL-17 produced in the supernatants by ELISA, possibly as a result of a higher number of Th17 producing cells. This may be as a result of the decrease in the amount of IL-2 measured in the supernatant by ELISA when compared to Th17(23) cells. IL-2 inhibits Th17 polarisation and also directly inhibits IL-17 production via signalling through STAT5 (Laurence et al. 2007). Given that the aim of this model was to identify a SNARE involved in the secretion of cytokine from a specific T-cell subset, conventional Th17(β) presented the best option for Th17 polarisation. They have been shown to exhibit less plasticity and when measured show an increase in the amount of IL-17 production and IL-17 producing cells, TGF-β was

therefore included in the antibody/recombinant protein cocktail used to generate $CD4^+$ Th17 cells.

Th1 cells are polarised and cloned *in vivo* in response to pathogenic invaders in the body. Macrophage and dendritic cells engulf pathogens and present molecules in the MHC complex on the cell surface. These antigen presenting cells (APCs) secrete large amounts of IL-12 into the environment surrounding the cells. Activation of T-cells by antigen through the TCR induces early IFN-γ production. IFN-γ produced early by activated T-cells *in vitro* leads to STAT1 activation and up-regulation of the IL-12 receptor. IL-12 signalling acting through STAT4 commits the T-cells to a Th1 differentiated cells by the up-regulation of T-bet and in turn, IFN-γ expression. IFN-γ can then act in an autocrine fashion to further induce T-bet expression in T-cells by signalling through the IFN-γ receptor, and establishing a self reinforcing feedback loop. IL-12 signalling also acts through a positive feedback loop by enhancing expression of its own receptor IL-12Rβ2 (Szabo et al. 2000; Schulz et al. 2009). IL-12 is necessary for commitment to Th1 cells and is secreted by APCs but not T-cells. It is therefore necessary to add recombinant IL-12 *in vitro* in order to provide this signal.

Th1 cells are directly inhibited by IL-4 producing Th2 cells. IL-4 drives GATA-3 expression and Th2 lineage commitment which directly inhibits Th1 development through two independent pathways; the direct inhibition of STAT4 induction which is necessary for T-bet activation, and the binding and active repressing of *Runx3* leading to direct inhibition of IFN-γ production (Ouyang et al. 1998; Usui et al. 2003; Yagi et al. 2010).

In order to obtain a Th1 cell subset, IL-12 and anti-IL4 anti-body were added to the culture media. This resulted in a marked increase in IFN-γ production relative to the other cytokines measured by ELISA and establishment of an autocrine feedback loop committing cells to the Th1 subset. T-bet is a master regulator of Th1 cells and leads to the secretion of IFN-γ (Szabo et al. 2000). In order to confirm Th1 lineage commitment, cells were measured for the expression of the transcription factor T-bet which was found to be significantly increased when compared to Th2 cells. CCR5 and CXCR3 are chemokine receptors expressed on the cell surface that have been reportedly up-regulated in Th1 cells (Qin et al. 1998). CXRCR3 has been associated with Th2 cells but CCR5 is unique to the Th1 subset. Up-regulation of CCR5 was observed in T-cells stimulated with IL-12 and anti-IL-4 antibody in this study.

Differentiation of Th2 cells is inhibited by IFN-γ produced early by Th1 and early activated T-helper cells. The addition of antibody to neutralise IFN-γ and the addition of IL-4 activates the transcription factors GATA-3 committing naïve T-helper cells to a Th2 lineage and inhibiting Th1 commitment (Zheng & Flavell 1997). Th2 cells were generated *in vitro* and characterised by cytokine production and the expression of GATA-3. The Th2 subset was optimised in the lab but the use of this model is not ideal to link SNARE expression to IL-4 production. Although IL-4 is the predominant cytokine produced by Th2 cells, it also secretes a number of others; IL-5, IL-9, IL-13 and IL-25 (Paul & Zhu 2010). This does not make Th2 cells a good cell line for this study but the development of the model was thought to be necessary for potential use as a comparative in later work.

This study established a model of T-helper cell polarisation for the generation of characterised Th1, Th2 and Th17 subsets producing predominantly IFN-γ, IL-4 and IL-17 cytokines respectively. This model will allow for the study of specific SNARE transport proteins regulating the secretion of signature cytokine produced in each subset of cells.

CHAPTER 4

SNARE EXPRESSION IN $CD4^+$ T-CELLS

4.1– INTRODUCTION

SNARE proteins were initially identified in the field of neurobiology as soluble synaptic trafficking proteins necessary for efficient transport between cellular organelles (Söllner et al. 1993). They were later identified as critical for intracellular transport in most, if not all eukaryotic pathways. Although well studied in neuronal signalling, the last 10 years has seen the emergence of a number of SNARE studies in immunological pathways. A lot of this work has been in granulocytes; mast cells, neutrophils and eosinophils (Stow et al. 2006). These studies focused on SNARE regulation in lytic granule release through regulated secretory pathways. Work in macrophages and cytotoxic T-lymphocytes (CTL) has also been carried out on regulated secretory pathways and mass release of pre-formed cytokine and lytic granules through SNARE regulated mechanisms (Murray, Wylie, et al. 2005; Qu et al. 2011). A detailed pathway has also been elucidated for the release of TNF-α from macrophages, identifying key SNARE complexes at different stages of release and a novel method of cell secretion through recycling endosomes (Murray, Kay, et al. 2005) . However, little work has been carried out to identify SNARE proteins involved in constitutive release of cytokines from $CD4^+$ T-helper cells. A study by Huse *et al* (2006) identified two multi-directional pathways for cytokine release in T-helper cells. This work used T-cell blasts in order to identify SNAREs involved in constitutive release through synaptic directed or multi-directional cytokine release (Huse et al. 2006). Huse *et al* (2006) co-localised SNARE proteins with two or more cytokines being released in synaptic or multi-direction pathways. However, although two pathways were identified using confocal microscopy to show different

SNARES in the same locality, SNARES complexes were not associated with the release or regulation of specific cytokines in T-helper cells.

In this chapter the aim was to use the clearly defined T-helper cell subsets Th1 and Th17 optimised in chapter 3 to screen SNARE expression and identify candidate SNARES involved in trafficking of cytokines in T-helper subsets. Using the established model of polarisation, T-cells were differentiated into Th1 and Th17 cells and kinetic studies of cytokine release identified optimal times to identify differences in SNARE mRNA expression between cell subsets.

In order to validate the relevance of any SNARE protein found to be associated with either Th1 or Th17, the expression of the SNARE was examined in inflammatory disease mediated by Th1 and Th17 cells. Therefore two murine models of ulcerative colitis were used to determine SNARE regulation during inflammatory disease.

4.2– RESULTS

4.2.1 – ANALYSIS OF IFN-γ AND IL-17 CYTOKINE LEVELS FROM POLARISED CD4⁺ T-HELPER CELLS OVER A 72hr TIME COURSE.

In order to identify the earliest time post-stimulation at which the IFN-γ and IL-17 cytokine levels were secreted in Th1 and Th17 cells respectively, a time course experiment was set up and supernatants were analysed at 2hr, 6hr, 12hr, 48hr and 72hrs following stimulation. The time point at which the levels of these cytokines differ from each other significantly will identify the point at which the cells have polarised into a T_H1 or Th17 subset and are actively secreting cytokine and would provide a logical point to analyse the differences in SNARE expression between Th1 and Th17 cells.

Cells were isolated from the spleens of BALB/c mice using the EasySep Mouse $CD4^+$ T Cell Enrichment Kit (Stemcell technologies #19752). $CD4^+$ cells were plated in triplicate at a concentration $2x10^6$ cells/ml in a 24-well plate, 500µl/well. The cells were then stimulated with anti-CD3 (5µg/ml) and anti-CD28 (2.5µg/ml), samples were removed at 2hr, 6hr, 12hr, 48hr and 72hrs and centrifuged at 2000RPM for 10mins to pellet the cells and collect the supernatant. The supernatant was assessed for levels of IFN-γ and IL-17 using ELISA duosets (R&D)**.**

The IFN-γ cytokine levels in Th1 polarised cells began to increase at 6 hours **[Figure 4.1]**. The level of IFN-γ measured from Th17 cells was almost undetectable at 6 hours. This trend continued with IFN-γ increasing significantly at 12hrs, 24hrs, 48hrs and 72hrs in Th1 samples, but remaining low for Th17 samples.

IL-17 levels in Th1 and Th17 polarised cells remained low for the first 12hrs following stimulation **[Figure 4.1]**. At 24hrs there was an increase in IL-17 which continued at 48 and 72 hours. In the Th1 polarised cells levels of IL-17 remained low over the time course **[Figure 4.1(B)].**

These data indicate a steady increase in IFN-γ from 2hrs onwards in Th1 cells with very significant levels at 48 and 72 hours. In the Th17 cells there is a steady increase from 24hrs with significant increases at 48 and 72hrs. The largest increase for both cytokines was therefore 48hrs after stimulation. This was selected as the most likely point to record a significant change in SNARE mRNA and protein levels, as all the proteins involved in secretion of IFN-γ and IL-17 were expressed and cells were polarised and actively secreting cytokine. The profile of cytokine secretion for the cells at this time point was as expected with significant levels of IFN-γ and low levels of IL-4 and IL-17 **[Figure 4.2].** In the Th17 cells at 48hrs the level of IL-17 is significantly higher than IFN-γ and IL-4. The 48hr time point was used as the initial screening point for further experiments to analyse SNARE mRNA and protein expression in Th1 and Th17 cells.

4.2.2 – IFN-γ AND IL-17 mRNA EXPRESSION IN Th1 AND Th17 POLARISED CD4⁺ T-CELLS AT 48hrs

The expression of mRNA for signature cytokines IFNγ and IL-17 was measured at 48hrs in Th1 and T_H17 cells in order to confirm the high expression of each in their respective subsets. An increase in expression of IFN-γ and IL-17 in Th1 and Th17 cells respectively would further confirm the polarisation of these cells after 48hrs and also indicate transcriptional activity in the T-cells at this time-point.

Cells were isolated from the spleens of BALB/c mice and $CD4^+$ T-cells were isolated using the EasySep Mouse $CD4^+$ T Cell Enrichment Kit (Stemcell technologies #19752). Cells were plated in 500µl/well at a concentration of $2x10^6$ cells/ml and stimulated with anti-CD3 (5µg/ml) and anti-CD28 (2.5µg/ml) for 48hrs in Th1 or Th17 polarising conditions for 48hrs in triplicate. Cells were then collected and centrifuged at 2000RPM for 10 mins and the supernatant was removed and stored at -20^OC for further analysis. The cell pellet was re-suspended in 350µl RA1 lysis buffer and 3.5µl DTT and mixed well before storing at -20^OC until RNA isolation was carried out using the RNA II Nucleospin® kit (Macherey-Nage) according to the manufacturer's instructions. The cDNA was generated using the High Capacity cDNA Reverse Transcriptase Kit (Applied Biosystems, USA) and random primers. The cDNA was diluted 1/12 in DEPC treated water and qPCR was carried out on the ABI Prism 7500 using Roche SYBR green mastermix and primers for IFN-γ (sigma) and IL-17 (IDT).

Samples were measured in triplicate for each assay and a non-template control was included in each target assay. Sample Ct values were normalised against two endogenous control genes; *GusB* and *TBP*. After normalisation of the samples, expression was calculated using the relative expression method and the Th1 cell subset was used as a calibrator giving the expression of the target gene in Th1 cells a value of 1.0 and calculating the expression in Th17 cells relative to this value. This gave an indication of the difference in expression of the target gene between the two T-cell subsets in terms of fold change.

As expected, the mRNA levels of expression for IFN-γ were significantly reduced in Th17 cells when compared to Th1 cells with a 5-fold decrease in expression to an

average of 0.2 **[Figure 4.3 (A)]**. Conversely, the mRNA expression of IL-17 in Th17 cells was significantly increased (4.5 fold) compared to Th1 cells **[Figure 4.3 (B)]**. These data show clearly an increase in mRNA expression of IFN-γ in Th1 cells and an increase in expression of IL-17 in Th17 cells when each subset is compared to each other and there is a clear difference in the transcriptional activity at the 48hr time point for cytokines of interest. The supernatants from these samples were assessed for cytokine levels in order to confirm the increase in expression of IFN-γ and IL-17 in line with an increase of mRNA expression.

These results confirm a Th1 and Th17 cell subset cytokine profile at 48hrs and the clear difference between the Th1 and Th17 subset at 48hrs indicated it to be a suitable point to examine differences in expression between polarised subsets. This mRNA was then used to measure the expression of SNARE proteins and assess the differences between Th1 and Th17 cells.

4.2.4 – DIFFERENCES IN R-SNARE EXPRESSION IN Th17 CELLS COMPARED TO Th1 CELLS USING qPCR ANALYSIS OF SAMPLES AT 48hrs.

Using the mRNA generated from the three experiments carried out in 4.2.2, mRNA expression of a number of R-SNARE targets was carried out using qRT-PCR analysis. R-SNAREs differ from the Q-SNARE family of proteins in their conserved amino acid contribution to the SNARE complex, R-SNAREs contribute an Arginine (R) to the ionic layer and Q-SNAREs contribute Glutamines (Q) (Fasshauer et al. 1998). R-SNAREs are pre-dominantly found on the membrane vesicle as opposed to the target membrane, it is

made up mainly of the VAMP family of SNAREs. The VAMP family of SNAREs that have been identified in immunological cells were targeted for analysis; VAMP2, VAMP3, VAMP4, VAMP7, VAMP8 and Sec22. Sequences of the primers used are detailed in **appendix C**.

Analysis was run on a total of 7 samples generated in 3 individual experiments. Samples were run on the ABI Prism 7500 using SYBR green mastermix and each target was run with a non-template control and tested in triplicate. Ct values were normalised to the homogenous controls *TBP* and *GusB*. The expression of the target mRNA was normalised setting the expression of the gene in the Th1 sample to a value of 1.0.

There was no significant change in the expression of VAMP3, VAMP4 or VAMP8 mRNA between Th1 and Th17 cells. However, there was a significant difference in expression of the remaining targets; VAMP2, VAMP7 and Sec22 **[Figure 4.4]**. Th17 cells had significantly higher expression of VAMP2 ($p<0.001$) and sec22 ($p<0.01$) compared to Th1 and Th17 cells had decreased expression of VAMP7 ($p<0.05$) when compared to Th1 cells.

4.2.5 – DIFFERENCES IN Qa-SNARE EXPRESSION IN Th17 CELLS COMPARED TO Th1 CELLS USING qPCR ANALYSIS OF SAMPLES AT 48hrs.

The next family of SNAREs to be analysed for differences in Th1 and Th17 cell subsets were the Q-SNAREs. These SNARES are broken up into 3 families; Qa, Qb and Qc. A SNARE complex is usually made up from a single R-SNARE and three Q-SNARES, one from each a, b and c. SNAREs contributing Qb and Qc motifs to the complex can be

sourced from a single SNARE (Qbc), or a combination of a Qb and Qc. However a single member of the Qa family is always part of the SNARE complex. This is an important contingent of SNAREs that is mainly made up of the Syntaxin (STX) family. The Qa SNARE targets measured were those previously identified in immune cells; STX2, STX4, STX5a, STX5L, STX6 and STX11. Primers used for the qRT-PCR analysis are listed in **Appendix C**. Samples were analysed using the ABI Prism 7500 and SYBR green master mix (Roche, USA). All targets were measured in triplicate with an NTC, results are representative of 3 experiments. Samples were tested for significance using the unpaired student t-test.

Th17 cells had a significant increase in expression of STX2 and STX11 ($p<0.001$) compared to Th1 cells **[Figure 4.5]**. No significant difference was detected for the remaining Qa SNARE targets analysed; STX 3, STX5a, STX5L and STX6. Although STX5a and STX5L did show a small increase of 0.5 fold, they were not statistically significant **[Figure 4.5]**.

4.2.6 – DIFFERENCES IN Qb AND Qbc-SNARE EXPRESSION IN Th17 CELLS COMPARED TO Th1 CELLS USING qPCR ANALYSIS OF SAMPLES AT 48hrs.

Qb and Qbc SNARES were the next families which contribute to the R-Qabc complex to be analysed. The Qb-SNARE Vti1b was examined for changes in mRNA expression in Th17 cells as it is a SNARE that has been identified in a number of immune pathways of cytokine release (Murray, Wylie, et al. 2005; Qu et al. 2011; Offenhäuser et al. 2011). SNAREs classified as Qbc are unique in that they contribute 2 conserved SNARE motifs

to the complex. This allows for the complex to be made up of 3 SNAREs as opposed to the 4 presumed to be required for formation of a 4-alpha helix bundle. SNAP23 is an ortholog to the well studied synaptic SNARE SNAP25. SNAP23 has been identified as a key SNARE in immune cell secretion pathways. Vti1b and SNAP23 were measured for mRNA expression at 48hrs**.** Samples were made up in SYBR green (Roche, USA) and analysed on an ABI Prism 7500. Samples were measured in triplicate and results are representative of 3 experiments, an NTC was included in the analysis of both targets.

No significant difference was detected for the mRNA expression of SNAP23 or Vti1b in Th17 cells when compared to Th1 cells at 48hrs **[Figure 4.6]**.

4.2.7 – CYTOKINE mRNA EXPRESSION LEVELS IN NAÏVE, Th1 AND Th17 CELLS AT 48hrs.

Having identified differences in mRNA expression of SNARE proteins between Th1 and Th17 cells subsets at 48hrs, we next wanted to compare the expression of these SNAREs in Th1 and Th17 cells with unstimulated naïve $CD4^+$ T-cells in order to determine if they were up-regulated in these differentiated cells. Before this was carried out we confirmed the expression of IFN-γ and IL-17 in the cell subsets, to include the naïve sample set. Th1 and Th17 Cells were generated as described above in 4.2.2. Naïve $CD4^+$ T-cells were isolated as in 4.2.2 but were not activated. $2x10^6$ cells were collected by centrifugation (1200RPM for 5 mins) and stored in RA1 buffer and 3.5µl DTT and mixed well before storing at -20^OC. Th1 and Th17 cells were collected after 48hrs and stored the same as naïve cells. RNA was isolated using the Nucleospin® RNA II kit according to the manufacturer's instructions. The cDNA was generated using the High Capacity cDNA Reverse Transcriptase Kit (Applied Biosystems, USA) and random primers. The

cDNA was diluted 1/12 in DEPC treated water as in 4.2.2. qPCR was carried out on the ABI Prism 7500 using Roche SYBR green mastermix and primers from IDT and Sigma. Samples were measured in triplicate for each assay and a non-template control was included for each target assay. Sample Ct values were normalised against *TBP*. After normalisation of the samples, IFN-γ expression was calculated using the relative expression method and the naïve cell subset was used as a calibrator giving the expression of the target gene in naïve cells a value of 1.0 and calculating the expression in Th1 and Th17 cells relative to this value. There was a significant increase in IFN-γ expression in the Th1 subset when compared to the naïve sample set and the Th17 subset **[Figure 4.7(a)]**.

Expression of IL-17 was measured the same way; however there was no expression measured for the naïve sample subset, therefore expression levels in Th17 cells were normalised to the Th1 subset **[Figure 4.7(B)].** The Th17 subset showed a significant increase in IL-17 mRNA expression when compared to the Th1 subset **[Figure 4.7(B)]**.

The expression levels of the cytokines IFN-γ and IL-17 in the naïve Th1 and Th17 subsets show high expression of IFN-γ in Th1 cells and high expression of IL-17 in the Th17 cells subset. The next step in the analysis of these subsets was to measure SNARE expression at this time point.

4.2.8 – SNARE mRNA EXPRESSION LEVELS IN NAÏVE, Th1 AND Th17 CELLS AT 48hrs.

The samples generated in **section 4.2.7** were used to analyse the differences in SNARE expression between the naïve, Th1 and Th17 subsets of cells. We selected SNAREs that were significantly different in their expression between Th1 and Th17 cells in the

previous experiments **[Section 4.2.4-6 above]**. These include the R-SNARE VAMP2 **[Section 4.2.4],** the Qa-SNAREs STX2 and STX11 **[Section 4.2.5]** and the control Qbc-SNAREs SNAP23 and Vti1b which showed no change in expression, but have been linked to cytokine secretion in a number of immune cells **[Section 4.2.6].**

Samples were measured in triplicate for each assay and a non-template control was included for each target gene. Sample Ct values were normalised against *TBP*. After normalisation of the samples, expression was calculated for each target SNARE using the relative expression method and the naïve cell subset was used as a calibrator giving the expression of the target gene in naïve cells a value of one and calculating the expression in T_H1 and T_H17 cells relative to this value **[Figure 4.8]**.

Figure 4.8 shows that the expression of VAMP2 in Th17 cells is increased compared to Th1 cells which confirmed previous results. It is also increased in the Th17 cells compared to the naïve cells but this was not statistically significant.

The expression of STX2 was significantly increased in Th17 cells compared to Th1 cells confirming the previous experiment. Expression in Th17 cells was the same as that of the naïve cells, however the expression of STX2 in the Th1 cells was decreased compared to the naïve cells. This indicates that the expression of STX2 SNARE mRNA is reduced in Th1 cells but remains unchanged in Th17 cells when normalised to naïve cells.

STX 11 expression was not detected in naïve cells and therefore the relative expression of STX 11 was calibrated by normalising the expression of STX11 in Th1 cells to one and calculating the relative expression in the Th17 cells. STX11 expression is significantly increased in Th17 cells compared to Th1 cells as previously shown in earlier

experiments. There was very low or no expression of STX11 mRNA in naïve cell samples **[Figure 4.8]**.

The last group to be measured were the Qb and Qbc SNAREs SNAP-23 and Vti1b. Although these SNAREs did not show a significant change in expression in the previous screening using Th1 and Th17 cells, it was important to include SNAREs that did not show any change in expression as a control group. These SNAREs have also been implicated in cytokine secretion in other cells of the immune system (Suzuki & Verma 2008; Martín-Martín et al. 2000)**.** **T**here was no significant change in expression of SNAP23 between Th1 and Th17 cell subsets **[Figure 4.8]**. There was also no significant change in expression between the three subsets for Vti1b relative to naïve cells **[Figure 4.8]**.

These data confirm that STX11 is increased following activation and polarisation into a Th17 cell subset. Although there are small differences in expression for STX2, VAMP2 and SNAP23, STX11 is of particular interest as it indicates an increase in the Th17 subset alone. STX11 was therefore hypothesized as a potential target for involvement in IL-17 secretion from T-cells. If STX11 is important in Th17 cells it should therefore also be up-regulated in inflammatory disease and infection where Th17 plays in important role. The next step in the study was to examine the role of STX11 in two murine models of colitis.

4.2.9 – STX11 mRNA EXPRESSION IN MOUSE MODELS OF COLITIS.

We examined the expression of STX11 and a number of other SNARE proteins in mouse models of inflammatory disease. To our knowledge there are no previous studies

examining the expression of these trafficking proteins in any inflammatory disease. The dextran sodium sulfate (DSS) model is well established as a chemically induced model of colitis in mice. It is believed to confer colitis like symptoms through direct toxicity to epithelial cells in the basal crypts situated in the gut, leading to a loss in mucosal barrier integrity and subsequent infiltration and inflammation (Wirtz et al. 2007). DSS induced colitis is a well studied model and a number of publications have identified a Th1/Th17 cell involvement in progression of disease (Alex et al. 2009; Ito et al. 2008). The DSS model was carried out in collaboration with Silvia Melgar in the Alimentary Pharmabiotic Centre, University College Cork. C57BL mice were randomly split into 5 groups. A control groups with 6 mice and 4 test groups with 6-8 mice. DSS (Sigma) was prepared fresh every day at a final concentration of 3% and administered to mice for 5 days *ad libitum*. The early acute mice were culled at day 7, late acute culled at day 12 and chronic mice culled at day 26. Mice were weighed and scored for daily disease activity (DDAI) based on stool composition, fur texture and posture every 3-4 days to monitor symptoms of gut inflammation. As expected, the control group maintained a healthy weight gain over 26 days. The DSS treated groups immediately began to lose weight with the biggest loss in weight observed at day 7, when the early acute mice were culled. Following this, late acute and chronic mice began to recover and gain weight. Late acute mice were culled at day 12 with a minor recovery in weight, while the chronic mice recovered to their original weight with a slight gain before day 26 **[Figure 4.9(a)]**. The DDAI showed a similar pattern of disease. No disease activity was observed in the control mice but there is a rapid increase in disease activity in all groups with mild recovery in the chronic group before the end point **[Figure 4.9(b)]**. When each group

came to the end-point of the experiment, two control mice were culled for analysis along with the treated group. The colons of each animal were removed and cleaned before measuring and weighing each colon individually. The weight and length of the colon are indicators of inflammation in the gut as the cell infiltration and inflammation increases the weight of the colon and also shrinks the colon in length. The colon length and weight from all treatment groups showed signs of inflammation with a significant increase in weight and decrease in colon length **[Figure 4.9(d),(e)]**. There was a minor increase in the average length of colons in the chronic group indicating a moderate recovery which is consistent with the rest of the data **[Figure 4.9(d)]**. After weighing and measuring colon length, a small section of distal colon was removed for histology. The tissue was cast in optimal cutting temperature (OCT) compound and snap frozen in liquid nitrogen before cutting into sections on a cryostat. The slides were then H&E stained for histological analysis. The H&E staining shows a healthy colon in the control group with good crypt formation and no infiltrating cells in the lower muscle layer of the gut. The early and late acute H&E staining shows a breakdown of crypt structures and infiltration of cells (purple spots) in the muscular layer with the worst infiltration evident in the late acute group. The chronic group shows some mild recovery with crypt structure evident and less infiltrating cells in the muscular layer consistent with the rest of the data **[Figure 4.9(e)]**. Collectively these results indicate a DSS induced model of colitis in the mice, with clear stages of colitis associated inflammation of the gut. A piece of the distal colon tissue was also removed and homogenised in order to extract RNA for qPCR analysis. The first parameters measured were the Th1 and Th17 cytokines IFN-γ and IL-17. The levels of expression in control mice were normalised to one and the other groups

measured were calculated as fold change in expression relative to the control group. IL-17 mRNA shows a significant 10-fold increase ($p<0.001$) in expression in the early acute group which is then significantly reduced in the late acute and chronic mice ($p<0.01$) **[Figure 4.10].** IFN-γ mRNA expression is significantly increased 10-fold ($p<0.05$) in the late acute mice. These results indicate that IL-17 and IFN-γ are predominantly expressed at different stages of the disease; an early acute IL-17 response which is then followed by a late acute and recovering IFN-γ response in the DSS induced colitis mice **[Figure 4.10]**. Having established the cytokine mRNA expression at the different stages of the DSS induced colitis, the SNARE targets identified as potential candidates involved in their secretion were assessed for mRNA expression levels. Syntaxin 11 mRNA expression was significantly increased in early acute DSS treated mice ($p<0.05$). This was concurrent with the increase in IL-17 mRNA expression observed at this stage of the disease. The level of STX11 then decreased to normal, if not reduced levels of mRNA expression at later stages of disease **[Figure 4.11].** A significant increase in VAMP7 mRNA expression levels was observed at the late acute stage of disease ($p<0.01$). These levels remained high in the chronic DSS treated mice **[Figure 4.11]** and correlated with an increase in IFN-γ at these stages. There was no significant change measured in the mRNA expression levels of STX2, VAMP2, SNAP23 and Vti1b SNARES in the DSS colitis model at any stage of disease **[Figure 4.11].**

Having identified the expression of IFN-γ and IL-17 in the stages of DSS colitis, and the relative expression levels of SNARE proteins in these mice it was clear that there was a correlation. IL-17 and IFN-γ are however expressed by a number of cells in the innate and adaptive immune system and the results obtained were from the whole tissue of a

distal portion of the colon. Therefore, the remainder of the colon was digested in order to remove the endothelial layers of cells and isolate the lamina propria. This layer of cells was then stained for with an anti-CD4 antibody in order to assess the percentage of $CD4^+$ cells present in the colon at the different stages of disease observed in DSS induced colitis. There was a significant increase in the number of $CD4^+$ cells from 5% in the control mice, to >20% of the total population of cells in the lamina propria of all treatment groups. Therefore, there is a significant number of $CD4^+$ cells T-cells in tissue isolated from the acute and chronic stages of disease in which the the levels of IFN-γ, IL-17 and SNARE mRNA expression levels were measured **[Figure 4.12].** Taken together this model corroborates the *in vitro* findings suggesting a link between IL-17 expression and STX11 expression. In order to confirm this link we looked at the Th17 dependent *Citrobacter rodentium* infection mouse model of colitis. *C. rodentium* is a pathogen that resides in the gut and induces transient colitis in healthy mice. Infection is usually cleared after 21 days (MacDonald et al. 2003; Bhinder et al. 2013).

C. rodentium work was carried out as before in collaboration with Silvia Melgar in the Alimentary Pharmabiotic Centre, University College Cork. C57BL mice in groups of 6-8 were inoculated orally by a 200µl gavage of approximately $200x10^9$ CFU *C. rodentium*. Mice were sacrificed at 9, 14, 21 and 28 days for tissue processing. The colons were removed and washed and the length and weight of each colon was measured individually as an indication of inflammation of the gut. There was a significant increase ($p<0.001$) in the colon weight at day 9 infected mice with recovery at days 14, 21 and 28 **[Figure 4.13]**. The average colon length in the infected mice was also significantly decreased at day 9 ($p<0.05$), with mild recovery at days 14, 21 and 28 **[Figure 4.13]**. These

parameters suggest colitis like symptoms of inflammation in the *C. rodentium* infected mice. Sections of the distal colon were homogenised and RNA was isolated for qPCR analysis.

The mRNA levels of expression for IFN-γ and IL-17 were assessed and a significant increase was observed in IL-17 mRNA expression at day 9 of the infection ($p<0.05$) **[Figure 4.14]**. This was decreased in the later stages of the infection with significantly decreased mRNA expression day 25 when compared to control mice ($p<0.01$). IFN-γ mRNA was not detected at significant levels at any stage of the infection **[Figure 4.14].** Candidate SNARES were assessed for levels of mRNA expression in the *C. rodentium* infected mice. There was a significant increase in STX11 mRNA expression in day 9 infected mice which was then reduced to control levels later in the infection ($p<0.01$) **[Figure 4.15].** This correlated with the increase in IL-17 observed at day 9 which subsequently decreased on days 14, 21 and 25 in the infection model. Interestingly, VAMP7 is significantly decreased on day 9 of infection ($p<0.05$) and levels remain low although not significant over the following days **[Figure 4.15].** VAMP2 ($p<0.05$), SNAP23 ($p<0.01$) and Vti1b ($p<0.05$) show a decrease in expression at day 9 of infection. However levels of expression return to normal in SNAP23 and VAMP2 with Vti1b mRNA expression remaining low in the later stages of *C. rodentium* infection. STX2 was increased on day 21 in infected mice ($p<0.05$) **[Figure 4.15]**.

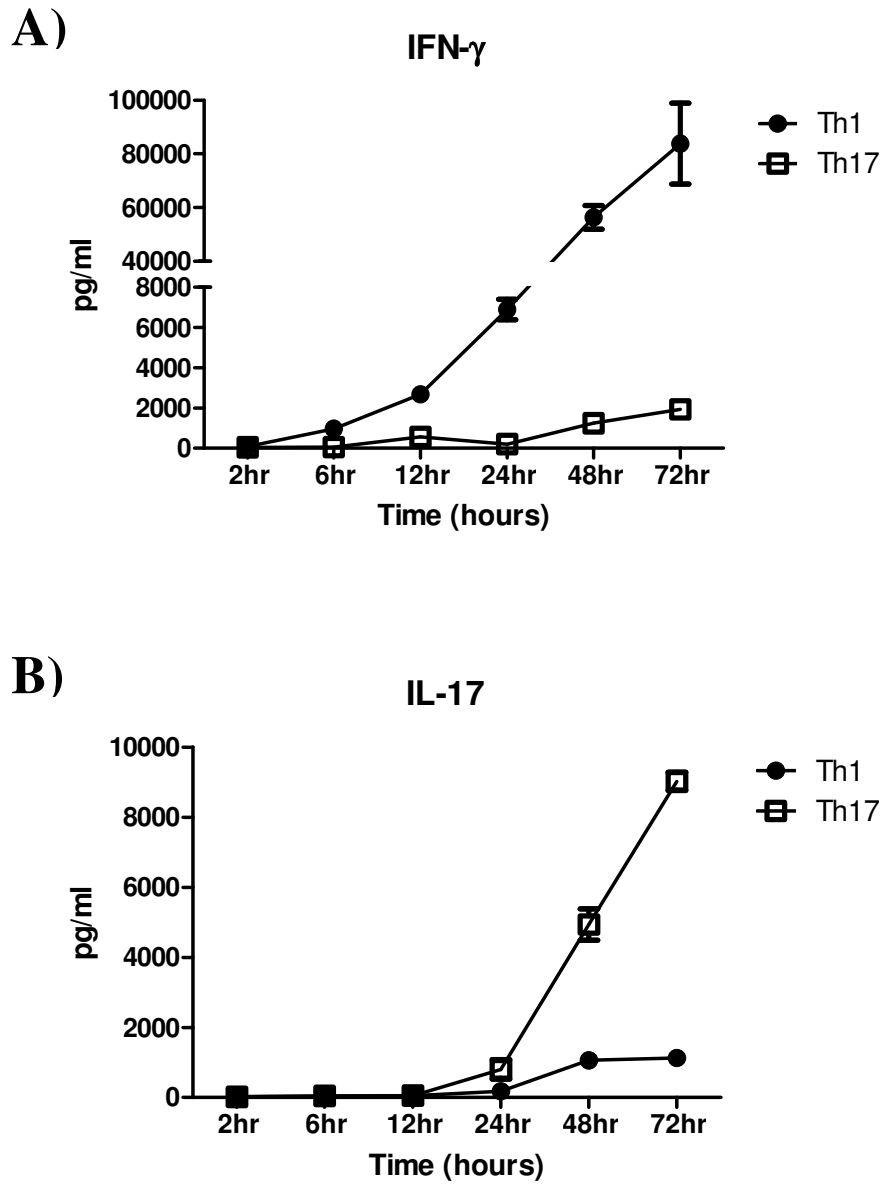

Figure 4.1 - Time course analysis of IFN-gamma and IL-17 secretion levels from T-cell subsets. $CD4^+$ cells were isolated from the spleens of BALB/c mice using the easysep magnetic isolation kit (stemcell cat#19752). Cells were plated at $2x10^6$/ml in a 24 well plate. Cells were stimulated with plate-bound anti-CD3 (5 ug/ml) plus anti-CD28 (2.5 ug/ml) in Th1 or Th17 polarising conditions for 3 days. Cells were collected at 2hrs, 6hrs, 12hrs, 24hrs, 48hrs and 72hrs. Cells were centrifuged at 2000RPM for 10mins and supernatants were collected and stored at -20°C before measuring for cytokine concentration by ELISA (R&D Duoset). A) IFN-γ levels measured in Th1 and Th17 polarised $CD4^+$ T-cells. B) IL-17 levels measured in Th1 and Th17 polarised $CD4^+$ T-cells.

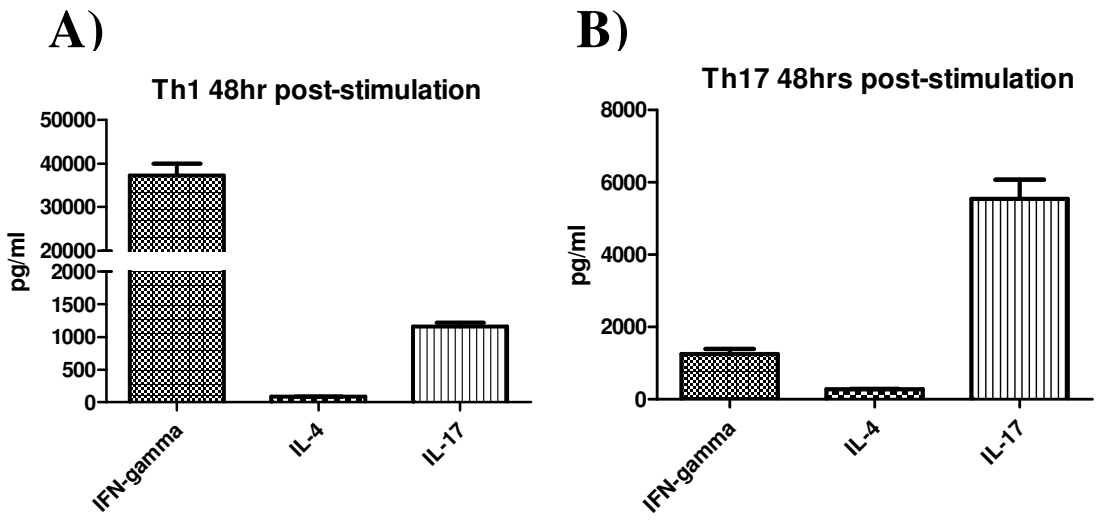

Figure 4.2 - Cytokine secretion 48hrs post stimulation Th1 vs Th17. $CD4^+$ cells were isolated from the spleens of female BALB/c mice aged 12-14 weeks using the easysep magnetic isolation kit. Cells were plated at $2x10^6$ cells/ml in a 24-well plate in either Th1 conditions: IL-2 (10ng/ml), IL-12 (10ng/ml) and anti-IL4 (10μg/ml) or Th17 conditions: IL1β (10ng/ml), IL-6 (20ng/ml), IL-23 (20ng/ml),TGF-β (0.2ng/ml), anti-IL-4 (10μg/ml) and anti-IFNγ (10μg/ml) and stimulated with coated anti-CD3 (5μg/ml) and anti-CD28 (2.5μg/ml) for 48 hours. Supernatants were collected and measured for IFN-γ, IL-4 and IL-17 cytokines using ELISA (R&D Duo sets). A) IFN-γ, IL-4 and IL-17 levels measured in Th1 polarised $CD4^+$ T-cells at 48hours. B) IFN-γ, IL-4 and IL-17 levels measured in Th17 polarised $CD4^+$ T-cells at 48hours. Experiment is representative of at least 3 individual experiments. Error bars represent the standard deviation of 3 technical replicates.

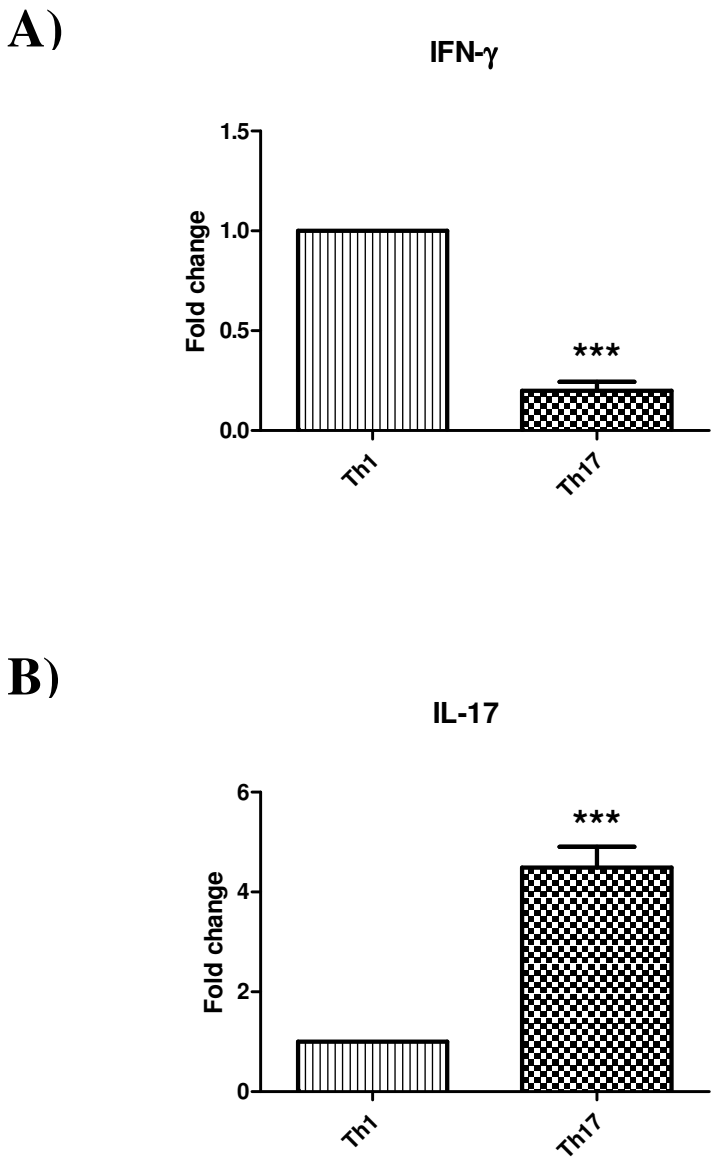

Figure 4.3 – Comparing mRNA expression of signature cytokines IFNγ and IL-17 in Th1 and Th17 cell subsets at 48hrs. $CD4^+$ cells were isolated from the spleens of female BALB/c mice aged 12-14 weeks using the easysep magnetic isolation kit. Cells were plated at $2x10^6$ cells/ml in a 24-well plate in either Th1 conditions: Il-2 (10ng/ml), IL-12 (10ng/ml) and anti-IL4 (10μg/ml) or Th17 conditions: IL1β (10ng/ml), IL-6 (20ng/ml), IL-23 (20ng/ml),TGF-β (0.2ng/ml), anti-IL-4 (10μg/ml) and anti-IFNγ (10μg/ml) and stimulated with coated anti-CD3 (5μg/ml) and anti-CD28 (2.5μg/ml) for 48 hours. The RNA was extracted from samples using nucleospin RNAII isolation columns (Macherey-Nage), equalised and converted to cDNA using the high capacity cDNA reverse transcription kit (Applied Biosystems). The cDNA was mixed with primers for *Ifnγ* (Sigma) and *Il17* (IDT) and FAST SYBR Mastermix (Roche) before analysing samples on the ABI Prism 7500. Groups were compared using relative quantitation; after normalising samples to *TBP* and *GusB,* Th1 was normalised to 1.0 and the expression in other groups is shown relative to this value**.** Results are means ±SD of 7 samples generated in 3 independent experiments measured in triplicate. An unpaired T-test was used to determine if differences between Th1 and Th17 groups were significantly different (***$p<0.001$).

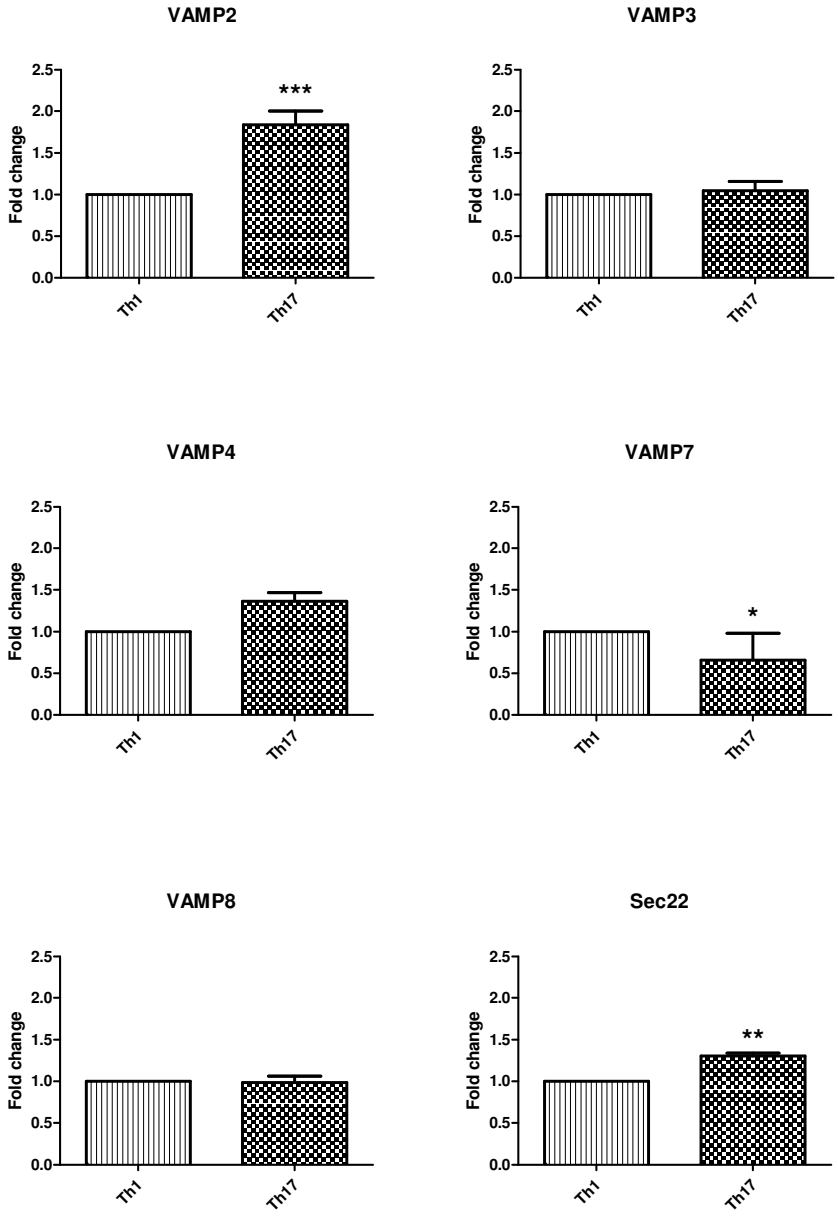

Figure 4.4 - R-SNARE mRNA expression in Th1 vs Th17 polarised T-helper cell subsets - $CD4^+$ cells were isolated from the spleens of female BALB/c mice aged 12-14 weeks using the easysep magnetic isolation kit. Cells were plated at $2x10^6$ cells/ml in a 24-well plate in either Th1 conditions: Il-2 (10ng/ml), IL-12 (10ng/ml) and anti-IL4 (10µg/ml) or Th17 conditions: IL1β (10ng/ml), IL-6 (20ng/ml), IL-23 (20ng/ml),TGF-β (0.2ng/ml), anti-IL-4 (10µg/ml) and anti-IFNγ (10µg/ml) and stimulated with coated anti-CD3 (5µg/ml) and anti-CD28 (5µg/ml) for 48 hours. Cells were collected and centrifuged at 1200RPM for 5mins, supernatant was removed for cytokine analysis. The RNA was extracted from samples using nucleospin RNAII isolation columns (Macherey-Nage), equalised and converted to cDNA using the high capacity cDNA reverse transcription kit (Applied Biosystems). The cDNA was mixed with primers for R-SNARE targets, and FAST SYBR Mastermix (Roche) before analysing samples on the ABI Prism 7500. Groups were compared using relative quantitation; after normalising samples to *TBP* and *GusB,* Th1 was normalised to 1.0 and the expression in other groups is shown relative to this value**.** Results are means ±SD of 7 samples generated in 3 independent experiments measured in triplicate. An unpaired T-test was used to determine if differences between Th1 and Th17 groups were significantly different (*$p<0.05$, **$p<0.01$and ***$p<0.001$).

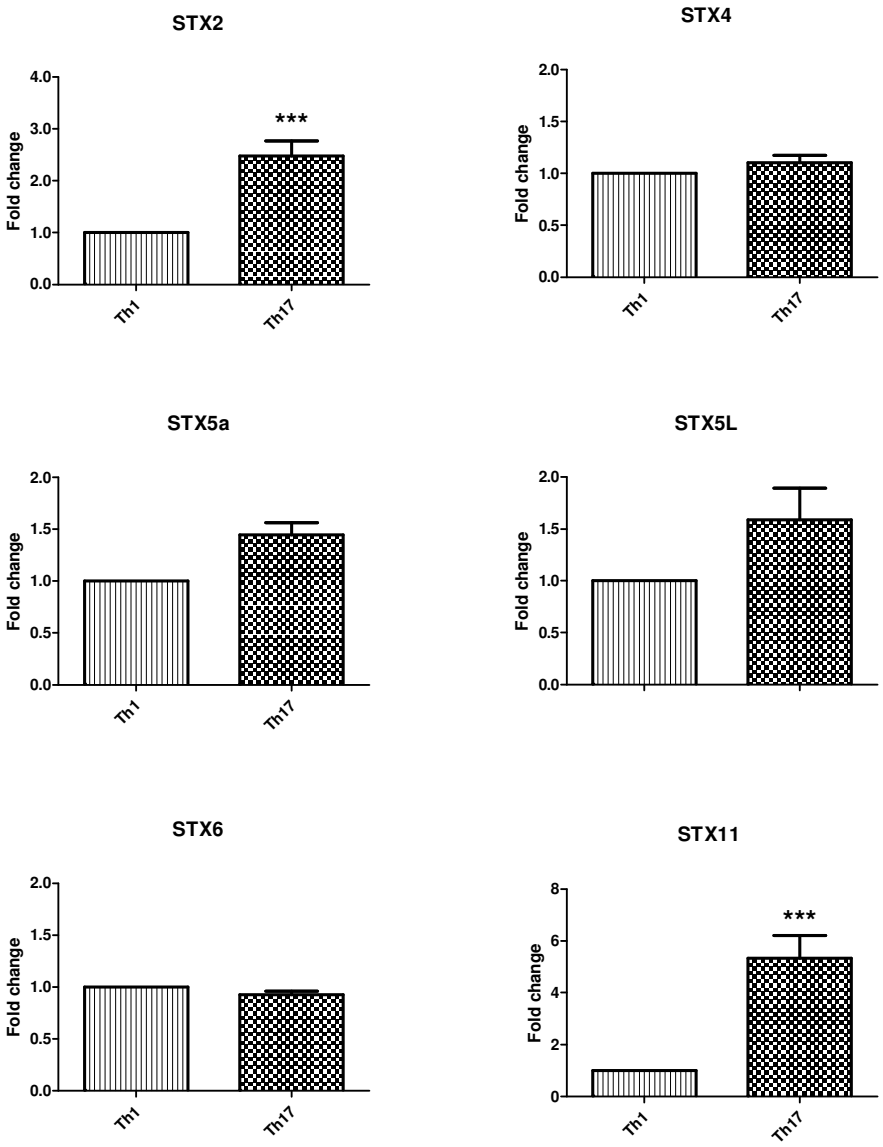

Figure 4.5 - Qa-SNARE mRNA expression in Th1 vs Th17 T-helper cell subsets - $CD4^+$ cells were isolated from the spleens of female BALB/c mice aged 12-14 weeks using the easysep magnetic isolation kit. Cells were plated at $2x10^6$ cells/ml in a 24-well plate in either Th1 conditions: Il-2 (10ng/ml), IL-12 (10ng/ml) and anti-IL4 (10µg/ml) or Th17 conditions: IL1β (10ng/ml), IL-6 (20ng/ml), IL-23 (20ng/ml),TGF-β (0.2ng/ml), anti-IL-4 (10µg/ml) and anti-IFNγ (10µg/ml) and stimulated with coated anti-CD3 (5µg/ml) and anti-CD28 (5µg/ml) for 48 hours. Cells were collected and centrifuged at 1200RPM for 5mins, supernatant was removed for cytokine analysis. The RNA was extracted from samples using nucleospin RNAII isolation columns (Macherey-Nage) and converted to cDNA using the high capacity cDNA reverse transcription kit (Applied Biosystems). The cDNA was mixed with primers for Qa SNARE targets (IDT) and FAST SYBR Mastermix (Roche) before analysing samples on the ABI Prism 7500. Groups were compared using relative quantitation; after normalising samples to *TBP* and *GusB,* Th1 was normalised to 1.0 and the expression in other groups is shown relative to this value**.** Results are means ±SD of 7 samples generated in 3 independent experiments and measured in triplicate. An unpaired T-test was used to determine if differences between Th1 and Th17 groups were significantly different (***$p<0.001$).

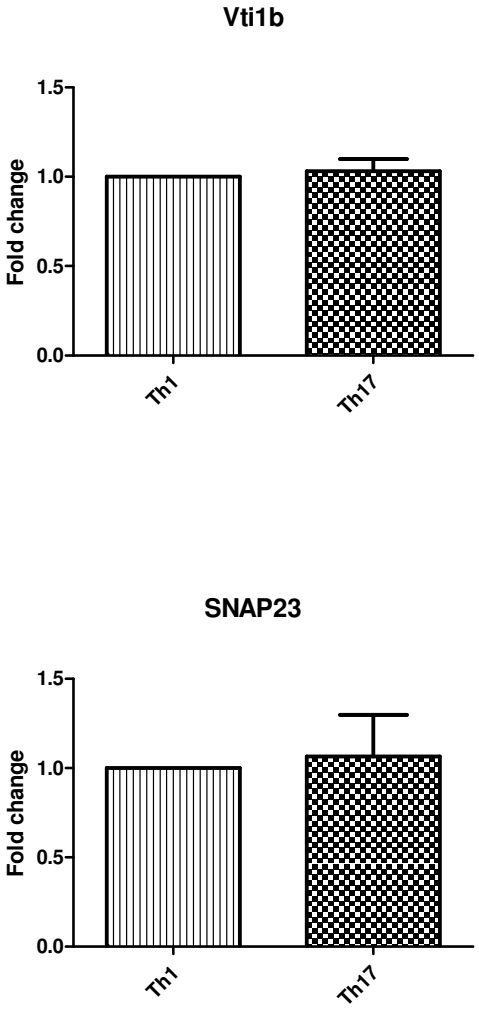

Figure 4.6 – Qb and Qbc SNARE mRNA expression in Th1 vs Th17 polarised T-helper cell subsets - $CD4^+$ cells were isolated from the spleens of female BALB/c mice aged 12-14 weeks using the easysep magnetic isolation kit. Cells were plated at $2x10^6$ cells/ml in a 24-well plate in either Th1 conditions: Il-2 (10ng/ml), IL-12 (10ng/ml) and anti-IL4 (10μg/ml) or Th17 conditions: IL1β (10ng/ml), IL-6 (20ng/ml), IL-23 (20ng/ml),TGF-β (0.2ng/ml), anti-IL-4 (10μg/ml) and anti-IFNγ (10μg/ml) and stimulated with coated anti-CD3 (5μg/ml) and anti-CD28 (5μg/ml) for 48 hours. Cells were collected and centrifuged at 1200RPM for 5mins, supernatant was removed for cytokine analysis. The RNA was extracted from samples using nucleospin RNAII isolation columns (Macherey-Nage)and 1μg of RNA was converted to cDNA using the high capacity cDNA reverse transcription kit (Applied Biosystems). The cDNA was mixed with primers for Vti1b and SNAP23 targets (IDT) and FAST SYBR Mastermix (Roche) before analysing samples on the ABI Prism 7500. Groups were compared using relative quantitation; after normalising samples to *TBP* and *GusB,* Th1 was normalised to 1.0 and the expression in other groups is shown relative to this value**.** Results are means ±SD of 7 samples generated in 3 independent experiments measured in triplicate. An unpaired T-test was used to determine if differences between Th1 and Th17 groups were significantly different.

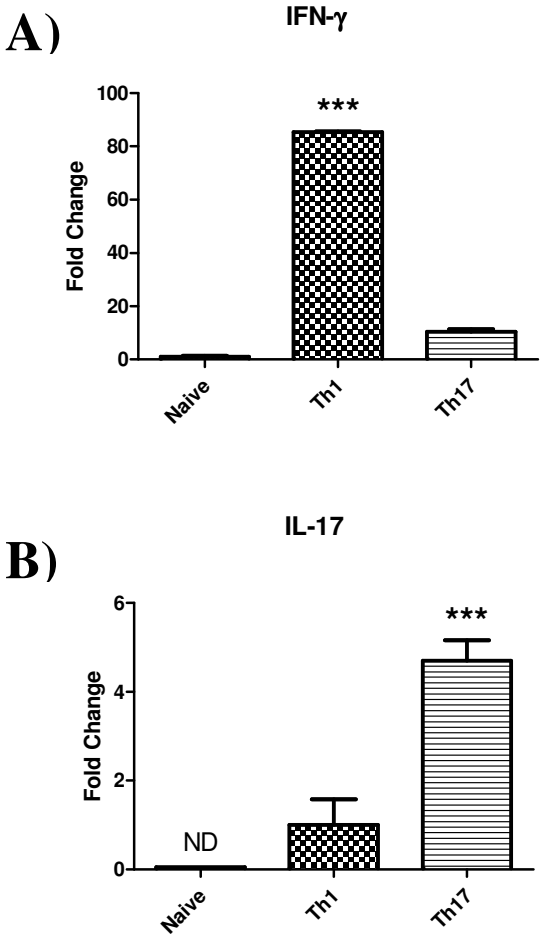

Figure 4.7 – Cytokine mRNA expression levels in Naïve, Th1 and Th17 cells at 48hrs. $CD4^+$ cells were isolated from the spleens of female BALB/c mice aged 12-14 weeks using the easysep magnetic isolation kit. Naïve cells were collected after isolation and prepped for RNA isolation by suspending in RA1 lysis buffer supplied by the RNAII nucleospin RNA isolation column kit. Remaining cells were plated at $2x10^6$ cells/ml in a 24-well plate in either Th1 conditions: Il-2 (10ng/ml), IL-12 (10ng/ml) and anti-IL4 (10μg/ml) or Th17 conditions: IL1β (10ng/ml), IL-6 (20ng/ml), IL-23 (20ng/ml),TGF-β (0.2ng/ml), anti-IL-4 (10μg/ml) and anti-IFNγ (10μg/ml) and stimulated with coated anti-CD3 (5μg/ml) and anti-CD28 (5μg/ml) for 48 hours. Cells were collected and centrifuged at 1200RPM for 5mins, supernatant was removed for cytokine analysis. The RNA was extracted from samples using nucleospin RNAII isolation columns (Macherey-Nage) and normalised amounts of RNA were converted to cDNA using the high capacity cDNA reverse transcription kit (Applied Biosystems). The cDNA was mixed with primers for IFNγ (Sigma) and IL-17 (IDT) and FAST SYBR Mastermix (Roche) before analysing samples on the ABI Prism 7500. Groups were compared using relative quantitation; after normalising samples to *TBP* and *GusB,* Th1 was normalised to 1.0 and the expression in other groups is shown relative to this value**.** Results are means ±SD of 7 samples generated in 3 independent experiments measured in triplicate. An unpaired T-test was used to determine if differences between Th1 and Th17 groups were significantly different (***$p<0.001$).

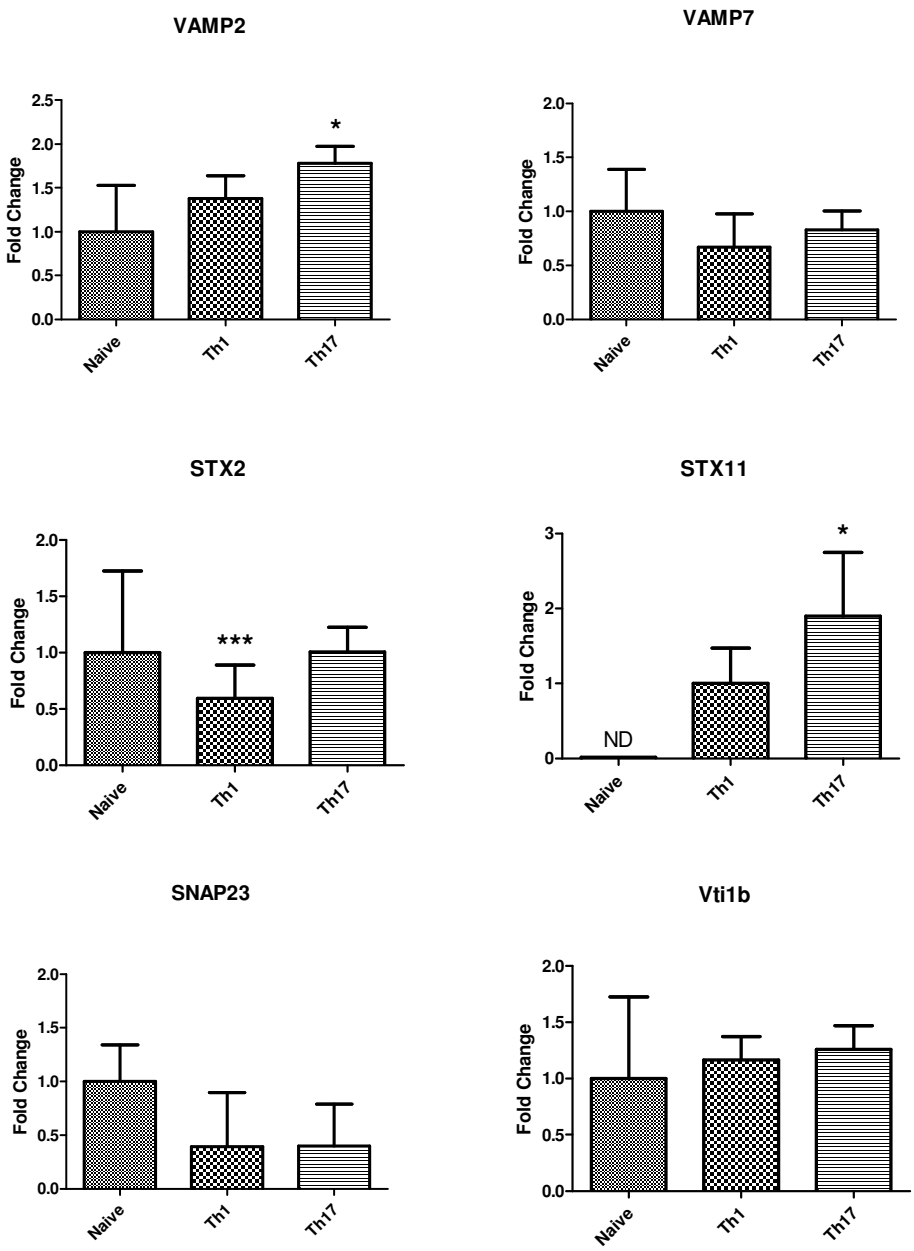

Figure 4.8 - SNARE mRNA expression levels in naïve, Th1 and Th17 cell lysates for targets of interest. $CD4^+$ cells were isolated from the spleens of female BALB/c mice aged 12-14 weeks using the easysep magnetic isolation kit. Naïve cells were collected after isolation RNA was isolated with the nucleospin RNAII isolation column kit. Remaining cells were plated at $2x10^6$ cells/ml in a 24-well plate in either Th1 conditions: Il-2 (10ng/ml), IL-12 (10ng/ml) and anti-IL4 (10µg/ml) or Th17 conditions: IL1β (10ng/ml), IL-6 (20ng/ml), IL-23 (20ng/ml),TGF-β (0.2ng/ml), anti-IL-4 (10µg/ml) and anti-IFNγ (10µg/ml) and stimulated with coated anti-CD3 (5µg/ml) and anti-CD28 (2.5µg/ml) for 48 hours. The RNA was extracted from samples and converted to cDNA using the high capacity cDNA reverse transcription kit (Applied Biosystems). The cDNA was mixed with primers for each SNARE mRNA target and FAST SYBR Mastermix (Roche) before analysing samples on the ABI Prism 7500. Groups were compared using relative quantitation; after normalising samples to *TBP* and *GusB,* Th1 was normalised to 1.0 and the expression in other groups is shown relative to this value**.** Results are means ±SD of 7 samples generated in 3 independent experiments measured in triplicate. An unpaired T-test was used to determine if differences between Th1 and Th17 groups were significantly different (***$p<0.001$).

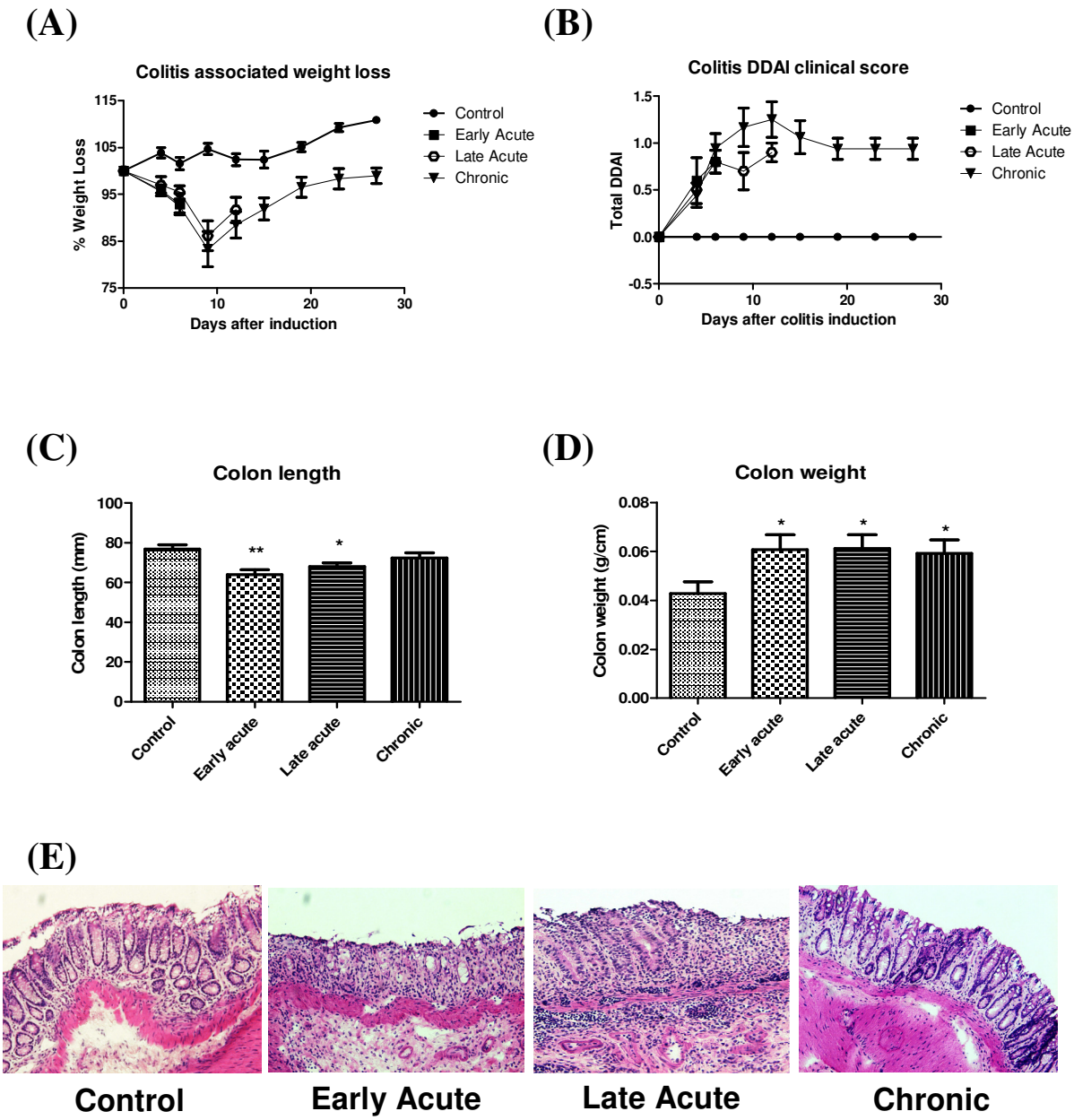

Figure 4.9 - Disease associated symptoms in the DSS colitis model – C57BL mice were grouped into a control group of 6 mice and 4 test groups. DSS was administered to mice in the drinking water for 5 days at a final concentration of 3%. Mice were weighed and disease scored based on fur texture/posture for a daily disease activity index (DDAI) every 3-4 days **(A)**. The average % weight change of the 4 groups is plotted to the end point for each group. The starting weight on Day 0 is plotted as 100% of the weight with the rest of the weight relative to this value. Two control mice were culled at the end point for each test group. There is a drop in body weight for all test groups after day 0 and a healthy gain in weight for control mice **(B)**. At the end point of each group the length **(C)** and weight **(D)** of each removed and washed colon was measured and used as an indication of inflammation in the colon. Sections of the distal colon were removed for histology and H&E staining in order to confirm inflammation. The control shows a healthy colon while infiltration and loss of crypt structure is evident in the acute slides with recovery in the chronic slides as expected **(E)**. Results are means ±SD of at least 5 mice, an unpaired T-test was used to determine if differences between groups were significant (*$p<0.05$, **$p<0.01$).

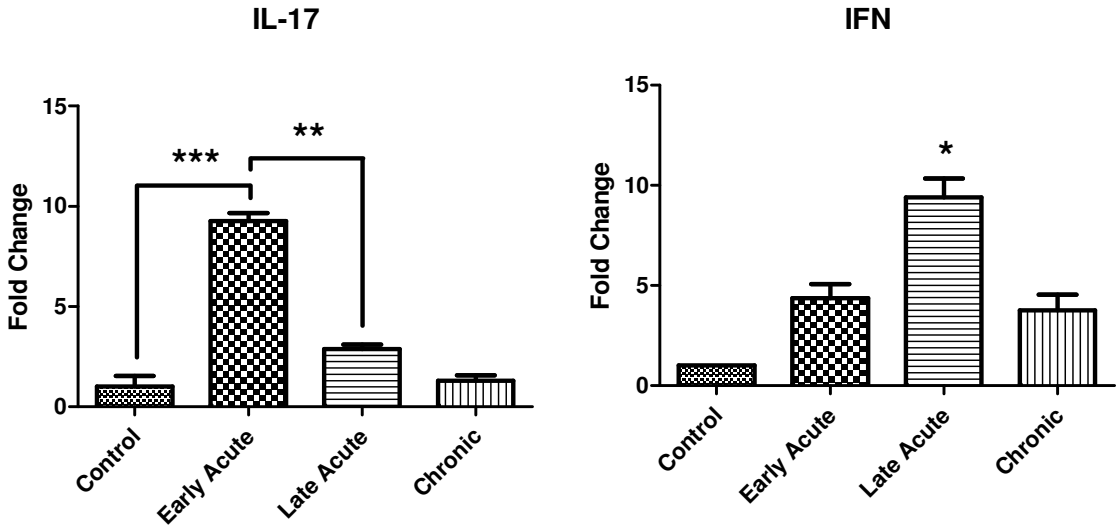

Figure 4.10 - cytokine mRNA in mouse model of colitis - C57BL mice were grouped into a control group of 6 mice and 4 test groups; early acute culled at day 7, late acute culled at day 12 and chronic mice culled at day 26. Tissue from each sample was weighed and homogenised using the Qiagen TissueLyser LT with stainless steel beads (5mm). Following homogenisation, RNA was extracted and quantitated on the nano-drop and equalised amounts of RNA were converted to cDNA using the high capacity cDNA mastermix (roche). The cDNA was mixed with primers for IFNγ (Sigma) and IL-17 (IDT) and FAST SYBR Mastermix (Roche) before analysing samples on the ABI Prism 7500. Groups were compared using relative quantitation; after normalising samples to *TBP* and *GusB,* the control group was normalised to 1.0 and the expression in other groups is shown relative to this value**.** Results are means ±SD of at least 5 mice measured in triplicate. An unpaired T-test was used to determine if differences between groups were significantly different (*$p<0.05$, **$p<0.01$, ***$p<0.001$).

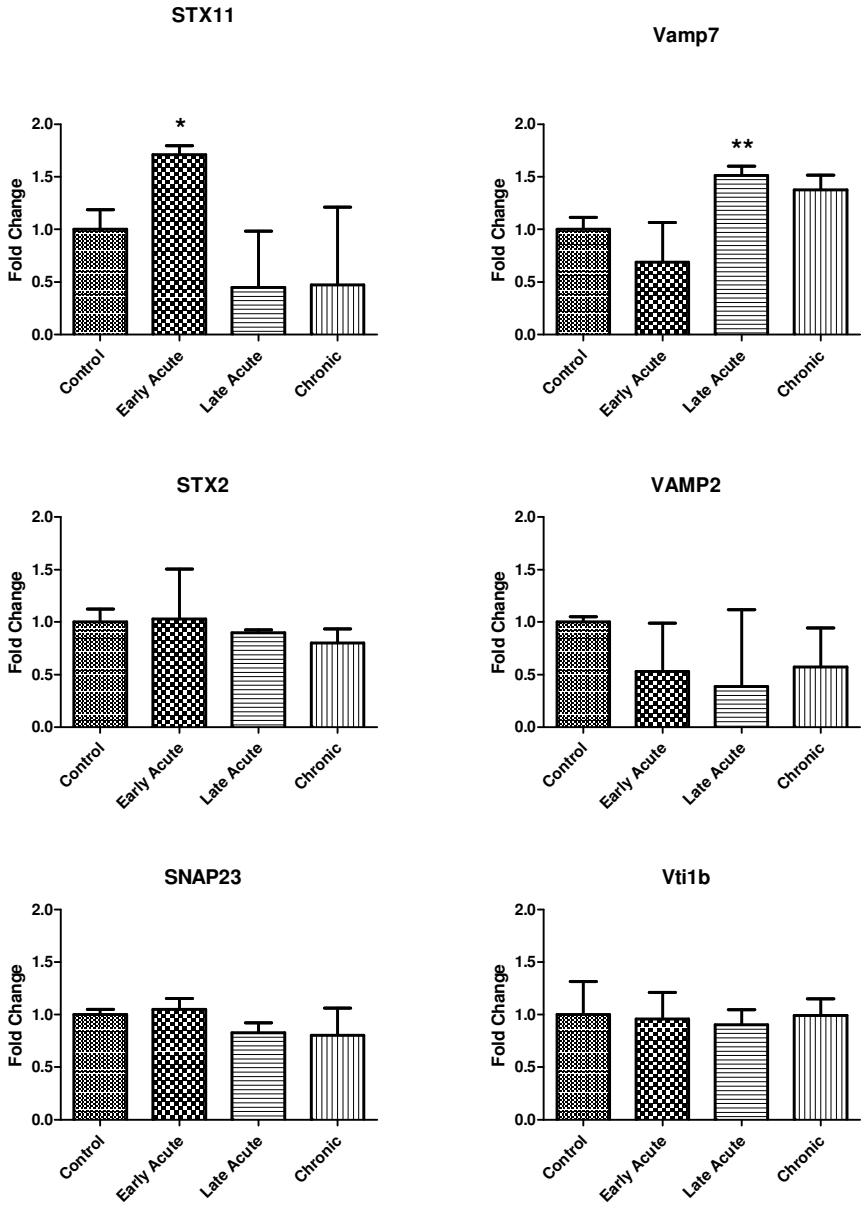

Figure 4.11 – SNARE mRNA analysis in DSS mouse model of Colitis - C57BL mice were grouped into a control group of 6 mice and 4 test groups; early acute culled at day 7, late acute culled at day 12 and chronic mice culled at day 26. DSS was administered to mice in the drinking water for 5 days at a final DSS concentration of 3%. Tissue from each sample was weighed and homogenised using the Qiagen TissueLyser LT with stainless steel beads (5mm). Following homgenisation, RNA was extracted and quantitated on the nano-drop and equalised amounts of RNA were converted to cDNA using the high capacity cDNA mastermix (roche). The cDNA was mixed with primers for each SNARE target mRNA and FAST SYBR Mastermix (Roche) before analysing samples on the ABI Prism 7500. Groups were compared using relative quantitation; after normalising samples to *TBP* and *GusB,* the control group was normalised to 1.0 and the expression in other groups are shown relative to this value**.** Results are means ±SD of at least 5 mice measured in triplicate. An unpaired T-test was used to determine if difference in expression between groups were significantly different (*$p<0.05$, **$p<0.01$).

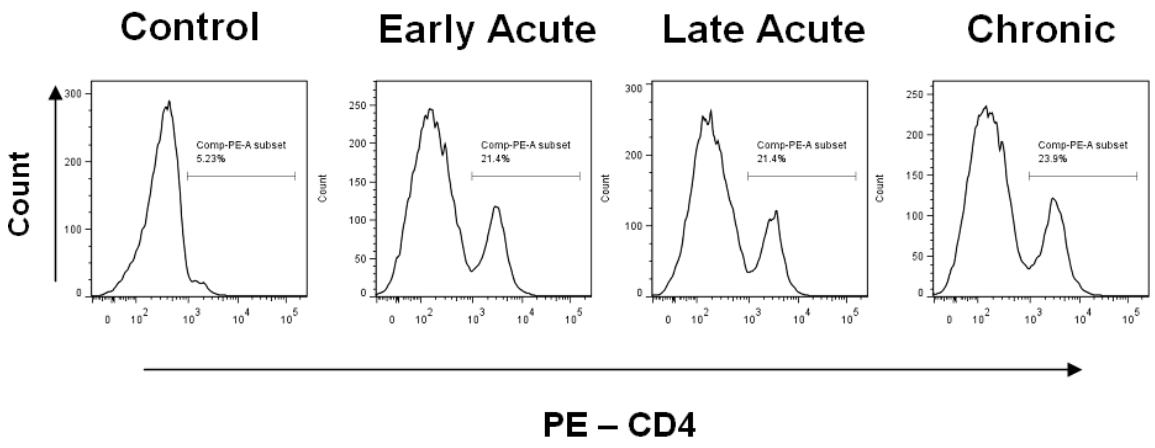

Figure 4.12 - CD4 expression in DSS model of Colitis – C57BL mice were grouped into a control group of 6 mice and 4 test groups; early acute culled at day 7, late acute culled at day 12 and chronic mice culled at day 26. DSS was administered to mice in the drinking water for 5 days. DSS water was prepared fresh every day with tap water and a final DSS concentration of 3%. Mice were weighed and disease scored based on fur texture/posture for a daily disease activity index every 3-4 days. The colon was removed from the mouse and disgested in enzymes to remove the endothelial layer of cells and isolate lamina propria cells. Cells were then stained for 30 mins with an anti-CD4 PE primary conjugated antibody (BD Bioscience) at 0.25µg/ml at room temperature. Cells were washed 3 times and analysed on the BD FACS Aria. Cells were gated to remove debris and gating shown indicates the percentage population positive for CD4 staining. The number of $CD4^+$ cells increases in the test groups when compared to the control group.

Colon Weight in *C. rodentium* infected mice

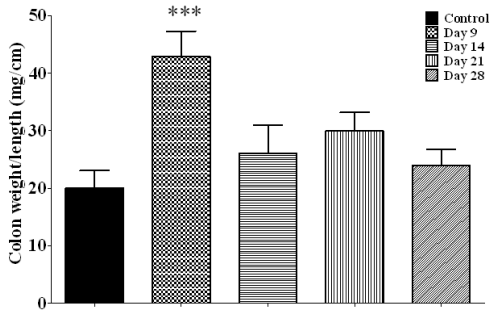

Colon Length in *C. rodentium* infected mice

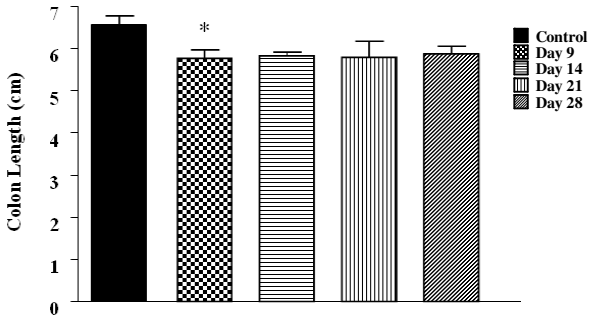

Figure 4.13 - Colon weight of mice infected with *Citrobacter rodentium* - C57BL mice were housed in groups of 6-8 mice and test mice were inoculated with *C. rodentium* orally by a 200µl gavage of approximately $200x10^9$ CFU *C. rodentium*. Mice were sacrificed at 9, 14, 21 and 28 days. Colons were collected from mice and the contents carefully removed before washing and patting dry. At the end point of each group the length and weight of each colon was measured individually and used as an indication of colitis in the mouse model. There is a significant increase in colon weight at day 9 with a recovery in the later days. There is a significant increase in colon length at day 9 with moderate recovery in the following days. Results are means ±SD of at least 5 mice, an unpaired T-test was used to determine if differences between groups were significant (*$p<0.05$, ***$p<0.001$).

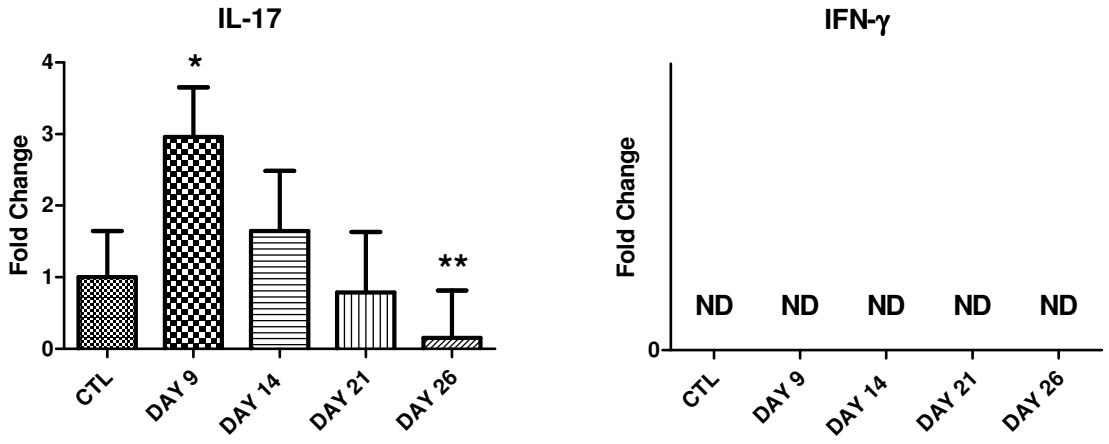

Figure 4.14 – Cytokine mRNA detection in *C. rodentium* infection model of colitis - C57BL mice were housed in groups of 6-8 mice and test mice were inoculated with a bioluminescent *C. rodentium* derivative orally by a 200µl gavage of approximately $200x10^9$ CFU *C. rodentium*. Mice were sacrificed at 9, 14, 21 and 28 days. %. The colon of each mouse was removed and the contents cleaned out in PBS before patting dry. The colon length and weight was measured and 0.5cm of distal colon was collected and stored in RNA later at 4^oC. The tissue from each sample was weighed and homogenised in RA1 buffer from the nucleospin RNAII isolation columns kit (Macherey-Nagel). Samples were homogenised using the Qiagen TissueLyser LT with stainless steel beads (5mm). Following homgenisation, RNA was extracted and quantitated on the nano-drop and 1µg of RNA was converted to cDNA using the high capacity cDNA reverse transcription kit (Applied Biosystems). The cDNA was mixed with primers for IL-17 (IDT) and FAST SYBR Mastermix (Roche) before analysing samples on the ABI Prism 7500. Groups were compared using relative quantitation; after normalising samples to *TBP* and *GusB,* the control group was normalised to 1.0. Results are means ±SD of at least 5 mice measured in triplicate. An unpaired T-test was used to determine if difference in expression between groups were significantly different (*$p<0.05$, **$p<0.01$).

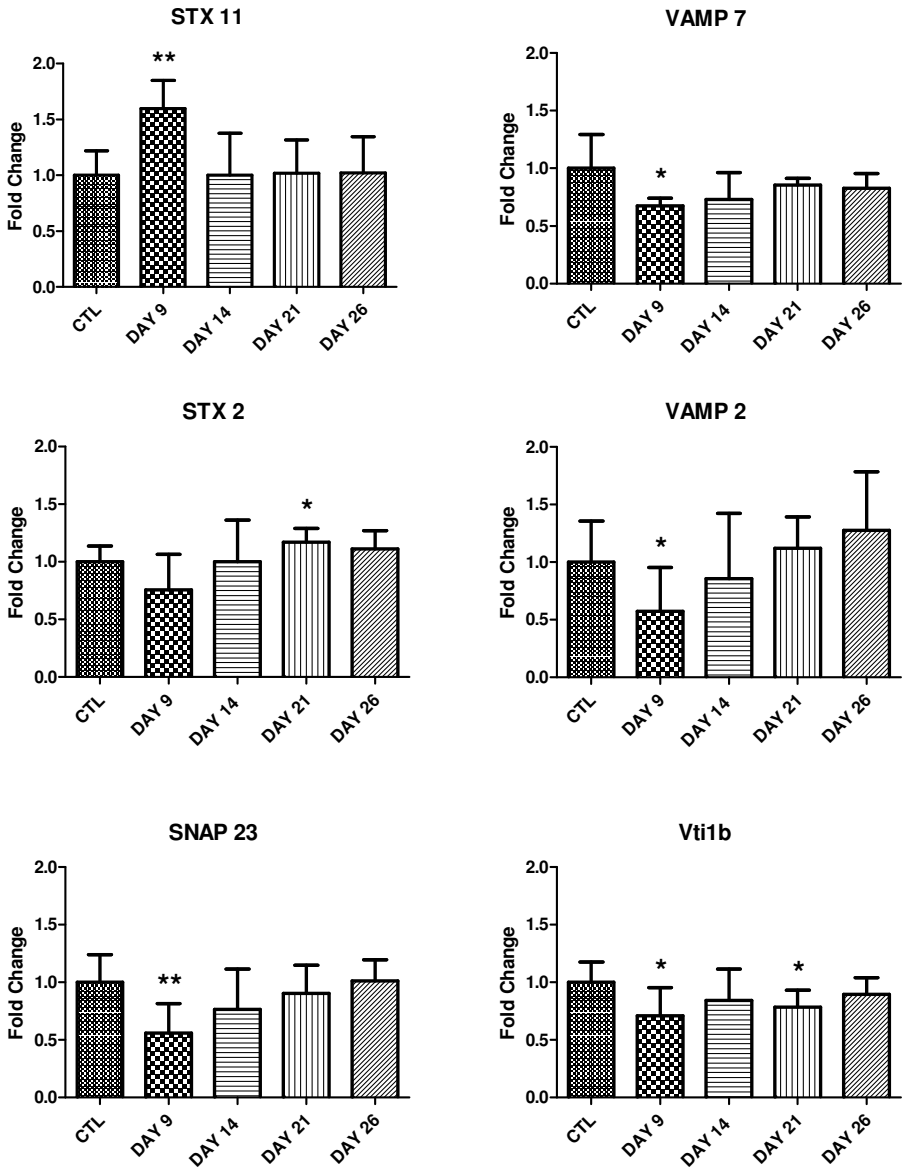

Figure 4.15 - SNARE mRNA analysis in *C. rodentium* infection model of colitis - - C57BL mice were housed in groups of 6-8 mice and test mice were inoculated with a bioluminescent *C. rodentium* derivative orally by a 200µl gavage of approximately 200x10^9 CFU *C. rodentium*. Mice were sacrificed at 9, 14, 21 and 28 days. %. The colon of each mouse was removed and the contents cleaned out in PBS before patting dry. The colon length and weight was measured and 0.5cm of distal colon was collected and stored in RNA later at 4^{o}C. The tissue from each sample was weighed and homogenised in RA1 buffer from the nucleospin RNAII isolation columns kit (Macherey-Nagel). Samples were homogenised using the Qiagen TissueLyser LT with stainless steel beads (5mm). Following homgenisation, RNA was extracted, quantitated on the nano-drop and converted to cDNA using the high capacity cDNA reverse transcription kit (Applied Biosystems) The cDNA was mixed with primers for IL-17 (IDT) and FAST SYBR Mastermix (Roche) before analysing samples on the ABI Prism 7500. Groups were compared using relative quantitation; after normalising samples to *TBP* and *GusB,* the control group was normalised to 1.0. Results are means ±SD of at least 5 mice measured in triplicate. An unpaired T-test was used to determine if difference in expression between groups were significantly different (*p<0.05, **p<0.01).

4.3 – DISCUSSION

Upon activation by anti-CD3 and anti-CD28 antibodies, T-cells undergo three phases of response leading to a polarised T-cell subset; activation, proliferation and polarisation. In order to polarise into Th1 and Th17 cells, naïve $CD4^+$ T-helper cells are activated in an environment containing recombinant cytokines which induce transcription factors and commit cells to the production of specific cytokines at the different stages of activation (Jelley-Gibbs et al. 2000). In order to analyse the differences in SNARE transcription and regulation between IFN-γ producing Th1 cells and IL-17 producing Th17 cells, it was necessary to identify a point at which each of these cytokines were highly expressed in their respective subset. The production of IFN-γ and IL-17 was assessed in polarised Th1 and Th17 cells over a 72 hour period. IFN-γ was produced early in activated T-helper cells, this has been shown by others and IFN-γ production is enhanced by the presence of IL-12 which activates STAT4 and is the first step in polarising T-cells to a Th1 subtype.(Schulz et al. 2009). IFN-γ production increased significantly at 48 hours and continued to increase at 72 hours. This is consistent with the study by Schulz *et al* (2009) showing a second significant increase in IFN-γ mRNA expression at 48 hours following commitment of Th1 cell polarisation and T-bet expression due to IL-12 signalling through the up-regulated IL-12Rβ2. This early IFN-γ response was not observed in the T-helper cells activated in Th17 conditions. Th17 cells had little or no IFN-γ or IL-17 production until 24 hours; neutralising IFN-γ antibody was included in the conditions for driving Th17 conditions and prevented the activation of T-bet via IFN-γ activation of STAT4.

T-bet represses Th17 differentiation through suppression of Runx1, the transcription factor activating RORγt (Lazarevic et al. 2011). Anti-IFN-γ antibody was included in the Th17 polarising conditions to inhibit T-bet expression, while the addition of IL-6 and TGF-β activates the Th17 master regulator RORγt. This resulted in IL-17 production at 24 hours with a significant increase measured at 48 hours. This is consistent with detailed studies of gene regulation describing induction of the signature cytokine mRNA *Il17a* at 20hrs post activation (Yosef et al. 2013). The cytokine and transcription factor data indicated 48hrs as an ideal time point to look at SNARE expression related to IFN-γ and IL-17 production. Furthermore, increased mRNA expression for the signature cytokines IFN-γ and IL17 were confirmed in their respective T-helper subset.

The SNARE family of proteins is defined by a conserved coiled-coil motif that is necessary for SNARE complex formation and membrane fusion. SNAREs are divided into 2 main families; R-SNARES are usually found on the vesicular membrane and have arginine (R) as the central functional residue in the SNARE motif. Q-SNARES are mainly found on the target membrane and are defined by a central glutamine (Q) residue. In order to form a complex and mediate membrane fusion, four SNARE motifs are required; one R-SNARE and two or three Q-SNAREs (Jahn & Scheller 2006). The R-SNARE family currently consists of seven proteins, all of which are vesicle associated membrane proteins (VAMPs) (Krzewski et al. 2011). VAMPs consist of a conserved family of proteins involved in constitutive and regulated release from a number of different cell types. VAMP1 and VAMP2 are conserved neuronal proteins involved in synaptic release (Trimble et al. 1988; Raptis et al. 2005). Although they have been shown to play a role in protein release from immunological cells, VAMP1 has not been

widely reported in immune cells and only in regulated release mechanisms (Mollinedo et al. 2006). Therefore VAMP1 was not included in this study. VAMP2 mRNA expression was increased in Th17 cells when compared to Th1 cells and may play a part in Th17 polarisation and/or exocytosis. VAMP2 is more widely distributed than VAMP1 and has been previously shown to play a role in small secretory vesicle release from neutrophils and eosinophils (Logan et al. 2006). In eosinophils VAMP2 was localised on small secretory vesicles that were rapidly mobilised following IFN-γ stimulation to release RANTES (Lacy et al. 2001). This secretion is regulated but demonstrates a role for VAMP2 in exocytosis of vesicles at the plasma membrane of an immunological cell. VAMP2 could act as the R-SNARE required to form a SNARE complex in Th1 or Th17 related constitutive cytokine release, however no significant change in VAMP2 was observed in the DSS model of colitis. Furthermore, VAMP2 was decreased in the *C. rodentium* infection model at day 9 and did not correlate with the *in vitro* study. A study in $CD8^+$ cytotoxic T-cells did not show accumulation of VAMP2 at the immunological synapse after activation, suggesting that it does not play a role in the final stages of exocytosis in T-cells (Pattu et al. 2012).

There was a small but significant decrease in VAMP7 expression in Th17 polarised cells compared to Th1 cells at 48 hours**.** An increase in mRNA expression of VAMP7 was observed in the late acute stage of DSS colitis, correlating with an increase in IFN-γ mRNA. Furthermore, VAMP7 mRNA was decreased in Th17 cells when compared to Th1 cells *in vitro,* and decreased on day 9 in the Th17 mediated *C. rodentium* infection *in vivo* when IFN-γ expression is absent. However, VAMP7 mRNA expression was not significantly increased in Th1 cells when compared to naïve $CD4^+$ T-cells *in vitro* and did

not correlate with the *in vivo* data showing regulation of VAMP7. Interestingly VAMP7 has been implicated in the secretion of de novo IFN-γ in NK T-cells. Knock-down of VAMP7 but not VAMP4 led to a decrease in IFN-γ secretion in response to different stimuli on NK cells. The ability of the cell to produce IFN-γ was not effected, but the IFN-γ was unable to leave the cells suggesting that VAMP7 is involved in its exocytosis from the cell (Krzewski et al. 2011). It is possible that VAMP7 may play a role in IFN-γ production in T-helper cells showing conservation between T-helper and NK T-cells. However, VAMP7 has been shown to be involved in other mechanisms in different cell types including degranulation in neutrophils and eosinophils (Mollinedo et al. 2006; Logan et al. 2006) and may have a number of roles depending on different cell types. The involvement of VAMP7 in de novo IFN-γ secretion warrants further investigation based on this study and those of others described but the lack of correlation between the *in vitro* and *in vivo* data did not make this a strong candidate to study further.

The Q-SNARE family is further divided into three sub-families Qa, Qb and Qc. One member of each is required to form a complex with R-SNAREs in a stable RQabc four helical bundle (Bock et al. 2001). Some SNAREs such as SNAP23 can contribute Qbc and form a complex with three members. The Qb and Qbc SNAREs SNAP23 and Vti1b showed no changes in expression between Th1 and Th17 cells at 48hours.

The syntaxin family of SNARE contribute the Qa-SNARE to the RQabc complex. Syntaxins 2, 4, 5a, 5L, 6 and 11 were assessed for changes in expression between Th1 and Th17 cells as these SNAREs have been reported to be involved in protein trafficking in immunological cells (Chen et al. 2000; Lowe et al. 2004; Murray, Wylie, et al. 2005;

Prekeris et al. 2000). The mRNA expression of STX2 was significantly increased in Th17 cells when compared to Th1 at 48hours. STX2 was originally believed to play a role in regulated granule release in platelets (Chen et al. 2000). However, this was later disputed when platelets from STX2 deficient mice indicated no loss of platelet secretory function and they went on further to show that the antibody used in the previous study was cross-reactive with STX11. Further analysis of STX2 mRNA expression in Th1 and Th17 polarised cells, compared to naïve $CD4^+$ T-helper cells showed a significant decrease in STX2 expression in the Th1 cell subset but no difference in expression between Th17 and naïve cells. Furthermore, there was no significant change in STX2 expression at any stage in the DSS model of colitis, indicating no correlation with the *in vitro* model. A small increase in mRNA expression was measured late in disease in the *C. rodentium* model. There is currently no evidence to suggest a role for STX2 in constitutive cytokine secretion in immune cells. STX2 has been identified in CTLs, but was not localised at the immunological synapse upon stimulation (Pattu et al. 2012). STX2 has also been localised on the membrane of platelet cells, although its function on the extracellular membrane still remains unclear, it is though to play a role in platelet-platelet fusion (Flaumenhaft et al. 2007). STX2 was not investigated further as a candidate for regulating cytokine secretion.

STX11 mRNA was significantly up-regulated in Th17 cells when compared to Th1 cells at 48 hours *in vitro*. When assessing SNAREs that exhibited a significant difference in expression between Th1 and Th17 subsets further, STX11 was the only SNARE that demonstrated little or no expression in naïve cells and was up-regulated in activated cells. STX11 and VAMP2 were the only SNAREs that demonstrated a significant increase in

expression in Th17 cells when compared to naïve T-helper cells**.** STX11 is an atypical SNARE in that it does not have a transmembrane domain to facilitate insertion into membrane structures. It is abundant in the immune system and is enriched in, but not exclusive to the thymus, spleen and lymph nodes (Prekeris et al. 2000). It has been identified as playing a role in a number of immune mechanisms (Bryceson et al. 2007; Ye et al. 2012; D'Orlando et al. 2013). Immune phagocytic cells are enriched in STX11 and early characterisation studies localised it on post-golgi compartments where it was hypothesized to play a regulatory role in SNARE complex formation (Prekeris et al. 2000). The *Stx11* gene mutation was recently identified as the cause of a rare autosomal recessive disorder; familial hemaphagocytic lymphohistocytosis (FHL) type-4 (zur Stadt et al. 2005). FHL is usually diagnosed within the first year of life in pediatric cases and patients with FHL present with high fever, hepatosplenomegaly and cytopenia. One of the hallmarks of the disease is hyperinflammation in patients which leads to hemophagocytosis, a condition in which the phagocytic immune cells begin to uncontrollably engulf host erythrocytes, leukocytes and platelets. Interestingly, other symptoms of FHL-4 are excessive production of pro-inflammatory cytokines but an inability to clear infections (Gholam et al. 2011). All of these symptoms suggest a dysregulation in cytokine production in STX11 deficient patients. It is clear that STX11 plays an important and specialised role in the immune system and may play involved in regulating intracellular trafficking in T-helper cells.

Importantly, this study shows a correlated increase in STX11 and IL-17 mRNA expression at the same stages of disease in both the DSS and *C. rodentium* models of

colitis. Analysis of mRNA expression in colonic tissue over the course of the DSS induced colitis revealed an initial increase in IL-17 mRNA expression in the early acute phase of disease on day 7 that decreased at later stages of disease**.** This was in parallel with a significant increase in STX11 mRNA expression at the same stage of disease and a decrease at later stages. This correlation was not seen for other SNAREs. These results suggest a link between IL-17 secretion and STX11 expression. Although IL-17 may be secreted from other cells present in the colonic tissue, we have also demonstrated that $CD4^+$ cells make up 22% of the cells in the lamina propria in treated mice. This increase in T-helper cell infiltration has been confirmed by others and studies have also indicated that the Th1/Th17 adaptive immune response plays a central role in inducing and sustaining IBD (Hall et al. 2011; Alex et al. 2009; Zenewicz et al. 2009; Liu et al. 2009; Abraham & Cho 2009). Furthermore, some of these studies describe an early Th17 response that induces IL-12 and IL-23 expression and initiates a late Th1 T-helper response (Feng et al. 2011; Ahern et al. 2010). Our data agrees with this as DSS induced colitis appears to switch to a Th1/IFN-γ response in the later stages of disease with a higher mRNA expression of IFN-γ in the late acute mice. This has been attributed in the literature to a class switch in IL-17 producing Th17 cells to IL17/IFN-γ double producing Th17 cells *in vivo* as discussed in **Chapter 3** (Ahern et al. 2010; Feng et al. 2011).

The DSS model of colitis shows that the initial IL-17/Th17 cell response correlates with an increase in STX11 in the early acute phase of the disease. Furthermore, the results from the DSS model concur well with the increased STX11 expression observed in the IL-17 producing Th17 cells *in vitro.*

The well established *C. rodentium* model of colitis further substantiated the association observed between STX11 and IL-17. *C. rodentium* is a natural rodent pathogen that inhabits the gut and induces transient distal colitis in healthy mice (MacDonald et al. 2003). *C. rodentium* was originally thought to be a Th1 inducing infection; however the discovery of the Th17 subset of cells led to this theory being revisited. A study of Th17 cells in IL-23-receptor knockout mice (*Il-23R*$^{-/-}$) infected with *C. rodentium* resulted in the discovery a central role for Th17 cells in clearing infection. In the study the Th17 response was shown to be independent of the IL-23R, but a sustained Th17 response was demonstrated to be dependent on IL-23R signalling (Mangan et al. 2006). This was later shown to be due to the necessity of IL-23R signalling in committing cells into a Th17 lineage after initial polarisation (McGeachy et al. 2009). High levels of Th17 cells were present in the colon at the height of the inflammatory response to infection on day 8. A lack of Il-23R in these mice led to a reduced ability to clear the infection highlighting the importance of Th17 cells in clearing *C. rodentium* infection (Mangan et al. 2006). In this chapter a significantly high level of IL-17 mRNA expression was measured at day 9 as expected and in agreement with the results in the study by Mangan *et al* (2006). There is a significant increase in STX11 mRNA expression on day 9 correlating with the increase in IL-17 mRNA expression. IL-17 expression is less prominent in the later stages of infection, and begins to drop off with a significant decrease on day 26. STX11 mRNA expression levels also return to control expression levels in parallel with the decreased IL-17 mRNA expression.

This chapter demonstrated that STX11 is up-regulated in Th17 cells *in vivo* and its expression is correlated to that of IL-17 in two *in vivo* models of inflammatory disease.

To our knowledge, this is the first time that a SNARE protein has been shown to be regulated during inflammatory disease of the gut and suggests a role for STX11 in Th17 cells. The next chapter will further explore the potential role for STX11 in Th17 cells.

CHAPTER 5

THE ROLE OF STX11 IN Th17 CELLS

5.1 – INTRODUCTION

In the previous chapter we demonstrated a clear correlation between increased IL-17 mRNA expression and increased STX11 mRNA expression in Th17 cells *in vitro*. STX11 expression in Th17 cells was also increased relative to the naïve T-helper cells suggesting a regulatory role in activated cells. Furthermore, STX11 mRNA expression is increased in parallel with IL-17 mRNA in two models of inflammation *in vivo* and is decreased in later stages of disease when IL-17 mRNA expression is low.

Recently a STX11 deficient (*Stx11*$^{-/-}$) mouse was generated and a murine model of FHL-4 was established in order to further explore the mechanisms by which STX11 regulates immune function. Studies using *Stx11*$^{-/-}$ cells confirmed the essential role for STX11 in NK and CTL function. Interestingly a study by D'Orlando *et al* (2013) looked in detail at the IFN-γ secretion in CD8^{+} CTL cells in *Stx11*$^{-/-}$ mice. This study confirmed the well recognised deficiency in granule release, but surprisingly showed that the cells also exhibited an over expression of IFN- γ, suggesting a loss in regulation of cytokine exocytosis (D'Orlando et al. 2013). High serum levels of circulating IFN-γ is a recognised symptom of FLH-4 and has also been shown to contribute to increased macrophage activation and phagocytosis, a hallmark of FHL (Sepulveda et al. 2013; Zhang et al. 2008). Taking this recent study into account and the results obtained in the previous chapter, we propose two possible roles for STX11 in T-helper cells. It is clear that there is a relationship between Th17 orchestrated IL-17 release and *Stx11* mRNA expression as shown in the previous chapter *in vitro* and *in vivo*. These data would suggest that STX11 is actively involved in transport and/or exocytosis of IL-17 from Th17 cells. However, given that STX11 has been implicated in negative regulation of

cellular processes and secretion through atypical SNARE behaviour, there is also a possibility that STX11 plays a role in negatively regulating IFN-γ. IFN-γ is typically not expressed in Th17 cells and therefore a negative regulatory role could explain the increase in STX11 in these cells observed in the previous chapter. The previous chapter also demonstrated that IL-17 is up-regulated in parallel with STX11 in the DSS and *C. rodentium* models of colitis in the early stages of disease. Interestingly, IFN-γ levels at these time points was low or not-detected. Furthermore, IFN-γ mRNA is expressed in the late acute stage of DSS and there is a return to control levels of STX11 mRNA expression**.** Therefore STX11 may play a role directly in Th17 secretion through regulation and transport of IL-17 from these cells; conversely, it may be involved in negatively regulating IFN-γ release, which may have consequences for Th17 cells. There is not enough evidence to suggest a prominence for either mechanism. In order to investigate these possible mechanisms and confirm the specific role for STX11 in Th17 cells, STX11 deficient mice (*Stx11*$^{-/-}$) developed by Udo Zur Stadt, were obtained through a collaboration with Silvia Bulfone-Paus at the Borstel Research Centre, Hamburg, Germany. $CD4^+$ cells from these mice were isolated and polarised into Th1 and Th17 cells and characterised *in vitro*.

5.2 – RESULTS

5.2.1 – CYTOKINE SECRETION FROM CD4⁺ T-HELPER CELLS ISOLATED FROM WILD TYPE AND Stx11$^{-/-}$ MICE AND CULTURED IN Th17 POLARISING CONDITIONS IN VITRO.

Having identified a potential role for STX11 in Th17 polarised cells, *Stx11*$^{-/-}$ mice were obtained from Silvia Bulfone-Paus' group in the Borstel Research Institute, Hamburg, Germany. Cells were isolated and cultured *in vitro* in Th1 and Th17 conditions optimised in the previous chapters and cell supernatants were assessed for cytokine secretion.

Spleenocytes and mesenteric lymph nodes from wild type (WT) and *Stx11*$^{-/-}$ mice were obtained from the Bulfone-Paus lab. $CD4^+$ cells were isolated from the spleens and lymph nodes using the EasySep Mouse $CD4^+$ T Cell Enrichment Kit (Stemcell). Naïve $CD4^+$ T-cells were also isolated from the spleenocytes using the EasySep Mouse Naïve $CD4^+$ T Cell Enrichment Kit (Stemcell). Cells were counted and plated at $2x10^6$cells/ml in 24 well plates in Th17 polarising conditions. Cells were stimulated with anti-CD3 (5μg/ml) and anti-CD28 (2.5μg/ml) for 4 days. Supernatants were collected and assessed for levels of IFN-γ, IL-17, IL-2, IL-10, IL-21 and TNF-α using ELISA duosets (R&D) and IL-21 using the Ready, Set, Go ELISA (eBioscience)**.**

IL-17 cytokine levels in the naïve Th17 polarised cells were significantly reduced ($p<0.001$) and IFN-γ levels were significantly increased in the cells from *Stx11*$^{-/-}$ mice compared to the wild type ($p<0.05$) **[Figure 5.1]**. While levels of IFN-γ are low in the WT cells as expected for a Th17 cell, but the *Stx11*$^{-/-}$ cells produced two-fold the amount

of IFN-γ **[Figure 5.1]**. Interestingly, IL-21 levels were completely reduced in *Stx11*$^{-/-}$ cells ($p<0.001$). IL-21 is a key cytokine produced early in polarised Th17 cells and is necessary for committing cells to this subset. IL-10 ($p<0.001$) and TNF-α ($p<0.05$) were also significantly reduced in *Stx11*$^{-/-}$ cells. IL-2 cytokine concentrations were at very low levels as expected in Th17 polarised cells, and there was no significant differences between WT and *Stx11*$^{-/-}$ cells **[Figure 5.1]**.

CD4^{+} T-cells isolated from the spleens of WT and *Stx11*$^{-/-}$ mice were cultured under the same conditions. Unlike the naïve CD4^{+} T-cells, there was no change observed in the levels of IL-17 cytokine secreted, with high concentrations of ~10ng/ml in WT and *Stx11*$^{-/-}$ cells. IFN-γ was significantly increased in the *Stx11*$^{-/-}$ CD4^{+} splenic cells ($P<0.001$). There was little or no IL-2 observed in the wild-type Th17 splenic T-cells as expected, however levels of IL-2 in the cells of *Stx11*$^{-/-}$ mice were significantly higher, this was also the case for IL-10 ($p<0.001$). TNF-α was moderately increased in the cells from *Stx11*$^{-/-}$ mice ($p<0.01$), while IL-21 levels were similar in WT and *Stx11*$^{-/-}$ cells **[Figure 5.2]**.

CD4^{+} T-cells were enriched from the mesenteric lymphnodes of WT and *Stx11*$^{-/-}$ mice and cultured in the same conditions as the naïve and splenic CD4^{+} T-cells over four days. Analysis of the cytokines in the supernatants show once again, a significant increase in the IFN-γ production in the Th17 polarised cells from *Stx11*$^{-/-}$ mice ($p<0.001$). There was no significant change observed in the supernatants from *Stx11*$^{-/-}$ cells for IL-17, IL-2 or TNF-α production. IL-10 production was increased in *Stx11*$^{-/-}$ cells ($p<0.05$), but there was a significant difference in the levels of IL-21 in the Th17 polarised lymph node cell supernatants. IL-21 was almost undetectable in the cell from WT mice and was increased

significantly in the *Stx11*$^{-/-}$ cell supernatants, this is in contrast to the naïve and splenic CD4^{+} cells supernatants measured **[Figure 5.3].**

5.2.2 – CYTOKINE SECRETION FROM CD4^{+} T-HELPER CELLS ISOLATED FROM WILD TYPE AND Stx11$^{-/-}$ MICE AND CULTURED IN Th1 POLARISING CONDITIONS IN VITRO.

Th17 polarised cells indicated some clear differences between secreted cytokine concentrations in WT and *Stx11*$^{-/-}$ cell supernatants. In order to ensure that the changes identified were specific to Th17 cells, Th1 cells were generated from WT and *Stx11*$^{-/-}$ mice as a comparison. Naïve CD4^{+} cells were isolated from the spleen and CD4^{+} cells were isolated from the spleens and lymph nodes using Easysep negative isolation kits (stemcell). Cells were plated at 2x10^{6} cells/ml and stimulated with plate bound 5μg/ml anti-CD3 and 2.5μg/ml soluble anti-CD28 antibodies for four days in Th1 polarising conditions. IL-2 was not added as a proliferative factor in the media so that IL-2 secretion from the cells could be accurately assessed. Supernatants from the Th1 polarised naïve CD4^{+} enriched cells showed no difference in the levels of IFN-γ, IL-17 or TNF-α after four days **[Figure5.4]**. There was a significant increase in the concentration of IL-10 ($p<0.01$) and IL-21 ($p<0.05$) measured *Stx11*$^{-/-}$ cell supernatants. Concentrations of IL-2 were significantly reduced in *Stx11*$^{-/-}$ naïve Th1 polarised cells supernatants ($P<0.001$) **[Figure 5.4]**.

Splenic CD4^{+} Th1 polarised cells show a similar trend for IL-17, IFN-γ and TNF-α with no difference between WT and *Stx11*$^{-/-}$ supernatants **[Figure 5.5]**. Again there was a decrease in the concentration of IL-2 from *Stx11*$^{-/-}$ cells ($p<0.05$) and an increase in IL-10

($p<0.001$). There was no change in IL-21 levels between WT and *Stx11*$^{-/-}$ splenic CD4^{+} isolated cells in contrast to the naïve cells **[Figure 5.5]**.

Th1 polarised CD4^{+} cells from the lymph nodes of WT and *Stx11*$^{-/-}$ mice showed no significant change in the concentrations of IFN-γ, IL-17, IL-21 and IL-2 **[Figure 5.6]**. TNF-α was significantly increased in the *Stx11*$^{-/-}$ cell ($p<0.05$) and IL-10 was also increased ($p<0.001$) in the *Stx11*$^{-/-}$ Th1 supernatants, similar to the naïve and splenic Th1 cell supernatants **[Figure 5.6]**.

5.2.3 – INTRA-CELLULAR CYTOKINE STAINING OF CD4^{+} T-HELPER CELLS ISOLATED FROM WILD TYPE AND Stx11$^{-/-}$ MICE AND CULTURED IN Th17 POLARISING CONDITIONS IN VITRO.

In order to determine the percentage of cells secreting IFN-γ and IL-17 from the total population, cells were stained for intracellular cytokines. Intracellular staining involves permeabilising the cell membrane using detergents to create pores and allow cytokine targeted antibodies to enter the cell. However, once cytokines leave the golgi apparatus in vesicles they are relatively unstable and are also able to leave the cells via the pores created by permeabilisation. In order to account for this and accurately stain cells for cytokines they produce, the cells are stimulated with PMA and ionomycin to aggressively activate the cells to produce cytokine. During this activation monensin is added to the cell culture. Monensin is a transport inhibitor that blocks intracellular transport and causes cytokines to accumulate in the golgi complex where they are less likely to leave the cells resulting in detectability being greatly increased (Prussin & Metcalfe 1995).

This method allows for single cell analysis of cytokine secretion. Cells were double stained and assessed for the percentage of cells producing IL-17 or IFN-γ or both.

WT and *Stx11*$^{-/-}$ cells were stimulated and stained for intracellular cytokines after four days of culture in Th17 polarising conditions. The cells were analysed on the BD FACS Aria and analysed using FlowJo software (Treestar). The gates were set using fluorescence minus one (FMO) controls to take into account autofluorescence and spilling of dyes into other channels. There were less IL-17 producing cells in the naïve CD4^{+} population of *Stx11*$^{-/-}$ cells with 10.1% in the WT and only 6.24% of the population in the *Stx11*$^{-/-}$ cells producing IL-17 **[Figure 5.7]**. This decrease was also observed in the lymph nodes with the WT cells having 0.19% and the *Stx11*$^{-/-}$ cells 0.48% **[Figure 5.7]** The IFN-γ producing cell population was increased in the *Stx11*$^{-/-}$ cells isolated from the spleen (0.3% to 0.77%) and the lymph nodes (0.019% to 0.048%).

No IFN-γ/IL-17 double producing cells (>0.1%) were detected in any of the cell populations **[Figure 5.7]**.

5.2.4 – INTRA-CELLULAR CYTOKINE STAINING OF CD4^{+} T-HELPER CELLS ISOLATED FROM WILD TYPE AND Stx11$^{-/-}$ MICE AND CULTURED IN Th1 POLARISING CONDITIONS IN VITRO.

Isolated cells were activated in Th1 polarising conditions for four days before re-activating with PMA and ionomycin in the presence of monensin. Cells were then stained with anti-IFN-γ and IL-17 primary conjugated antibodies and analysed on the BD FACS Aria. The data were analysed using FlowJo software (Treestar).

There was a significant increase in the *Stx11*$^{-/-}$ Th1 polarised naive cells with a large increase in the number of IFN-γ producing cells. The WT cells had an 18.5% IFN-γ producing population and the *Stx11*$^{-/-}$ had a 32.2% IFN-γ producing population, an almost 2-fold increase **[Figure 5.8]**. This increase was not evident in the spleen and lymph node CD4^{+} cells. Very small numbers (<1%) of cells were identified as IL-17 producing cells in any of the WT and *Stx11*$^{-/-}$ cells populations **[Figure 5.8]**.

5.2.5 – RORγt STAINING OF CD4^{+} T-HELPER CELLS ISOLATED FROM WILD TYPE AND Stx11$^{-/-}$ MICE AND CULTURED IN Th17 AND Th1 POLARISING CONDITIONS IN VITRO.

The previous sections have described a significant decrease in the concentration of IL-17 in the supernatants of *Stx11*$^{-/-}$ cells polarised in Th17 conditions for four days *in vitro* **[section 5.2.1]**. We have also shown that the number of IL-17 producing cells is decreased in some Th17 polarised cell populations, particularly the naïve cell population **[section 5.2.3].** In order to attribute this reduction in IL-17 secretion to dysregulation in cytokine trafficking due to a lack of STX11, it was necessary to confirm the commitment of the cells to a Th17 subset. RORγt expression is required for the polarisation of a Th17 cells from naïve T-helpers (Ivanov et al. 2006). Therefore, the expression of the master regulator and transcription factor RORγt was assessed in Th1 and Th17 polarised cells from WT and *Stx11*$^{-/-}$ mice. Chapter 2 of this study and work by others has shown that RORγt expression peaks at 18hrs after stimulation in Th17 polarising conditions (Yosef et al. 2013). At this time point cells were removed from culture and fixed with 3% PAF and permeabilised with 1% Tween-20. Cells were then stained with an APC conjugated

anti-RORγt antbody and analysed on the FACS Aria. Data were analysed using FlowJo software (Treestar). The data are presented as the percentage of RORγt expressing cells in the total cell population following 18hrs stimulation in either Th1 or Th17 polarising conditions.

The naïve Th17 polarised cells were 21.5% positive for RORγt expression in the WT population. This was significantly reduced to 5.2% in the *Stx11*$^{-/-}$ cells **[Figure 5.9)**. A similar reduction was observed in the splenic CD4^{+} cells, with a 22.4% positive RORγt population in the WT cells and 8% RORγt positive population in the *Stx11*$^{-/-}$ cells, and the CD4^{+} T-cells isolated from the lymph nodes, with 29.5% of the population of RORγt positive cells compared to 20.8% in the *Stx11*$^{-/-}$ cells **[Figure5.9]**. RORγt expression was also measured in the Th1 polarised cell populations. 10% of the WT naïve Th1 polarised cells stained positive for RORγt expression. This was decreased to 5.9% in the *Stx11*$^{-/-}$ cells **[Figure 5.10]**. No change was observed in the splenic isolated CD4^{+} T-cells and the lymph node CD4^{+} cells had a 10.7% RORγt population, which was marginally increased to 12.4% in the *Stx11*$^{-/-}$ cells **[Figure5.10]**.

5.2.6 – PROLIFERATION OF Th17 POLARISED CELLS ISOLATED FROM WILD TYPE AND Stx11$^{-/-}$ *MICE.*

Proliferation is an important factor in T-cell activation and polarisation. Levels of cytokines accumulated over four days show differences between polarised cells from WT and *Stx11*$^{-/-}$ mice. However, an increased proliferation rate would result in more generations of cytokine producing cells which may not be reflected in the cell number or viability due to increased cell cycling. This may have an impact on the results observed in the supernatant cytokine measurements. In order to assess the effects lack of STX11

on proliferation rates in Th1 and Th17 polarised cells, the cells were stained with CFSE as described previously **[section 3.2.6]**. Cells were removed from culture daily and stained with propidium iodide in order to exclude the dead cells. Cells were analysed on the BD FACS Aria and the data were analysed using FlowJo software (Treestar). The histograms show the number of peaks measured on day one, two and three of cell culture. Each peak represents a generation of cells. The raw data was anaylsed using the proliferation analysis algorithm on the FlowJo software which calculates the approximate number of cells in each generation of cells. The data is represented in three graphs comparing the WT and *Stx11*$^{-/-}$ cells. The percentage divided is the total number of cells in the population which underwent proliferation.

In the WT Th17 cells on day four, 70% of the total cells had divided compared to just 40% of the *Stx11*$^{-/-}$ cells **[Figure 5.11]**. A reduction was also observed in the division index. The division index is the average number of divisions that the cells undergo. This includes the undivided peak and is therefore representative of the whole system and not just the dividing system. The bottom graph represents the profile of proliferation to allow easy comparison between WT and *Stx11*$^{-/-}$ cells where each point represents the total percentage of cells in each generation of divided cells. It is clear from these profiles that more of the WT cells were in later generations and had undergone more divisions **[Figure 5.11]**. The effect was not as significant in splenic and lymph node CD4^{+} cells; however the trend was the same. The percentage divided and the division index was decreased in the *Stx11*$^{-/-}$ cells for both populations and the profiles indicated more cells in the later generations of WT cells compared to *Stx11*$^{-/-}$ cells **[Figure 5.12 and 5.13]**.

Therefore, in the absence of STX11, proliferation was affected in all populations of isolated Th17 polarised cells and was most evident in naïve Th17 polarised cells.

5.2.7 – PROLIFERATION OF Th1 POLARISED CELLS ISOLATED FROM WILD TYPE AND *Stx11*$^{-/-}$ MICE.

We also examined the effect of STX11 deficiency on the proliferation of T1 polarised cells. Th1 naïve *Stx11*$^{-/-}$ cells had a reduced percentage of total cells divided; 35% compared to the 74% in the WT **[Figure 5.14]**. The division index was also reduced. The proliferation profile comparing the WT and *Stx11*$^{-/-}$ cells demonstrates the significant difference between the profiles of these cells, with the majority of the *Stx11*$^{-/-}$ cells having a low number of divisions **[Figure 5.14]**. This difference in proliferation was not observed in the splenic or lymph node isolated $CD4^+$ cells **[Figure 5.15 and 5.16]**. The percentage divided and division index were similar for both the splenic and lymph node isolated cells and the proliferation profile for splenic and lymph node cell populations were almost identical for the WT and *Stx11*$^{-/-}$ cells **[Figure 5.15 and 5.16]**.

5.2.8 – CELL COUNTS AND VIABILITY OF Th1 And Th17 POLARISED CELLS ISOLATED FROM WILD TYPE AND *Stx11*$^{-/-}$ MICE.

Having identified differences between proliferation in Th1 and Th17 cell subsets from WT and *Stx11*$^{-/-}$ cells, the viability and cells numbers was assessed to identify any other differences in the absence of STX11 in order to correctly interpret the data collected.

The numbers of cells in culture following four days of stimulation in Th1 or Th17 conditions were counted using a haemocytometer and trypan blue dead cell exclusion.

The numbers were graphed comparing WT and *Stx11*$^{-/-}$ cells in both Th1 and Th17 cells. The naïve Th1 cells had similar numbers in the WT and *Stx11*$^{-/-}$ cells **[Figure 5.17]**. The naïve Th17 polarised cells however had a significant difference in the cell numbers on day four. The WT cell numbers were almost 3-fold higher than the Th17 polarised *Stx11*$^{-/-}$ cells **[Figure 5.17]**. The cell viability was assessed using PI staining, and cells were analysed on the BD FACS Aria flow cytometer. Live cells do not allow PI to enter the cells and stain the nucleus, therefore cells negative for PI staining were gated and the graph represents the percentage of viable cells from the total number of cells measured. The viability of the naïve Th1 polarised *Stx11*$^{-/-}$ cells was increased compared to the wild type with 58% viability measured in the *Stx11*$^{-/-}$ cells compared to 43% in the WT cells **[Figure 5.17].** There was no difference in the Th17 polarised cells between WT and *Stx11*$^{-/-}$**.** Finally the viability of the cells over the four days was plotted and WT and *Stx11*$^{-/-}$ cell viability was compared in both Th1 and Th17 polarised cells. There was an increase in viability in the Th1 polarised naïve cells from *Stx11*$^{-/-}$ mice on days 2, 3 and 4, while the WT Th17 cells had a higher viability then the *Stx11*$^{-/-}$ mice on days 1, 2 and 3 **[Figure 5.17]**.

There are no significant changes observed between the WT and *Stx11*$^{-/-}$ cell counts in the splenic CD4^{+} cells **[Figure 5.18]**. The cell viability was similar between WT and *Stx11*$^{-/-}$ Th1 polarised cells over the four days, while the WT Th17 polarised cells appear to have higher viability on days 1 and 2 with similar viability to *Stx11*$^{-/-}$ cells on days 3 and 4 **[Figure 5.18]**. The lymph node isolated CD4^{+} cells show an increased cell viability in the Th1 polarised WT cells compared to the cells from *Stx11*$^{-/-}$ mice on days 2 an 3 with similar levels on day 4. The Th17 polarised WT cells have an increased viability on days

2 and 3 with similar viability on day 4 with no significant increase compared to Th1 polarised *Stx11*$^{-/-}$ cells **[Figure 5.19].**

5.2.9 – mRNA EXPRESSION OF SIGNATURE Th17 GENES AND CONFIRMATION OF Th17 POLARISATION IN NAÏVE CELLS FROM WT MICE.

These results on cell numbers and viability and the previous sections assessing proliferation must be taken in to account when analysing and interpreting the concentrations of IFNγ and IL-17 secreted in the supernatants over the four days of cell culture. Over the four days the cells undergo a number of changes in gene regulation and cytokine secretion. Gene expression differences between the WT and *Stx11*$^{-/-}$ cells can give an indication on the state of the cell after four days in culture. mRNA expression was therefore assessed in naïve polarised T-helper cells in order to collect more information on the effects of STX11 deficiency on cytokine gene expression, and polarisation of the cells.

The splenic naïve T-cells represent a pure population of cells which were then polarised into Th1 and Th17 cells. The splenic and lymph node cell populations contain central and effector memory cells which may already be differentiated into Th1 and Th17 cells and therefore may affect the results observed in the *Stx11*$^{-/-}$ cells on differentiation or cytokine regulation. Differences in cell differentiation and proliferation were previously detected in **section 5.2.3, 4, 6 and 7** in the naïve cells, which were not as evident in the $CD4^+$ isolated cells from spleen and lymph nodes. Therefore, the mRNA expression

from cytokine and transcription factor genes was analysed in the pure naïve polarised cell populations in order to identify differences between WT and *Stx11*$^{-/-}$ cells.

RNA was isolated from the Naïve CD4^{+} WT cells using the RNA II Nucleospin® kit (Macherey-Nage) according to the manufacturer's instructions. The cDNA was generated from 0.5µg of RNA using the High Capacity cDNA Reverse Transcriptase Kit (Applied Biosystems, USA) and random primers. The cDNA was diluted 1/10 in DEPC treated water and qPCR was carried out on the ABI Prism 7500 using Roche SYBR green mastermix and primers directed to the targets were obtained from sigma or IDT as listed in **Appendix C**. We first examined the Th1 and T17 profiles in the WT cells to establish that we had a distinct fully polarised Th1 and Th17 population. Th17 cells showed high expression of IL-17, IL-21 and RORγt and low expression of IFN-γ and T-bet **[Figure 5.20].** The Il-23 receptor, which is critical for maintenance and commitment of Th17 cells, had similar expression in Th1 and T17 cells **[Figure 5.20].** These results were in agreement with the cytokine data generated for the Th17 cells showing high production of IL-17 and IL-21, and low production of IFN-γ in these cells. The RORγt mRNA expression levels also corroborated the intracellular staining of RORγt protein in the naïve WT cells. Having confirmed the Th17 profile of cells using mRNA, expression of STX11 was measured to confirm the results observed in our previous studies using naïve CD4^{+} cells. STX11 expression was significantly increased in the Th17 polarised cells ($P<0.001$). STX11 expression was also measured in the *Stx11*$^{-/-}$ cells and was not detected as expected. The RNA generated was used to assess genes associated with cytokine production, polarisation and cell phenotype in order to identify differences in gene expression between the WT and *Stx11*$^{-/-}$ cells.

5.2.10 – mRNA EXPRESSION OF TRANSCRIPTION FACTOR GENES IN POLARISED NAÏVE CELLS FROM WT AND *Stx11*$^{-/-}$ MICE.

The mRNA expression levels of the master regulator genes RORγt (Th17), T-bet (Th1) and Foxp3 (Treg) were assessed in the cells stimulated in Th17 polarising conditions. The expression measured in the *Stx11*$^{-/-}$ cells were expressed relative to WT Th17 cells which were normalised to one. The Th17 cells surprisingly show a small increase in RORγt expression on day four (1-1.5-fold), this is despite a decrease at 18hrs as shown by intracellular protein staining, when RORγt is highly expressed during polarisation. There was a significant increase in the expression of T-bet and Foxp3 **[Figure 5.22].** Suggesting a difference in phenotype between the WT and *Stx11*$^{-/-}$ cells activated in Th17 polarising conditions.

No significant difference in the mRNA expression of the transcription factors RORγt, T-bet or FoxP3 were observed on day four in Th1 polarised naïve T-cells from WT and *Stx11*$^{-/-}$ mice **[Figure 5.23].**

5.2.11 – mRNA EXPRESSION OF CYTOKINE GENES IN POLARISED NAÏVE CELLS FROM WT AND *Stx11*$^{-/-}$ MICE.

IL-17 is the key cytokine secreted by Th17 cells and as observed in the previous sections IL-17 secretion is down-regulated in naïve Th17 cells in the absence of STX11. To assess cytokine gene expression in these cells, qPCR was used to measure mRNA expression in Th17 polarised cells from WT and *Stx11*$^{-/-}$ mice. In agreement with the previous results, IL-17 mRNA expression was significantly lower in cells from *Stx11*$^{-/-}$

mice. IFN-γ mRNA expression was significantly increased (8-fold) in the *Stx11*$^{-/-}$ cells in agreement with earlier results showing an increase in IFN-γ in cell supernatants collected over the four days. mRNA expression of the *Il21* gene, necessary for early Th17 polarisation, was significantly decreased in *Stx11*$^{-/-}$ cells compared to WT Th17 polarised cells. IL-2 mRNA expression was also significantly decreased in the *Stx11*$^{-/-}$ cells. There was no change observed in IL-10 mRNA expression in the *Stx11*$^{-/-}$ cells **[Figure 5.24]**. Taken together these results show a decrease in IL-17 and IL-21 at gene expression level while IFN-γ expression is significantly increased. This would indicate a difference in the cell phenotypes following activation in these conditions, and a dysregulation of Th17 polarisation in the absence of STX11.

We also examined the cytokine expression in Th1 cells and showed that there was a similar increase in IFN-γ mRNA expression in the *Stx11*$^{-/-}$ cells ($P<0.01$) **[Figure 5.25].** This correlates with the measured increase in IFN-γ secretion in the supernatants from these cells and the increase in IFN-γ producing cells observed in the earlier intracellular staining. Surprisingly, IL-2 was higher in the *Stx11*$^{-/-}$ cells compared to the WT on day four **[Figure 5.25]**. IL-21 mRNA expression is increased in the *Stx11*$^{-/-}$ cells (>15-fold) **[Figure 5.25]**. IL-21 is secreted late in Th1 cells and this significant increase in IL-21 at the gene level is in agreement with the earlier ELISA carried out on the supernatants of these cells. IL-21 production has been reported to induce IL-10 mRNA expression, which we also showed to be increased in the *Stx11*$^{-/-}$ cells **[Figure 5.25]** and was also in agreement with the earlier ELISA data.

5.2.12 – mRNA EXPRESSION OF CYTOKINE RECEPTOR GENES IN POLARISED NAÏVE CELLS FROM WT AND Stx11$^{-/-}$ MICE.

Cytokine receptors are indicative of the phenotypic state of a cell and increases in receptor proteins on the surface can be a result of polarisation, activation or cell exhaustion. In order to assess the state of these cells the cytokine receptors for IL-23, IL-2 (CD25) and IFN-γ were compared in Th17 polarised cells from WT and *Stx11*$^{-/-}$ mice. IFN-γR has been indentified on late stage Th17 cells which can class switch to a double producing cell. IFN-γR1 mRNA expression levels were significantly reduced in Th17 polarised cells from *Stx11*$^{-/-}$ mice ($p<0.001$) **[Figure 5.26]**. IL-23 receptor signalling on T-cells is necessary for lineage commitment and expansion of Th17 cells. There is a significant decrease in the expression of IL-23R in the cells from *Stx11*$^{-/-}$ mice ($P<0.001$) **[Figure 5.26]**. There was no significant difference observed in the IL-2Ra mRNA expression levels comparing naïve *Stx11*$^{-/-}$ cells to WT cells **[Figure 5.26]**.

The mRNA expression of the cell surface receptor genes for IFN-γR1, IL-2RA and IL-23R were also assessed in the Th1 polarised cells from WT and *Stx11*$^{-/-}$ mice. IFN-γR1 is significantly reduced in the *Stx11*$^{-/-}$ cells ($P<0.001$) **[Figure 5.27]**. This is concurrent with a minor reduction in IL-2RA which is responsible for proliferation and maintenance of Th1 cells. There is no significant difference in IL-23R mRNA expression between the WT and *Stx11*$^{-/-}$ cells **[Figure 5.27]**.

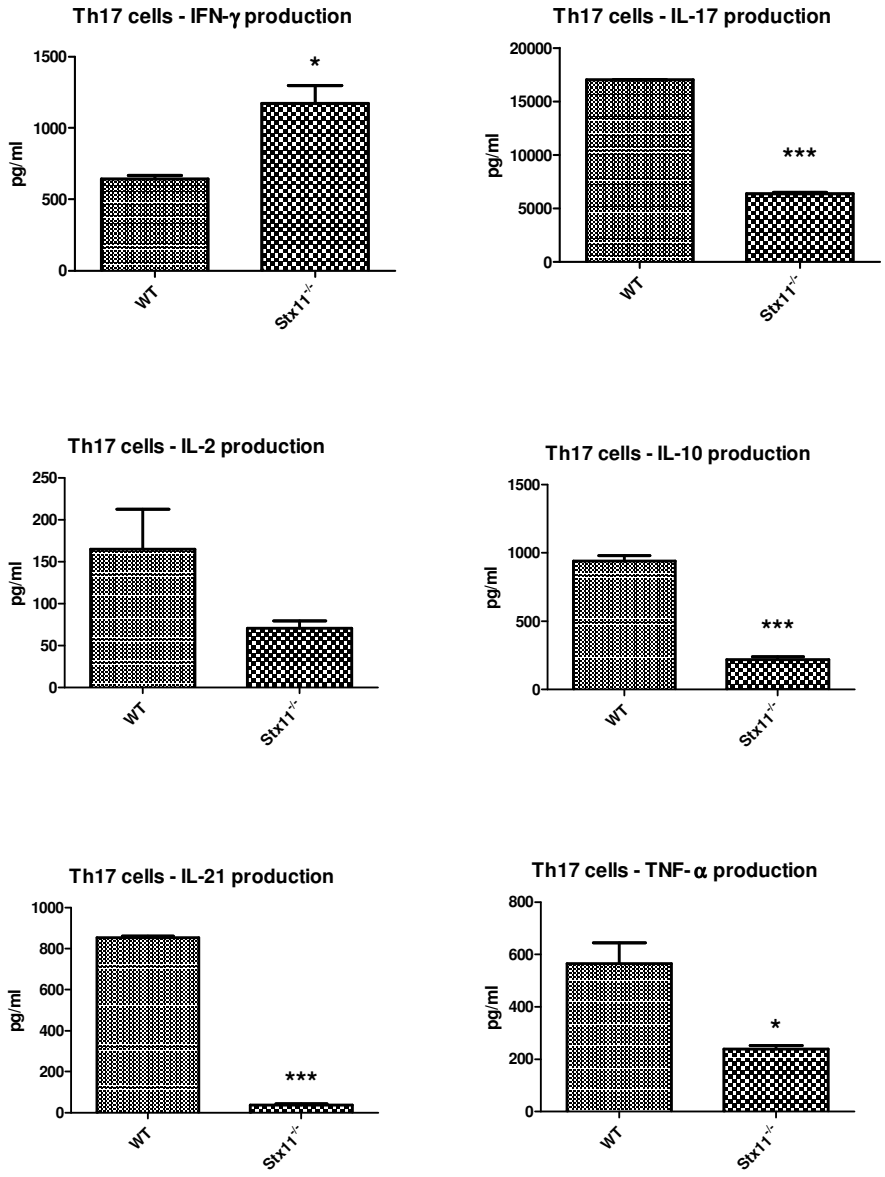

Figure 5.1 – Cytokine concentration in supernatants from wild type and *Stx11*$^{-/-}$ naive splenic CD4^{+} T-cells activated in Th17 polarising conditions and measured by ELISA. Spleens were isolated from 8 wild type and 8 *Stx11*$^{-/-}$ mice**.** Spleenocytes were enriched for Naïve CD4^{+} T-cells using the EasySep™ Mouse Naïve CD4^{+} T-Cell Isolation Kit (Stemcell). Cells were counted and plated at 2x10^{6} cells/ml and stimulated with plate bound anti-CD3 antibody (5μg/ml) and soluble anti-CD28 antibody (2.5μg/ml) in Th17 conditions: IL1β (10ng/ml), IL-6 (20ng/ml), IL-23 (20ng/ml),TGF-β (0.2ng/ml), anti-IL-4 (10μg/ml) and anti-IFNγ (10μg/ml) for 4 days. Cells were centrifuged (2000RPM for 10 mins) and supernatants were collected and assessed for concentrations of IFN-γ, IL-17, IL-2, IL-10 and TNF-α using R&D duoset ELISA kits. IL -21 was assessed using the IL-21 ready, set, go ELISA kit (eBioscience). Results are means ±SEM of three groups each consisting of cells pooled from two mice and measured in triplicate. An unpaired T-test was used to determine if differences between WT and *Stx11*$^{-/-}$ mice were significantly different (*p<0.05 and ***p<0.001).

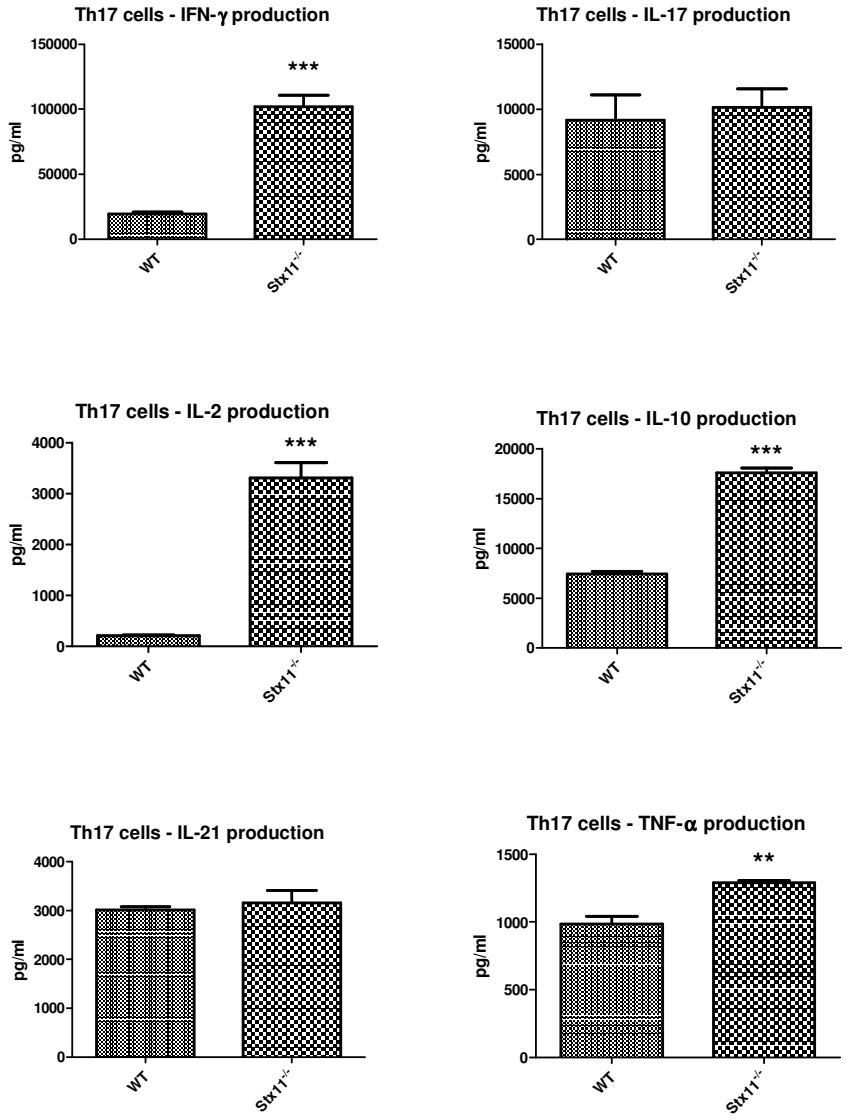

Figure 5.2- Cytokine concentrations in supernatants from wild type and *Stx11*$^{-/-}$ CD4^{+} T- splenic cells activated in Th17 polarising conditions and measured by ELISA. Spleens were isolated from 8 wild type and 8 *Stx11*$^{-/-}$ mice**.** Spleenocytes were enriched for CD4^{+} T-cells using the EasySep™ Mouse CD4^{+} T-Cell Isolation Kit (Stemcell). Cells were counted and plated at 2x10^{6} cells/ml and stimulated with plate bound anti-CD3 antibody (5μg/ml) and soluble anti-CD28 antibody (2.5μg/ml) in Th17 conditions: IL1β (10ng/ml), IL-6 (20ng/ml), IL-23 (20ng/ml), TGF-β (0.2ng/ml), anti-IL-4 (10μg/ml) and anti-IFNγ (10μg/ml) for 4 days. Cells were centrifuged (2000RPM for 10 mins) and supernatants were collected and assessed for concentrations of IFN-γ, IL-17, IL-2, IL-10 and TNF-α using R&D duoset ELISA kits. Il-21 was assessed using the IL-21 ready, set, go ELISA kit (eBioscience). Results are means ±SEM of three groups each consisting of cells pooled from two mice and measured in triplicate. An unpaired T-test was used to determine if differences between WT and *Stx11*$^{-/-}$ mice were significantly different (**p<0.01and ***p<0.001).

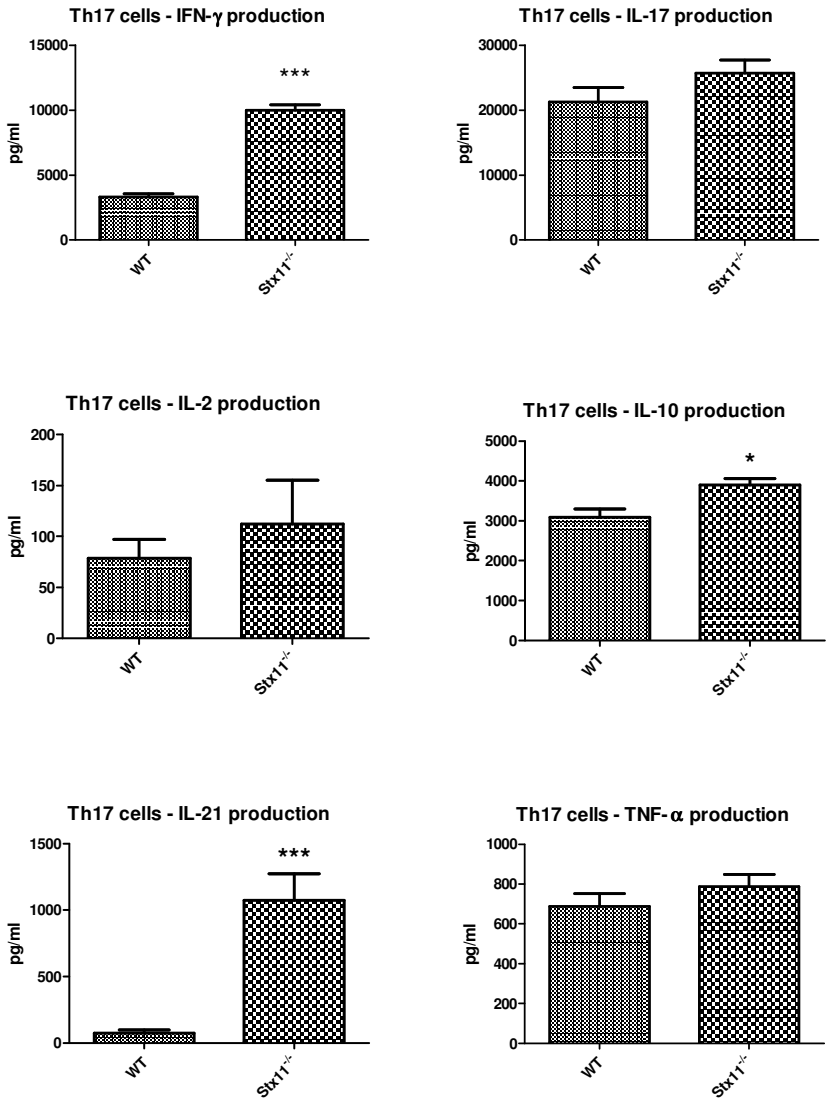

Figure 5.3 - Cytokine concentration in supernatants from wild type and *Stx11*$^{-/-}$ lymph node CD4+ T-cells activated in Th17 polarising conditions and measured by ELISA. Mesenteric lymph nodes were isolated from 8 wild type and 8 *Stx11*$^{-/-}$ mice**.** Lymph nodes were enriched for CD4^{+} T-cells using the EasySep™ Mouse CD4^{+} T-Cell Isolation Kit (Stemcell). Cells were counted and plated at 2x10^{6} cells/ml and stimulated with plate bound anti-CD3 antibody (5μg/ml) and soluble anti-CD28 antibody (2.5μg/ml) in Th17 conditions: IL1β (10ng/ml), IL-6 (20ng/ml), IL-23 (20ng/ml),TGF-β (0.2ng/ml), anti-IL-4 (10μg/ml) and anti-IFNγ (10μg/ml) for 4 days. Cells were centrifuged (2000RPM for 10 mins) and supernatants were collected and assessed for concentrations of IFN-γ, IL-17, IL-2, IL-10 and TNF-α using R&D duoset ELISA kits. Il-21 was assessed using the IL-21 ready, set, go ELISA kit (eBioscience). Results are means ±SEM of three groups each consisting of cells pooled from two mice and measured in triplicate. An unpaired T-test was used to determine if differences between WT and *Stx11*$^{-/-}$ mice were significantly different (*p<0.05 and ***p<0.001).

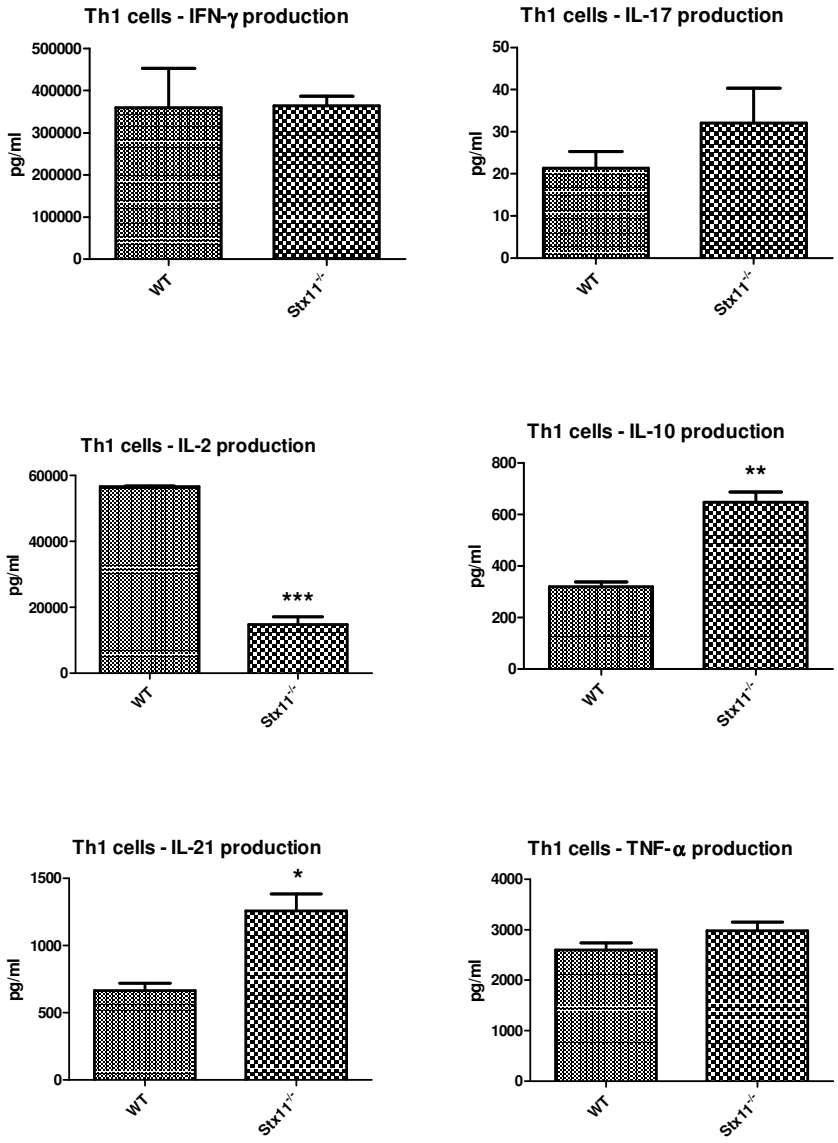

Figure 5.4 - Cytokine concentrations in supernatants from wild type and *Stx11*$^{-/-}$ naïve CD4+ T-cells activated in Th1 polarising conditions and measured by ELISA. Spleens were isolated from 8 wild type and 8 Stx11$^{-/-}$ mice**.** Spleenocytes were enriched for Naïve CD4^{+} T-cells using the EasySep™ Mouse Naïve CD4^{+} T Cell Isolation Kit (Stemcell). Cells were counted and plated at 2x10^{6} cells/ml and stimulated with plate bound anti-CD3 antibody (5µg/ml) and soluble anti-CD28 antibody (2.5µg/ml) in Th1 polarising conditions: IL12 (10ng/ml) and anti-IL-4 (10µg/ml) for 4 days. Cells were centrifuged (2000RPM for 10 mins) and supernatants were collected and assessed for concentrations of IFN-γ, IL-17, IL-2, IL-10 and TNF-α using R&D duoset ELISA kits. Il-21 was assessed using the IL-21 ready, set, go ELISA kit (eBioscience). Results are means ±SEM of three groups each consisting of cells pooled from two mice and measured in triplicate. An unpaired T-test was used to determine if differences between WT and *Stx11*$^{-/-}$ mice were significantly different (*p<0.05, **p<0.01 and ***p<0.001).

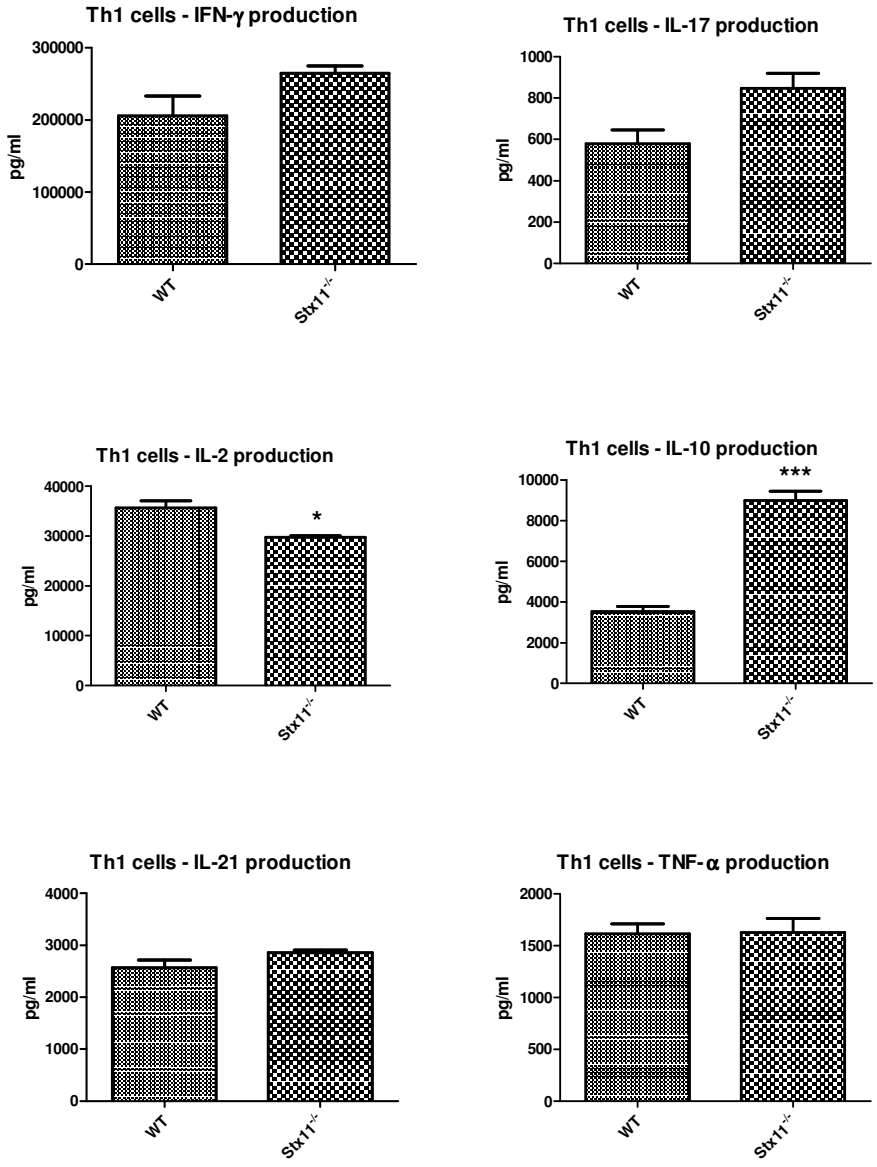

Figure 5.5 - Cytokine concentrations in supernatants from wild type and *Stx11*$^{-/-}$ splenic CD4+ T-cells activated in Th1 polarising conditions and measured by ELISA. Spleens were isolated from 8 wild type and 8 Stx11$^{-/-}$ mice**.** Spleenocytes were enriched for CD4^{+} T-cells using the EasySep™ Mouse CD4^{+} T-Cell Isolation Kit (Stemcell). Cells were counted and plated at 2x10^{6} cells/ml and stimulated with plate bound anti-CD3 antibody (5µg/ml) and soluble anti-CD28 antibody (2.5µg/ml) in Th1 polarising conditions: IL12 (10ng/ml) and anti-IL-4 (10µg/ml) for 4 days. Cells were centrifuged (2000RPM for 10 mins) and supernatants were collected and assessed for concentrations of IFN-γ, IL-17, IL-2, IL-10 and TNF-α using R&D duoset ELISA kits. Il-21 was assessed using the IL-21 ready, set, go ELISA kit (eBioscience). Results are means ±SEM of three groups each consisting of cells pooled from two mice and measured in triplicate. An unpaired T-test was used to determine if differences between WT and *Stx11*$^{-/-}$ mice were significantly different (*p<0.05 and ***p<0.001).

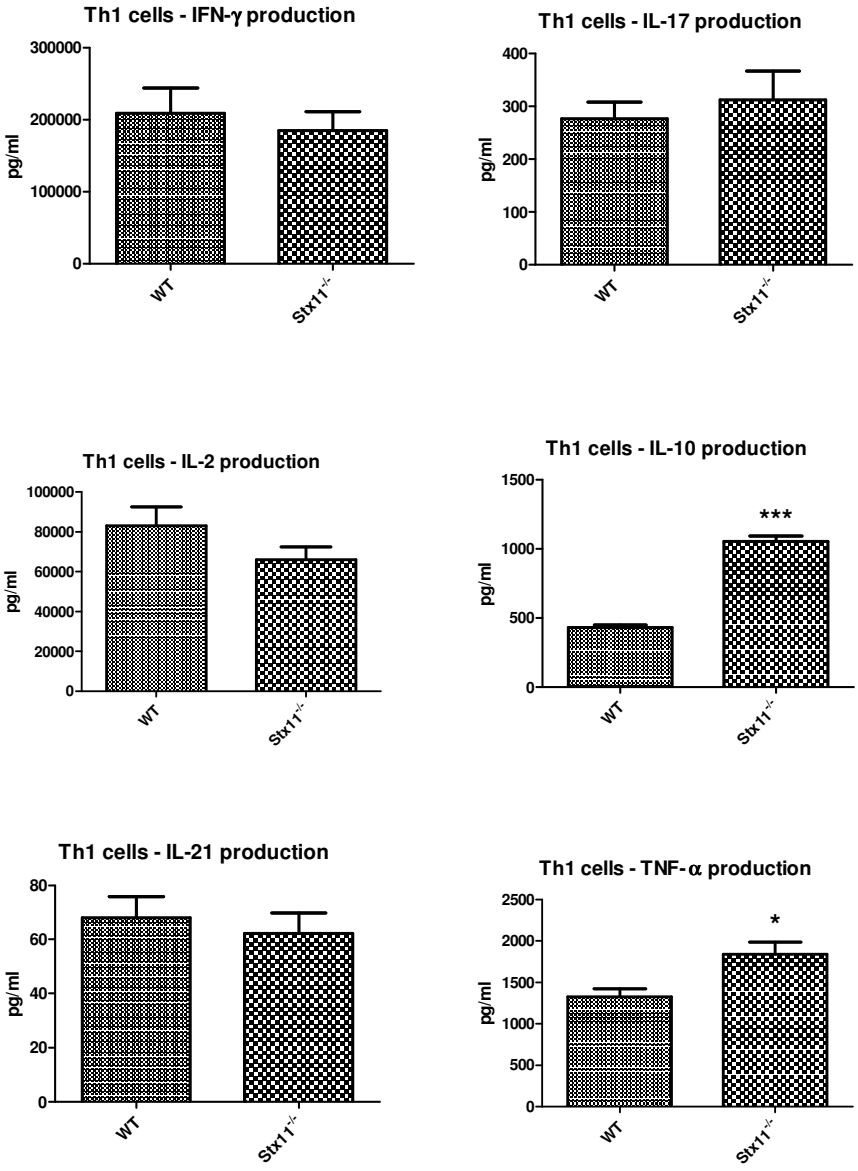

Figure 5.6 - Cytokine concentration in supernatants from wild type and *Stx11*$^{-/-}$ lymph node CD4+ T-cells activated in Th1 polarising conditions and measured by ELISA. Mesenteric lymph nodes were isolated from 8 wild type and 8 Stx11$^{-/-}$ mice**.** Lymph nodes were enriched for CD4^{+} T-cells using the EasySep™ Mouse CD4^{+} T-Cell Isolation Kit (Stemcell). Cells were counted and plated at 2x10^{6} cells/ml and stimulated with plate bound anti-CD3 antibody (5μg/ml) and soluble anti-CD28 antibody (2.5μg/ml) in Th17 conditions: Th1 polarising conditions: IL12 (10ng/ml) and anti-IL-4 (10μg/ml) for 4 days. Cells were centrifuged (2000RPM for 10 mins) and supernatants were collected and assessed for concentrations of IFN-γ, IL-17, IL-2, IL-10 and TNF-α using R&D duoset ELISA kits. Il-21 was assessed using the IL-21 ready, set, go ELISA kit (eBioscience). Results are means ±SEM of three groups each consisting of cells pooled from two mice and measured in triplicate. An unpaired T-test was used to determine if differences between WT and *Stx11*$^{-/-}$ mice were significantly different (*p<0.05 and ***p<0.001).

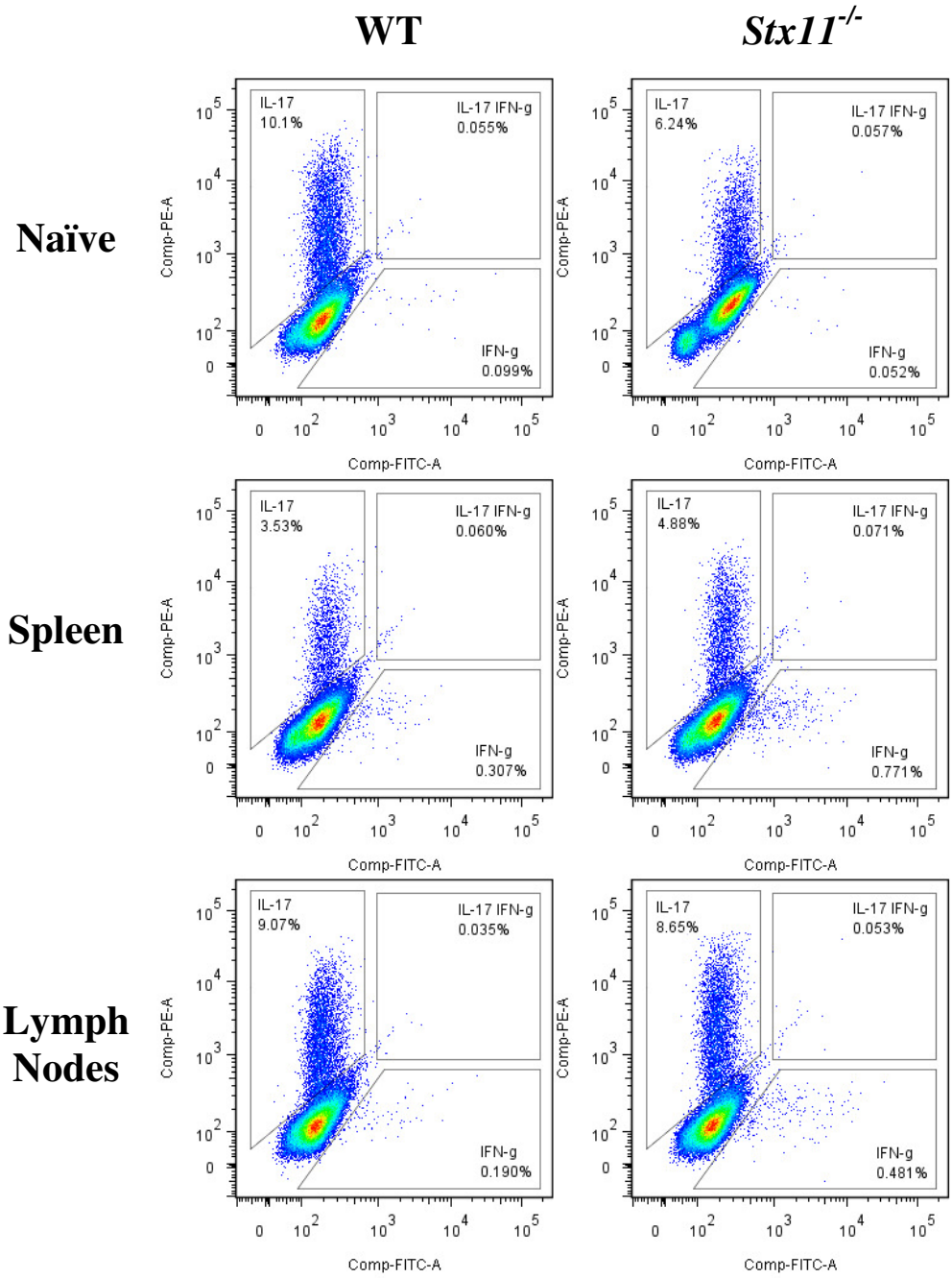

Figure 5.7 - Intracellular cytokine staining of cells isolated from wild type and *Stx11*$^{-/-}$ mice and activated in Th17 polarising conditions *in vitro*. Spleens and mesenteric lymph nodes were isolated from 8 wild type and 8 *Stx11*$^{-/-}$ mice**.** Spleenocytes were enriched for Naïve CD4^{+} T-cells and spleenocytes and lymph nodes were enriched for CD4^{+} T-cells using Easysep isolation kits (stemcell) Cells were counted and plated at 2x10^{6} cells/ml and stimulated with plate bound anti-CD3 antibody (5µg/ml) and soluble anti-CD28 antibody (2.5µg/ml) in Th17 polarising conditions for 4 days. On day 4, cells were stimulated with PMA (1µg/ml) and ionomycin (50ng/ml) for 4 hours. Monensin was added for the last 2 hours. Cells were the centrifuged and fixed with 3% PAF and permeabilised with saponin (0.5%). Cells were double stained with FITC conjugated anti-IFN-γ and PE conjugated PE antibodies. Cells were analysed on the FACS aria (BD) and data were analysed using Flowjo software. Plots show the percentage of cells expressing IFN-γ, IL-17 or both. Representative graphs are shown comparing the percentage of IL-17 and IFN-γ expressing cells isolated from WT vs. *Stx11*$^{-/-}$ mice.

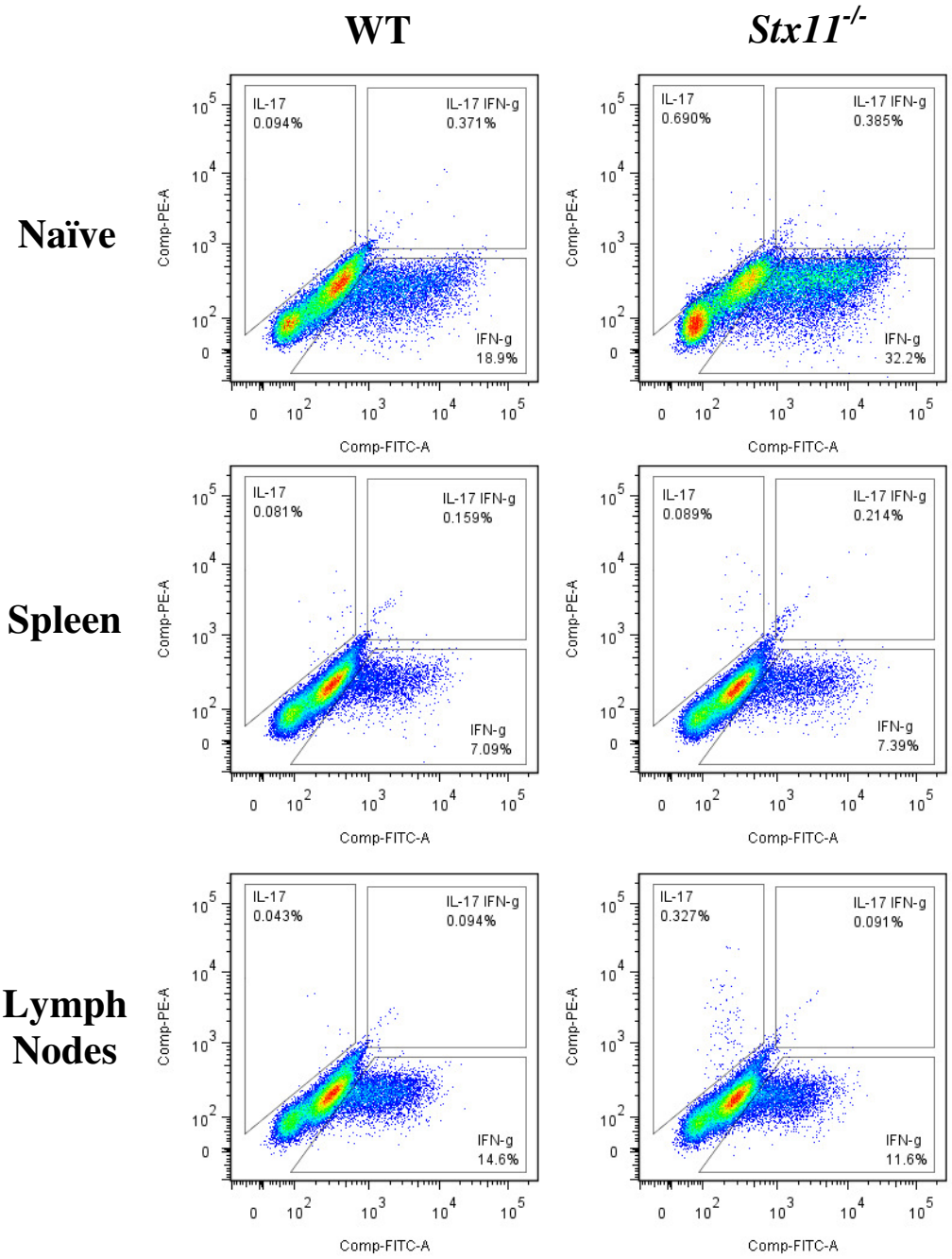

Figure 5.8- Intracellular cytokine staining of cells isolated from wild type and *Stx11*$^{-/-}$ mice and activated in Th1 polarising conditions *in vitro*. Spleens and mesenteric lymph nodes were isolated from 8 wild type and 8 *Stx11*$^{-/-}$ mice**.** Spleenocytes were enriched for Naïve CD4^{+} T-cells and spleenocytes and lymph nodes were enriched for CD4^{+} T-cells using Easysep isolation kits (stemcell) Cells were counted and plated at 2x10^{6} cells/ml and stimulated with plate bound anti-CD3 antibody (5µg/ml) and soluble anti-CD28 antibody (2.5µg/ml) in Th1 polarising conditions for 4 days. On day 4, cells were stimulated with PMA (1µg/ml) and ionomycin (50ng/ml) for 4 hours. Monensin was added for the last 2 hours. Cells were the centrifuged and fixed with 3% PAF and permeabilised with saponin (0.5%). Cells were double stained with FITC conjugated anti-IFN-γ and PE conjugated PE antibodies. Cells were analysed on the FACS aria (BD) and data were analysed using Flowjo software. Plots show the percentage of cells expressing IFN-γ, IL-17 or both. Representative graphs are shown comparing the percentage of IL-17 and IFN-γ expressing cells isolated from WT vs. *Stx11*$^{-/-}$ mice.

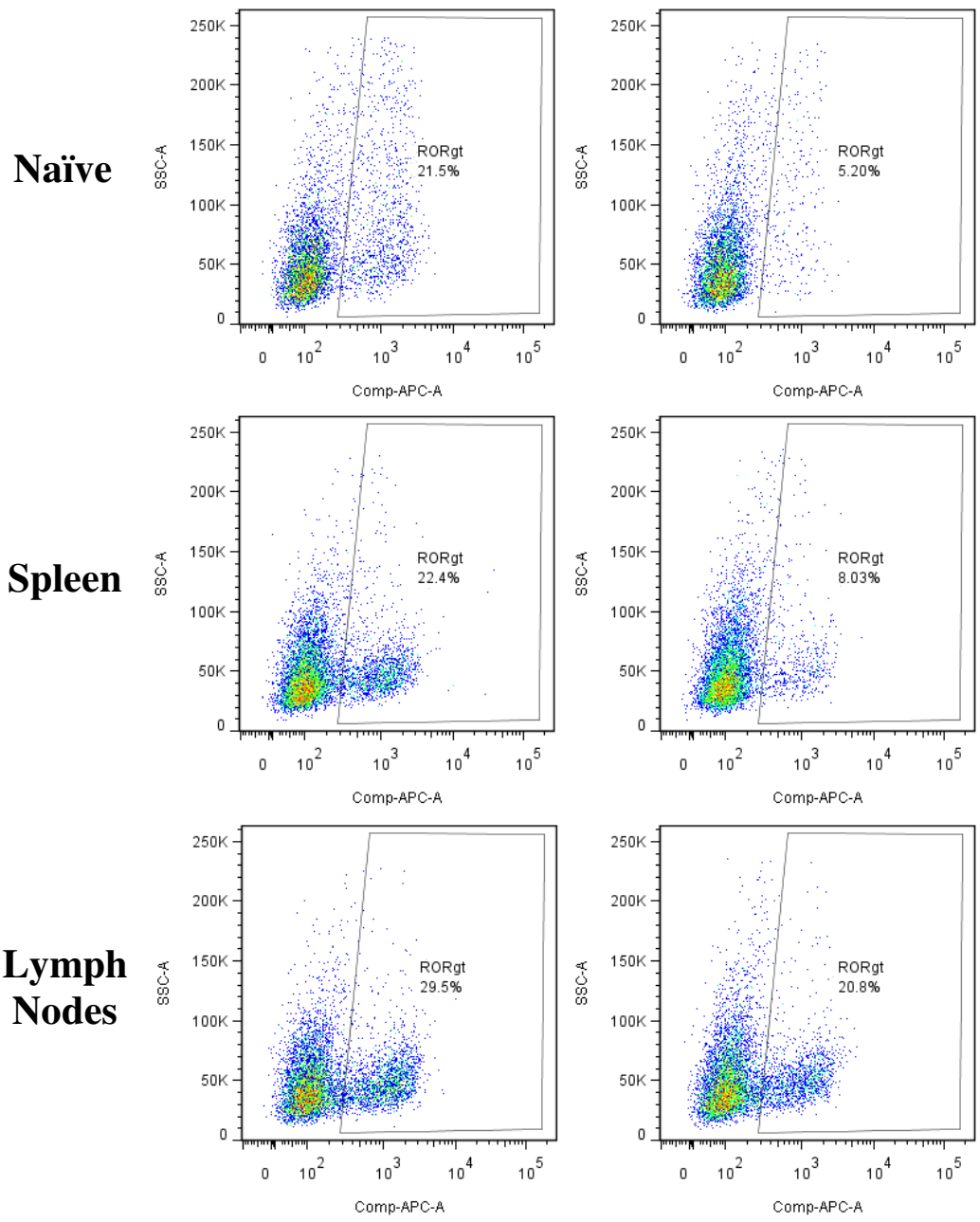

Figure 5.9 - Intracellular transcription factor staining of cells isolated from wild type and *Stx11*$^{-/-}$ mice and activated in Th17 polarising conditions *in vitro*. Spleens and mesenteric lymph nodes were isolated from 8 wild type and 8 *Stx11*$^{-/-}$ mice**.** Spleenocytes were enriched for Naïve CD4^{+} T-cells and spleenocytes and lymph nodes were enriched for CD4^{+} T-cells using Easysep isolation kits (stemcell) Cells were counted and plated at 2x10^{6} cells/ml and stimulated with plate bound anti-CD3 antibody (5µg/ml) and soluble anti-CD28 antibody (2.5µg/ml) in Th17 polarising conditions for 18hrs. Cells were then centrifuged and fixed with 3% PAF and permeabilised with triton-x100 (1%). Cells were stained with APC conjugated anti-RORγt antibody. Cells were analysed on the FACS aria (BD) and data were analysed using Flowjo software. Plots show the percentage of cells expressing RORγt. Representative graphs are shown comparing the percentage of RORγt expressing cells isolated from WT vs. *Stx11*$^{-/-}$ mice

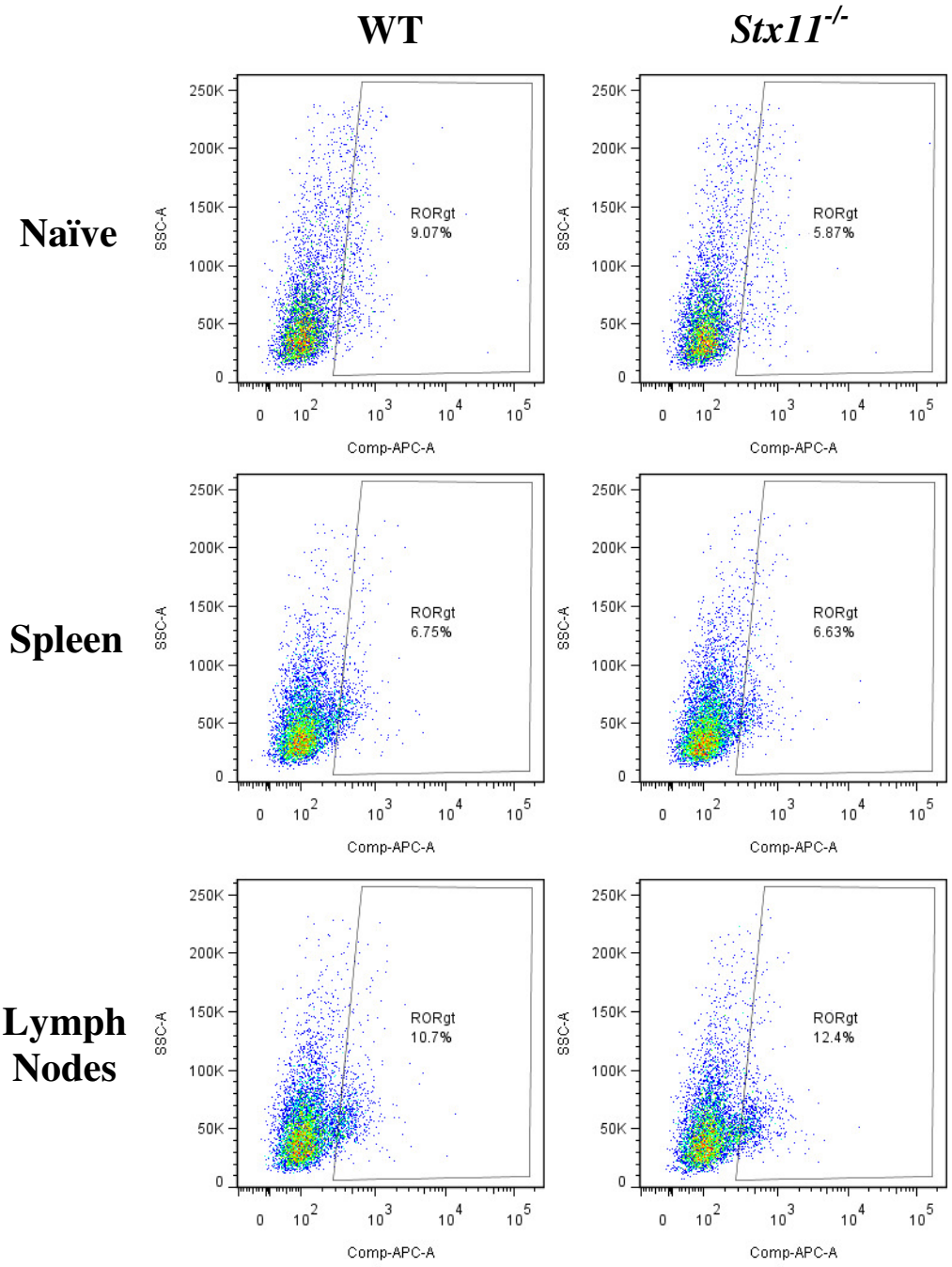

Figure 5.10 - Intracellular transcription factor staining of RORγt in cells isolated from wild type and *Stx11*$^{-/-}$ mice and activated in Th1 polarising conditions *in vitro*. Spleens and mesenteric lymph nodes were isolated from 8 wild type and 8 *Stx11*$^{-/-}$ mice**.** Spleenocytes were enriched for Naïve CD4^{+} T-cells and spleenocytes and lymph nodes were enriched for CD4^{+} T-cells using Easysep isolation kits (stemcell) Cells were counted and plated at 2x10^{6} cells/ml and stimulated with plate bound anti-CD3 antibody (5µg/ml) and soluble anti-CD28 antibody (2.5µg/ml) in Th1 polarising conditions for 18hrs. Cells were then centrifuged and fixed with 3% PAF and permeabilised with triton-x100 (1%). Cells were stained with APC conjugated anti-RORγt antibody. Cells were analysed on the FACS aria (BD) and data were analysed using Flowjo software. Plots show the percentage of cells expressing RORγt. Representative graphs are shown comparing the percentage of RORγt expressing cells isolated from WT vs. *Stx11*$^{-/-}$

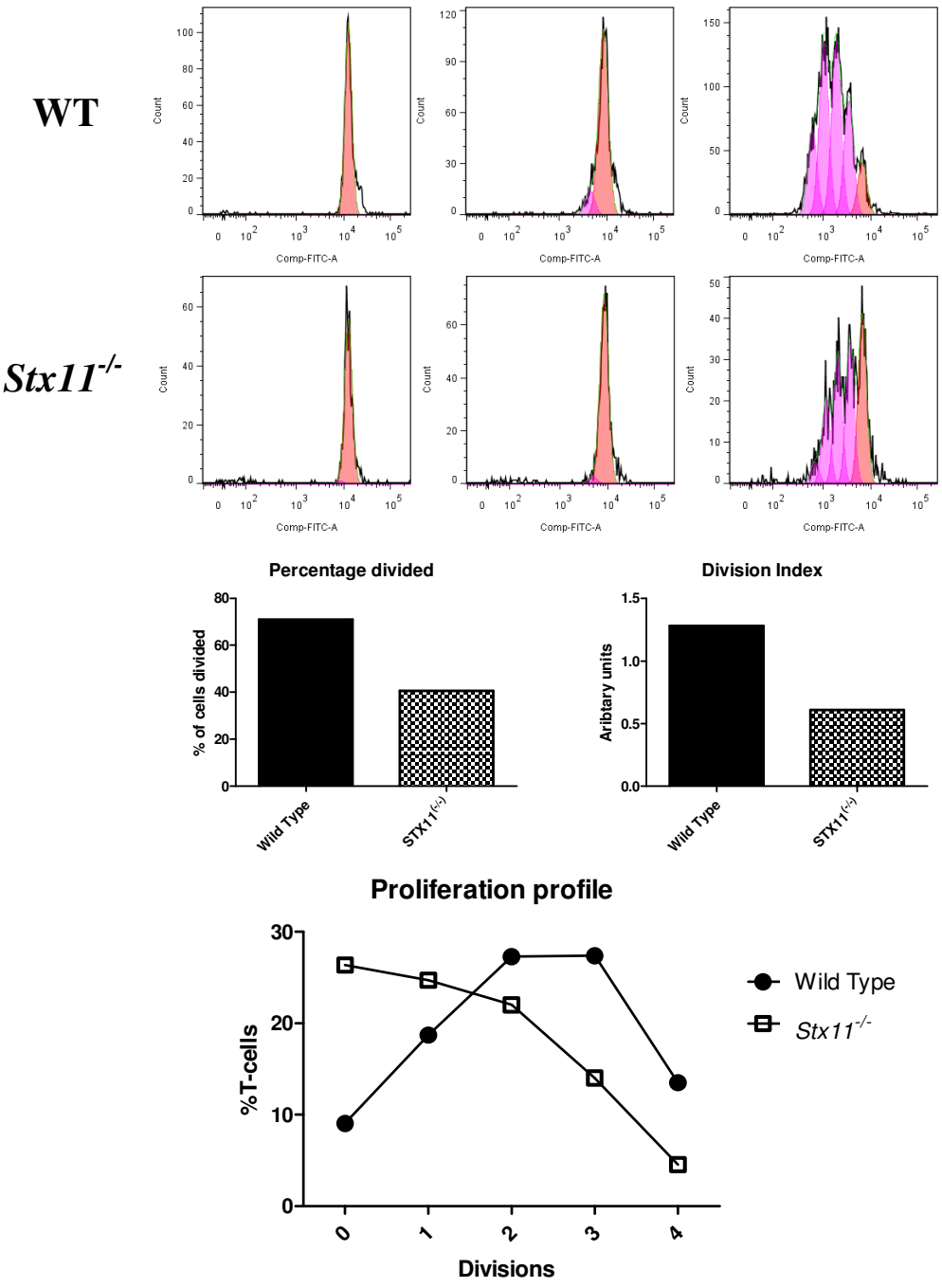

Figure 5.11 - Proliferation study of naïve cells isolated from wild type and *Stx11*$^{-/-}$ mice activated in Th17 polarising conditions. Spleens were isolated from 8 wild type and 8 *Stx11*$^{-/-}$ mice**.** Spleenocytes were enriched for Naïve CD4^{+} T-cells using Easysep isolation kits (Stemcell). Cells were stained with CFSE dye for 5 mins in PBS/FBS at RT before washing twice in PBS. Cells were counted and plated at 2x10^{6} cells/ml and stimulated with plate bound anti-CD3 antibody (5µg/ml) and soluble anti-CD28 antibody (2.5µg/ml) in Th17 polarising conditions. Cells were sampled daily removing 50µl of cells and staining with propidium iodide immediately before analysis on the BD FACS Aria. The data was analysed using FlowJo analysis software (Treestar). Cells were gated on live cells and CFSE was plotted and analysed using the proliferation algorithm on the FlowJo software in order to calculate the percentage of divided cells, the proliferation index and the number of cells in each generation of day four of cell culture.

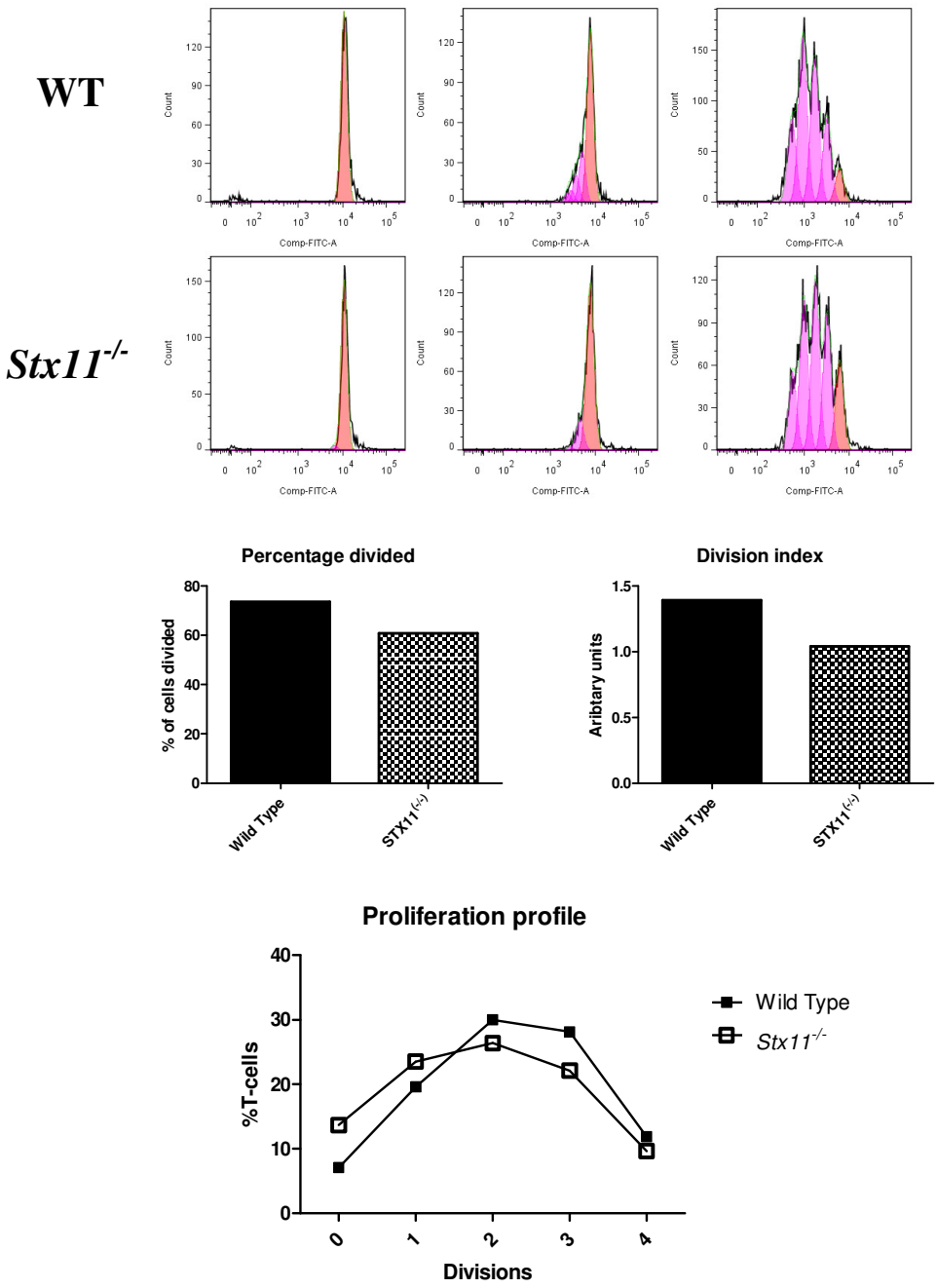

Figure 5.12 - Proliferation study of splenic CD4$^+$ cells isolated from wild type and *Stx11*$^{-/-}$ mice activated in Th17 polarising conditions. Spleens were isolated from 8 wild type and 8 *Stx11*$^{-/-}$ mice**.** Spleenocytes were enriched for CD4$^+$ T-cells using Easysep isolation kits (Stemcell). Cells were stained with CFSE dye for 5 mins in PBS/FBS at RT before washing twice in PBS. Cells were counted and plated at 2x10^6 cells/ml and stimulated with plate bound anti-CD3 antibody (5µg/ml) and soluble anti-CD28 antibody (2.5µg/ml) in Th17 polarising conditions. Cells were sampled daily removing 50µl of cells and staining with propidium iodide immediately before analysis on the BD FACS Aria. The data was analysed using FlowJo analysis software (Treestar). Cells were gated on live cells and CFSE was plotted and analysed using the proliferation algorithm on the FlowJo software in order to calculate the percentage of divided cells, the proliferation index and the number of cells in each generation of day four of cell culture.

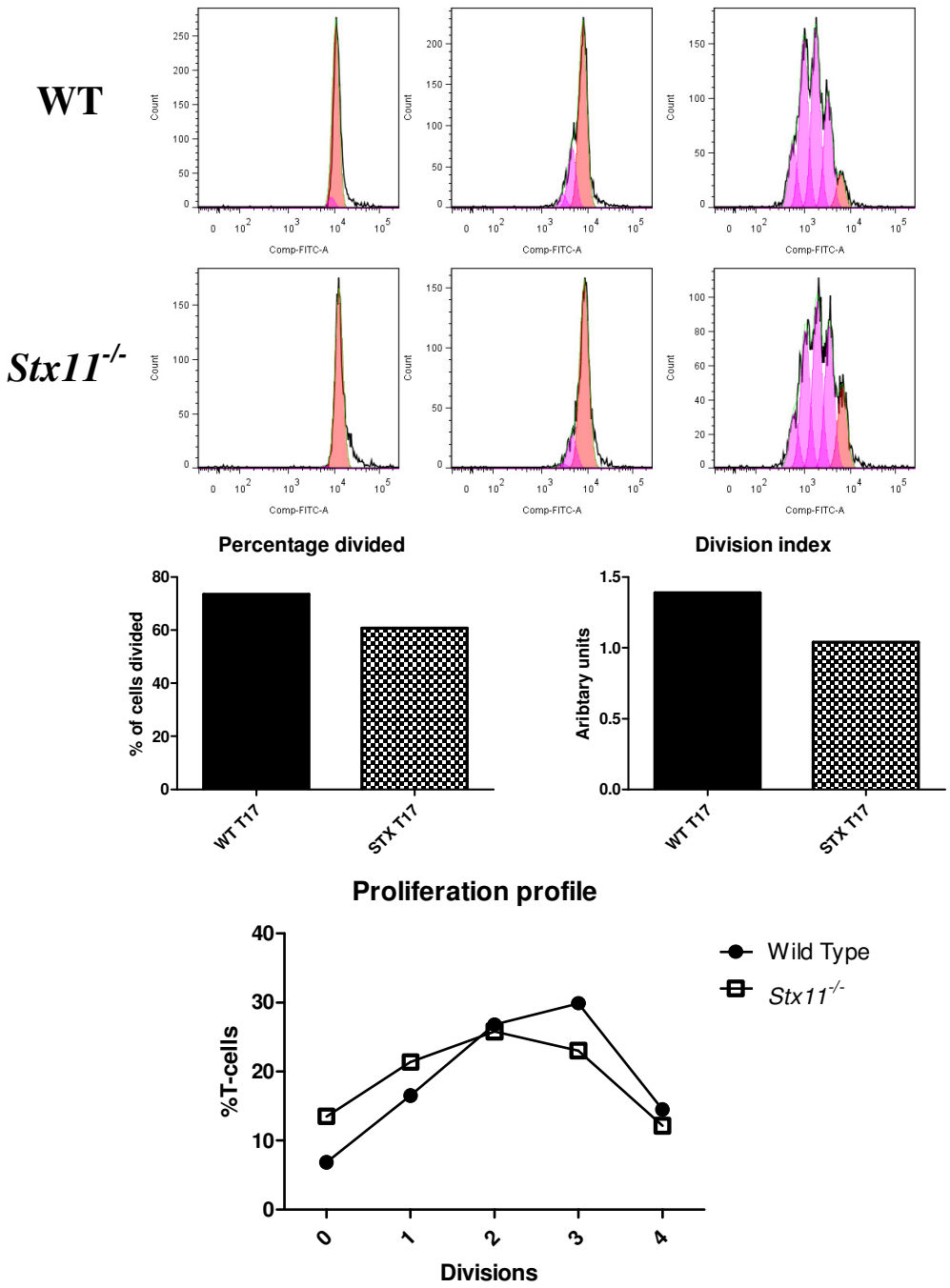

Figure 5.13 - Proliferation study of mesenteric lymph node CD4$^+$ cells isolated from wild type and *Stx11*$^{-/-}$ mice activated in Th17 polarising conditions. Mesenteric lymph nodes were isolated from 8 wild type and 8 *Stx11*$^{-/-}$ mice**.** The mesenteric lymph nodes cell solution was enriched for CD4$^+$ T-cells using Easysep isolation kits (Stemcell). Cells were stained with CFSE dye for 5 mins in PBS/FBS at RT before washing twice in PBS. Cells were counted and plated at 2x10^6 cells/ml and stimulated with plate bound anti-CD3 antibody (5µg/ml) and soluble anti-CD28 antibody (2.5µg/ml) in Th17 polarising conditions. Cells were sampled daily removing 50µl of cells and staining with propidium iodide immediately before analysis on the BD FACS Aria. The data was analysed using FlowJo analysis software (Treestar). Cells were gated on live cells and CFSE was plotted and analysed using the proliferation algorithm on the FlowJo software in order to calculate the percentage of divided cells, the proliferation index and the number of cells in each generation of day four of cell culture

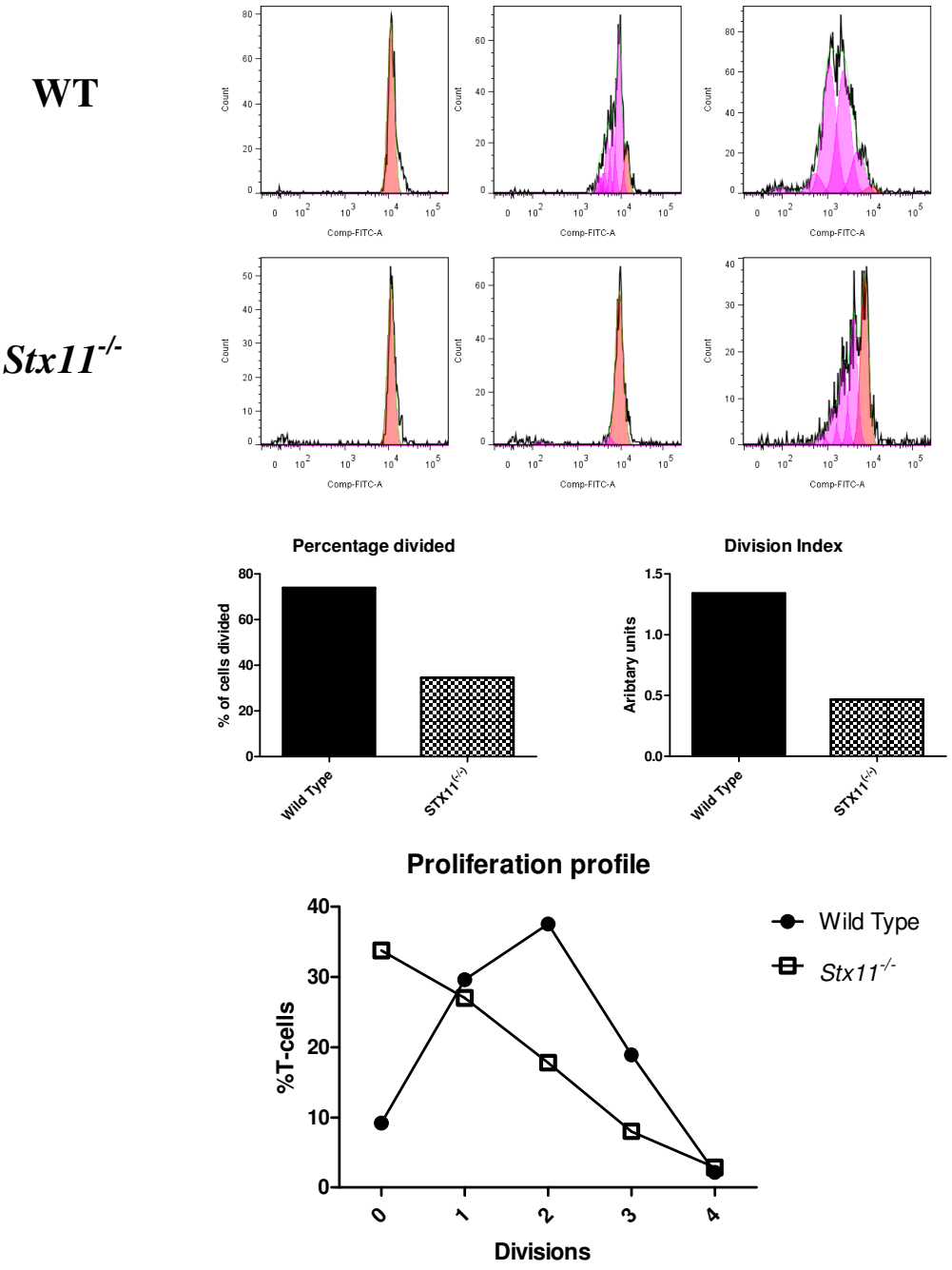

Figure 5.14 - Proliferation study of naïve cells isolated from wild type and *Stx11*$^{-/-}$ mice activated in Th1 polarising conditions. Spleens were isolated from 8 wild type and 8 *Stx11*$^{-/-}$ mice**.** Spleenocytes were enriched for Naïve CD4^{+} T-cells using Easysep isolation kits (Stemcell). Cells were stained with CFSE dye for 5 mins in PBS/FBS at RT before washing twice in PBS. Cells were counted and plated at 2x10^{6} cells/ml and stimulated with plate bound anti-CD3 antibody (5µg/ml) and soluble anti-CD28 antibody (2.5µg/ml) in Th1 polarising conditions. Cells were sampled daily removing 50µl of cells and staining with propidium iodide immediately before analysis on the BD FACS Aria. The data was analysed using FlowJo analysis software (Treestar). Cells were gated on live cells and CFSE was plotted and analysed using the proliferation algorithm on the FlowJo software in order to calculate the percentage of divided cells, the proliferation index and the number of cells in each generation of day four of cell culture.

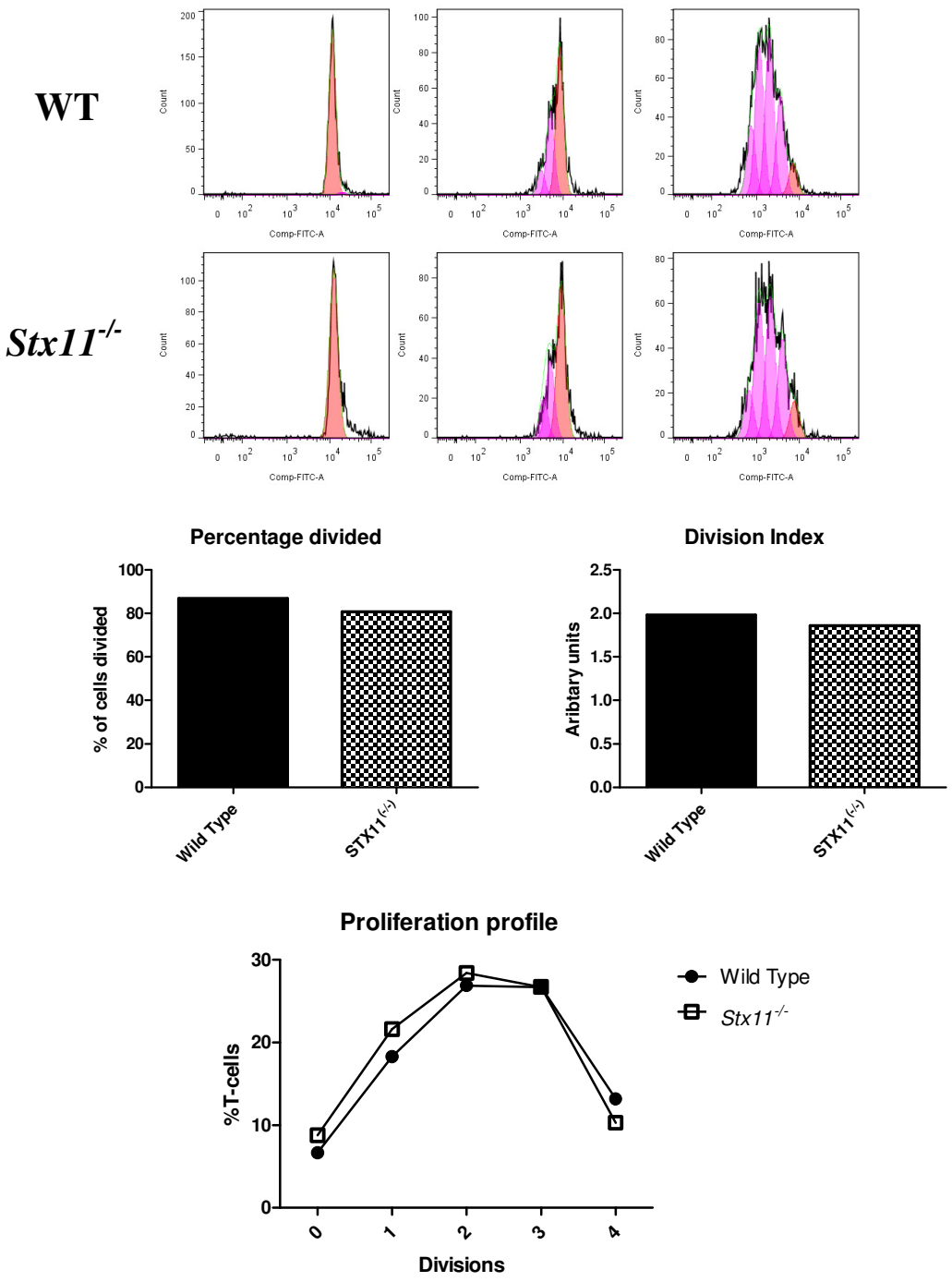

Figure 5.15 - Proliferation study of splenic CD4$^+$ cells isolated from wild type and *Stx11*$^{-/-}$ mice activated in Th1 polarising conditions. Spleens were isolated from 8 wild type and 8 *Stx11*$^{-/-}$ mice**.** Spleenocytes were enriched for CD4$^+$ T-cells using Easysep isolation kits (Stemcell). Cells were stained with CFSE dye for 5 mins in PBS/FBS at RT before washing twice in PBS. Cells were counted and plated at 2x10^6 cells/ml and stimulated with plate bound anti-CD3 antibody (5µg/ml) and soluble anti-CD28 antibody (2.5µg/ml) in Th1 polarising conditions. Cells were sampled daily removing 50µl of cells and staining with propidium iodide immediately before analysis on the BD FACS Aria. The data was analysed using FlowJo analysis software (Treestar). Cells were gated on live cells and CFSE was plotted and analysed using the proliferation algorithm on the FlowJo software in order to calculate the percentage of divided cells, the proliferation index and the number of cells in each generation of day four of cell culture

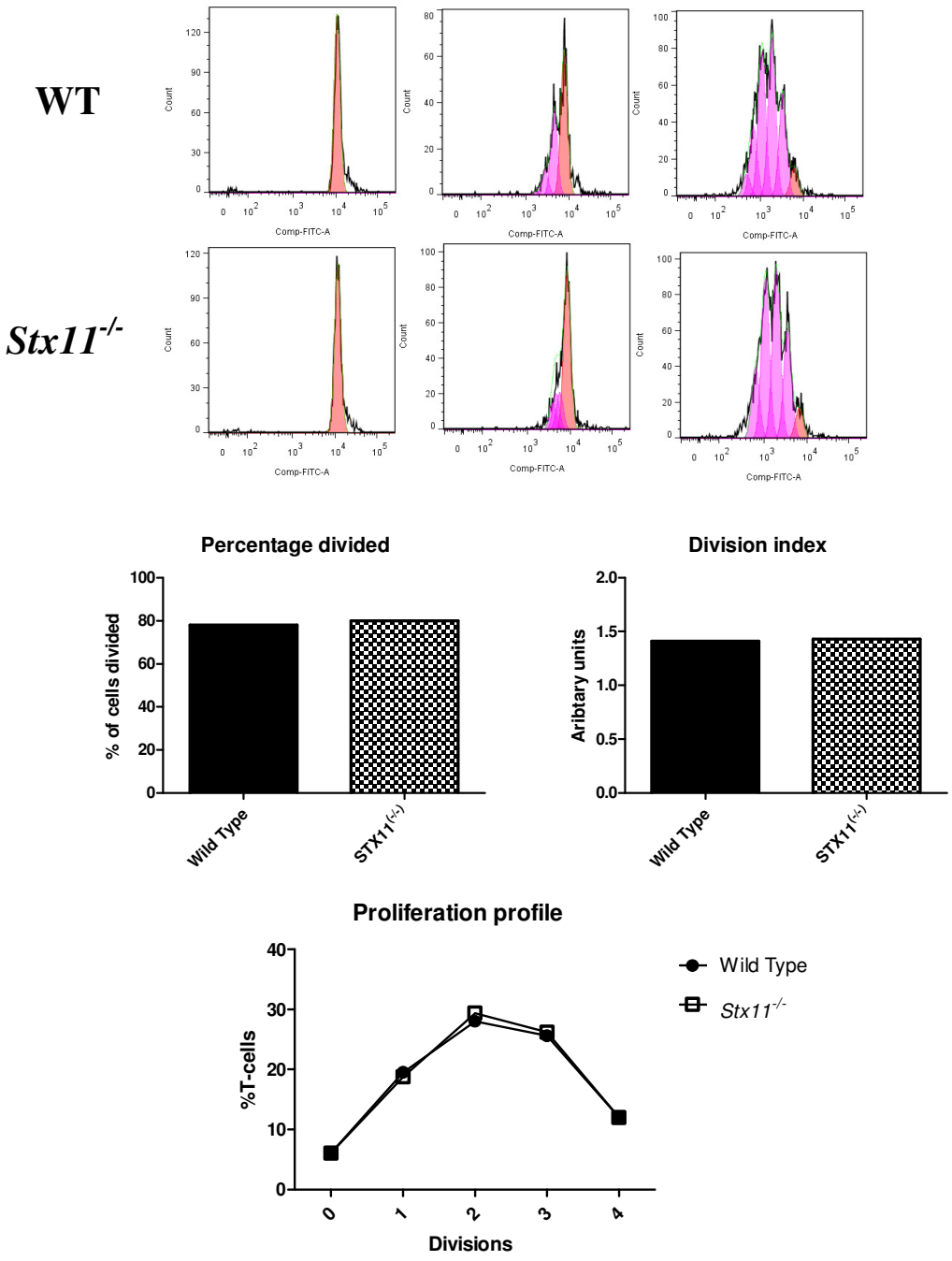

Figure 5.16 - Proliferation study of mesenteric lymph node CD4$^+$ cells isolated from wild type and *Stx11*$^{-/-}$ mice activated in Th1 polarising conditions. Mesenteric lymph nodes were isolated from 8 wild type and 8 *Stx11*$^{-/-}$ mice**.** The mesenteric lymph nodes cell solution was enriched for CD4$^+$ T-cells using Easysep isolation kits (stemcell). Cells were stained with CFSE dye for 5 mins in PBS/FBS at RT before washing twice in PBS. Cells were counted and plated at 2x10^6 cells/ml and stimulated with plate bound anti-CD3 antibody (5µg/ml) and soluble anti-CD28 antibody (2.5µg/ml) in Th1 polarising conditions. Cells were sampled daily removing 50µl of cells and staining with propidium iodide immediately before analysis on the BD FACS Aria. The data was analysed using FlowJo analysis software (treestar). Cells were gated on live cells and CFSE was plotted and analysed using the proliferation algorithm on the FlowJo software in order to calculate the percentage of divided cells, the proliferation index and the number of cells in each generation of day four of cell culture

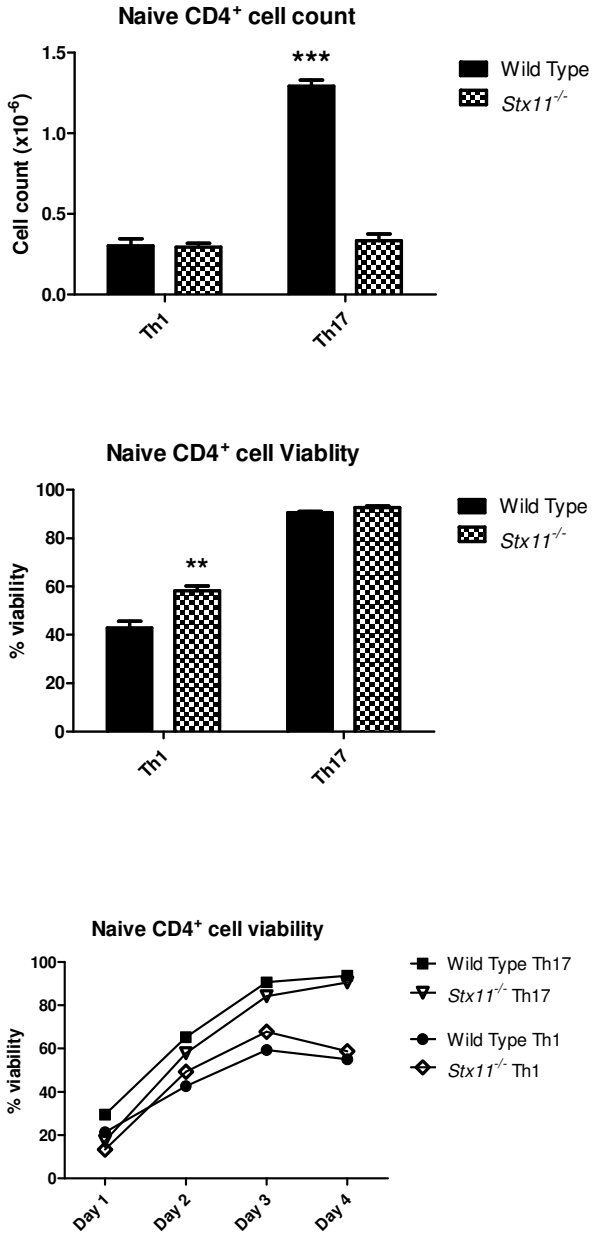

Figure 5.17 - Cell viability study of naive CD4$^+$ cells isolated from WT and *Stx11*$^{-/-}$ mice activated in Th1 and Th17 polarising conditions. Spleens were isolated from 8 wild type and 8 *Stx11*$^{-/-}$ mice**.** Spleenocytes were enriched for Naïve CD4$^+$ T-cells using Easysep isolation kits (Stemcell). Cells were counted and plated at 2x10^6 cells/ml and stimulated with plate bound anti-CD3 antibody (5µg/ml) and soluble anti-CD28 antibody (2.5µg/ml) in Th1 polarising conditions. Cells were sampled daily removing 50µl of cells and staining with propidium iodide immediately before analysis on the BD FACS Aria. The data was analysed using FlowJo analysis software (Treestar). Cells were gated on live cells and the percentage of non-stained cells was plotted daily. On day four cells were counted using a haemocytometer and trypan blue dead cell exclusion. Cell numbers and viability on day four are means ±SEM of three groups each consisting of cells pooled from two mice. An unpaired T-test was used to determine if differences between WT and *Stx11*$^{-/-}$ mice were significantly different (**p<0.01 and ***p<0.001).

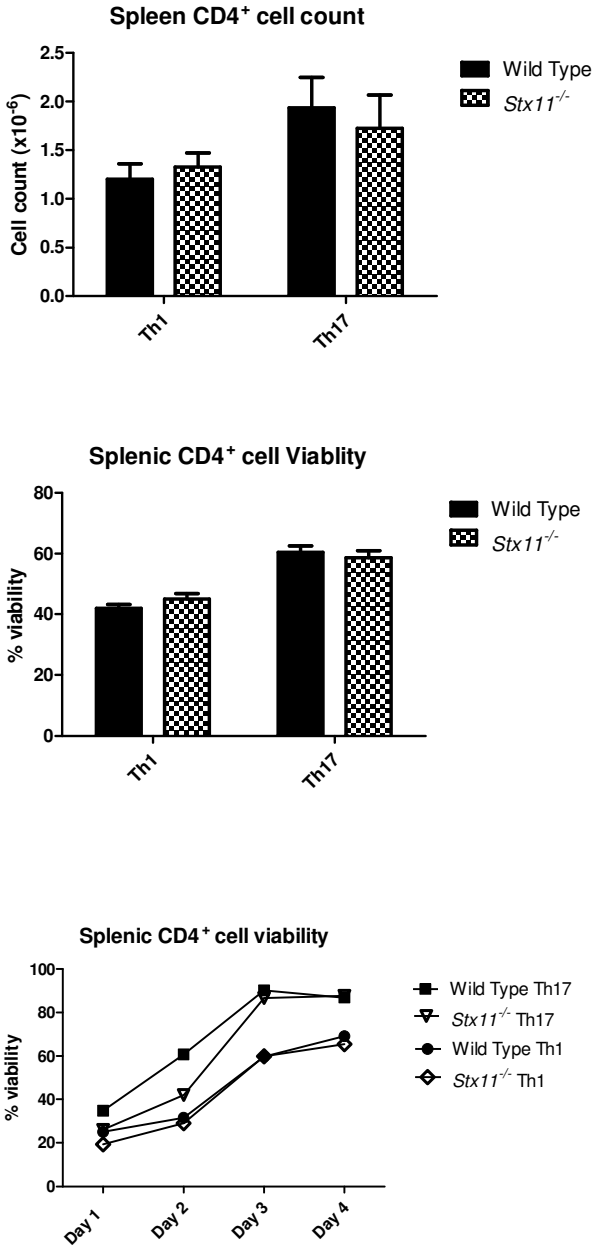

Figure 5.18 - Cell viability study of splenic CD4$^+$ cells isolated from WT and *Stx11*$^{-/-}$ mice activated in Th1 and Th17 polarising conditions. Spleens were isolated from 8 wild type and 8 *Stx11*$^{-/-}$ mice**.** Spleenocytes were enriched for CD4$^+$ T-cells using Easysep isolation kits (Stemcell). Cells were counted and plated at 2x10^6 cells/ml and stimulated with plate bound anti-CD3 antibody (5µg/ml) and soluble anti-CD28 antibody (2.5µg/ml) in Th1 polarising conditions. Cells were sampled daily removing 50µl of cells and staining with propidium iodide immediately before analysis on the BD FACS Aria. The data was analysed using FlowJo analysis software (Treestar). Cells were gated on live cells and the percentage of non-stained cells was plotted daily. On day four cells were counted using a haemocytometer and trypan blue dead cell exclusion. Cell numbers and viability on day four are means ±SEM of three groups each consisting of cells pooled from two mice. An unpaired T-test was used to determine if differences between WT and *Stx11*$^{-/-}$ mice were significantly different.

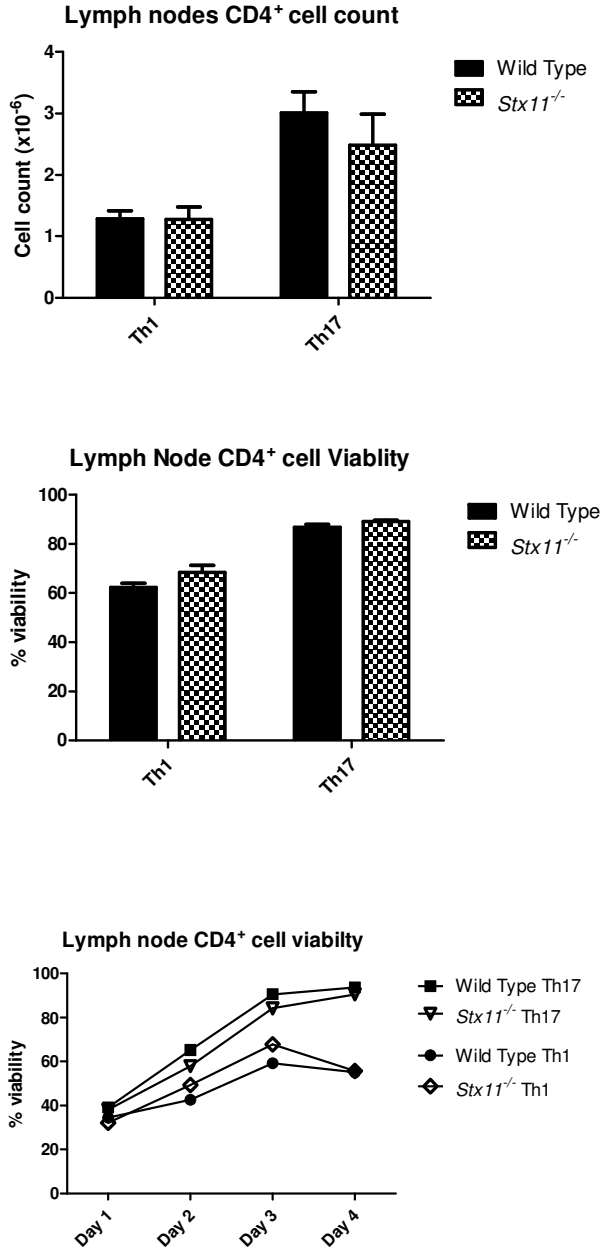

Figure 5.19 - Cell viability study of mesenteric lymph node CD4$^+$ cells isolated from WT and *Stx11*$^{-/-}$ mice activated in Th1 and Th17 polarising conditions. Mesenteric lymph nodes were isolated from 8 wild type and 8 *Stx11*$^{-/-}$ mice**.** The mesenteric lymph node cell solution was enriched for CD4$^+$ T-cells using Easysep isolation kits (Stemcell). Cells were counted and plated at 2x10^6 cells/ml and stimulated with plate bound anti-CD3 antibody (5µg/ml) and soluble anti-CD28 antibody (2.5µg/ml) in Th1 polarising conditions. Cells were sampled daily removing 50µl of cells and staining with propidium iodide immediately before analysis on the BD FACS Aria. The data was analysed using FlowJo analysis software (Treestar). Cells were gated on live cells and the percentage of non-stained cells was plotted daily. On day four cells were counted using a haemocytometer and trypan blue dead cell exclusion. Cell numbers and viability on day four are means ±SEM of three groups each consisting of cells pooled from two mice. An unpaired T-test was used to determine if differences between WT and *Stx11*$^{-/-}$ mice were significantly different

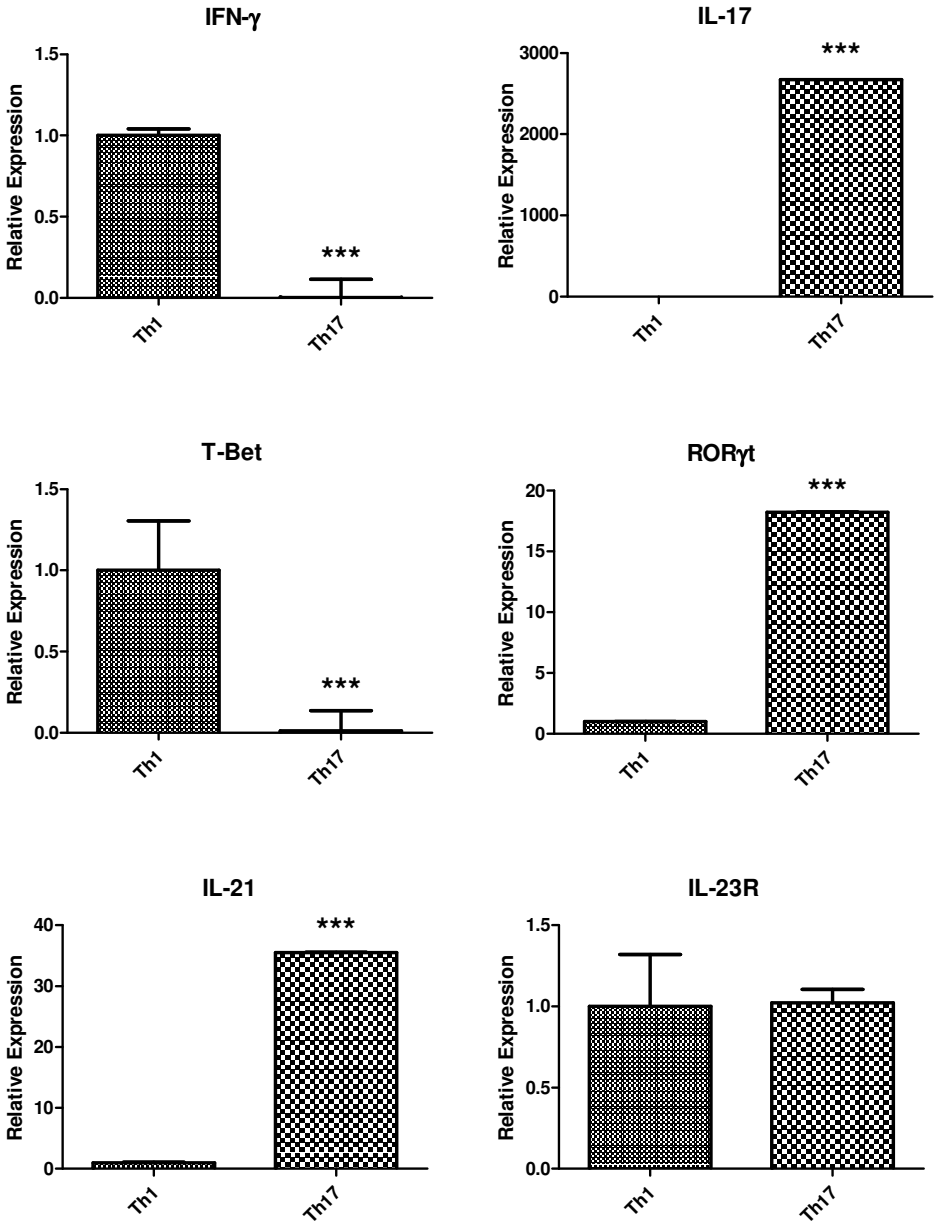

Figure 5.20 – mRNA expression of genes specific for Th1 and Th17 subsets in polarised cells from wild type mice. Spleens were isolated from 8 wild type and 8 *Stx11*$^{-/-}$ mice**.** Spleenocytes were enriched for Naïve CD4^{+} T-cells using Easysep isolation kits (Stemcell). Cells were counted and plated at 2x10^{6} cells/ml and stimulated with plate bound anti-CD3 antibody (5µg/ml) and soluble anti-CD28 antibody (2.5µg/ml) in Th1 or Th17 polarising conditions for four days. RNA was purified using the using nucleospin RNAII isolation columns (Macherey-Nage) and equalised amounts of RNA were converted to cDNA using the high capacity cDNA mastermix (Roche). The cDNA was mixed with primers for *Il17, Tbx21, Rorc, Il21, Il23r* (IDT) and *Ifnγ* (Sigma) and FAST SYBR Mastermix (Roche) before analysing samples on the ABI Prism 7500. Groups were compared using relative quantitation; after normalising samples to *TBP* and *GusB,* the Th1 control group was normalised to 1.0 and the expression in other groups is shown relative to this value**.** Results are means ±SD of 3 groups with 2 mice in each group and measured in triplicate. An unpaired T-test was used to determine if differences between groups were significantly different (***p<0.001).

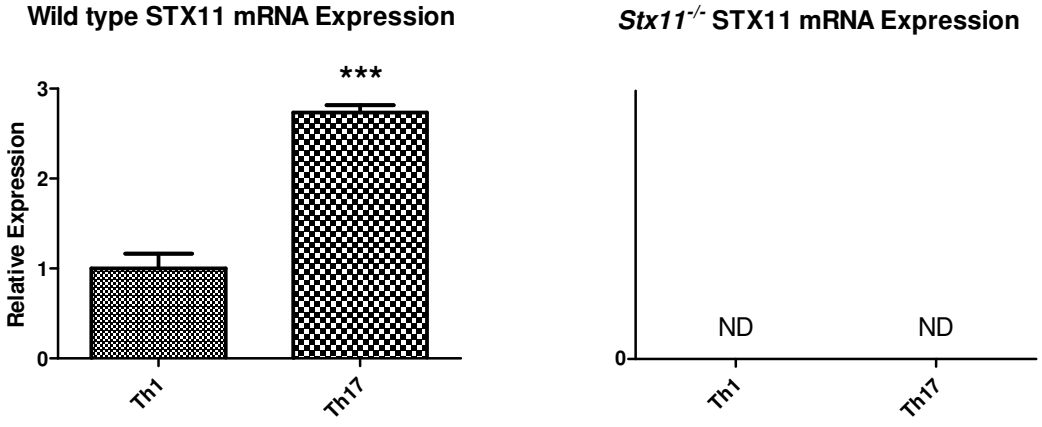

Figure 5.21 - STX11 mRNA expression expression in Th1 and Th17 polarised cells from wild type and *Stx11*$^{-/-}$ mice. Spleens were isolated from 8 wild type and 8 *Stx11*$^{-/-}$ mice**.** Spleenocytes were enriched for Naïve CD4^{+} T-cells using Easysep isolation kits (Stemcell). Cells were counted and plated at 2x10^{6} cells/ml and stimulated with plate bound anti-CD3 antibody (5µg/ml) and soluble anti-CD28 antibody (2.5µg/ml) in Th1 or Th17 polarising conditions for four days. RNA was purified using the using nucleospin RNAII isolation columns (Macherey-Nage) and equalised amounts of RNA were converted to cDNA using the high capacity cDNA mastermix (Roche). The cDNA was mixed with primers for *Stx11* (IDT) and FAST SYBR Mastermix (Roche) before analysing samples on the ABI Prism 7500. Groups were compared using relative quantitation; after normalising samples to *TBP* and *GusB,* the Th1 control group was normalised to 1.0 and the expression in other groups is shown relative to this value**.** Results are means ±SD of 3 groups with 2 mice in each group and measured in triplicate. An unpaired T-test was used to determine if differences between groups were significantly different (***p<0.001).

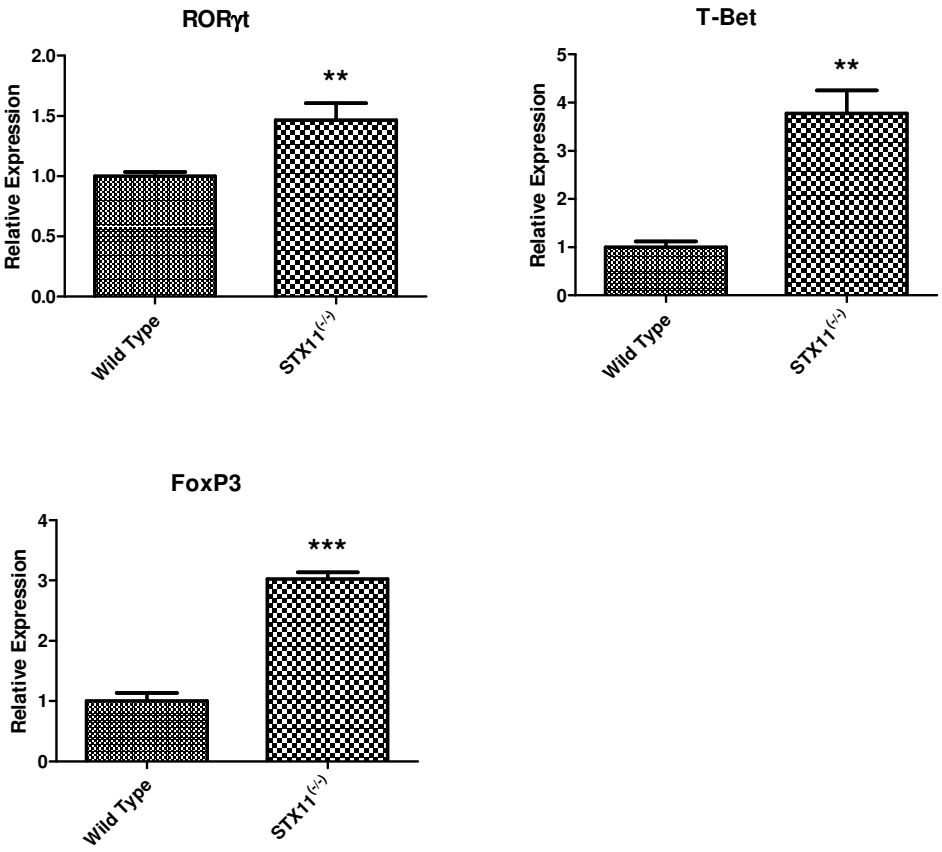

Figure 5.22 – Transcription factors mRNA expression in Th17 polarised cells from wild type and *Stx11*$^{-/-}$ mice. Spleens were isolated from 8 wild type and 8 *Stx11*$^{-/-}$ mice**.** Spleenocytes were enriched for Naïve CD4^{+} T-cells using Easysep isolation kits (Stemcell). Cells were counted and plated at 2x10^{6} cells/ml and stimulated with plate bound anti-CD3 antibody (5µg/ml) and soluble anti-CD28 antibody (2.5µg/ml) in Th17 polarising conditions for four days. RNA was purified using the using nucleospin RNAII isolation columns (Macherey-Nage) and equalised amounts of RNA were converted to cDNA using the high capacity cDNA mastermix (Roche). The cDNA was mixed with primers for *Rorc, Tbx21* and *Foxp3* (IDT) and FAST SYBR Mastermix (Roche) before analysing samples on the ABI Prism 7500. Groups were compared using relative quantitation; after normalising samples to *TBP* and *GusB,* the Th1 control group was normalised to 1.0 and the expression in other groups is shown relative to this value**.** Results are means ±SD of 3 groups with 2 mice in each group and measured in triplicate. An unpaired T-test was used to determine if differences between groups were significantly different (**p<0.01 and ***p<0.001).

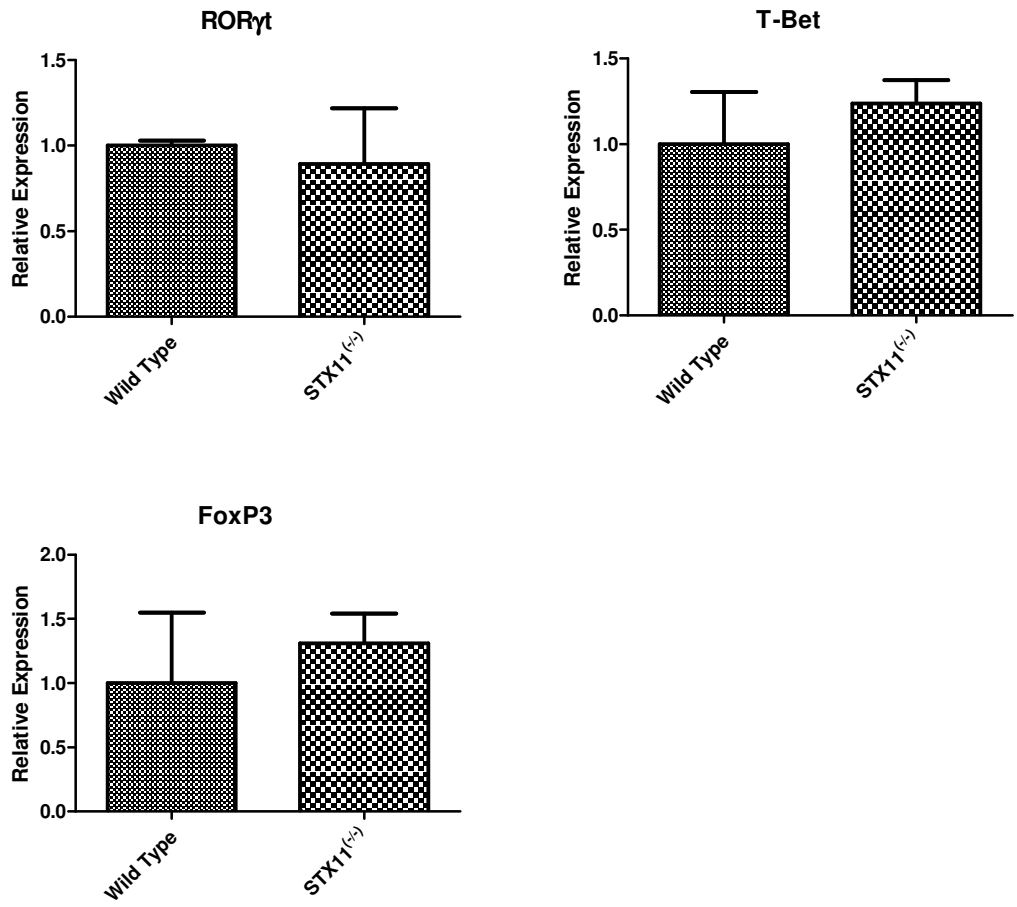

Figure 5.23 – Transcription factors mRNA expression in Th1 polarised cells from wild type and *Stx11*$^{-/-}$ mice. Spleens were isolated from 8 wild type and 8 *Stx11*$^{-/-}$ mice**.** Spleenocytes were enriched for Naïve CD4^{+} T-cells using Easysep isolation kits (Stemcell). Cells were counted and plated at 2x10^{6} cells/ml and stimulated with plate bound anti-CD3 antibody (5µg/ml) and soluble anti-CD28 antibody (2.5µg/ml) in Th1 polarising conditions for four days. RNA was purified using the using nucleospin RNAII isolation columns (Macherey-Nage) and equalised amounts of RNA were converted to cDNA using the high capacity cDNA mastermix (Roche). The cDNA was mixed with primers for *Rorc, Tbx21* and *Foxp3* (IDT) and FAST SYBR Mastermix (Roche) before analysing samples on the ABI Prism 7500. Groups were compared using relative quantitation; after normalising samples to *TBP* and *GusB,* the Th1 control group was normalised to 1.0 and the expression in other groups is shown relative to this value**.** Results are means ±SD of 3 groups with 2 mice in each group and measured in triplicate. An unpaired T-test was used to determine if differences between groups were significantly different (**p<0.01 and ***p<0.001).

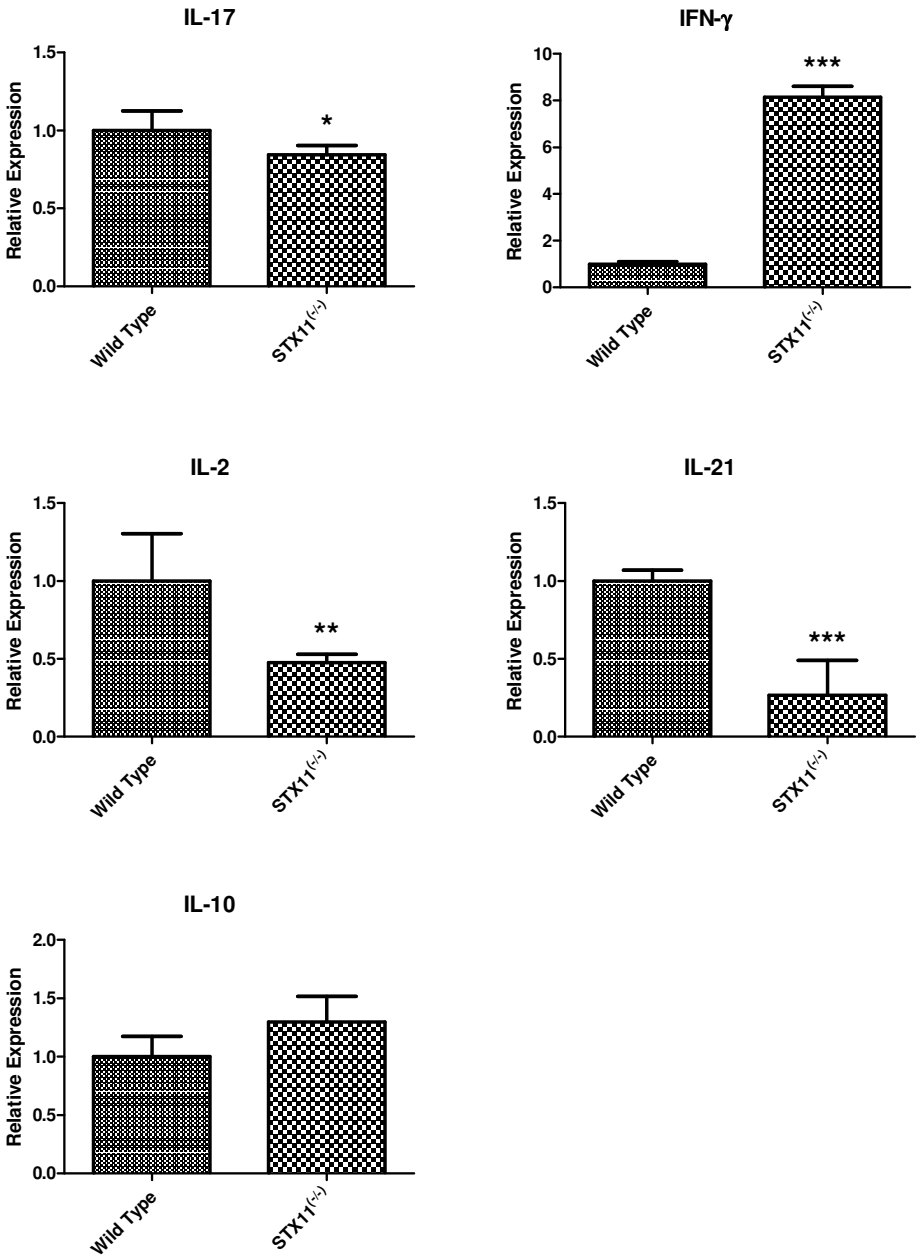

Figure 5.24 – Cytokine mRNA expression in Th17 polarised cells from wild type and *Stx11*$^{-/-}$ mice. Spleens were isolated from 8 wild type and 8 *Stx11*$^{-/-}$ mice**.** Spleenocytes were enriched for Naïve CD4^{+} T-cells using Easysep isolation kits (Stemcell). Cells were counted and plated at 2x10^{6} cells/ml and stimulated with plate bound anti-CD3 antibody (5µg/ml) and soluble anti-CD28 antibody (2.5µg/ml) in Th17 polarising conditions for four days. RNA was purified using the using nucleospin RNAII isolation columns (Macherey-Nage) and equalised amounts of RNA were converted to cDNA using the high capacity cDNA mastermix (Roche). The cDNA was mixed with primers for *Il17, Il2, Il21, Il10* (IDT) and *Ifnγ* (Sigma) and FAST SYBR Mastermix (Roche) before analysing samples on the ABI Prism 7500. Groups were compared using relative quantitation; after normalising samples to *TBP* and *GusB,* the Th1 control group was normalised to 1.0 and the expression in other groups is shown relative to this value**.** Results are means ±SD of 3 groups with 2 mice in each group and measured in triplicate. An unpaired T-test was used to determine if differences between groups were significantly different (*p<0.05, **p<0.01 and ***p<0.001).

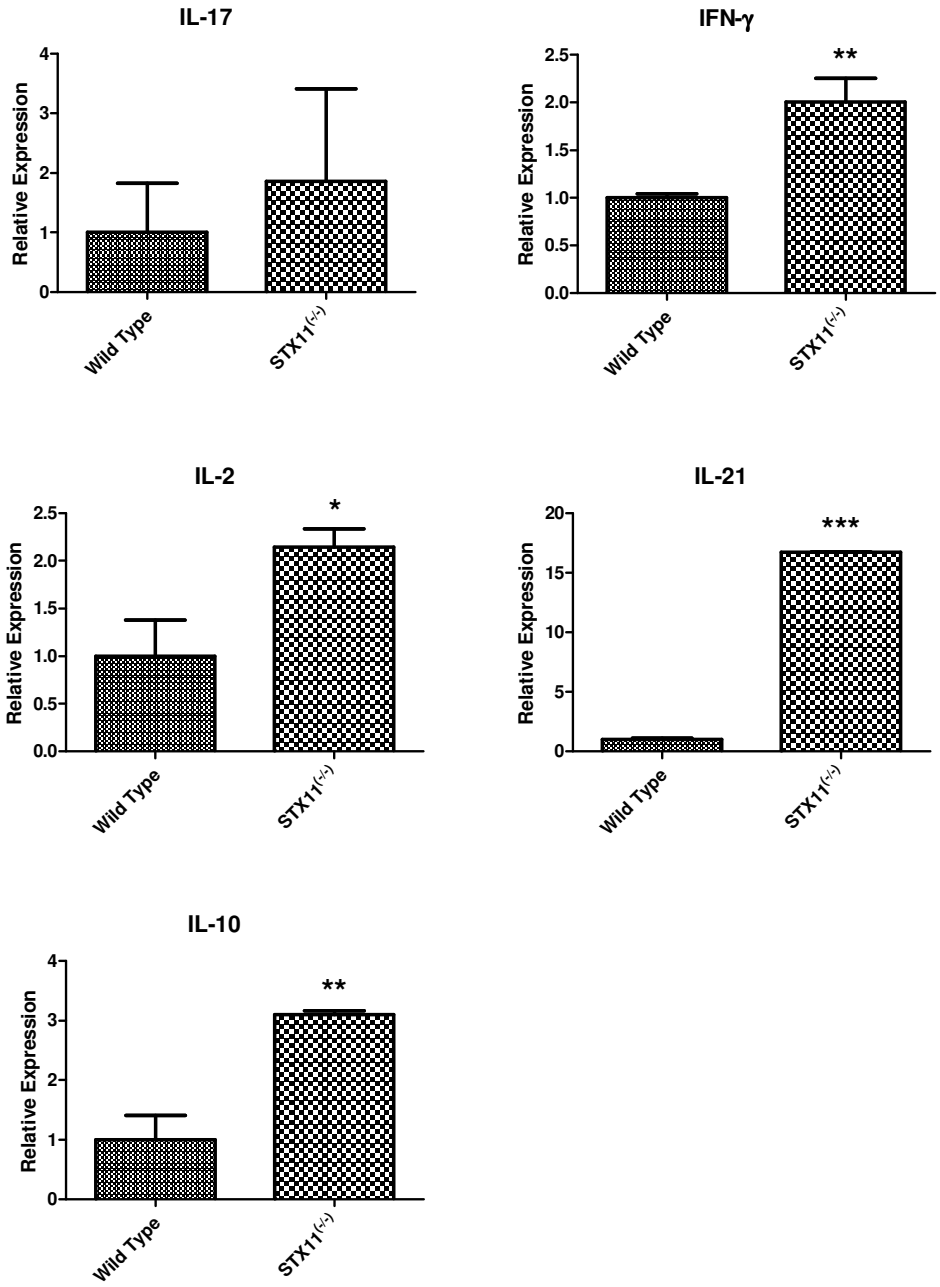

Figure 5.25 – Cytokine mRNA expression in Th1 polarised cells from wild type and *Stx11*$^{-/-}$ mice. Spleens were isolated from 8 wild type and 8 *Stx11*$^{-/-}$ mice**.** Spleenocytes were enriched for Naïve CD4^{+} T-cells using Easysep isolation kits (Stemcell). Cells were counted and plated at 2x10^{6} cells/ml and stimulated with plate bound anti-CD3 antibody (5µg/ml) and soluble anti-CD28 antibody (2.5µg/ml) in Th1 polarising conditions for four days. RNA was purified using the using nucleospin RNAII isolation columns (Macherey-Nage) and equalised amounts of RNA were converted to cDNA using the high capacity cDNA mastermix (Roche). The cDNA was mixed with primers for *Il17, Il2, Il21, Il10* (IDT) and *Ifnγ* (Sigma) and FAST SYBR Mastermix (Roche) before analysing samples on the ABI Prism 7500. Groups were compared using relative quantitation; after normalising samples to *TBP* and *GusB,* the Th1 control group was normalised to 1.0 and the expression in other groups is shown relative to this value**.** Results are means ±SD of 3 groups with 2 mice in each group and measured in triplicate. An unpaired T-test was used to determine if differences between groups were significantly different (*p<0.05, **p<0.01 and ***p<0.001).

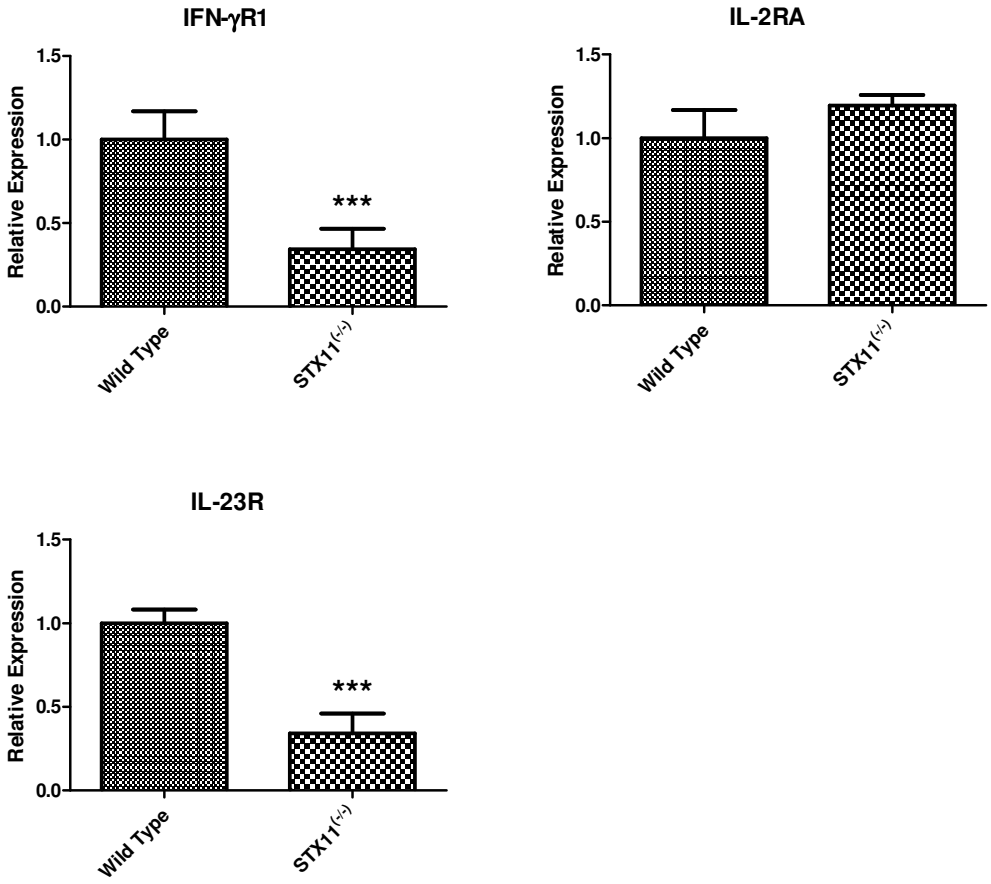

Figure 5.26 – cytokine receptor Cytokine mRNA expression Th17 polarised cells from wild type and *Stx11*$^{-/-}$ mice. Spleens were isolated from 8 wild type and 8 *Stx11*$^{-/-}$ mice**.** Spleenocytes were enriched for Naïve CD4^{+} T-cells using Easysep isolation kits (Stemcell). Cells were counted and plated at 2x10^{6} cells/ml and stimulated with plate bound anti-CD3 antibody (5μg/ml) and soluble anti-CD28 antibody (2.5μg/ml) in Th17 polarising conditions for four days. RNA was purified using the using nucleospin RNAII isolation columns (Macherey-Nage) and equalised amounts of RNA were converted to cDNA using the high capacity cDNA mastermix (Roche). The cDNA was mixed with primers for *Ifnγrα, Il2r,*and *Il23r* (IDT) and FAST SYBR Mastermix (Roche) before analysing samples on the ABI Prism 7500. Groups were compared using relative quantitation; after normalising samples to *TBP* and *GusB,* the Th1 control group was normalised to 1.0 and the expression in other groups is shown relative to this value**.** Results are means ±SD of 3 groups with 2 mice in each group and measured in triplicate. An unpaired T-test was used to determine if differences between groups were significantly different (***p<0.001).

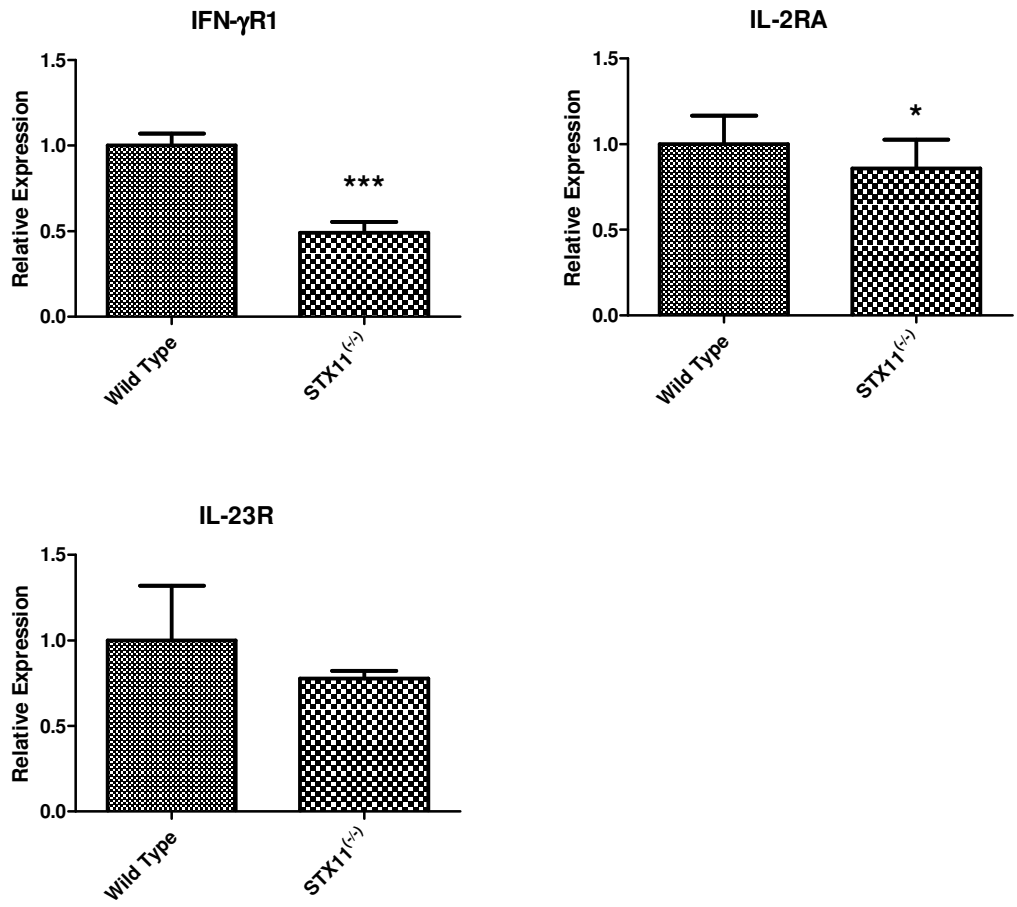

Figure 5.27 – cytokine receptor Cytokine mRNA expression Th1 polarised cells from wild type and *Stx11*$^{-/-}$ mice. Spleens were isolated from 8 wild type and 8 *Stx11*$^{-/-}$ mice**.** Spleenocytes were enriched for Naïve CD4^{+} T-cells using Easysep isolation kits (Stemcell). Cells were counted and plated at 2x10^{6} cells/ml and stimulated with plate bound anti-CD3 antibody (5μg/ml) and soluble anti-CD28 antibody (2.5μg/ml) in Th1 polarising conditions for four days. RNA was purified using the using nucleospin RNAII isolation columns (Macherey-Nage) and equalised amounts of RNA were converted to cDNA using the high capacity cDNA mastermix (Roche). The cDNA was mixed with primers for *Ifnγrα Il2r,*and *Il23r* (IDT) and FAST SYBR Mastermix (Roche) before analysing samples on the ABI Prism 7500. Groups were compared using relative quantitation; after normalising samples to *TBP* and *GusB,* the Th1 control group was normalised to 1.0 and the expression in other groups is shown relative to this value**.** Results are means ±SD of 3 groups with 2 mice in each group and measured in triplicate. An unpaired T-test was used to determine if differences between groups were significantly different (***p<0.001).

5.3– DISCUSSION

The results from chapter 4 propose a regulatory function for STX11 in Th17 cells. STX11 is up-regulated in Th17 cells when compared to Th1 cells suggesting a role for STX11 in IL-17 trafficking. STX11 is enriched in immune cells and is expressed at high levels in the thymus, spleen and lymph nodes (Prekeris et al. 2000). The importance of STX11 in the immune system is highlighted by a deficiency in humans that results in the immune deficiency syndrome, hemophagocytic lymphohistiocytosis (HLH). In particular, a familial form of HLH (FHL-4) is characterised by a mutation in *Stx11*. Infection in patients with FHL-4 can lead to uncontrolled and ineffective immune responses with symptoms including hyperinflammation, cytopenias and haemophagocytosis. Hemophagocytosis is a characteristic feature of the syndrome and although it may be initially absent, it is the primary manifestation of FHL and distinguishes it from other immune deficiency syndromes (Janka 2012). Identification of FHL-4 as a STX11 autosomal recessive disorder led to cells from these patients being used to investigate dysfunctions in the immune response in the absence of STX11, particularly CTLs, NK cells and phagocytic macrophages.

A mouse model of FHL-4 was recently established in two independent labs using *Stx11*$^{-/-}$ mice generated in-house. Infection of STX11 deficient mice with the lymphocytic choriomeningitis virus (LCMV) reproduced manifestations of FHL (Kögl et al. 2013; Sepulveda et al. 2013). The mice were generated by the deletion of exon 3 (the only coding exon in *Stx11*) in a C57BL/6 background which led to a STX11 protein expression defect (Sepulveda et al. 2013). The mice had normal immune cell

development and proportions of NK, B, T and APC cells in the thymus, lymph nodes and spleen. Furthermore, normal ratios of $CD8^+$ to $CD4^+$ T-cells were observed (Sepulveda et al. 2013). When infected with LCMV the mice displayed impaired degranulation in CTL and NK cells associated with HLH. The role of $CD4^+$ T-cells in this model was not investigated despite the vital role of $CD4^+$ T-cells in inflammation, a clear role of other T-cells in the progression of this disease, and the possible haemopoetic conservation of mechanisms between $CD4^+$ and $CD8^+$ T-cells (Starr et al. 2003). Through collaboration with Silvia Bulfone-Paus in the Borstel Research Centre in Germany cells from *Stx11*$^{-/-}$ mice were obtained in order to investigate the regulatory role of STX11 in $CD4^+$ T-helper cells. $CD4^+$ T-cells were isolated from the spleen and mesenteric lymph nodes of wild type and *Stx11*$^{-/-}$ mice. Given that Th17 cells play a central role in gut immune regulation and that the *in vivo* data collected from the colitis models in the previous chapter indicated an increase in STX11 mRNA expression when IL-17 is highly expressed, both spleen and mesenteric lymph node cells (MLN) were isolated for comparison. MLNs are the draining lymph nodes located along the colon and contain high amounts of $CD4^+$ T-cells. $CD4^+$ T-cells were isolated from the spleen and MLNs using the Easysep negative isolation kit (stemcells). The $CD4^+$ enriched cell solution consisted of naïve and memory phenotype $CD4^+$ T-cells. Memory phenotype cells are generated during an immune response when cells react to an antigen during inflammation. Some of these responders survive and form antigen-specific memory T-cells that can mount an efficient immune response following future interactions with the antigen. However, memory T-cells are also found in small numbers in normal naïve mice, accounting for 10-20% of T-cells in young mice (Sprent & Surh 2011). This conversion into a memory phenotype is due in

part to environmental antigens, but also priming by self antigens, as these cells are present in neonates and mice maintained in germ and antigen free environments (Sprent & Surh 2011). These cells consist of central and effector memory cells that may be already committed to a specific T-helper cell lineage. The presence of these cells can influence the polarisation and cytokine secretion of the cells in culture. Therefore, naïve isolated T-helper cells were enriched to exclude central and effector memory $CD4^+$ cells. When polarised they represent pure subsets with minimal contaminating cells secreting cytokines that could influence the cells polarisation or mask the pure naïve polarised cell response. These cells represent a small percentage of the total spleenocytes (5-10%) but they are capable of cloning into measured responses and can produce high levels of cytokine. Although these cells are isolated from the spleen, they will be referred to as the naïve cell population, while $CD4^+$ cell populations from the spleen and mesenteric lymph nodes will be referred to as splenic and MLN populations.

Using these populations from WT and *Stx11*$^{-/-}$ mice, the cytokine secretion levels were evaluated following four days of culture in Th1 or Th17 polarising conditions. The naïve WT cells cultured and polarised in Th17 conditions produced high levels of IL-17 as expected. This was dramatically reduced in the *Stx11*$^{-/-}$ naïve Th17 cells. Taken in isolation, this would suggest that STX11 is involved in secretion of IL-17 as the results in the previous chapter would suggest. However, this reduction in IL-17 secretion was not observed in the splenic or MLN Th17 polarised cells. As this population contains central and effector memory cells that are already committed to the Th17 lineage, and secreting IL-17, it is possible that the lack of *Stx11*$^{-/-}$ may not have a specific effect on trafficking of IL-17 in $CD4^+$ T-helper cells, but rather affect the polarisation and commitment to a

Th17 subset. Indeed, the IL-17 cytokine levels measured in the Th1 polarised cells from naïve, splenic and MLN populations were low as expected but no significant change observed between the cell populations, further indicating no effect on the secretion of IL-17 in the absence of STX11.

The reduction in cytokine levels in the naïve Th17 cells from *Stx11*$^{-/-}$ mice was not exclusive to IL-17. IL-10, TNF-α and IL-21 were all significantly reduced in the cells isolated from *Stx11*$^{-/-}$ mice. However, IFN-γ was significantly increased in Th17 polarised cells from *Stx11*$^{-/-}$ mice. Although levels were low in comparison to Th1 cells, the concentration in the supernatants of cells from *Stx11*$^{-/-}$ mice was 2-fold higher compared to the WT cells. Furthermore, IFN-γ was also significantly increased in both the splenic and MLN CD4^{+} Th17 polarised cells from *Stx11*$^{-/-}$ mice, showing consistency in both the naïve and memory cells. Surprisingly, this increase was not observed in the supernatants from *Stx11*$^{-/-}$ mice polarised into IFN-γ producing Th1 cells from the naïve, splenic or MLN populations.

The decrease in IL-17 is specific to the naïve Th17 cells from *Stx11*$^{-/-}$ mice but not the mixed naïve and memory populations. Furthermore, the lack of IL-17 secretion and measured increase in IFN-γ would suggest that these are not in fact Th17 polarised cells despite the environment in which they were stimulated. There is a significant reduction in the concentration of IL-21 measured in the supernatants from the naïve *Stx11*$^{-/-}$ Th17 polarised cells which would also suggest a problem with the polarisation of these cells. Upon activation in the presence of IL-6, T-helper cells induce IL-21 production which initiates a positive feed back loop in Th17 cell polarisation and drives IL-17 production in a STAT3 dependant manner (Wei et al. 2007). There is no difference in the IL-21

concentration measured in the supernatants of $CD4^+$ splenic cells from WT and *Stx11*$^{-/-}$ mice and there is an increase in IL-21 in the MLN supernatants from *Stx11*$^{-/-}$ mice. There is also no change in the IL-17 levels in these cells which would again suggest inhibition of Th17 polarisation of naïve cells from the *Stx11*$^{-/-}$ mice alone. The presence of effector memory cells in the splenic and MLN $CD4^+$ population is the main difference between these cells and the naïve population. Given that they secrete IL-17 and IL-21 at normal levels, perhaps they are only mildly affected by the lack of STX11 due to the presence of memory Th17 cells.

TNF-α is significantly reduced in the *Stx11*$^{-/-}$ cells, at less than half the concentration measured for the WT Th17 polarised cells. TNF-α production has been reported in Th17 cells and a study by Veldhoen *et al* (2006) demonstrated that the addition of TNF-α can augment the IL-17 response from Th17 cells. However, a previous study using *TNF-α*$^{-/-}$ mice has shown that TNF-α is not necessary for the generation of IL-17 producing cells (Nakae et al. 2002), leading Veldhoen *et al* (2006) to surmise that TNF-α secreted primarily from APCs aids in the augmentation of Th17 responses. However, despite there being no apparent requirement for TNF-α in the polarisation of Th17 cells, it is possible that TNF-α secreted by Th17 cells acts in an autocrine manner to enhance IL-17 production in these cells. TNF-α secretion is indeed decreased in the naïve *Stx11*$^{-/-}$ cells but is increased in the supernatants from the splenic $CD4^+$ Th17 polarised cells from *Stx11*$^{-/-}$ mice. This may be due to other sources of TNF-α in the mixed cell population.

IL-10 production was initially associated with Th2 cells and identified as having a suppressive effect on the Th1 population (Fiorentino 1989). IL-10 is also a characteristic cytokine of Tregs which suppresses T-helper cells in the immune response, particularly

Th17 cells, and controls inflammation (Wing & Sakaguchi 2010). Recently IL-10 production has been associated with Th1 polarised cells and is thought to act through a self-limiting, negative feed back loop late in T-cell activation. IL-10 suppression contracts the Th1 cell population following the immune response and controls inflammation when clearing infection (Trinchieri 2007). IL-10 secretion is not limited to Th1 and Th2 cells, and Th17 cells have been demonstrated to secrete IL-10 in what is thought to be part of a self-limiting mechanism. A detailed epigenetic study of the Th17 cell polarisation programme demonstrated the induction of IL-10 family regulatory cytokines in the "transition to late phase" stage of polarisation (Yosef et al. 2013). Furthermore, in pathogenic models of disease, IL-10 secretion from Th17 cells was demonstrated following continuous antigen stimulation in which Th17 cells down-regulated IL-17 production and up-regulated IL-10 (Zielinski et al. 2012). This IL-10 secretion in the late stage of the inflammation is thought to be more prevalent in non-pathogenic Th17 cells that do not switch to IFN-γ/IL-17 double producers. As discussed in earlier chapters these cells are programmed in the absence of TGF-β, however IL-β has also been linked to this control during infection *in vivo* (Zielinski et al. 2012) and was present in the Th17 polarising cocktail when these cells were activated. IL-10 production is significantly reduced in the naïve *Stx11*$^{-/-}$ Th17 polarised cells. The fact that *Il10* gene induction occurs early (t=20hr) in the Th17 cell polarisation programming (Yosef et al. 2013), and is significantly reduced in these cells, indicates further the inhibition of Th17 cell polarisation as the reason for the reduction in IL-17 production.

In order to investigate the loss of IL-17, and the hypothesis that Th17 differentiation in the naïve cells from the *Stx11*$^{-/-}$ mice is inhibited, the cells were stained for the

transcription factor RORγt. The cells were stained at 18hr, the point at which Th17 polarised cells highly express RORγt as shown in chapter 3 and by others (Yosef et al. 2013). In agreement with the cytokine analysis of these cells, there were fewer RORγt expressing cells in not only the naïve, but also the splenic and MLN Th17 polarised cells from the *Stx11*$^{-/-}$ mice. This under expression of the master regulator for Th17 cells at 18hrs would indicate that the polarisation of the Th17 cells was affected in the absence of STX11. As IL-17 production is controlled by the transcription of RORγt via activation of STAT3 and transcription of the *Il17a* gene, this would directly effect IL-17 production and offer an explanation for the significant decrease in IL-17 concentration in the supernatant of these cells.

To confirm the decrease in IL-17 production in the naïve Th17 polarised cells from *Stx11*$^{-/-}$ mice, the cells were re-stimulated with PMA and ionomycin in the presence of monensin, trapping any cytokine produced by the cell in the golgi apparatus. The cells produce cytokine according to their transcriptional programming and the cytokine is trapped in the golgi apparatus allowing for stable intracellular cytokine staining. This allows for the assessment of the percentage of the cell population producing IFN-γ and IL-17 after four days of culture *in vitro*. Intracellular staining for IL-17 and IFN-γ in the naïve Th17 polarised cells from the WT and *Stx11*$^{-/-}$ mice confirmed the decrease in IL-17 producing cells. This decrease was not observed in the mixed $CD4^+$ splenic and MLN isolated cells suggesting that this is a result of the naïve cells not polarising into IL-17 producing cells. Also of interest was the IFN-γ production from these cells. Although IFN-γ is produced in very small amounts in Th17 polarising conditions, there was an increase in the percentage of IFN-γ producing cells in the $CD4^+$ splenic and MLN

isolated Th17 polarised cells. This result was also supported by the increase in the concentration of IFN-γ in the supernatants of Th17 polarised cells from *Stx11*$^{-/-}$ mice. However, despite the significant increase in IFN-γ in the supernatants of naïve Th17 polarised *Stx11*$^{-/-}$ cells, there was no increase observed in the percentage of IFN-γ producing naïve Th17 polarised cells.

Intracellular staining of the naïve Th1 polarised cells demonstrated an almost 2-fold increase in the number of IFN-γ producing cells from *Stx11*$^{-/-}$ mice compared to WT. This was not reflected in the supernatants collected from these cells after four days culture *in vitro*. This increase in IFN-γ producing cells was also not observed in the CD4^{+} splenic and MLN cells isolated from *Stx11*$^{-/-}$ mice. It is possible that there is a suppressive effect on the cells from a population of central or effector memory cells that is not present in the naïve cell population, or that the cells have undergone a high number of cell divisions and this has lead to a decreased ability to produce IFN-γ at gene expression level. The MLN and splenic cells contain a complex mix of memory and naïve phenotype cells that make it difficult to come to a conclusion without defining these cell populations.

In order to determine if the cell viability or proliferation was affected by STX11 deficiency, the proliferation and cell numbers of the different cell populations were studied in more detail. CFSE stably labels cytosolic molecules in the cell and the division of cells equally divides the dye resulting in a sequential halving of fluorescence. This allows for quantitation of the number of dividing cells in each generation of stained cells (Quah et al. 2007). Using this information it is possible to build a proliferation profile in order to compare the proliferation of polarised cells from WT and *Stx11*$^{-/-}$ mice.

The number of cells and viability over the four days of *in vitro* culture were also assessed for all WT and *Stx11*$^{-/-}$ cells from naïve, splenic and MLN populations. The naïve Th17 polarised cells show an immediate difference in the proliferation profiles of the cells from WT and *Stx11*$^{-/-}$ mice. The number of cells divided and the division index is significantly reduced. These cells show a similar viability >90% following four days *in vitro*, however when the cells were counted on day four, there is almost 3-fold increase in the number of WT naïve Th17 polarised cells compared to those isolated from *Stx11*$^{-/-}$ mice. Therefore, the proliferation of these cells is greatly affected in the absence of STX11. This may be due to the apparent inhibitory effects of STX11 deficiency on Th17 differentiation. The commitment and expansion of Th17 cells is dependant on the IL-23 receptor (IL-23R) (McGeachy et al. 2009) and its expression is significantly down-regulated in Th17 polarised cells from *Stx11*$^{-/-}$ mice**.** The inhibition of Th17 differentiation in these cells seems to have led to IL-23R not being up-regulated and not allowing the cells to expand, however still maintaining cell viability. In the absence of Th17 polarisation, our data shows that the growth factor IL-2 can expand undifferentiated cells, this has been also been shown by others (Liao et al. 2011). However, supernatants measured from these cells show low levels of IL-2 in WT and *Stx11*$^{-/-}$ samples. Therefore the reduction in cell numbers can be explained by the inhibition of Th17 cell polarisation of these cells. This would also contribute to the reduced levels of IL-17 measured in the supernatants of these cells. This abated proliferation of the naïve Th17 polarised cells from the *Stx11*$^{-/-}$ mice is also seen to a lesser extent in the CD4^{+} cells isolated from the spleen and MLN of these mice.

The increase in the percentage of IFN-γ producing cells in the naïve Th1 polarised cells from *Stx11*$^{-/-}$ mice is contradictory to the measured levels of IFN-γ in the supernatants from these cells. Measured concentrations of IFN-γ in supernatants from Th1 *Stx11*$^{-/-}$ cells show no significant change when compared to Th1 polarised cells from WT mice. However, the proliferation profile of the naïve cells revealed a deficiency in the proliferation of naïve Th1 polarised cells from *Stx11*$^{-/-}$ mice. The naïve cells show a dramatically reduced proliferation rate with the percentage of divided cells dropping from 75% in the WT cells to just 35% in the cells from *Stx11*$^{-/-}$ mice. The division index is also reduced from 1.3 to just 0.5 average divisions per cell. This was not observed in the splenic or MLN CD4^{+} isolated cells. There is a measured increase in the number of IFN-γ producing cells following re-stimulation on day four, as well as an increase in IFN-γ mRNA expression. However, proliferation deficiency may account for no measured increase in IFN-γ in the supernatants from naïve Th1 *Stx11*$^{-/-}$ cells. Over-expression of IFN-γ by the naïve Th1 *Stx11*$^{-/-}$ cells may induce an early T-cell phenotype change. This would account for the lack of proliferation despite the similar cell numbers and viability compared to the cells from the WT mice. Th1 cells undergo a change in phenotype following constant antigenic stimulation and secretion. This cell phenotype is characterised by production of IL-10 which is increased in concentration in the supernatants from the *Stx11*$^{-/-}$ cells. Interestingly, Th1 cells have been shown to have an increased capacity to produce IFN-γ following successive rounds of proliferation (Gett 1998). It is possible that the over-expression of IL-10 in the *Stx11*$^{-/-}$ cells triggers an early phenotypic change usually controlled by over production of IFN-γ in proliferating Th1 cells. The *Stx11*$^{-/-}$ cells also have a measured increase in IL-21, which has also been

demonstrated to be secreted in high levels by late Th1 polarised cells in infection (Sarra et al. 2010). IL-21 induces IL-10 secretion and may act in a self limiting negative feed back loop with IL-10. Switching off of IL-2 production is also a hallmark of T-cell exhaustion (Wherry 2011) and this is demonstrated in these cells by a reduction in the measured levels of IL-2 in the supernatants from the naïve Th1 polarised cells from *Stx11*$^{-/-}$ mice.

The data suggest that there is a dysregulation in the IFN-γ secretion from the naïve Th1 and Th17 polarised cells from *Stx11*$^{-/-}$ mice which is causing over secretion of IFN-γ in the Th1 cells and also causing inhibition of Th17 differentiation *in vitro*. To investigate this inhibition of Th17 polarisation and the effects of over expression of IFN-γ in Th1 cells, RNA was isolated from the naïve Th1 and Th17 polarised, WT and *Stx11*$^{-/-}$ cells. mRNA levels were assessed to determine gene expression following four days of *in vitro* cell culture. The Th17 polarised *Stx11*$^{-/-}$ cells showed a significant increase in T-bet and FoxP3 mRNA expression relative to the WT cells. Flow analysis of these cells clearly indicated a measured decrease in RORγt expression at 18hrs compared to the WT cells. From these results it would seem that the *Stx11*$^{-/-}$ cells are unable to effectively differentiate into Th17 cells when stimulated in polarising conditions due to the presence of over produced IFN-γ. It is clear that these cells did not polarise into a classical Th17 subset of cells in the absence of STX11.

Taking these results together there is clear evidence for dysregulation of IFN-γ secretion in Th1 and Th17 cells lacking STX11. In Naïve T-helper cells this has the effect of driving Th1 into a self limiting phenotype producing IL-21 and IL-10 and down-regulating activating surface markers IFN-γR1 and IL-2Rα, leading to a suppression of

proliferation *in vitro*. These cells are still capable of producing IFN-γ when restimulated directly via PKC in contrast to the splenic and MLN cells which have undergone 4-5 rounds of division.

In Th17 polarised cells, the apparent lack of control of IFN-γ in cells from *Stx11*$^{-/-}$ mice at the early stages of polarisation disrupts the programming of these cells into Th17 cells. The presence of IFN-γ inhibits Th17 polarisation and this is evident by the decrease in RORγt expression at 18hrs and a decrease in IL-17 and IL-21 production, which was confirmed at mRNA level. This is supported by a decrease in IL-23R and IL-17 mRNA expression in the *Stx11*$^{-/-}$ cells. Increased expression of FoxP3 and T-bet in the *Stx11*$^{-/-}$ cells were also indicative of a non-classical Th17 polarised phenotype of cells.

Taken together, results obtained in the Th1 and Th17 models individually indicate a regulatory role for STX11 in IFN-γ secretion. This suggests an early requirement for STX11 induction in naïve T-helper cells necessary for polarisation of cells into a Th17 cell subtype via control of IFN-γ secretion.

CHAPTER 6

GENERAL DISCUSSION

6.1– GENERAL DISCUSSION

Th17 cells are essential in the clearance of extracellular pathogens. They maintain gut homeostasis in a careful balance with regulatory T-cells, but in their capacity to produce IL-17 and other pro-inflammatory cytokines needed to clear infection, they have also been implicated in the induction of several autoimmune diseases (Bettelli et al. 2007). Cytokine signalling from Th17 and other T-helper cells is central to the regulation of the adaptive immune response but despite this, there is little known about the trafficking pathways involved in cytokine exocytosis from these cells. SNAREs have been identified as fundamental trafficking proteins required for intracellular membrane-membrane fusion events in eukaryotic cells (Jahn & Scheller 2006). Furthermore they are localised and carry out their function in specific organelles which has allowed researchers to "map out" the specific trafficking pathway of cytokines from immune cells. This has led to the mapping of TNF-α secretion from macrophages and elucidation of an original exocytotic pathway through recycling endosomes that is implicitly linked to the phagocytic activity of these cells (Stow et al. 2006). Identification of these trafficking pathways and the proteins that regulate them will lead to a better understanding of cytokine secretion during inflammation and may present potential therapeutic targets in disease.

In this study we have identified a regulatory requirement for the SNARE syntaxin 11 (STX11) in IFN-γ control in T-helper cells. Further more there is a requirement for STX11 regulation of IFN-γ for naïve T-helper cells to undergo efficient Th17 cell polarisation. IFN-γ is a potent inhibitor of Th17 cell polarisation via its suppression of the master regulator transcription factor RORγt. IFN-γ induces T-bet expression in activated T-helper cells and this inhibits RORγt expression driving T-cells in the direction of a Th1 phenotype

and in order to efficiently polarise a Th17 cell population *in vitro,* antibodies are added to neutralise IFN-γ activity (Lazarevic et al. 2011). Activated T-helper cells are capable of producing large amounts of IFN-γ within hours of TCR activation and *Ifnγ* gene expression is not repressed in polarised Th17 cells until the late to transition phase of the differentiation programme at 20hrs when the *Il17* cytokine gene is induced (Yosef et al. 2013). Therefore further regulatory mechanisms are required to control early secretion of IFN-γ and allow naïve T-helper cells to polarise into a Th17 cell subset.

STX11 is not like a typical syntaxin SNARE as it lacks a transmembrane domain. Despite this fact, STX11 still appears to be a syntaxin protein in that it is ~35kDa in size with two identified regions capable of forming coiled-coil structures to facilitate zippering with other SNARE proteins. It has been shown to bind with SNAP23 and VAMP2 efficiently *in vitro* demonstrating typical SNARE behaviour (Valdez et al. 1999). STX11 has also been localised on cell membranes despite the absence of an anchoring domain. This may be due in part to the presence of a C-terminal cysteine rich domain which is an ideal target site for palmitoylation. Palmitoylation is not unusual in SNARE regulation and has been studied in the SNAP25 family, including the immune rich variant SNAP23 (Pallavi & Nagaraj 2003). Although STX11 has a cysteine rich domain that is a putative palmitoylation site, Prekeris *et al* (2000) demonstrated that this site was not necessary for STX11 to associate with the membrane. Instead they show that STX11 binds to other SNARE proteins and that its membrane association is dependant on this interaction. Furthermore, they show that in the presence of α-SNAP and NSF, when NSF activity is inhibited STX11 is not assembled in a 20S complex with other SNAREs. The authors discovered that STX11 dissociated to its monomeric form and did not form part of a complex suggesting that STX11, despite its

ability to bind to other SNAREs, does not form part of a typical SNARE complex. In this study Prekeris *et al* (2000) suggested that STX11 may play a regulatory role by competing with transmembrane bound SNAREs and preventing SNARE assembly and fusing of membranes.

The idea that STX11 can act in a regulatory manner was later explored in a study in which Offenhäuser *et al* (2011) demonstrated that STX11 binds to Vti1b and makes Vti1b unavailable for the formation of membrane fusing SNARE complex's in macrophages. The authors show that Vti1b is involved in late endosome, lysosome and membrane transport, and that a loss of STX11 results in an increase in this trafficking to the cell surface, contributing to increased phagocytosis (Offenhäuser et al. 2011). Offenhäuser *et al* (2011) also showed that in normal conditions STX11 forms part of a large SNARE complex. However, when NSF activity is inhibited using NEM, SNAREs remain in a trans SNARE complex and STX11 is eluted in a smaller monomeric form, not forming part of a typical complex. This corroborates the observations made by Prekeris *et al* (2000) and their hypothesis that STX11 plays a regulatory role in immune cell function through competitive binding of fusogenic SNAREs preventing complex formation (Prekeris et al. 2000).

Our data has shown that *in vitro* Th17 polarised cells increased expression of STX11 following activation but levels remain low in naïve and IFN-γ producing Th1 cells. Furthermore, the expression of STX11 is increased in Th17 mediated models of inflammation *in vivo* when levels of IL-17 mRNA are increased and there is little or no IFN-γ mRNA expression. To our knowledge, this is the first study showing regulation of a

SNARE protein in a model of inflammatory disease and suggests that STX11 is involved in regulating the Th17 response *in vivo*.

Our data also shows that naïve T-helper cells from STX11 deficient mice were unable to efficiently differentiate into a Th17 subset *in vitro* compared to wild type cells. Cells from *Stx11*$^{-/-}$ mice had a reduced number of IL-17 producing cells, decreased expression of RORγt and low mRNA expression of essential Th17 related genes expressing IL-23R and IL-21. Interestingly this population also had increased numbers of IFN-γ producing cells, higher levels of secreted IFN-γ in the supernatant and increased IFN-γ and T-bet mRNA expression compared to WT cells. Furthermore, Th1 polarised cells from the *Stx11*$^{-/-}$ mice showed a significant increase in the number of IFN-γ producing cells. Dysregulation of IFN-γ production in T-cells from *Stx11*$^{-/-}$ mice has been previously described. In two studies confirming STX11 involvement in dysfunctional degranulation from $CD8^+$ T-cells, the authors also describe significantly increased levels of IFN-γ from these cells (Kögl et al. 2013; D'Orlando et al. 2013).

IFN-γ inhibits the differentiation of purified naïve $CD4^+$ T-cells into a Th17 cell subset (Lazarevic et al. 2011). We propose that in order to effectively polarise into Th17 cells, naïve T-cells activated in Th17 conditions upregulate STX11 in order to control basal secretion of IFN-γ production and prevent inhibition of Th17 differentiation. RORγt expression is decreased in *Stx11*$^{-/-}$ mice at 18hrs indicating that early stage Th17 polarisation may be inhibited by the increased levels of IFN-γ present; therefore STX11 expression is required early in the differentiation programme. Interestingly, STAT3 deficient mice fail to upregulate IL-17 and fail to induce severe disease in an EAE mouse model of multiple sclerosis (MS) (Yang et al. 2007). Early STAT3 activation is critical and

can be provided by a combination of IL-1, IL-6 and IL-21. Naïve $CD4^+$ T-cells are capable of differentiating into Th17 cells in the absence of IL-6 once IL-21, IL-23 and TGF-β are present (Korn et al. 2007). Similarly, Th17 cells can be generated *in vivo* in *Il21*$^{-/-}$ or *Il21R*$^{-/-}$ mice when IL-1β, IL-6 and TNFα are present (Sonderegger et al. 2008). These conditions resulted in diminished Th17 responses, and strong STAT3 activation may be required to increase STX11 expression and the regulation of IFN-γ necessary for efficient Th17 polarisation.

Our data shows that TGF-β1 is also dispensable in the generation of Th17 cells in the presence of IL-6, IL-1β and IL-23; however, the total numbers of IL-17 producing cells were significantly reduced. This is in agreement with a study by Ghoreschi *et al* (2010) who also demonstrated that Th17 cells generated in the absence of TGF-β1 expressed both RORγt and T-bet transcription factors. As well as demonstrating a reduced number of IL-17 producing cells, of particular interest is the fact that these cells were shown to be capable of becoming double producers of IFN-γ and IL-17 (Ghoreschi et al. 2010). Interestingly, in our study and the study carried out by Ghoreschi *et al* (2010), an anti-IFN-γ antibody was used to neutralise its activity *in vitro* to generate Th17 cells in the absence of TGF-β1. We would therefore suggest that TGF-β may responsible for driving STX11 expression in order to regulate IFN-γ expression.

In fact the naïve T-helper cells from *Stx11*$^{-/-}$ mice polarised in Th17 conditions show the same characteristics as the Th17 cells generated in the absence of TGF-β1 described in detail by Ghoreschi *et al* (2010). *Rorc* (RORγt) and *Il17* promoter region trimethylation was decreased in the cells polarised in the absence of TGF-β. *Rorc* mRNA expression was also reduced (Ghoreschi et al. 2010), correlating with our data showing reduced *Rorc* and

Il17 mRNA expression in *Stx11*$^{-/-}$ Th17 polarised cells. Our data also shows that naïve Th17 polarised *Stx11*$^{-/-}$ cells had reduced numbers of IL-17 producing cells and increased IFN-γ and T-bet mRNA expression, as well as a measured increase in IFN-γ in the supernatants from these cells. Furthermore, Ghoreschi *et al* (2010) showed that cells generated in the absence of TGF-β1 do not express IL-10. Our data shows that supernatants from *Stx11*$^{-/-}$ cells activated in Th17 polarising conditions have a significanlty reduced concentration of IL-10, and IL-10 mRNA expression in these cells is also significantly decreased compared to the wild type cells. Therefore naïve Th17 cells polarised in the absence of TGF-β1 have the same characterisitcs as naïve Th17 *Stx11*$^{-/-}$ cells and TGF-β signalling may lead to increased expression of STX11 to control IFN-γ production in Th17 polarisation. The exact role of TGF-β in Th17 differentiation is not fully understood and it is believed to inhibit T-bet expression in order to allow RORγt transcription and polarisation of a Th17 subset (Lee et al. 2009). TGF-β1 has been shown to inhibit Th1 cell development which is in part due to the suppression of T-bet (I.-K. Park et al. 2005). IFN-γ is a potent activator of T-bet and TGF-β may also induce STX11 expression in order to control IFN-γ production and break the feedback loop. Furthermore, studies in mice expressing a mutant form of TGF-β subunit receptor II (dnTGF-βRII) on T-cells demonstrate that it interferes with the generation of Th17 cells in an EAE mouse model of MS (Ghoreschi et al. 2010). The lamina propria of these mice had reduced numbers of IL-17 producing $CD4^+$ T-cells. Interestingly, there was also increased proportions of IFN-γ producing $CD4^+$ T-cells in the dnTGF-βRII mice compared to wild type, which was also confirmed in mice lacking TGF-R1 on $CD4^+$ T-cells (Ghoreschi et al. 2010).

Systematically high concentrations of IFN-γ are also found in patients with the STX11 deficiency culminating in the autoimmune disorder Familial hemophagocytic lymphohistiocytosis – 4 (FHL-4). These patients present with fever, cytopenia and hyper-inflammation and are prone to autoimmune disease. Characteristic traits of disease are over-activation of macrophages leading to hemophagocytosis, and impaired $CD8^+$ T-cells and NK cell cytotoxicity (Janka 2012).

As discussed above, loss of STX11 regulation in macrophages leads to the increased phagocytosis and TNF-α secretion that is observed in FHL-4 patients (Offenhäuser et al. 2011). The authors also suggested a role for STX11 in regulation of dendritic cells (DCs). STX11 transcription and protein expression is up-regulated in bone marrow-derived DCs (BMDCs) within 24hrs suggesting STX11 is regulated in these cells (Offenhäuser et al. 2011). Work in our own lab has demonstrated an increase in STX11 mRNA expression in the JAWS DC cell line within 1 hr of activation with toll like receptor (TLR) agonists (Collins., unpublished). Interestingly BMDCs stimulated with TLR agonists produce low levels of IFN-γ, and are capable of increased production when stimulated in the presence of IL-12 (Hochrein et al. 2001). STX11 may therefore play a similar regulatory role in IFN-γ regulation in DCs, indeed BMDCs isolated from *Stx11*$^{-/-}$ mice in our lab show increased levels of IFN-γ production compared to wild type controls when stimulated with TLR agonists (Collins., unpublished).

Extracellular pathogens have been described and implicated in cases of FHL including protozoa, bacterial and fungal infections. In fact, untreated FHL is rapidly fatal and most patients die from bacterial or fungal infections attributed in part to neutropenia (Janka 2012). Neutrophils have emerged as important mediators of Th17 controlled immune

resistance to extracellular pathogens (Mantovani et al. 2011). Th17 cells produce CXCL8, a neutrophil chemo-attractant which is not produced by Th1 cells (Pelletier et al. 2010). IL-17A and IL-17F also stimulate epithelial cells to secrete granulopoietic factors and chemokines that favour recruitment, activation and prolonged survival of neutrophils in inflammation (Mantovani et al. 2011). Our data shows that in the absence of STX11, Th17 differentiation of T-cells is inhibited which may impair neutrophil recruitment and may in part explain the inability of FHL-4 patients lacking functional STX11 to clear fungal infections. To our knowledge there are currently no data published on the $CD4^+$ T-helper populations present in FHL-4 patients and further study is required to establish if decreased $CD4^+$ IL-17 producing populations play a role in progression of disease.

Our data shows that there is an increase in the number of IFN-γ producing cells in $Stx11^{-/-}$ Th1 polarised $CD4^+$ T-cells compared to wild type cells. This has been previously described in $CD8^+$ T-cells, suggesting that T-cells share a common regulatory mechanism (D'Orlando et al. 2013; Kögl et al. 2013). Contrary to this finding, naïve Th1 *Stx11*$^{-/-}$ cells had reduced levels of measured IFN-γ in supernatants despite increased mRNA expression of IFN-γ. Interestingly, these cells had drastically reduced proliferation rates compared to wild type cells despite an increase in cell viability. Significantly high levels of IL-10 and IL-21 were measured in the supernatants from the Th1 *Stx11*$^{-/-}$ cells, mRNA expression of these genes were also increased significantly. IL-10 and IL-21 expression have been associated with Th1 cells late in development and are associated with an exhaustive T-cell state that acts as a self limiting mechanism to control the immune response (Salek-Ardakani & Schoenberger 2013; Saraiva et al. 2009). It is possible that the suppressive

effects of these cytokines inhibited proliferation of these cells *in vitro*. A mouse model of FHL-4 has been generated by infecting $Stx11^{-/-}$ mice with lymphocytic choriomeningitis virus (LCMV) which present all clinical and lab features of hemophagocytic lymphohistiocytosis (HLH) (Kögl et al. 2013; Sepulveda et al. 2013). Interestingly, Kögl *et al* (2013) showed that in contrast to mice with HLH caused by a lack in $CD8^+$ associated perforin, the *Stx11*$^{-/-}$ mouse model was non-fatal and unable to clear LCMV infection; this was attributed to an exhausted phenotype in $CD8^+$ CTLs. Despite elevated levels of IFN-γ producing cells and IFN-γ serum levels in early disease, $CD8^+$ CTLs from *Stx11*$^{-/-}$ mice took on an exhausted phenotype which could be reversed by blocking inhibitory pathways. An exhausted phenotype has been described in $CD8^+$ and $CD4^+$ T-cells and interestingly IFN-γ production is correlated with an advanced state of exhaustion before deletion (Yi et al. 2010) explaining the ability of these suppressed cells to be stimulated to secrete IFN-γ. In our experiment the inhibitory pathways were bypassed by the stimulation of the cells with PMA and ionomycin, as they are direct chemical inducers of protein kinase c and intracellular calcium channels (Carter et al. 2002).

These data begin to suggest a role for T-helper cells in developing FHL-4 in STX11 deficient patients. This work and others have shown that STX11 is critical for regulating IFN-γ secretion in T-cells. We have also shown that this inhibits the generation of Th17 cells *in vitro*. Among the clinical feature of HLH are high serum levels of pro-inflammatory cytokines including IFN-γ. HLH is usually fatal in early infants if untreated, however, HLH in STX11 deficient patients develop less severe disease associated with late onset, alleviated symptoms and longer periods of disease free remission compared to patients with perforin deficiency (Kögl et al. 2013). Th1 responses are responsible for

clearance of intracellular pathogens and secrete large amounts of pro-inflammatory cyokines in order to mediate clearance. Inability to control Th1 cells leads to severe autoimmune inflammation (Cope et al. 2011) thus, the reduced severity in FHL-4 patients could be attributed to an induced $CD4^+$ exhausted phenotype in Th1 cells deficient in STX11. Furthermore, patients are unable to clear extracellular pathogens which can result in onset of symptoms and death, this may be attributed to a lack of a Th17 driven immune response. The exact mechanism for T-cell switching to an exhausted phenotype is not well understood but may be related to STX11 regulation, trafficking in the cell or IFN-γ secretion and signalling. The use of these *Stx11*$^{-/-}$ cells may present a good model for studying the T-cell exhaustion pathway and provide some answers on its mechanism.

While our data outline a possible regulatory function for STX11 in the differentiation of Th17 cells, further investigation is required to study this mechanism *in vivo*. These data suggest that there is a role for T-helper cells in FHL-4 and it will be of great interest to further investigate Th17 cells in patients and murine models of disease. Furthermore, although the DSS and *C. rodentuim* Th17 mediated models of inflammatory disease in this study agree with the *in vitro* data and clearly show a regulated increase of STX11 in correlation with IL-17 production and reduced IFN-γ; there is a need to investigate Th17 differentiation of $CD4^+$ cells in isolation *in vivo*. Adoptive transfer of $CD45RB^{HI}$ cells from wild type mice into immune deficient mice lacking mature B- and T-cell lymphocytes leads to the development of colitis (Ostanin et al. 2009). The adoptive transfer model of colitis is well studied and inflammation has been linked to the development of Th17 cells in the gut of the immune deficient mice (Shale et al. 2013). Adoptive transfer of naïve cells

from *Stx11*$^{-/-}$ mice into immune deficient mice presents an ideal model for *in vivo* study of STX11 regulation in Th17 differentiation of CD4^{+} T-helper cells.

In summary we propose a novel mechanism that upon activation in Th17 polarising conditions, STAT3 or more than likely TGF-β1 mediated signalling induces CD4^{+} T-cells to upregulate the expression of STX11. STX11 then inhibits IFN-γ production preventing the T-bet mediated inhibition of RORγt and allows cells to differentiate into a Th17 phenotype. Furthermore we suggest a role for CD4^{+} T-cells in FHL-4 STX11 deficient patients in which CD4^{+} Th1 cells become exhausted due to dysregulated IFN-γ production and suppress the immune response leading to decreased severity in disease. In parallel, inhibition of Th17 cell leaves patients susceptible to extracellular pathogens. Further study of the mechanics of STX11 regulation in Th17 and Th1 cells will lead to elucidation of the trafficking pathways in these cells and a better understanding of their regulation in disease.

CHAPTER 7

BIBLIOGRAPHY

Abraham, C. & Cho, J., 2009. Interleukin-23/Th17 pathways and inflammatory bowel disease. *Inflammatory bowel diseases*, 15(7), pp.1090–100. Available at: http://www.ncbi.nlm.nih.gov/pubmed/19253307 [Accessed June 25, 2013].

Abraham, S.N. & St John, A.L., 2010. Mast cell-orchestrated immunity to pathogens. *Nature reviews. Immunology*, 10(6), pp.440–52. Available at: http://www.ncbi.nlm.nih.gov/pubmed/20498670 [Accessed May 21, 2013].

Afkarian, M. et al., 2002. T-bet is a STAT1-induced regulator of IL-12R expression in naïve CD4+ T cells. *Nature immunology*, 3(6), pp.549–57. Available at: http://www.ncbi.nlm.nih.gov/pubmed/12006974 [Accessed June 9, 2013].

Aggarwal, S. et al., 2003. Interleukin-23 promotes a distinct CD4 T cell activation state characterized by the production of interleukin-17. *The Journal of biological chemistry*, 278(3), pp.1910–4. Available at: http://www.jbc.org.remote.library.dcu.ie/content/278/3/1910 [Accessed May 25, 2013].

Ahern, P.P. et al., 2010. Interleukin-23 drives intestinal inflammation through direct activity on T cells. *Immunity*, 33(2), pp.279–88. Available at: http://www.pubmedcentral.nih.gov/articlerender.fcgi?artid=3078329&tool=pmcentrez&rendertype=abstract [Accessed May 31, 2013].

Aidoo, A. et al., 1991. Comparative-Study of Intracellular Glutathione Content in Rat Lymphocyte-Cultures Treated with 2-Mercaptoethanol and Interleukin-2. *Cell biology and toxicology*, 7(3), pp.215–227.

Alex, P. et al., 2009. Distinct cytokine patterns identified from multiplex profiles of murine DSS and TNBS-induced colitis. *Inflammatory bowel diseases*, 15(3), pp.341–52. Available at: http://www.pubmedcentral.nih.gov/articlerender.fcgi?artid=2643312&tool=pmcentrez&rendertype=abstract [Accessed June 15, 2013].

Banchereau, J. & Steinman, R.M., 1998. Dendritic cells and the control of immunity. *Nature*, 392(6673), pp.245–52. Available at: http://www.nature.com.remote.library.dcu.ie/nature/journal/v392/n6673/full/392245a0.html [Accessed May 22, 2013].

Barber, D.L., Wherry, E.J. & Ahmed, R., 2003. Cutting edge: rapid in vivo killing by memory CD8 T cells. *Journal of immunology (Baltimore, Md.□: 1950)*, 171(1), pp.27–31. Available at: http://www.jimmunol.org.remote.library.dcu.ie/content/171/1/27.full [Accessed July 6, 2013].

Barbi, J., Pardoll, D. & Pan, F., 2013. Metabolic control of the Treg/Th17 axis. *Immunological reviews*, 252(1), pp.52–77. Available at: http://www.ncbi.nlm.nih.gov/pubmed/23405895.

Basu, R., Hatton, R.D. & Weaver, C.T., 2013. The Th17 family: flexibility follows function. *Immunological reviews*, 252(1), pp.89–103. Available at: http://www.ncbi.nlm.nih.gov/pubmed/23405897.

Becher, B., Durell, B.G. & Noelle, R.J., 2002. Experimental autoimmune encephalitis and inflammation in the absence of interleukin-12. *The Journal of clinical investigation*, 110(4), pp.493–7. Available at: /pmc/articles/PMC150420/?report=abstract [Accessed June 25, 2013].

Benado, A., Nasagi-Atiya, Y. & Sagi-Eisenberg, R., 2009. Protein trafficking in immune cells. *Immunobiology*, 214(6), pp.403–21. Available at: http://dx.doi.org/10.1016/j.imbio.2008.11.011 [Accessed July 16, 2013].

Bettelli, E. et al., 2006. Reciprocal developmental pathways for the generation of pathogenic effector TH17 and regulatory T cells. *Nature*, 441(7090), pp.235–8. Available at: http://www.nature.com.remote.library.dcu.ie/nature/journal/v441/n7090/full/nature04753.html [Accessed May 22, 2013].

Bettelli, E., Oukka, M. & Kuchroo, V.K., 2007. T(H)-17 cells in the circle of immunity and autoimmunity. *Nature immunology*, 8(4), pp.345–350.

Bevan, M.J., 2004. Helping the CD8(+) T-cell response. *Nature reviews. Immunology*, 4(8), pp.595–602. Available at: http://www.ncbi.nlm.nih.gov/pubmed/15286726 [Accessed May 23, 2013].

Bhinder, G. et al., 2013. The Citrobacter rodentium mouse model: studying pathogen and host contributions to infectious colitis. *Journal of visualized experiments: JoVE*, (72), p.e50222. Available at: http://www.ncbi.nlm.nih.gov/pubmed/23462619 [Accessed June 6, 2013].

Block, M.R. & Rothman, J.E., 1992. Purification of N-ethylmaleimide-sensitive fusion protein. *Methods in enzymology*, 219, pp.300–9. Available at: http://www.ncbi.nlm.nih.gov/pubmed/1488002 [Accessed July 18, 2013].

Bluestone, J. a et al., 2009. The functional plasticity of T cell subsets. *Nature reviews. Immunology*, 9(11), pp.811–6. Available at: http://www.pubmedcentral.nih.gov/articlerender.fcgi?artid=3075537&tool=pmcentrez&rendertype=abstract.

Bock, J.B. et al., 2001. A genomic perspective on membrane compartment organization. *Nature*, 409(6822), pp.839–41. Available at: http://www.ncbi.nlm.nih.gov/pubmed/11237004 [Accessed June 24, 2013].

Borregaard, N., Sørensen, O.E. & Theilgaard-Mönch, K., 2007. Neutrophil granules: a library of innate immunity proteins. *Trends in immunology*, 28(8), pp.340–5. Available at: http://www.ncbi.nlm.nih.gov/pubmed/17627888 [Accessed May 21, 2013].

Bouguermouh, S. et al., 2009. CD28 co-stimulation down regulates Th17 development. D. Unutmaz, ed. *PloS one*, 4(3), p.e5087. Available at: http://dx.plos.org/10.1371/journal.pone.0005087 [Accessed June 17, 2013].

Bour-Jordan, H. et al., 2011. Intrinsic and extrinsic control of peripheral T-cell tolerance by costimulatory molecules of the CD28/B7 family. *Immunological reviews*, 241, pp.180–205.

Bradley, L.M., Atkins, G.G. & Swain, S.L., 1992. Long-term CD4+ memory T cells from the spleen lack MEL-14, the lymph node homing receptor. *Journal of immunology (Baltimore, Md.: 1950)*, 148(2), pp.324–31. Available at: http://www.ncbi.nlm.nih.gov/pubmed/1345918 [Accessed June 17, 2013].

Bryceson, Y.T. et al., 2007. Defective cytotoxic lymphocyte degranulation in syntaxin-11 deficient familial hemophagocytic lymphohistiocytosis 4 (FHL4) patients. *Blood*, 110(6), pp.1906–15. Available at: http://bloodjournal.hematologylibrary.org/content/110/6/1906.short [Accessed June 25, 2013].

Budd, R.C. et al., 1987. Distinction of virgin and memory T lymphocytes. Stable acquisition of the Pgp-1 glycoprotein concomitant with antigenic stimulation. *Journal of immunology (Baltimore, Md.□: 1950)*, 138(10), pp.3120–9. Available at: http://www.ncbi.nlm.nih.gov/pubmed/3106474 [Accessed June 17, 2013].

Bustin, S.A. et al., 2009. The MIQE guidelines: minimum information for publication of quantitative real-time PCR experiments. *Clinical chemistry*, 55(4), pp.611–22. Available at: http://www.clinchem.org/content/55/4/611.full [Accessed October 25, 2012].

Carter, L.L. et al., 2002. PD-1:PD-L inhibitory pathway affects both CD4+ and CD8+ T cells and is overcome by IL-2. *European Journal of Immunology*, 32(3), pp.634–643. Available at: http://www.ncbi.nlm.nih.gov/pubmed/11857337 [Accessed June 21, 2013].

Chang, H.-C. et al., 2010. The transcription factor PU.1 is required for the development of IL-9-producing T cells and allergic inflammation. *Nature immunology*, 11(6), pp.527–34. Available at:

http://www.nature.com.remote.library.dcu.ie/ni/journal/v11/n6/abs/ni.1867.html [Accessed May 25, 2013].

Chang, M.P., Strehler, B.L. & Makinodan, T., 1982. Requirement of 2-Mercaptoethanol for Invitro Growth-Factor Production by T-Cells and Vulnerability of the Response to Age. *Mechanisms of ageing and development*, 20(1), pp.65–73.

Chen, D. et al., 2000. Molecular mechanisms of platelet exocytosis: role of SNAP-23 and syntaxin 2 in dense core granule release. *Blood*, 95(3), pp.921–9. Available at: http://www.ncbi.nlm.nih.gov/pubmed/10648404 [Accessed June 24, 2013].

Chen, Z., Laurence, A. & O'Shea, J.J., 2007. Signal transduction pathways and transcriptional regulation in the control of Th17 differentiation. *Seminars in immunology*, 19(6), pp.400–8. Available at: http://www.pubmedcentral.nih.gov/articlerender.fcgi?artid=2323678&tool=pmcentrez&rendertype=abstract [Accessed June 9, 2013].

Chopra, R.K. et al., 1989. Phorbol myristate acetate and calcium ionophore A23187-stimulated human T cells do not express high-affinity IL-2 receptors. *Immunology*, 66(1), pp.54–60.

Chung, Y. et al., 2009. Critical regulation of early Th17 cell differentiation by interleukin-1 signaling. *Immunity*, 30(4), pp.576–587. Available at: http://www.pubmedcentral.nih.gov/articlerender.fcgi?artid=2705871&tool=pmcentrez&rendertype=abstract [Accessed May 31, 2013].

Clary, D.O. & Rothman, J.E., 1992. Purification of soluble N-ethylmaleimide-sensitive fusion attachment proteins from bovine brain microsomes. *Methods in enzymology*, 219, pp.319–30. Available at: http://www.ncbi.nlm.nih.gov/pubmed/1488004 [Accessed July 18, 2013].

Clement, L.T., Tilden, A.B. & Dunlap, N.E., 1985. Analysis of the monocyte Fc receptors and antibody-mediated cellular interactions required for the induction of T cell proliferation by anti-T3 antibodies. *Journal of immunology (Baltimore, Md.□: 1950)*, 135(1), pp.165–71. Available at: http://www.ncbi.nlm.nih.gov/pubmed/3923099 [Accessed June 17, 2013].

Cope, A. et al., 2011. The Th1 life cycle: molecular control of IFN-γ to IL-10 switching. *Trends in immunology*, 32(6), pp.278–86. Available at: http://www.ncbi.nlm.nih.gov/pubmed/21531623 [Accessed May 29, 2013].

Cote-Sierra, J. et al., 2004. Interleukin 2 plays a central role in Th2 differentiation. *Proceedings of the National Academy of Sciences of the United States of America*, 101(11), pp.3880–5. Available at: http://www.pnas.org/content/101/11/3880.full [Accessed June 13, 2013].

Crotty, S., 2011. Follicular helper CD4 T cells (TFH). *Annual review of immunology*, 29, pp.621–63. Available at: http://www.annualreviews.org/doi/abs/10.1146/annurev-immunol-031210-101400 [Accessed May 23, 2013].

Curotto de Lafaille, M.A. & Lafaille, J.J., 2009. Natural and adaptive foxp3+ regulatory T cells: more of the same or a division of labor? *Immunity*, 30(5), pp.626–35. Available at: http://www.ncbi.nlm.nih.gov/pubmed/19464985 [Accessed May 23, 2013].

D'Orlando, O. et al., 2013. Syntaxin 11 is required for NK and $CD8^+$ T-cell cytotoxicity and neutrophil degranulation. *European journal of immunology*, 43(1), pp.194–208. Available at: http://www.ncbi.nlm.nih.gov/pubmed/23042080 [Accessed June 16, 2013].

Das, V. et al., 2004. Activation-Induced Polarized Recycling Targets T Cell Antigen Receptors to the Immunological Synapse: Involvement of SNARE Complexes. , 20(5), pp.577–588. Available at: http://linkinghub.elsevier.com/retrieve/pii/S1074761304001062.

Delprete, G.F. et al., 1991. Purified Protein Derivative Of Mycobacterium-Tuberculosis And Excretory-Secretory Antigen(S) Of Toxocara-Canis Expand Invitro Human T-Cells With Stable And Opposite (Type-1 T-Helper Or Type-2 T-Helper) Profile Of Cytokine Production. *JOURNAL OF CLINICAL INVESTIGATION*, 88(1), pp.346–350.

Dressel, R. et al., 2010. The exocytosis of lytic granules is impaired in Vti1b- or Vamp8-deficient CTL leading to a reduced cytotoxic activity following antigen-specific activation. *Journal of immunology (Baltimore, Md.□: 1950)*, 185(2), pp.1005–14. Available at: http://www.ncbi.nlm.nih.gov/pubmed/20543108 [Accessed July 19, 2013].

Duerr, R.H. et al., 2006. A genome-wide association study identifies IL23R as an inflammatory bowel disease gene. *Science (New York, N.Y.)*, 314(5804), pp.1461–3. Available at: http://www.ncbi.nlm.nih.gov/pubmed/17068223 [Accessed May 25, 2013].

Duhen, T. et al., 2009. Production of interleukin 22 but not interleukin 17 by a subset of human skin-homing memory T cells. *Nature immunology*, 10(8), pp.857–63. Available at: http://www.ncbi.nlm.nih.gov/pubmed/19578369 [Accessed June 11, 2013].

Eyerich, S. et al., 2009. Th22 cells represent a distinct human T cell subset involved in epidermal immunity and remodeling. *The Journal of clinical investigation*, 119(12), pp.3573–85. Available at: http://www.pubmedcentral.nih.gov/articlerender.fcgi?artid=2786807&tool=pmcentrez&rendertype=abstract [Accessed June 11, 2013].

Fasshauer, D. et al., 1998. Conserved structural features of the synaptic fusion complex: SNARE proteins reclassified as Q- and R-SNAREs. *Proceedings of the National Academy of Sciences of the United States of America*, 95(26), pp.15781–15786. Available at: http://www.pnas.org/content/95/26/15781.long [Accessed June 24, 2013].

Feng, T. et al., 2011. Th17 cells induce colitis and promote Th1 cell responses through IL-17 induction of innate IL-12 and IL-23 production. *Journal of immunology (Baltimore, Md.□: 1950)*, 186(11), pp.6313–8. Available at: http://www.jimmunol.org/content/186/11/6313.long [Accessed May 31, 2013].

Ferber, I.A. et al., 1996. Mice with a disrupted IFN-gamma gene are susceptible to the induction of experimental autoimmune encephalomyelitis (EAE). *Journal of immunology (Baltimore, Md.□: 1950)*, 156(1), pp.5–7. Available at: http://www.jimmunol.org.remote.library.dcu.ie/content/156/1/5.abstract [Accessed May 26, 2013].

Fink, P.J., 2013. The biology of recent thymic emigrants. *Annual review of immunology*, 31, pp.31–50. Available at: http://www.ncbi.nlm.nih.gov/pubmed/23121398 [Accessed May 30, 2013].

Fiorentino, D.F., 1989. Two types of mouse T helper cell. IV. Th2 clones secrete a factor that inhibits cytokine production by Th1 clones. *Journal of Experimental Medicine*, 170(6), pp.2081–2095. Available at: http://jem.rupress.org.remote.library.dcu.ie/content/170/6/2081 [Accessed July 2, 2013].

Flaumenhaft, R. et al., 2007. SNAP-23 and syntaxin-2 localize to the extracellular surface of the platelet plasma membrane. *Blood*, 110(5), pp.1492–501. Available at: http://www.pubmedcentral.nih.gov/articlerender.fcgi?artid=1975852&tool=pmcentrez&rendertype=abstract [Accessed June 24, 2013].

Fontenot, J.D., Gavin, M.A. & Rudensky, A.Y., 2003. Foxp3 programs the development and function of CD4+CD25+ regulatory T cells. *Nature immunology*, 4(4), pp.330–6. Available at: http://www.ncbi.nlm.nih.gov/pubmed/12612578 [Accessed May 21, 2013].

Foster, B. et al., 2007. Detection of intracellular cytokines by flow cytometry. *Current protocols in immunology / edited by John E.Coligan ...[et al.]*, Chapter 6, p.Unit 6.24.

Gajewski, T.F. & Fitch, F.W., 1988. Anti-proliferative effect of IFN-gamma in immune regulation. I. IFN-gamma inhibits the proliferation of Th2 but not Th1 murine helper T lymphocyte clones. *Journal of immunology (Baltimore, Md.: 1950)*, 140(12), pp.4245–4252. Available at:

http://www.jimmunol.org.remote.library.dcu.ie/content/140/12/4245.abstract [Accessed July 9, 2013].

Germain, R.N., 2002. T-cell development and the CD4?CD8 lineage decision. *Nature Reviews Immunology*, 2(5).

Gett, A. V., 1998. Cell division regulates the T cell cytokine repertoire, revealing a mechanism underlying immune class regulation. *Proceedings of the National Academy of Sciences*, 95(16), pp.9488–9493. Available at: http://www.pnas.org/content/95/16/9488.long [Accessed July 3, 2013].

Gholam, C. et al., 2011. Familial haemophagocytic lymphohistiocytosis: advances in the genetic basis, diagnosis and management. *Clinical & Experimental Immunology*, 163(3), pp.271–283. Available at: http://doi.wiley.com/10.1111/j.1365-2249.2010.04302.x [Accessed April 22, 2013].

Ghoreschi, K. et al., 2010. Generation of pathogenic TH 17 cells in the absence of TGF-β 2 signalling. *Nature*, 467(7318), pp.967–971. Available at: http://www.scopus.com/inward/record.url?eid=2-s2.0-77958584113&partnerID=40&md5=435517d608081995143a279ade9e15a1.

Gocke, A.R. et al., 2007. T-bet regulates the fate of Th1 and Th17 lymphocytes in autoimmunity. *Journal of immunology (Baltimore, Md.□: 1950)*, 178(3), pp.1341–8. Available at: http://www.ncbi.nlm.nih.gov/pubmed/17237380 [Accessed July 15, 2013].

Greaves, J. et al., 2010. Palmitoylation of the SNAP25 protein family: specificity and regulation by DHHC palmitoyl transferases. *The Journal of biological chemistry*, 285(32), pp.24629–38. Available at: http://www.pubmedcentral.nih.gov/articlerender.fcgi?artid=2915699&tool=pmcentrez&rendertype=abstract [Accessed July 13, 2013].

Greenwald, R.J., 2005. THE B7 FAMILY REVISITED. *Annual Review of Immunology*, 23(1).

Le Gros, G., 1990. Generation of interleukin 4 (IL-4)-producing cells in vivo and in vitro: IL-2 and IL-4 are required for in vitro generation of IL-4- producing cells. *Journal of Experimental Medicine*, 172(3), pp.921–929. Available at: http://jem.rupress.org/content/172/3/921.abstract [Accessed July 8, 2013].

Guo, Z., Turner, C. & Castle, D., 1998. Relocation of the t-SNARE SNAP-23 from lamellipodia-like cell surface projections regulates compound exocytosis in mast cells. *Cell*, 94(4), pp.537–48. Available at: http://www.ncbi.nlm.nih.gov/pubmed/9727496 [Accessed July 19, 2013].

Häger, M., Cowland, J.B. & Borregaard, N., 2010. Neutrophil granules in health and disease. *Journal of internal medicine*, 268(1), pp.25–34. Available at: http://www.ncbi.nlm.nih.gov/pubmed/20497300 [Accessed June 4, 2013].

Hall, L.J. et al., 2011. Induction and activation of adaptive immune populations during acute and chronic phases of a murine model of experimental colitis. *Digestive diseases and sciences*, 56(1), pp.79–89. Available at: http://www.springerlink.com/content/l39p6180x6l5r431/ [Accessed March 26, 2012].

Hardy, R.R. & Hayakawa, K., 2001. B cell development pathways. *Annual review of immunology*, 19, pp.595–621. Available at: http://www.ncbi.nlm.nih.gov/pubmed/11244048 [Accessed June 18, 2013].

Haribhai, D. et al., 2011. A requisite role for induced regulatory T cells in tolerance based on expanding antigen receptor diversity. *Immunity*, 35(1), pp.109–22. Available at: http://www.cell.com/immunity/fulltext/S1074-7613(11)00259-7 [Accessed May 31, 2013].

Harrington, L.E. et al., 2005. Interleukin 17-producing CD4+ effector T cells develop via a lineage distinct from the T helper type 1 and 2 lineages. *Nature immunology*, 6(11), pp.1123–1132.

Hochrein, H. et al., 2001. Differential production of IL-12, IFN-alpha, and IFN-gamma by mouse dendritic cell subsets. *Journal of immunology (Baltimore, Md.□: 1950)*, 166(9), pp.5448–55. Available at: http://www.ncbi.nlm.nih.gov/pubmed/11313382 [Accessed July 23, 2013].

Hohenstein, A.C. & Roche, P.A., 2001. SNAP-29 Is a Promiscuous Syntaxin-Binding SNARE. *Biochemical and biophysical research communications*, 285(2), pp.167–171. Available at: http://www.sciencedirect.com.remote.library.dcu.ie/science/article/B6WBK-45S4J2G-MJ/2/12f9f9bb19f933cf5d15efe8537a69c7.

Hohl, T.M. et al., 1998. Arrangement of subunits in 20 S particles consisting of NSF, SNAPs, and SNARE complexes. *Molecular cell*, 2(5), pp.539–48. Available at: http://www.ncbi.nlm.nih.gov/pubmed/9844627 [Accessed July 1, 2013].

Hong, W., 2005. SNAREs and traffic. *Biochimica et biophysica acta*, 1744(2), pp.120–44. Available at: http://www.ncbi.nlm.nih.gov/pubmed/15893389 [Accessed May 21, 2013].

Hsieh, C.-S. et al., 1993. Development of T(H)1 CD4(+) T cells through IL-12 produced by Listeria-induced macrophages. *Science*, 260, pp.547–49.

Hsu, V.W. & Prekeris, R., 2010. Transport at the recycling endosome. *Current opinion in cell biology*, 22(4), pp.528–34. Available at: http://dx.doi.org/10.1016/j.ceb.2010.05.008 [Accessed May 23, 2013].

Huse, M. et al., 2006. T cells use two directionally distinct pathways for cytokine secretion. *Nature immunology*, 7(3), pp.247–255.

Huse, M., Quann, E.J. & Davis, M.M., 2008. Shouts, whispers and the kiss of death: directional secretion in T cells. *Nature immunology*, 9(10), pp.1105–1111.

Hwang, E.S. et al., 2005. T Helper Cell Fate Specified by Kinase-Mediated Interaction of T-Bet with GATA-3. *Science*, 307(5708), pp.430–433. Available at: http://www.jstor.org/stable/3840063.

Inui, K., Oreffo, R.O.C. & Triffitt, J.T., 1997. Effects of beta mercaptoethanol on the proliferation and differentiation of human osteoprogenitor cells. *Cell biology international*, 21(7), pp.419–425.

Ito, R. et al., 2008. Involvement of IL-17A in the pathogenesis of DSS-induced colitis in mice. *Biochemical and biophysical research communications*, 377(1), pp.12–6. Available at: http://www.ncbi.nlm.nih.gov/pubmed/18796297 [Accessed May 25, 2013].

Ivanov, I.I. et al., 2009. Induction of intestinal Th17 cells by segmented filamentous bacteria. *Cell*, 139(3), pp.485–98. Available at: http://www.pubmedcentral.nih.gov/articlerender.fcgi?artid=2796826&tool=pmcentrez&rendertype=abstract [Accessed May 30, 2013].

Ivanov, I.I. et al., 2006. The orphan nuclear receptor RORgammat directs the differentiation program of proinflammatory IL-17+ T helper cells. *Cell*, 126(6), pp.1121–1133.

Jacobson, N.G. et al., 1995. Interleukin 12 signaling in T helper type 1 (Th1) cells involves tyrosine phosphorylation of signal transducer and activator of transcription (Stat)3 and Stat4. *The Journal of experimental medicine*, 181(5), pp.1755–62. Available at: http://www.pubmedcentral.nih.gov/articlerender.fcgi?artid=2191986&tool=pmcentrez&rendertype=abstract [Accessed June 24, 2013].

Jahn, R. & Scheller, R.H., 2006. SNAREs - engines for membrane fusion. *Nature Reviews Molecular Cell Biology*, 7(9), pp.631–643.

Janeway, C.A. & Medzhitov, R., 2002. Innate immune recognition. *Annual review of immunology*, 20, pp.197–216. Available at: http://www.annualreviews.org.remote.library.dcu.ie/doi/abs/10.1146/annurev.immunol.20.083001.084359 [Accessed May 23, 2013].

Janka, G.E., 2012. Familial and acquired hemophagocytic lymphohistiocytosis. *Annual review of medicine*, 63, pp.233–46. Available at: http://www.annualreviews.org/doi/abs/10.1146/annurev-med-041610-134208 [Accessed March 11, 2013].

Jelley-Gibbs, D.M. et al., 2000. Two distinct stages in the transition from naive CD4 T cells to effectors, early antigen-dependent and late cytokine-driven expansion and differentiation. *Journal of immunology (Baltimore, Md.□: 1950)*, 165(9), pp.5017–26. Available at: http://www.ncbi.nlm.nih.gov/pubmed/11046030 [Accessed June 23, 2013].

Jiang, S. & Dong, C., 2013. A complex issue on CD4(+) T-cell subsets. *Immunological reviews*, 252(1), pp.5–11. Available at: http://www.ncbi.nlm.nih.gov/pubmed/23405891 [Accessed July 5, 2013].

Jolly, C. & Sattentau, Q.J., 2007. Regulated secretion from CD4+ T cells. *Trends in immunology*, 28(11), pp.474–81. Available at: http://www.ncbi.nlm.nih.gov/pubmed/17962070 [Accessed July 19, 2013].

Kandere-Grzybowska, K. et al., 2003. IL-1 induces vesicular secretion of IL-6 without degranulation from human mast cells. *Journal of immunology (Baltimore, Md.□: 1950)*, 171(9), pp.4830–6. Available at: http://www.ncbi.nlm.nih.gov/pubmed/14568962 [Accessed July 19, 2013].

Kaplan, M.H. et al., 1996. Stat6 Is Required for Mediating Responses to IL-4 and for the Development of Th2 Cells. *Immunity*, 4(3), pp.313–319. Available at: http://www.cell.com.remote.library.dcu.ie/immunity/fulltext/S1074-7613(00)80439-2 [Accessed July 10, 2013].

Kenneth Murphy Mark Walport, P.T., 2008. *Janeway's Immunobiology*, New York and London: Garland Science, Taylor & Francis group, LLC.

Kögl, T. et al., 2013. Hemophagocytic lymphohistiocytosis in syntaxin-11-deficient mice: T-cell exhaustion limits fatal disease. *Blood*, 121(4), pp.604–13. Available at: http://www.ncbi.nlm.nih.gov/pubmed/23190531 [Accessed June 3, 2013].

Korn, T. et al., 2009. IL-17 and Th17 Cells. *Annual review of immunology*, 27, pp.485–517. Available at: http://www.annualreviews.org.remote.library.dcu.ie/doi/abs/10.1146/annurev.immunol.021908.132710 [Accessed May 21, 2013].

Korn, T. et al., 2007. IL-21 initiates an alternative pathway to induce proinflammatory T(H)17 cells. *Nature*, 448(7152), pp.484–7. Available at: http://www.ncbi.nlm.nih.gov/pubmed/17581588 [Accessed May 26, 2013].

Krummel, M.F. et al., 2000. Differential clustering of CD4 and CD3 zeta during T cell recognition. *Science*, 289(5483), pp.1349–1352.

Krzewski, K. et al., 2011. VAMP4- and VAMP7-expressing vesicles are both required for cytotoxic granule exocytosis in NK cells. *European journal of immunology*, 41(11), pp.3323–9. Available at: http://www.pubmedcentral.nih.gov/articlerender.fcgi?artid=3438144&tool=pmcentrez&rendertype=abstract [Accessed June 16, 2013].

Lacy, P. et al., 2001. Fusion protein vesicle-associated membrane protein 2 is implicated in IFN-gamma-induced piecemeal degranulation in human eosinophils from atopic individuals. *The Journal of allergy and clinical immunology*, 107(4), pp.671–8. Available at: http://dx.doi.org/10.1067/mai.2001.113562 [Accessed June 24, 2013].

Lacy, P. & Stow, J.L., 2011. Cytokine release from innate immune cells: association with diverse membrane trafficking pathways. *Blood*, 118(1), pp.9–18. Available at: http://www.ncbi.nlm.nih.gov/pubmed/21562044 [Accessed July 5, 2013].

Laurence, A. et al., 2007. Interleukin-2 signaling via STAT5 constrains T helper 17 cell generation. *Immunity*, 26(3), pp.371–81. Available at: http://www.ncbi.nlm.nih.gov/pubmed/17363300 [Accessed May 31, 2013].

Lazarevic, V. et al., 2011. T-bet represses T(H)17 differentiation by preventing Runx1-mediated activation of the gene encoding RORγt. *Nature immunology*, 12(1), pp.96–104. Available at: http://dx.doi.org/10.1038/ni.1969 [Accessed June 4, 2013].

Lee, Y. et al., 2012. Induction and molecular signature of pathogenic TH17 cells. *Nature immunology*, 13(10), pp.991–9. Available at: http://www.pubmedcentral.nih.gov/articlerender.fcgi?artid=3459594&tool=pmcentrez&rendertype=abstract [Accessed May 31, 2013].

Lee, Y.K. et al., 2009. Late developmental plasticity in the T helper 17 lineage. *Immunity*, 30(1), pp.92–107. Available at: http://dx.doi.org/10.1016/j.immuni.2008.11.005 [Accessed May 31, 2013].

Lenschow, D.J., Walunas, T.L. & Bluestone, J.A., 1996. CD28/B7 system of T cell costimulation. *Annual Review of Immunology*, 14, pp.233–258.

Leshem, B., Yogev, D. & Fiorentini, D., 1999. Heat inactivation of fetal calf serum is not required for in vitro measurement of lymphocyte functions. *Journal of immunological methods*, 223(2), pp.249–254.

Liao, W., Lin, J.-X. & Leonard, W.J., 2011. IL-2 family cytokines: new insights into the complex roles of IL-2 as a broad regulator of T helper cell differentiation. *Current opinion in immunology*, 23(5), pp.598–604. Available at:

http://www.pubmedcentral.nih.gov/articlerender.fcgi?artid=3405730&tool=pmcentrez&rendertype=abstract [Accessed June 6, 2013].

Littleton, J.T. et al., 2001. SNARE-complex disassembly by NSF follows synaptic-vesicle fusion. *Proceedings of the National Academy of Sciences of the United States of America*, 98(21), pp.12233–8. Available at: http://www.pubmedcentral.nih.gov/articlerender.fcgi?artid=59797&tool=pmcentrez&rendertype=abstract [Accessed July 18, 2013].

Littman, D.R. & Rudensky, A.Y., 2010. Th17 and regulatory T cells in mediating and restraining inflammation. *Cell*, 140(6), pp.845–858.

Liu, Z.-J. et al., 2009. Potential role of Th17 cells in the pathogenesis of inflammatory bowel disease. *World journal of gastroenterology: WJG*, 15(46), pp.5784–8. Available at: http://www.pubmedcentral.nih.gov/articlerender.fcgi?artid=2791270&tool=pmcentrez&rendertype=abstract [Accessed June 25, 2013].

Logan, M.R. et al., 2006. A critical role for vesicle-associated membrane protein-7 in exocytosis from human eosinophils and neutrophils. *Allergy*, 61(6), pp.777–84. Available at: http://www.ncbi.nlm.nih.gov/pubmed/16677249 [Accessed June 23, 2013].

Loo, L.S. et al., 2009. A role for endobrevin/VAMP8 in CTL lytic granule exocytosis. *European journal of immunology*, 39(12), pp.3520–8. Available at: http://www.ncbi.nlm.nih.gov/pubmed/19830729 [Accessed May 24, 2013].

Lorentz, A. et al., 2012. The SNARE Machinery in Mast Cell Secretion. *Frontiers in immunology*, 3, p.143. Available at: http://www.pubmedcentral.nih.gov/articlerender.fcgi?artid=3367400&tool=pmcentrez&rendertype=abstract [Accessed July 19, 2013].

Lowe, M. et al., 2004. Caspase-mediated cleavage of syntaxin 5 and giantin accompanies inhibition of secretory traffic during apoptosis. *Journal of cell science*, 117(Pt 7), pp.1139–50. Available at: http://www.ncbi.nlm.nih.gov/pubmed/14970262 [Accessed June 27, 2013].

Lu, Y. & Durkin, J.P., 1997. Protein kinase C in IL-2 signal transduction. *Immunologic research*, 16(4), pp.355–374.

Ma, C.S. et al., 2012. The origins, function, and regulation of T follicular helper cells. *The Journal of experimental medicine*, 209(7), pp.1241–53. Available at: http://www.pubmedcentral.nih.gov/articlerender.fcgi?artid=3405510&tool=pmcentrez&rendertype=abstract [Accessed May 21, 2013].

Macatonia, S.E. et al., 1993. Dendritic cells and macrophages are required for Th1 development of CD4+ T cells from alpha beta TCR transgenic mice: IL-12 substitution for macrophages to stimulate IFN-gamma production is IFN-gamma-dependent. *International immunology*, 5(9), pp.1119–28. Available at: http://www.ncbi.nlm.nih.gov/pubmed/7902129 [Accessed July 11, 2013].

MacDonald, T.T. et al., 2003. Host defences to Citrobacter rodentium. *International Journal of Medical Microbiology*, 293(1), pp.87–93. Available at: http://www.sciencedirect.com/science/article/pii/S143842210470140X.

MacLennan, I.C., 1994. Germinal centers. *Annual review of immunology*, 12, pp.117–39. Available at: http://www.ncbi.nlm.nih.gov/pubmed/8011279 [Accessed May 22, 2013].

Malsam, J., Kreye, S. & Soellner, T.H., 2008. Membrane fusion: SNAREs and regulation. *Cellular and Molecular Life Sciences*, 65(18), pp.2814–2832.

Mangan, P.R. et al., 2006. Transforming growth factor-beta induces development of the T(H)17 lineage. *Nature*, 441(7090), pp.231–4. Available at: http://www.nature.com.remote.library.dcu.ie/nature/journal/v441/n7090/full/nature04754.html [Accessed May 21, 2013].

Mantovani, A. et al., 2011. Neutrophils in the activation and regulation of innate and adaptive immunity. *Nature reviews. Immunology*, 11(8), pp.519–31. Available at: http://www.ncbi.nlm.nih.gov/pubmed/21785456 [Accessed May 23, 2013].

Martín-Martín, B. et al., 2000. Involvement of SNAP-23 and syntaxin 6 in human neutrophil exocytosis. *Blood*, 96(7), pp.2574–83. Available at: http://www.ncbi.nlm.nih.gov/pubmed/11001914 [Accessed June 15, 2013].

Mauri, C., 2010. Regulation of immunity and autoimmunity by B cells. *Current Opinion in Immunology*, 22(6), pp.761–767. Available at: http://www.sciencedirect.com/science/article/pii/S0952791510001597.

Maynard, C.L. et al., 2012. Reciprocal interactions of the intestinal microbiota and immune system. *Nature*, 489(7415), pp.231–41. Available at: http://www.ncbi.nlm.nih.gov/pubmed/22972296 [Accessed June 2, 2013].

McGeachy, M.J. et al., 2007. TGF-beta and IL-6 drive the production of IL-17 and IL-10 by T cells and restrain T(H)-17 cell-mediated pathology. *Nature immunology*, 8(12), pp.1390–7. Available at: http://www.nature.com.remote.library.dcu.ie/ni/journal/v8/n12/abs/ni1539.html [Accessed July 15, 2013].

McGeachy, M.J. et al., 2009. The interleukin 23 receptor is essential for the terminal differentiation of interleukin 17-producing effector T helper cells in vivo. *Nature*

immunology, 10(3), pp.314–24. Available at: http://www.pubmedcentral.nih.gov/articlerender.fcgi?artid=2945605&tool=pmcentrez&rendertype=abstract [Accessed May 27, 2013].

McKenzie, B.S., Kastelein, R.A. & Cua, D.J., 2006. Understanding the IL-23-IL-17 immune pathway. *Trends in immunology*, 27(1), pp.17–23. Available at: http://www.ncbi.nlm.nih.gov/pubmed/16290228 [Accessed May 23, 2013].

Melo, R.C.N. et al., 2008. Mechanisms of eosinophil secretion: large vesiculotubular carriers mediate transport and release of granule-derived cytokines and other proteins. *Journal of leukocyte biology*, 83(2), pp.229–36. Available at: http://www.pubmedcentral.nih.gov/articlerender.fcgi?artid=2734949&tool=pmcentrez&rendertype=abstract [Accessed July 18, 2013].

Miossec, P., Korn, T. & Kuchroo, V.K., 2009. Interleukin-17 and type 17 helper T cells. *The New England journal of medicine*, 361(9), pp.888–898.

Mollinedo, F. et al., 2006. Combinatorial SNARE complexes modulate the secretion of cytoplasmic granules in human neutrophils. *Journal of immunology (Baltimore, Md.: 1950)*, 177(5), pp.2831–41. Available at: http://www.ncbi.nlm.nih.gov/pubmed/16920918 [Accessed June 23, 2013].

Mollinedo, F. et al., 2003. Role of vesicle-associated membrane protein-2, through Q-soluble N-ethylmaleimide-sensitive factor attachment protein receptor/R-soluble N-ethylmaleimide-sensitive factor attachment protein receptor interaction, in the exocytosis of specific and tertiary. *JOURNAL OF IMMUNOLOGY*, 170(2), pp.1034–1042.

Mombaerts, P. et al., 1992. RAG-1-deficient mice have no mature B and T lymphocytes. *Cell*, 68(5), pp.869–77. Available at: http://www.ncbi.nlm.nih.gov/pubmed/1547488 [Accessed May 27, 2013].

Mosmann, T.R. et al., 1986. Two types of murine helper T cell clone. I. Definition according to profiles of lymphokine activities and secreted proteins. *Journal of immunology (Baltimore, Md.: 1950)*, 136(7), pp.2348–2357.

Moss, M.L. et al., 1997. Structural features and biochemical properties of TNF-alpha converting enzyme (TACE). *Journal of neuroimmunology*, 72(2), pp.127–9. Available at: http://www.ncbi.nlm.nih.gov/pubmed/9042103 [Accessed July 18, 2013].

Murphy, C.A. et al., 2003. Divergent pro- and antiinflammatory roles for IL-23 and IL-12 in joint autoimmune inflammation. *The Journal of experimental medicine*, 198(12), pp.1951–7. Available at: http://jem.rupress.org.remote.library.dcu.ie/content/198/12/1951 [Accessed June 26, 2013].

Murray, R.Z., Kay, J.G., et al., 2005. A role for the phagosome in cytokine secretion. *Science (New York, N.Y.)*, 310(5753), pp.1492–5. Available at: http://www.sciencemag.org/content/310/5753/1492.abstract [Accessed May 23, 2013].

Murray, R.Z., Wylie, F.G., et al., 2005. Syntaxin 6 and Vti1b form a novel SNARE complex, which is up-regulated in activated macrophages to facilitate exocytosis of tumor necrosis Factor-alpha. *The Journal of biological chemistry*, 280(11), pp.10478–83. Available at: http://www.ncbi.nlm.nih.gov/pubmed/15640147 [Accessed May 25, 2013].

Nakae, S. et al., 2002. Antigen-specific T cell sensitization is impaired in IL-17-deficient mice, causing suppression of allergic cellular and humoral responses. *Immunity*, 17(3), pp.375–87. Available at: http://www.ncbi.nlm.nih.gov/pubmed/12354389 [Accessed July 2, 2013].

Nicoletti, I. et al., 1991. A rapid and simple method for measuring thymocyte apoptosis by propidium iodide staining and flow cytometry. *Journal of immunological methods*, 139(2), pp.271–279.

Nobrega, A.F., Maldonado, M.S. & Dos Reis, G.A., 1986. Analysis of isolated and combined effects of calcium ionophore and phorbol ester on T lymphocyte activation. *Clinical and experimental immunology*, 65(3), pp.559–569.

O'Garra, A., Stockinger, B. & Veldhoen, M., 2008. Differentiation of human T(H)-17 cells does require TGF-beta! *Nature immunology*, 9(6), pp.588–590.

Offenhäuser, C. et al., 2011. Syntaxin 11 binds Vti1b and regulates late endosome to lysosome fusion in macrophages. *Traffic (Copenhagen, Denmark)*, 12(6), pp.762–73. Available at: http://www.ncbi.nlm.nih.gov/pubmed/21388490 [Accessed June 24, 2013].

Ostanin, D. V et al., 2009. T cell transfer model of chronic colitis: concepts, considerations, and tricks of the trade. *American journal of physiology. Gastrointestinal and liver physiology*, 296(2), pp.G135–46. Available at: http://www.pubmedcentral.nih.gov/articlerender.fcgi?artid=2643911&tool=pmcentrez&rendertype=abstract [Accessed May 31, 2013].

Ouyang, W. et al., 1998. Inhibition of Th1 development mediated by GATA-3 through an IL-4-independent mechanism. *Immunity*, 9(5), pp.745–755.

Pagan, J.K. et al., 2003. The t-SNARE syntaxin 4 is regulated during macrophage activation to function in membrane traffic and cytokine secretion. *Current biology□: CB*, 13(2), pp.156–60. Available at: http://www.ncbi.nlm.nih.gov/pubmed/12546791 [Accessed July 18, 2013].

Pallavi, B. & Nagaraj, R., 2003. Palmitoylated peptides from the cysteine-rich domain of SNAP-23 cause membrane fusion depending on peptide length, position of cysteines, and extent of palmitoylation. *The Journal of biological chemistry*, 278(15), pp.12737–44. Available at: http://www.jbc.org/content/278/15/12737.full [Accessed May 21, 2013].

Park, H. et al., 2005. A distinct lineage of CD4 T cells regulates tissue inflammation by producing interleukin 17. *Nature immunology*, 6(11), pp.1133–1141.

Park, I.-K. et al., 2005. TGF-beta1 inhibits T-bet induction by IFN-gamma in murine CD4+ T cells through the protein tyrosine phosphatase Src homology region 2 domain-containing phosphatase-1. *Journal of immunology (Baltimore, Md.□: 1950)*, 175(9), pp.5666–74. Available at: http://www.ncbi.nlm.nih.gov/pubmed/16237056 [Accessed July 23, 2013].

Pattu, V. et al., 2012. SNARE protein expression and localization in human cytotoxic T lymphocytes. *European journal of immunology*, 42(2), pp.470–5. Available at: http://www.ncbi.nlm.nih.gov/pubmed/22120889 [Accessed March 2, 2012].

Paul, W.E. & Zhu, J., 2010. How are T(H)2-type immune responses initiated and amplified? *Nature Reviews Immunology*, 10(4), pp.225–235.

Paumet, F. et al., 2000. Soluble NSF attachment protein receptors (SNAREs) in RBL-2H3 mast cells: functional role of syntaxin 4 in exocytosis and identification of a vesicle-associated membrane protein 8-containing secretory compartment. *Journal of immunology (Baltimore, Md.□: 1950)*, 164(11), pp.5850–7. Available at: http://www.ncbi.nlm.nih.gov/pubmed/10820264 [Accessed July 19, 2013].

Pelletier, M. et al., 2010. Evidence for a cross-talk between human neutrophils and Th17 cells. *Blood*, 115(2), pp.335–43. Available at: http://www.ncbi.nlm.nih.gov/pubmed/19890092 [Accessed May 21, 2013].

Poirier, M.A. et al., 1998. The synaptic SNARE complex is a parallel four-stranded helical bundle. *Nature structural biology*, 5(9), pp.765–769. Available at: http://dx.doi.org/10.1038/1799.

Powrie, F. & Mason, D., 1990. OX-22high CD4+ T cells induce wasting disease with multiple organ pathology: prevention by the OX-22low subset. *The Journal of experimental medicine*, 172(6), pp.1701–8. Available at: http://www.pubmedcentral.nih.gov/articlerender.fcgi?artid=2188779&tool=pmcentrez&rendertype=abstract [Accessed July 12, 2013].

Prekeris, R., Klumperman, J. & Scheller, R.H., 2000. Syntaxin 11 is an atypical SNARE abundant in the immune system. *European journal of cell biology*, 79(11), pp.771–80. Available at: http://www.ncbi.nlm.nih.gov/pubmed/11139139 [Accessed June 24, 2013].

Prussin, C. & Metcalfe, D.D., 1995. Detection of intracytoplasmic cytokine using flow cytometry and directly conjugated anti-cytokine antibodies. *Journal of immunological methods*, 188(1), pp.117–28. Available at: http://www.ncbi.nlm.nih.gov/pubmed/8551029 [Accessed June 28, 2013].

Purvis, H.A. et al., 2010. Low-strength T-cell activation promotes Th17 responses. *Blood*, 116(23), pp.4829–37. Available at: http://www.pubmedcentral.nih.gov/articlerender.fcgi?artid=3223073&tool=pmcentrez&rendertype=abstract [Accessed May 25, 2013].

Qin, S. et al., 1998. The chemokine receptors CXCR3 and CCR5 mark subsets of T cells associated with certain inflammatory reactions. *The Journal of clinical investigation*, 101(4), pp.746–754. Available at: http://www.jci.org/articles/view/1422.

Qu, B. et al., 2011. Docking of lytic granules at the immunological synapse in human CTL requires Vti1b-dependent pairing with CD3 endosomes. *Journal of immunology (Baltimore, Md.□: 1950)*, 186(12), pp.6894–904. Available at: http://www.ncbi.nlm.nih.gov/pubmed/21562157 [Accessed May 27, 2013].

Quah, B.J., Warren, H.S. & Parish, C.R., 2007. Monitoring lymphocyte proliferation in vitro and in vivo with the intracellular fluorescent dye carboxyfluorescein diacetate succinimidyl ester. *Nature protocols*, 2(9), pp.2049–2056.

Raptis, A. et al., 2005. Distribution of synaptobrevin/VAMP 1 and 2 in rat brain. *Journal of chemical neuroanatomy*, 30(4), pp.201–11. Available at: http://www.ncbi.nlm.nih.gov/pubmed/16169186 [Accessed June 23, 2013].

Reefman, E. et al., 2010. Cytokine secretion is distinct from secretion of cytotoxic granules in NK cells. *Journal of immunology (Baltimore, Md.□: 1950)*, 184(9), pp.4852–62. Available at: http://www.ncbi.nlm.nih.gov/pubmed/20368273 [Accessed June 5, 2013].

Rennick, D.M., Fort, M.M. & Davidson, N.J., 1997. Studies with IL-10-/- mice: an overview. *Journal of leukocyte biology*, 61(4), pp.389–96. Available at: http://www.ncbi.nlm.nih.gov/pubmed/9103224 [Accessed July 15, 2013].

Romagnani, S., 1994. Lymphokine production by human T cells in disease states. *Annual review of immunology*, 12, pp.227–57. Available at: http://www.ncbi.nlm.nih.gov/pubmed/8011282 [Accessed July 9, 2013].

Russell, J.H.L., 2002. Lymphocyte-Mediated Cytotoxicity. *Annual Review of Immunology.*, 20(1), p.323.

De Saint Basile, G., Ménasché, G. & Fischer, A., 2010. Molecular mechanisms of biogenesis and exocytosis of cytotoxic granules. *Nature reviews. Immunology*,

10(8), pp.568–79. Available at: http://www.ncbi.nlm.nih.gov/pubmed/20634814 [Accessed May 27, 2013].

Sakaguchi, S. et al., 1995. Immunologic self-tolerance maintained by activated T cells expressing IL-2 receptor alpha-chains (CD25). Breakdown of a single mechanism of self-tolerance causes various autoimmune diseases. *Journal of immunology (Baltimore, Md.□: 1950)*, 155(3), pp.1151–64. Available at: http://www.ncbi.nlm.nih.gov/pubmed/7636184 [Accessed June 9, 2013].

Salek-Ardakani, S. & Schoenberger, S.P., 2013. T cell exhaustion: a means or an end? *Nature immunology*, 14(6), pp.531–533. Available at: http://dx.doi.org/10.1038/ni.2619 [Accessed May 21, 2013].

Saraiva, M. et al., 2009. Interleukin-10 production by Th1 cells requires interleukin-12-induced STAT4 transcription factor and ERK MAP kinase activation by high antigen dose. *Immunity*, 31(2), pp.209–19. Available at: http://www.pubmedcentral.nih.gov/articlerender.fcgi?artid=2791889&tool=pmcentrez&rendertype=abstract [Accessed May 25, 2013].

Sarra, M. et al., 2010. Interferon-gamma-expressing cells are a major source of interleukin-21 in inflammatory bowel diseases. *Inflammatory bowel diseases*, 16(8), pp.1332–9. Available at: http://www.ncbi.nlm.nih.gov/pubmed/20186935 [Accessed June 20, 2013].

Schroder, K. et al., 2004. Interferon-gamma: an overview of signals, mechanisms and functions. *Journal of leukocyte biology*, 75(2), pp.163–89. Available at: http://www.jleukbio.org/content/75/2/163.full [Accessed May 21, 2013].

Schulz, E.G. et al., 2009. Sequential Polarization and Imprinting of Type 1 T Helper Lymphocytes by Interferon-^{3} and Interleukin-12. *Immunity*, 30(5), pp.673–683. Available at: http://linkinghub.elsevier.com/retrieve/pii/S1074761309001848 [Accessed June 4, 2013].

Seddon, B., Tomlinson, P. & Zamoyska, R., 2003. Interleukin 7 and T cell receptor signals regulate homeostasis of CD4 memory cells. *Nature immunology*, 4(7), pp.680–686.

Seder, R.A. et al., 1993. Interleukin 12 acts directly on CD4+ T cells to enhance priming for interferon gamma production and diminishes interleukin 4 inhibition of such priming. *Proceedings of the National Academy of Sciences of the United States of America*, 90(21), pp.10188–92. Available at: http://www.pubmedcentral.nih.gov/articlerender.fcgi?artid=47739&tool=pmcentrez&rendertype=abstract [Accessed July 11, 2013].

Sepulveda, F.E. et al., 2013. Distinct severity of HLH in both human and murine mutants with complete loss of cytotoxic effector PRF1, RAB27A, and STX11. *Blood*,

121(4), pp.595–603. Available at: http://www.ncbi.nlm.nih.gov/pubmed/23160464 [Accessed June 25, 2013].

Shale, M., Schiering, C. & Powrie, F., 2013. CD4(+) T-cell subsets in intestinal inflammation. *Immunological reviews*, 252(1), pp.164–82. Available at: http://www.ncbi.nlm.nih.gov/pubmed/23405904 [Accessed July 2, 2013].

Shimoda, K. et al., 1996. Lack of IL-4-induced Th2 response and IgE class switching in mice with disrupted Stat6 gene. *Nature*, 380(6575), pp.630–3. Available at: http://www.nature.com.remote.library.dcu.ie/nature/journal/v380/n6575/abs/380630a0.html [Accessed May 23, 2013].

Shurety, W. et al., 2000. Localization and post-Golgi trafficking of tumor necrosis factor-alpha in macrophages. *Journal of interferon & cytokine research□: the official journal of the International Society for Interferon and Cytokine Research*, 20(4), pp.427–38. Available at: http://www.ncbi.nlm.nih.gov/pubmed/10805378 [Accessed July 18, 2013].

Smith, K.A., 1988. Interleukin-2: inception, impact, and implications. *Science (New York, N.Y.)*, 240(4856), pp.1169–1176.

Smith, K.A., Gilbride, K.J. & Favata, M.F., 1980. Lymphocyte activating factor promotes T-cell growth factor production by cloned murine lymphoma cells. *Nature*, 287(5785), pp.853–5. Available at: http://www.ncbi.nlm.nih.gov/pubmed/6776414 [Accessed March 27, 2013].

Söllner, T. et al., 1993. A protein assembly-disassembly pathway in vitro that may correspond to sequential steps of synaptic vesicle docking, activation, and fusion. *Cell*, 75(3), pp.409–418. Available at: http://apps.webofknowledge.com.remote.library.dcu.ie/full_record.do?product=WOS&search_mode=Refine&qid=29&SID=P2jpo2loIdP1Ki8kIIP&page=1&doc=1 [Accessed June 16, 2013].

Sonderegger, I. et al., 2008. IL-21 and IL-21R are not required for development of Th17 cells and autoimmunity in vivo. *European journal of immunology*, 38(7), pp.1833–8. Available at: http://www.ncbi.nlm.nih.gov/pubmed/18546146 [Accessed June 20, 2013].

Sprent, J. & Surh, C.D., 2011. Normal T cell homeostasis: the conversion of naive cells into memory-phenotype cells. *Nature Immunology*, 131(6), pp.478–484.

Zur Stadt, U. et al., 2005. Linkage of familial hemophagocytic lymphohistiocytosis (FHL) type-4 to chromosome 6q24 and identification of mutations in syntaxin 11. *Human molecular genetics*, 14(6), pp.827–34. Available at: http://www.ncbi.nlm.nih.gov/pubmed/15703195 [Accessed April 23, 2013].

Stanley, A.C. & Lacy, P., 2010. Pathways for cytokine secretion. *Physiology (Bethesda, Md.)*, 25(4), pp.218–29. Available at: http://physiologyonline.physiology.org/content/25/4/218 [Accessed May 22, 2013].

Starr, T.K., Jameson, S.C. & Hogquist, K.A., 2003. Positive and negative selection of T cells. *Annual review of immunology*, 21, pp.139–76.

Stinchcombe, J.C. & Griffiths, G.M., 2007. Secretory mechanisms in cell-mediated cytotoxicity. *Annual review of cell and developmental biology*, 23, pp.495–517. Available at: http://www.ncbi.nlm.nih.gov/pubmed/17506701 [Accessed May 27, 2013].

Stow, J.L., Manderson, A.P. & Murray, R.Z., 2006. SNAREing immunity: the role of SNAREs in the immune system. *Nature reviews.Immunology*, 6(12), pp.919–929.

Stow, J.L. & Murray, R.Z., 2013. Intracellular trafficking and secretion of inflammatory cytokines. *Cytokine & growth factor reviews*, 24(3), pp.227–39. Available at: http://www.sciencedirect.com.remote.library.dcu.ie/science/article/pii/S1359610113000294 [Accessed June 16, 2013].

Sutton, R.B. et al., 1998. Crystal structure of a SNARE complex involved in synaptic exocytosis at 2.4 angstrom resolution. *Nature*, 395(6700), pp.347–353.

Suzuki, K. & Verma, I.M., 2008. Phosphorylation of SNAP-23 by IkappaB kinase 2 regulates mast cell degranulation. *Cell*, 134(3), pp.485–95. Available at: http://www.pubmedcentral.nih.gov/articlerender.fcgi?artid=2586340&tool=pmcentrez&rendertype=abstract [Accessed June 15, 2013].

SWAIN, S.L. et al., 1990. Il-4 Directs The Development Of Th2-Like Helper Effectors. *Journal of Immunology*, 145(11), pp.3796–3806.

Szabo, S.J. et al., 2000. A novel transcription factor, T-bet, directs Th1 lineage commitment. *Cell*, 100(6), pp.655–669.

Szabo, S.J. et al., 2002. Distinct effects of T-bet in T(H)1 lineage commitment and IFN-gamma production in CD4 and CD8 T cells. *Science*, 295(5553), pp.338–342.

Takahashi, T. et al., 1998. Immunologic self-tolerance maintained by CD25+CD4+ naturally anergic and suppressive T cells: induction of autoimmune disease by breaking their anergic/suppressive state. *International immunology*, 10(12), pp.1969–80. Available at: http://www.ncbi.nlm.nih.gov/pubmed/9885918 [Accessed July 12, 2013].

Takeda, K. et al., 1996. Essential role of Stat6 in IL-4 signalling. *Nature*, 380(6575), pp.627–30. Available at:

http://www.nature.com.remote.library.dcu.ie/nature/journal/v380/n6575/abs/380627a0.html [Accessed May 23, 2013].

Thornton, A.M. & Shevach, E.M., 1998. CD4+CD25+ immunoregulatory T cells suppress polyclonal T cell activation in vitro by inhibiting interleukin 2 production. *The Journal of experimental medicine*, 188(2), pp.287–96. Available at: http://www.pubmedcentral.nih.gov/articlerender.fcgi?artid=2212461&tool=pmcentrez&rendertype=abstract [Accessed July 12, 2013].

Tian, T., Yu, S. & Ma, D., 2013. Th22 and related cytokines in inflammatory and autoimmune diseases. *Expert opinion on therapeutic targets*, 17(2), pp.113–25. Available at: http://informahealthcare.com.remote.library.dcu.ie/doi/abs/10.1517/14728222.2013.736497 [Accessed July 24, 2013].

Tiwari, N. et al., 2008. VAMP-8 segregates mast cell-preformed mediator exocytosis from cytokine trafficking pathways. *Blood*, 111(7), pp.3665–74. Available at: http://www.ncbi.nlm.nih.gov/pubmed/18203950 [Accessed July 19, 2013].

Trifari, S. et al., 2009. Identification of a human helper T cell population that has abundant production of interleukin 22 and is distinct from T(H)-17, T(H)1 and T(H)2 cells. *Nature immunology*, 10(8), pp.864–71. Available at: http://www.ncbi.nlm.nih.gov/pubmed/19578368 [Accessed June 11, 2013].

Triglia, R.P. & Linscott, W.D., 1980. Titers of nine complement components, conglutinin and C3b-inactivator in adult and fetal bovine sera. *Molecular immunology*, 17(6), pp.741–748.

Trimble, W.S., Cowan, D.M. & Scheller, R.H., 1988. VAMP-1: a synaptic vesicle-associated integral membrane protein. *Proceedings of the National Academy of Sciences of the United States of America*, 85(12), pp.4538–42. Available at: http://www.pubmedcentral.nih.gov/articlerender.fcgi?artid=280466&tool=pmcentrez&rendertype=abstract [Accessed June 23, 2013].

Trinchieri, G., 2007. Interleukin-10 production by effector T cells: Th1 cells show self control. *The Journal of experimental medicine*, 204(2), pp.239–43. Available at: http://jem.rupress.org.remote.library.dcu.ie/content/204/2/239 [Accessed July 2, 2013].

Usui, T. et al., 2003. GATA-3 Suppresses Th1 Development by Downregulation of Stat4 and Not through Effects on IL-12Rβ2 Chain or T-bet. *Immunity*, 18(3), pp.415–428. Available at: http://www.cell.com/immunity/fulltext/S1074-7613(03)00057-8 [Accessed June 13, 2013].

Vahedi, G. et al., 2013. Helper T-cell identity and evolution of differential transcriptomes and epigenomes. *Immunological reviews*, 252(1), pp.24–40. Available at: http://www.ncbi.nlm.nih.gov/pubmed/23405893.

Vaidyanathan, V. V, Puri, N. & Roche, P. a, 2001. The last exon of SNAP-23 regulates granule exocytosis from mast cells. *The Journal of biological chemistry*, 276(27), pp.25101–6. Available at: http://www.ncbi.nlm.nih.gov/pubmed/11350976 [Accessed May 25, 2013].

Valdez, A.C. et al., 1999. Syntaxin 11 is associated with SNAP-23 on late endosomes and the trans-Golgi network. *Journal of cell science*, 112 (Pt 6, pp.845–54. Available at: http://www.ncbi.nlm.nih.gov/pubmed/10036234 [Accessed July 1, 2013].

Veldhoen, M. et al., 2006. TGFbeta in the context of an inflammatory cytokine milieu supports de novo differentiation of IL-17-producing T cells. *Immunity*, 24(2), pp.179–89. Available at: http://www.ncbi.nlm.nih.gov/pubmed/16473830 [Accessed May 31, 2013].

Wei, L. et al., 2007. IL-21 is produced by Th17 cells and drives IL-17 production in a STAT3-dependent manner. *The Journal of biological chemistry*, 282(48), pp.34605–10. Available at: http://www.jbc.org/content/282/48/34605 [Accessed May 27, 2013].

Wherry, E.J., 2011. T cell exhaustion. *Nature Immunology*, 131(6), pp.492–499. Available at: http://dx.doi.org/10.1038/ni.2035 [Accessed May 21, 2013].

Wing, K. & Sakaguchi, S., 2010. Regulatory T cells exert checks and balances on self tolerance and autoimmunity. *Nature immunology*, 11(1), pp.7–13.

Wirtz, S. et al., 2007. Chemically induced mouse models of intestinal inflammation. *Nature protocols*, 2(3), pp.541–6. Available at: http://dx.doi.org/10.1038/nprot.2007.41 [Accessed May 25, 2013].

Woska, J.R. & Gillespie, M.E., 2011. Small-interfering RNA-mediated identification and regulation of the ternary SNARE complex mediating RBL-2H3 mast cell degranulation. *Scandinavian journal of immunology*, 73(1), pp.8–17. Available at: http://www.ncbi.nlm.nih.gov/pubmed/21128998 [Accessed June 16, 2013].

Yagi, R. et al., 2010. The transcription factor GATA3 actively represses RUNX3 protein-regulated production of interferon-gamma. *Immunity*, 32(4), pp.507–17. Available at: http://www.cell.com/immunity/fulltext/S1074-7613(10)00129-9 [Accessed June 13, 2013].

Yamane, H. & Paul, W.E., 2012. Cytokines of the γ(c) family control CD4+ T cell differentiation and function. *Nature immunology*, 13(11), pp.1037–44. Available at:

http://www.nature.com.remote.library.dcu.ie/ni/journal/v13/n11/full/ni.2431.html [Accessed May 31, 2013].

Yamane, H. & Paul, W.E., 2013. Early signaling events that underlie fate decisions of naive CD4(+) T cells toward distinct T-helper cell subsets. *Immunological reviews*, 252(1), pp.12–23. Available at: http://www.ncbi.nlm.nih.gov/pubmed/23405892.

Yang, L. et al., 2008. IL-21 and TGF-beta are required for differentiation of human T(H)17 cells. *Nature*, 454(7202), pp.350–2. Available at: http://www.pubmedcentral.nih.gov/articlerender.fcgi?artid=2760130&tool=pmcentrez&rendertype=abstract [Accessed June 3, 2013].

Yang, X.O. et al., 2007. STAT3 regulates cytokine-mediated generation of inflammatory helper T cells. *The Journal of biological chemistry*, 282(13), pp.9358–63. Available at: http://www.jbc.org.remote.library.dcu.ie/content/282/13/9358 [Accessed May 30, 2013].

Ye, S. et al., 2012. Syntaxin-11, but not syntaxin-2 or syntaxin-4, is required for platelet secretion. *Blood*, 120(12), pp.2484–92. Available at: http://bloodjournal.hematologylibrary.org/content/120/12/2484.long [Accessed June 5, 2013].

Yi, J.S., Cox, M.A. & Zajac, A.J., 2010. T-cell exhaustion: characteristics, causes and conversion. *Immunology*, 129(4), pp.474–81. Available at: http://www.pubmedcentral.nih.gov/articlerender.fcgi?artid=2842494&tool=pmcentrez&rendertype=abstract [Accessed May 31, 2013].

Yosef, N. et al., 2013. Dynamic regulatory network controlling T(H)17 cell differentiation. *Nature*, 496(7446), pp.461–8. Available at: http://www.ncbi.nlm.nih.gov/pubmed/23467089 [Accessed May 21, 2013].

Yoshida, A. et al., 1994. IFN-gamma induces IL-12 mRNA exression by a murine cell line, J774. *Biochemical and biophysical research communications*, 198(3), pp.857–861.

Zenewicz, L.A., Antov, A. & Flavell, R.A., 2009. CD4 T-cell differentiation and inflammatory bowel disease. *Trends in molecular medicine*, 15(5), pp.199–207. Available at: http://www.sciencedirect.com.remote.library.dcu.ie/science/article/pii/S1471491409000598 [Accessed May 25, 2013].

Zerial, M. & McBride, H., 2001. Rab proteins as membrane organizers. *Nature reviews. Molecular cell biology*, 2(2), pp.107–17. Available at: http://www.ncbi.nlm.nih.gov/pubmed/11252952 [Accessed May 31, 2013].

Zhang, S. et al., 2008. Syntaxin-11 is expressed in primary human monocytes/macrophages and acts as a negative regulator of macrophage engulfment of apoptotic cells and IgG-opsonized target cells. *British journal of haematology*, 142(3), pp.469–79. Available at: http://www.ncbi.nlm.nih.gov/pubmed/18547321 [Accessed May 25, 2013].

Zheng, W. & Flavell, R.A., 1997. The transcription factor GATA-3 is necessary and sufficient for Th2 cytokine gene expression in CD4 T cells. *Cell*, 89(4), pp.587–596.

Zhou, L. et al., 2007. IL-6 programs T(H)-17 cell differentiation by promoting sequential engagement of the IL-21 and IL-23 pathways. *Nature immunology*, 8(9), pp.967–974. Available at: http://www.ncbi.nlm.nih.gov/pubmed/17581537 [Accessed May 26, 2013].

Zhou, L. et al., 2008. TGF-beta-induced Foxp3 inhibits T(H)17 cell differentiation by antagonizing RORgammat function. *Nature*, 453(7192), pp.236–40. Available at: http://www.pubmedcentral.nih.gov/articlerender.fcgi?artid=2597437&tool=pmcentrez&rendertype=abstract [Accessed May 21, 2013].

Zhu, J. et al., 2004. Conditional deletion of Gata3 shows its essential function in T(H)1-T(H)2 responses. *Nature immunology*, 5(11), pp.1157–65. Available at: http://www.nature.com.remote.library.dcu.ie/ni/journal/v5/n11/abs/ni1128.html [Accessed June 8, 2013].

Zhu, J. et al., 2006. GATA-3 promotes Th2 responses through three different mechanisms: induction of Th2 cytokine production, selective growth of Th2 cells and inhibition of Th1 cell-specific factors. *Cell research*, 16(1), pp.3–10. Available at: http://www.ncbi.nlm.nih.gov/pubmed/16467870 [Accessed June 9, 2013].

Zhu, J., 2010. Transcriptional regulation of Th2 cell differentiation. *Immunology and cell biology*, 88(3), pp.244–249.

Zhu, J., Yamane, H. & Paul, W.E., 2010. Differentiation of effector CD4 T cell populations (*). *Annual review of immunology*, 28, pp.445–89. Available at: http://www.pubmedcentral.nih.gov/articlerender.fcgi?artid=3502616&tool=pmcentrez&rendertype=abstract [Accessed May 21, 2013].

Zhu, P. et al., 2010. IL-2 mRNA stabilization upon PMA stimulation is dependent on NF90-Ser647 phosphorylation by protein kinase CbetaI. *Journal of immunology (Baltimore, Md.□: 1950)*, 185(9), pp.5140–9. Available at: http://www.jimmunol.org/content/185/9/5140.long [Accessed June 17, 2013].

Zielinski, C.E. et al., 2012. Pathogen-induced human TH17 cells produce IFN-γ or IL-10 and are regulated by IL-1β. *Nature*, 484(7395), pp.514–8. Available at: http://www.ncbi.nlm.nih.gov/pubmed/22466287 [Accessed April 3, 2012].

APPENDICES

APPENDIX A – MEDIA AND BUFFERS

COMPLETE RPMI 1640 500 ml

Heat inactivated Foetal bovine serum (FBS)	10%
Penicillin/streptomycin/L-glutamine Culture Cocktail	2%
(Gives a final concentration of 2 mM L-glutamine,	
100 μ g/ml penicillin and 100 U/ml streptomycin)	

PHOSPHATE BUFFERED SALINE (PBS)

$Na_2HPO_4.2H_2O$	8.0 mM
KH_2PO_4	1.5 mM
NaCl	137 mM
KCl	2.7 mM

Dissolve in H_2O and pH to 7.4

TRIS BUFFERED SALINE (TBS) pH 7.6

NaCl	1.5 M
Trizma Base	0.2 M

Dissolve dH_2O pH to 7.6

TBST

Add 0.05% Tween-20 to 1x TBS

FACS BUFFER

FCS	2%
NaN_3	0.05%

Dissolved in PBS

SORTING BUFFER

FCS	1%
EDTA	1 mM
HEPES	25 mM

Dissolved in PBS

TAE BUFFER

TRIS	40 mM
ACETIC ACID	20 mM
EDTA	1 mM

Dissolved in H_2O

APPENDIX B – PRIMER EFFICIENCY CURVES

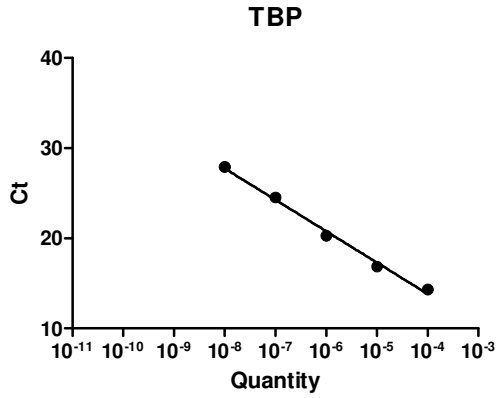

R^2 = 0.9937 **Efficiency** = 93.8%

Dynamic Range = 14-28 Ct

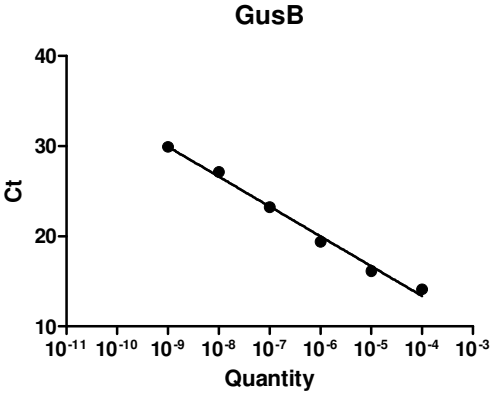

R^2 = 0.9925 **Efficiency** = 100.5%

Dynamic Range = 14-30 Ct

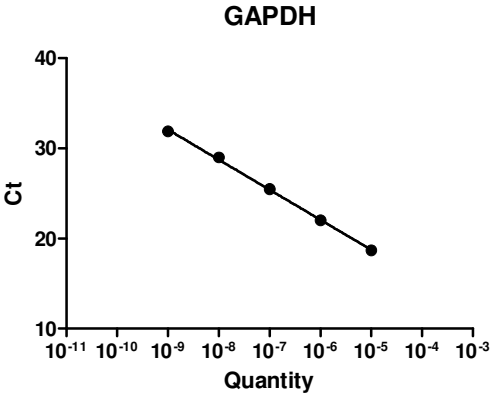

R^2 = 0.9989 **Efficiency** = 99.7%

Dynamic Range = 19-32 Ct

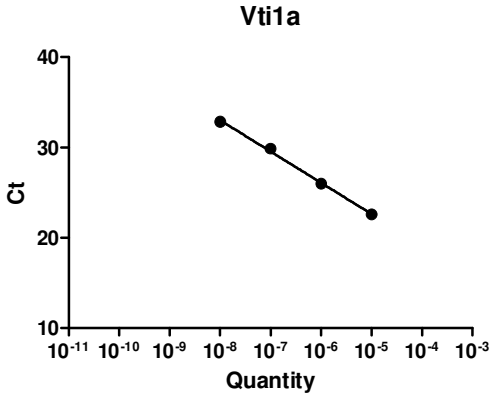

R^2 = 0.9976 **Efficiency** = 94.5%

Dynamic Range = 23-33 Ct

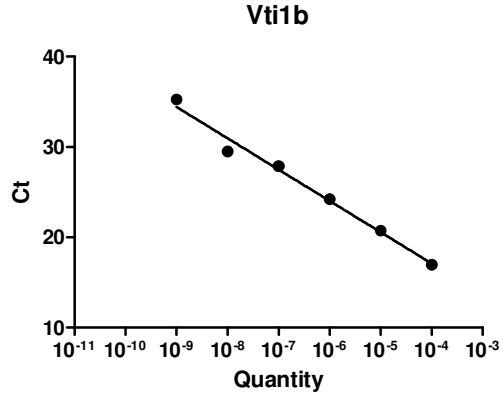

R^2 = 0.9989 **Efficiency** = 94.3%

Dynamic Range = 17-35 Ct

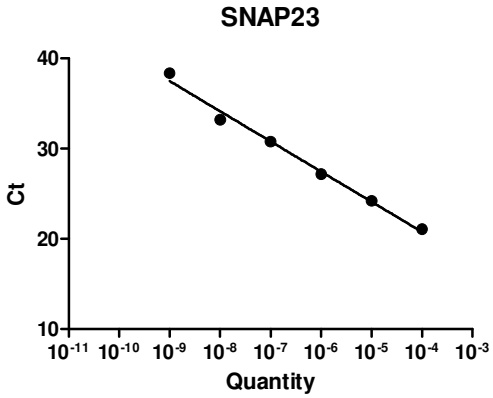

R^2 = 0.9908 **Efficiency** = 99.3%

Dynamic Range = 21-35 Ct

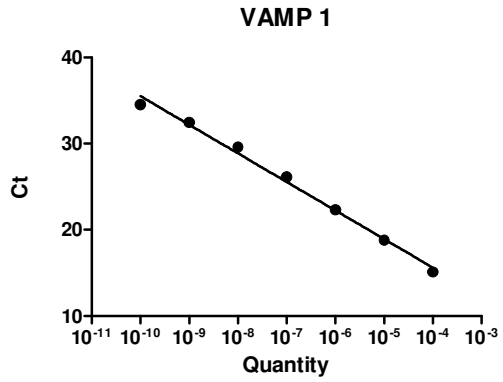

R^2 = 0.9933 **Efficiency** = 100.2%

Dynamic Range = 15-35 Ct

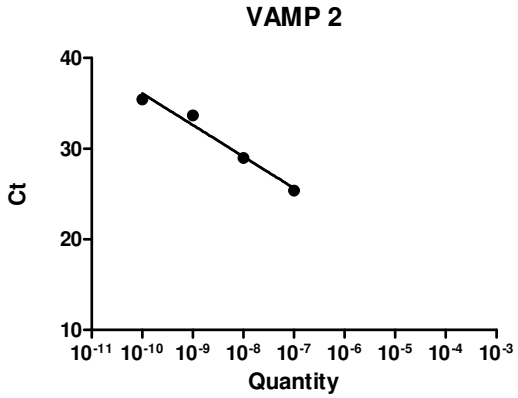

R^2 = 0.9733 **Efficiency** = 93.6%

Dynamic Range = 25-35 Ct

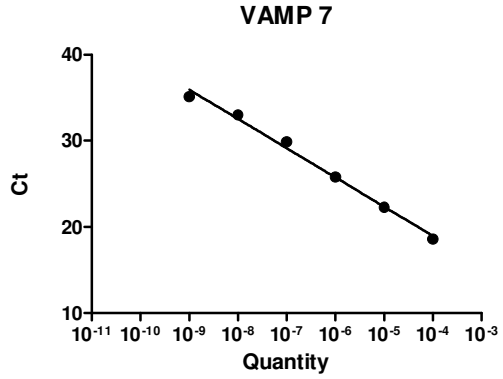

R^2 = 0.9922 **Efficiency** = 96.9%

Dynamic Range = 19-35 Ct

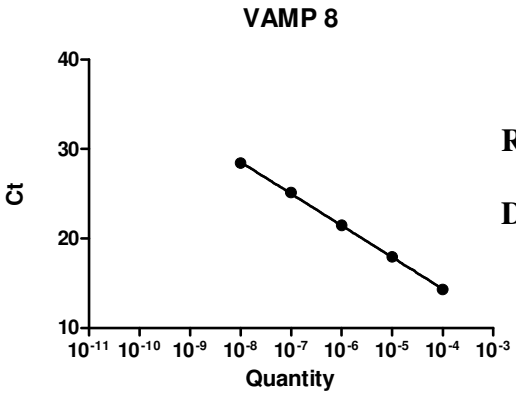

R^2 = 0.9997 **Efficiency** = 91.4%

Dynamic Range = 14-28 Ct

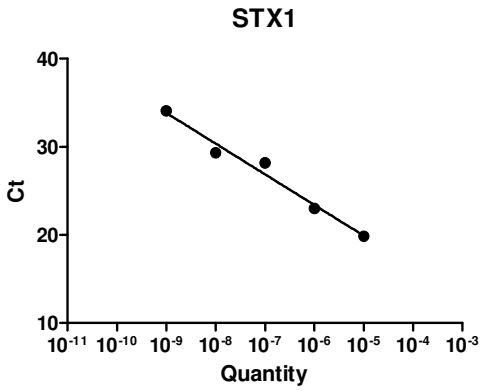

R^2 = 0.9760 **Efficiency** = 93.6%

Dynamic Range = 30-34 Ct

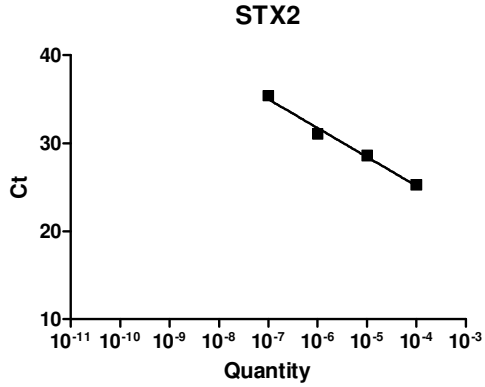

R^2 = 0.9760 **Efficiency** = 101.7%

Dynamic Range = 25-35 Ct

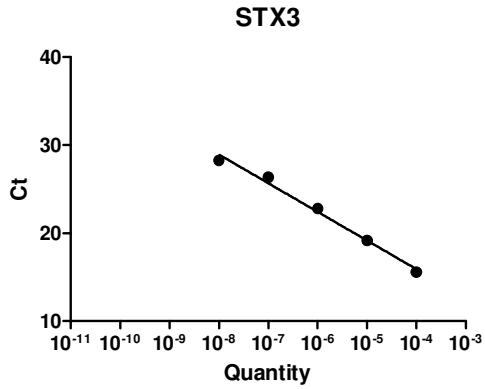

R^2 = 0.9894 **Efficiency** = 102.9%

Dynamic Range = 16-28 Ct

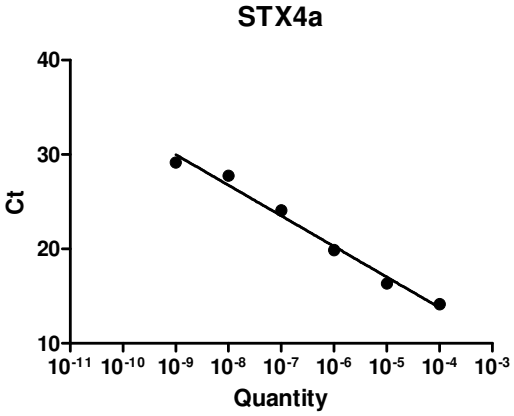

R^2 = 0.9851 **Efficiency** = 103.4%

Dynamic Range = 14-29 Ct

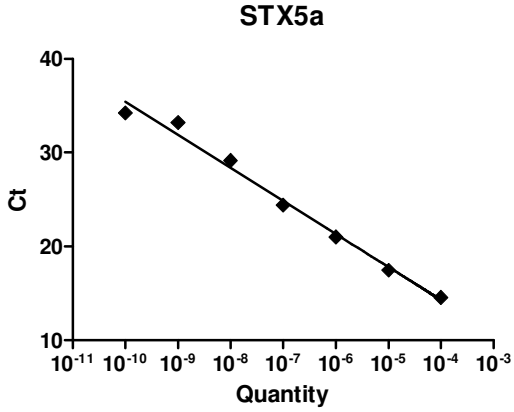

R^2 = 0.9879 **Efficiency** = 92.1%

Dynamic Range = 15-34 Ct

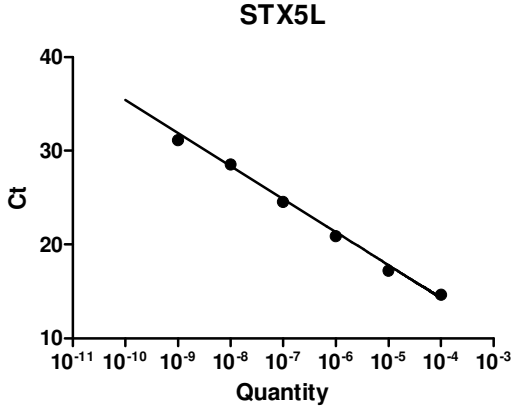

R^2 = 0.9958 **Efficiency** = 95.7%

Dynamic Range = 15-31 Ct

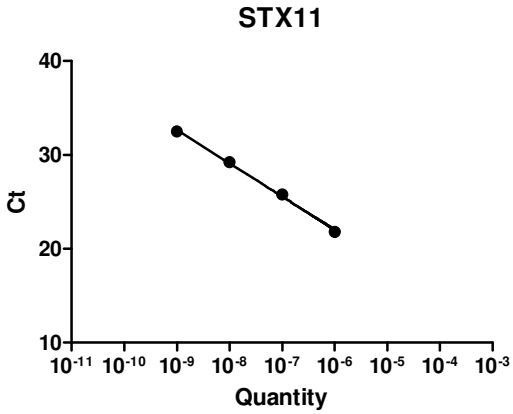

R^2 = 0.9978 **Efficiency** = 91.5%

Dynamic Range = 22-33 Ct

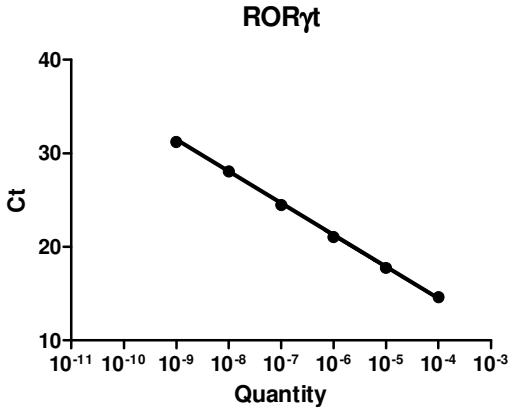

R^2 = 0.9997 **Efficiency** = 98.8%

Dynamic Range = 15-32 Ct

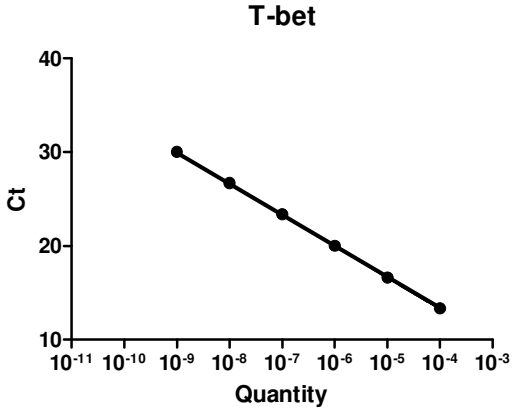

R^2 = 1.000 **Efficiency** = 99.9%

Dynamic Range = 13-30 Ct

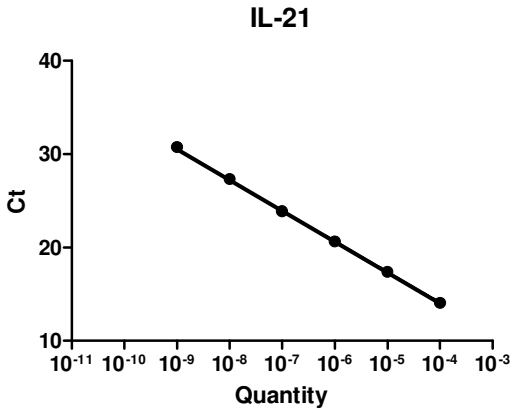

R^2 = 0.9998 **Efficiency** = 99.8%

Dynamic Range = 14-31 Ct

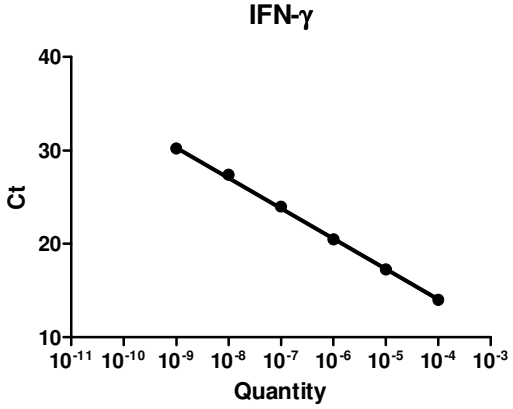

R^2 = 0.9993 **Efficiency** = 101.78%

Dynamic Range = 14-30 Ct

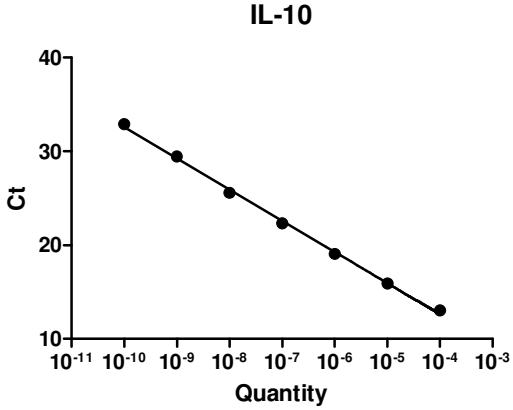

R^2 = 0.9982 **Efficiency** = 99.7%

Dynamic Range = 13-33 Ct

APPENDIX C – PRIMER SEQUENCES

IDT PRIMER SEQUENCES

Gusb
Primer 1 5'-GAG AACTGGTAT AAG ACG CAT CA-3'
Primer 2 5'-GAA CAG CCT TCT GGT ACT CC-3'

Tbp
Primer 1 5'-TTC ACC AAT GACTCC TAT GAC C-3'
Primer 2 5'-CAA GTT TAC AGC CAA GAT TCA CG-3'

Stx11
Primer 1 5'-GAA GCA GTA GAG AGC GTA GAA C-3'
Primer 2 5'-TCCTGG ACA ATT CTT GAA GCT C-3'

Il17a
Primer 1 5'-AGA CTA CCT CAA CCGTTC CA-3'
Primer 2 5'-GAG CTT CCC AGATCA CAG AG-3'

Il23r
Primer 1 5'-CAT CCC ACG AAC CTC AGA AG-3'
Primer 2 5'-CAA GAA GAC CAT TCC CGA CAA-3'

Tbx21
Primer 1 5'-TTC AAC CAG CAC CAG ACA G-3'
Primer 2 5'-CAA GAC CAC ATC CAC AAA CAT C-3'

Il2r
Primer 1 5'-CTG CCT CTT CCT GCT CAT C-3'
Primer 2 5'-GCT CTG ACT TTT CTA GCT TGC T-3'

Il21
Primer 1 5'-TGA CTT GGATCC TGA ACT TCT ATC-3'
Primer 2 5'-GGT TTG ATG GCT TGA GTT TGG-3'

Il2
Primer 1 5'-GCA GGATGG AGA ATT ACA GGA A-3'
Primer 2 5'-GCA GAG GTC CAA GTT CAT CTT C-3'

Ifngr1
Primer 1 5'-TTG AAC CCT GTC GTATGC TG-3'
Primer 2 5'-ATG ATC AGA AAT GTT GGT GCA G-3'

Rorc
Primer 1 5'-TCT GCA AGA CTC ATC GAC AAG-3'
Primer 2 5'-GAG GTG CTG GAA GAT CTG C-3'

SIGMA PRIMER SEQUENCES

Ifng

Primer 1 5'-ATG AAC GCT ACA CAC TGC ATC-3'
Primer 2 5'-CCA TCC TTT TGC CAG TTC CTC-3'

Sec22

Primer 1 5’-GCT AAC AAT TTG TCC AGT CTA TC-3’
Primer 2 5’-AAC CGC ACA TAC ACT ATC AG-3’

Snap23

Primer 1 5’-GTT CTT GCT CAG GCT TCC-3’
Primer 2 5’-CCA ACC AAC CAA TAC CAA TAA TG-3

Stx1

Primer 1 5’-CAC CCA CTG CTC CAT TCT-3’
Primer 2 5’-CAC ACA CTG TCA CAA GAT CAT-5’

Stx2

Primer 1 5’-GGT GGC AAA GGT GAT GTT-3’
Primer 2 5’-CAG GTA TGG TCG GAG TCA-3’

StX3

Primer 1 5’-CCA CAA CCA CTA GCA TCA TAA-3’
Primer 2 5’-CTC AAG AGA TAT TCC GCC TTA A-3’

Stx4

Primer 1 5’-GGT GTC AAG TGT GAG AGA G-3’
Primer 2 5’-AAC CTC ATC TTC ATC GTC TG-3’

Vamp1

Primer 1 5’-CCC TCT GTT TGC TTT CTC A-3’
Primer 2 5’-CGT TGT CTT CGG GTA GTG-3’

Vamp2

Primer 1 5’-CTC CTT CCC TTG GAT TTA ACC-3’
Primer 2 5’-TGA AAC AGA CAG CGT ATG C-3’

Vamp7

Primer 1 5’-GAT GGA GAC TCA AGC ACA AG-3’
Primer 2 5’-GAC ACA ATG ATA TAG ATG AAC ACA AT-3’

Vamp8

Primer 1 5’-GGC GAA GTT CTG CTT TGA-3’
Primer 2 5’-CTT GAC TCC CTC CAC CTC-3’

Vti1b

Primer 1 5’-TAC CTT GGA GAA CGA GCA T-3’
Primer 2 5’-TGG ACA TTG AGC GAA GAA TC-3’